

Investigation on adverse biochemical alterations in HepG2 cells during hyperinsulinemia and possible reversal with vanillic acid

by

Sreelekshmi Mohan
10BB16A39017

A thesis submitted to the
Academy of Scientific & Innovative Research
for the award of the degree of
DOCTOR OF PHILOSOPHY

in

SCIENCE

Under the supervision of
Prof. (Dr) K G Ragh



CSIR-National Institute for Interdisciplinary Science and Technology
(NIIST), Thiruvananthapuram.



Academy of Scientific and Innovative Research
AcSIR Headquarters, CSIR-HRDC campus
Sector 19, Kamla Nehru Nagar,
Ghaziabad. U.P. – 201 002. India

November 2021



राष्ट्रीय अंतर्विषयी विज्ञान तथा प्रौद्योगिकी संस्थान
NATIONAL INSTITUTE FOR INTERDISCIPLINARY SCIENCE AND TECHNOLOGY

वैज्ञानिक तथा औद्योगिक अनुसंधान परिषद्
इंडस्ट्रियल इस्टेट पी. ओ. पाप्पनकोड, तिरुवनंतपुरम, भारत - 695 019

Council of Scientific and Industrial Research
Industrial Estate P.O., Pappanamcode, Thiruvananthapuram, India-695 019

CERTIFICATE

This is to certify that the work incorporated in this Ph.D. thesis entitled, "Investigation on adverse biochemical alterations in HepG2 cells during hyperinsulinemia and possible reversal with vanillic acid", submitted by Sreelekshmi Mohan to the Academy of Scientific and Innovative Research (AcSIR) in partial fulfillment of the requirements for the award of the Degree of Doctor of Philosophy in Biological Sciences, embodies original research work carried-out by the student. We, further certify that this work has not been submitted to any other University or Institution in part or full for the award of any degree or diploma. Research materials obtained from other sources and used in this research work have been duly acknowledged in the thesis. Images(s), illustration(s), figure(s), table(s) etc., used in the thesis from other sources(s), have also been duly cited and acknowledged.

Sreelekshmi Mohan

Date: 26/11/2021

Dr. K G Raghu

Date: 26/11/2021

Statements of Academic Integrity

I, Sreelekshmi Mohan, a Ph.D. student of the Academy of Scientific and Innovative Research (AcSIR) with Registration No. 10BB16A39017 hereby undertake that, the thesis entitled "Investigation on adverse biochemical alterations in HepG2 cells during hyperinsulinemia and possible reversal with vanillic acid" has been prepared by me and that the document reports original work carried out by me and is free of any plagiarism in compliance with the UGC Regulations on "Promotion of Academic Integrity and Prevention of Plagiarism in Higher Educational Institutions (2018)" and the CSIR Guidelines for "Ethics in Research and in Governance (2020)".



Signature of the Student

Date: 26/11/2021

Place: Thiruvananthapuram

It is hereby certified that the work done by the student, under my supervision, is plagiarism-free in accordance with the UGC Regulations on "Promotion of Academic Integrity and Prevention of Plagiarism in Higher Educational Institutions (2018)" and the CSIR Guidelines for "Ethics in Research and in Governance (2020)".



Signature of the Supervisor

Dr. K G Raghu

Thiruvananthapuram

Acknowledgements

I dedicate this page to express my sincere gratitude and appreciation to those who made possible support and guidance to make this PhD thesis possible.

First and foremost I would like to extend my sincere gratitude to my supervisor, Dr. K. G. Raghu, Principal Scientist, NIIST-CSIR for introducing me to the enthusiastic world of science and for his creative suggestions, encouragement, and his dedicated help throughout my doctoral research. I am deeply grateful to him for providing me necessary lab facilities and excellent supervision at each stage of my study and helping me to complete this work. His understanding, encouragement and personal guidance have provided a good basis for this thesis. His enthusiasm, integral view on research, and mission for providing a high quality work has made a deep impression on me. I am proud to become one of the research students of Dr. K.G. Raghu.

I offer my profound gratitude to Dr. A. Ajayaghosh, Director, CSIR-NIIST, Thiruvananthapuram, for allowing me to be a part of this institution and providing the necessary facilities to me for carrying out the work.

I would like to express my sincere gratitude to Mr. M.M. Sreekumar, Dr. B.S. Dileep Kumar, former Heads of Division and Mr. V.V. Venugopal, HOD, Agro-Processing and Technology Division for their support.

I take this opportunity to thank the Doctoral Advisory Committee: Dr. S. Priya, Dr. P. Jayamurthy and Dr. Kaustabh Kumar Maiti, for their valuable comments and encouragement, which has helped me to orderly complete my research. I am also grateful to the AcSIR coordinators Dr. Luxmi Varma, Dr. C. H. Suresh and Dr. V Karunakaran for guiding me throughout the working tenure and helping me in fulfilling AcSIR requirements for the completion of my work. I am obliged to Dr. M Arumugam, for giving excellent support for the fulfilment of the AcSIR coursework and other requirements in the faculty of biological sciences.

Also I express my thanks to scientists of Agro-Processing and Technology Division, Dr. Jayamurthy P, Dr. P. Nisha, Dr. B. S. Dileep Kumar, Dr. M.V. Reshma, Dr. Anjineyulu Kothakota, Dr. R. Venkatesh, Mr. T. Venkatesh and technical staff Dr. Beena Joy and Sri. D.R. Soban Kumar of Agro-Processing and Technology Division for their valuable suggestions during the divisional meetings and I am thankful to one and all for their kind suggestions. All

the former and present members of Agro-Processing and Technology Division have been more helpful and co-operative and I am thankful to all for their support. I also wish to thank Mrs. Divya Mohan and Ms. Ishwarya who mentally support and help me in my work during my pregnancy

My sincere thanks go to all my former labmates Dr. Reshma P.L, Dr. Vandana S, Dr. Anusree S.S, Dr. Sithara Thomas, Dr. Dhanya R, Dr. Syama H.P and Mrs. Saranya for giving me valuable advices.

I also would like to thank Dr. Jubi Jacob, Dr. Jamsheena, Dr. Silpa G and Mrs. Geethu Gopinath and Mr. Sanu Thankachan for their support, care, help and encouragement. They also taught and familiarized me to analyze and interpret my data and helped me to clarify the various doubts that I have faced during my studies.

My appreciation extends to my present lab colleagues for having helped me in various ways. Initially, my special thanks to Mrs. Eveline Mariya Anto who helped and encouraged me to overcome the hard period of my PhD. I also thank Dr. Salin Raj P and Dr. Anupama Nair and Dr. Preetha Rani, those who have given me the proper directions to do my work and taught me the basics of cell culture with patience during the initial period of my PhD. I am also grateful to Dr. Sindhu G, DHR young scientist who supported me in my western blot analysis.

I would express my sincere gratitude to Dr. Soumya R.S, Dr. Genu George, Dr. Shyni G.L, Ms. Sruthi C.R, Dr. Swapna Sasi U.S, Ms. Poornima M.R and Ms. Roopasree O.J for supporting and helping me in various phases of my PhD. I also wish to thank to Mr. Billu Abraham, Ms. Surya Lakshmi, Ms. Lakshmi Sundhar, Ms. Lakshmi S, Ms. Anusha, Ms. Lakshmi K, Ms. Tanya M.S, Ms. Anaga Nair, Ms. Gopika, Dr. Varsha K, Mr. Sreejith, Mr. Pratheesh S Nair and all other friends of APTD, CSIR-NIIST for supporting and helping me throughout.

It is my duty to thank all the members of the library, administrative, academic programme committee, IT lab and technical staff of NIIST for their help.

I also extend my heartfelt thanks to my seniors and all friends in other divisions of NIIST for their help and support.

I am also thankful to the University Grants Commission (UGC) for financial assistance in the form of research fellowship.

My special regards to my teachers who taught me at different stages of education and gave me the wings and dreams to fly over the amazing world of science, and enabled me to experience the beauty of a deep sense of knowledge. Their effort and dedication made it possible to see this day.

I owe my deep sense of gratitude and regard to my family and my son for their prayers, affection, encouragement, understanding, mental support and patience which have always been mentally strengthened me and helped me to the successful completion of my dream. Their constant support and sacrifice will remain my inspiration and my strength throughout my life, and without their help I would not have been able to complete this thesis.

Finally, but not the least, I thank the Almighty who has always been with me throughout my research work and filled me with strength, patience, and good thoughts and also showering his blessing on me on each and every moment. GOD decided and helped me to reach this very special and important milestone moment in my academic life.

Sreelekshmi Mohan

Table of contents

Chapter1 Intoduction and Literature Survey	1
1.1 Diabetes mellitus.....	1
1.2 Insulin resistance and hyperinsulinemia.....	4
1.3 Diagnostic criteria for hyperinsulinemia and insulin resistance.....	6
1.3.1 Hyperinsulinemic-euglycemic clamp.....	7
1.3.2 Fasting insulin.....	8
1.3.3 Oral glucose tolerance test.....	8
1.3.4 HOMA-IR.....	9
1.3.5 Insulinogenic index.....	10
1.3.6 Quantitative insulin sensitivity check index (QUICKI).....	10
1.3.7 Glucose effectiveness.....	11
1.3.8 C-reactive protein.....	12
1.3.9 Soluble CD36.....	12
1.3.10 Insulin growth factor binding protein-1.....	12
1.3.11 Adiponectin.....	13
1.3.12 HbA1c.....	13
1.3.13 Protein kinase C.....	14
1.4 Causes and pathophysiology of hyperinsulinemia.....	14
1.5 Metabolic consequences of hyperinsulinemia.....	17
1.5.1 Hyperinsulinemia and diabetes.....	18
1.5.2 Hyperinsulinemia and NAFLD.....	19
1.5.3 Hyperinsulinemia and pregnancy	19
1.5.4 Hyperinsulinemia and obesity.....	19
1.5.5 Hyperinsulinemia associated mitochondrial dysfunctions and ER stress: role of MAM.....	20
1.6 Management and Pharmacotherapies of hyperinsulinemia.....	23
1.7 Natural products with antidiabetic activity.....	24

1.8	Vanillic acid.....	26
1.9	Hypothesis and Objectives.....	28

Chapter 2 Establishment of hyperinsulinemia induced insulin resistance in HepG2 cells and effect of vanillic acid (VA).....48

2.1	Introduction.....	48
2.2	Materials and methods.....	51
2.3	Results.....	59
2.3.1	High insulin induced cell death in HepG2 cells.....	59
2.3.2	Induction of insulin resistance through hyperinsulinemic shock in HepG2 cells.....	60
2.3.3	Cytotoxicity of VA.....	61
2.3.4	Cell viability of VA during hyperinsulinemia created insulin resistance in HepG2 cells.....	62
2.3.5	Effect of VA on ROS generation.....	63
2.3.6	Effect of hyperinsulinemia created insulin resistance on SOD levels.....	64
2.3.7	VA increases the GPx levels.....	66
2.3.8	Hyperinsulinemia reduced the GSH and G6PDH activity.....	66
2.3.9	Hyperinsulinemia induces damage to cellular lipids and proteins.....	67
2.4	Discussion.....	69

Chapter 3 Consequences of hyperinsulinemia in glucose metabolism in HepG2 cells and amelioration with VA.....80

3.1	Introduction.....	80
3.2	Materials and methods.....	83
3.3	Results.....	90
3.3.1	Flow cytometric analysis of glucose uptake.....	90
3.3.2	Effect of hyperinsulinemia created insulin resistance on the insulin signaling pathway.....	91
3.3.3	Effect of hyperinsulinemia created insulin resistance on glycolysis via the regulation of GK.....	92
3.3.4	Docking of VA to GK.....	93
3.3.5	GK activation is linked with the hepatic BAD expression.....	94
3.3.6	Hyperinsulinemia enhances the glycogenesis in the liver.....	95
3.3.7	Effect of hyperinsulinemia on hepatic gluconeogenesis.....	96

3.3.8	Sorbitol assay.....	97
3.3.9	Antiglycation capacity of VA.....	98
3.3.10	Production of AGE during high insulin.....	99
3.4	Discussion.....	101

Chapter 4 Hyperinsulinemia mediated alteration in lipid metabolism and inflammation in HepG2 creates an ambience for NAFLD and amelioration with

VA.....	116	
4.1	Introduction.....	116
4.2	Materials and methods.....	121
4.3	Results.....	128
4.3.1	Hyperinsulinemia enhanced the lipid droplet accumulation in HepG2 cells.....	128
4.3.2	Effect of hyperinsulinemia on fatty acid uptake.....	129
4.3.3	Hyperinsulinemia created insulin resistance up-regulate the hepatic lipogenesis.....	130
4.3.4	Hyperinsulinemia enhanced the triglyceride accumulation and DGAT-2 activity in hepatocytes.....	132
4.3.5	Effect of hyperinsulinemia on DPP4 inhibition.....	133
4.3.6	Effect of hyperinsulinemia in NF- κ B transcription activity.....	134
4.3.7	Hyperinsulinemia potentiate the progression of inflammation.....	135
4.4	Discussion.....	137

Chapter 5 Repercussion of hyperinsulinemia on mitochondria and ER- mitochondria calcium signaling in HepG2

cells.....	151	
5.1	Introduction.....	151
5.2	Materials and methods.....	157
5.3	Results.....	164
5.3.1	Effect of VA on mitochondrial superoxide production.....	164
5.3.2	Mitochondrial content.....	165
5.3.3	Aconitase activity.....	166
5.3.4	Effect of vanillic acid on $\Delta\psi_m$	167
5.3.5	Mitochondrial biogenesis regulated by VA.....	168
5.3.6	Mitochondrial fission and fusion proteins.....	170
5.3.7	ATP levels and oxygen consumption.....	171

5.3.8	Hyperinsulinemia induced intracellular calcium overload.....	172
5.3.9	Effect of VA on mPTP opening.....	173
5.3.10	Hyperinsulinemia and calcium dysregulation.....	174
5.3.11	Hyperinsulinemia causes ER stress.....	176
5.3.12	VA reduced the dysregulations in MAM during hyperinsulinemia.....	177
5.4	Discussion.....	180
Chapter 6 Summary and Conclusion.....		202

List of figures

Figure No.	Caption	Page No.
1.1	Insulin resistance and hyperinsulinemia	5
1.2	Causes of hyperinsulinemia	16
1.3	Vanillic acid: A methoxybenzoic acid	26
2.1	Cell viability of high insulin	59
2.2	Induction of IR through hyperinsulinemic shock in HepG2 cells	61
2.3	Cell viability of VA	62
2.4	Cell viability of VA during hyperinsulinemia	63
2.5	Intracellular reactive oxygen species generation determined using DCFDA	64
2.6	Activity of SOD during hyperinsulinemia	65
2.7	Glutathione peroxidase (GPx) activity	66
2.8	Total glutathione (GSH) levels and G6PDH activity	67
2.9	Estimation of Lipid peroxidation product and protein carbonyl content	68

3.1	Hepatic glucose metabolism	81
-----	----------------------------	----

3.2	Glucose uptake using 2-NBDG	90
3.3	Analysis of insulin signaling pathway	92
3.4	Effect of hyperinsulinemia on glycolysis	93
3.5	Molecular docking	94
3.6	Effect of VA on GK and BAD	95
3.7	Hyperinsulinemia and glycogenesis	96
3.8	Effect of hyperinsulinemia in gluconeogenesis	97
3.9	Effect of VA on polyol pathway	98
3.10	Antiglycation capacity of VA	98
3.11	Hyperinsulinemia and glycation	99-100
4.1	Effect of hyperinsulinemia on hepatic lipid metabolism	120
4.2	Lipid droplet accumulation	128-129
4.3	Effect of hyperinsulinemia in free fatty acid uptake	130
4.4	Hepatic lipogenesis	132
4.5	Effect of hyperinsulinemia on TG accumulation & DGAT2 levels	133

4.6	Determination of DDPIV inhibition	134

4.7	NF- κ B translocation during hyperinsulinemia	135
4.8	Hyperinsulinemia & inflammation	136
5.1	Hyperinsulinemia and mitochondrial superoxide	164
5.2	Effect of hyperinsulinemia in mitochondrial content	165-166
5.3	Effect of hyperinsulinemia in aconitase activity	167
5.4	Mitochondrial transmembrane potential ($\Delta\psi_m$) determined using JC1 staining	168
5.5	Immunoblot analysis of proteins involved in mitochondrial biogenesis	169
5.6	Analysis of proteins involved in mitochondrial dynamics	170
5.7	Mitochondrial bioenergetics	171
5.8	Effect of hyperinsulinemia in calcium dysregulation	172-173
5.9	Hyperinsulinemia & mPTP opening	174
5.10	ER & calcium	175
5.11	Effect of hyperinsulinemia on ER stress	177
5.12	Hyperinsulinemia & MAM	179

6.1	Schematic representation of adverse biochemical alterations in HepG2 cells during hyperinsulinemia and proposed mechanism of action of VA	209
-----	---	-----

Abbreviations

2-DG	- 2-deoxy-D-glucose
2-NBDG	- 2-[N-(7-nitrobenz-2-oxa-1,3-diazol-4-yl) amino]-2-deoxy-D-glucose
ACC	- Acetyl CoA carboxylase
AGEs	- Advanced glycation end products
AKT	- Protein kinase B
AMPK	- Activated protein kinase
ANOVA	- One-way analysis of variance
ATF6	- Activating transcription factor 6
BAT	- Brown adipose tissue
BCA	- Bicinchoninic acid
BSA	- Bovine serum albumin
Ca ²⁺	- Calcium
CD36	- Cluster of differentiation 36
CHOP	- C/EBP homologous protein
ChREBP	- Carbohydrate regulatory element binding protein
CPT1	- Carnitine palmitoyltransferase 1
CRP	- C-reactive protein
CVD	- Cardiovascular disease
Cyp D	- Cyclophilin D
DCF	- 2,7-dichlorofluorescein
DCFH-DA	- 2,7-dichlorodihydrofluorescein diacetate
DDOST	- Dolichyl-diphospho-oligosaccharide-protein glycosyltransferase non-catalytic subunit

DGAT	- Diacylglycerol acyl transferase
DMEM	- Dulbecco's modified eagle's medium
DMSO	- Dimethylsulfoxide
DNL	- <i>De novo</i> lipogenesis
DPP4	- Dipeptidyl peptidase- 4
DTNB	- 5, 5'-dithio-bis-2- (nitrobenzoic acid)
DTT	- Dithiothreitol
ECL	- Chemiluminescence
EDTA	- Ethylene diamine tetra acetic acid
ER	- Endoplasmic reticulum
ERAD	- ER-associated degradation
ETC	- Electron transport chain
FABP	- Fatty acid binding protein
FAS	- Fatty acid synthase
FATPs	- Fatty acid transport proteins
FBS	- Fetal bovine serum
FFAs	- Free fatty acids
G-6-P	- Glucose-6-phosphatase
G6PDH	- Glucose-6-phosphate dehydrogenase
GDM	-Gestational diabetes mellitus
GIP	- Glucose-dependent insulinotropic polypeptide
GK	- Glucokinase
GKRP	- Glucokinase regulatory protein
GLP-1	- Glucagon-like peptide-1
Glut2	- Glucose transporter 2
GPx	- Glutathione peroxidase
GRP75	- Glucose regulatory protein 75
GRP78	- Glucose regulatory protein 78
GS	- Glycogen synthase
GSH	- Reduced glutathione

GSK3 β	- Glycogen synthase kinase-3 β
GTT	- Glucose tolerance test
H ₂ O ₂	- Hydrogenperoxides
HbA1c	- Glycated haemoglobin
HDL	- High density lipoprotein
HEPES	- 4-(2-hydroxyethyl)-1-piperazineethanesulfonic acid
HGP	- Hepatic glucose production
HI	- Hyperinsulinemia
HMG CoA	- 3-hydroxy-3-methylglutaryl-coenzyme A
HOMA-IR	- Homeostatic model assessment insulin resistance
HRP	- Horseradish peroxidase
IDE	- Insulin degrading enzyme
IDF	- International diabetes federation
IGF-1	- Insulin growth factor-1
IGFBP-1	- Insulin growth factor binding protein-1
IGI	- Insulinogenic index
IGTT	- Intravenous glucose tolerance test
IP3R	- Inositol 1,4,5-trisphosphate receptor
IRE1	- Inositol-requiring transmembrane kinase/endoribonuclease 1
IRS2	- Insulin receptor substrate
ITT	- Insulin tolerance test
JNK	- c-jun N-terminal kinase
K ₂ HPO ₄	- Dipotassium phosphate
K ₂ PO ₄	- Potassium phosphate
KH ₂ PO ₄	- Potassium dihydrogen phosphate
KRB	- Krebs-Ringer Bicarbonate
MAM	- Mitochondria associated ER-membrane
MFN2	- Mitofusin-2
mtGPAT	- Mitochondrial glycerol-3-phosphate-acyltransferase
mTORC2	- Mammalian target of rapamycin 2

MTT	- 3-(4,5-dimethyl-thiazol-2-yl)-2,5-diphenyl tetrazolium bromide
Na ₂ HPO ₄	- Disodium hydrogen phosphate
NAC	- N-acetyl cysteine
NAFLD	- Non-alcoholic fatty liver disease
NASH	- Non-alcoholic steatohepatitis
NF-κB	- Nuclear factor kappa B
OGTT	- Oral glucose tolerance test
OS	- Oxidative stress
p-AKT	- Phosphorylated protein kinase B
PAL-1	- Plasminogen activator inhibitor type-1
p-BAD	- Phosphorylated Bcl-2 associated death receptor
PBS	- Phosphate buffered saline
PDI	- Protein disulfide isomerase
PEPCK	- Phosphoenolpyruvate carboxykinase
PERK	- Protein kinase RNA-like ER kinase
PGC-1α	- Peroxisome proliferator-activated receptor-γ coactivator
PI3K	- Phosphatidylinositol -3 kinase
PKC	- Protein kinase C
PP2A	- Protein phosphatase 2A
PPAR	- Peroxisome proliferator-activated receptor
PPARγ	- Peroxisome proliferator-activated receptor γ
PTEN	- Phosphatase and tensin homolog
PVDF	- Polyvinylidene difluoride
QUICKI	- Quantitative insulin sensitivity check index
RAGE	- Receptor for advanced glycation end products
RIPA	- Radioimmunoprecipitation assay
RISC	- Relationship between insulin sensitivity and cardiovascular disease study
ROS	- Reactive oxygen species
SDS	- Sodium dodecyl sulfate
SEM	- Standard error of the mean

SERCA	- Sarcoplasmic/endoplasmic reticulum calcium ATPase
Sig-1R	- Sigma-1 receptors
SIRT1	- Sirtuin 1
SOD1	- Superoxide dismutase 1
SOD2	- Superoxide dismutase 2
SPSS	- Statistical Package for the Social Sciences
SREBP1c	- Sterol regulatory element binding protein 1c
T1DM	-Insulin dependent diabetes mellitus
T2DM	- Insulin independent diabetes mellitus
TBST	- Tris buffered saline-Tween 20
TG	- Triglycerides
UPR	- Unfolded protein response
XBP1	- X-box binding protein 1

Chapter 1

Introduction and Literature Survey

1.1 Diabetes mellitus

Diabetes is a more dangerous situation to global health that never respects any socioeconomic status or national boundaries. It is a long term heterogeneous disorder that happen when the body cannot make enough insulin or cannot utilise the produced insulin effectively (Ayepola et al., 2014). Due to less insulin or cells are unable to respond to insulin properly which results in the decreased absorption of glucose from the blood. So the blood glucose level is increased and this is technically called hyperglycemia. The persistent hyperglycemia for a longer time during diabetes leads to the development of the micro and macro vascular complications which finally leads to damages to the organs like heart, liver, kidney, nerves and blood vessels (Ayepola et al., 2014). Both the micro and macro vascular complications are the main players behind the morbidity and mortality in diabetes (Fowler, 2008). Diabetes nephropathy, neuropathy and retinopathy are the micro vascular complications while stroke, peripheral artery disease and coronary artery disease are the macro vascular complications (Lewis and Xu, 2008). Among the microvascular complications diabetic retinopathy is the most crucial one and it is the major causative agent of most eye diseases in the world (Fowler, 2008). Organs like pancreas, liver and kidney play predominant roles in diabetes. Insulin is the major enzyme that participates in glucose metabolism and diabetes, it maintains a normal blood glucose level during fed state. Pancreas is the main organ that controls the glucose metabolism by producing both insulin and glucagon. In the Islets of Langerhans, β -cells are responsible for the production of insulin where glucagon is secreted by α -cells (Cook et al., 2005).

The main types of diabetes are insulin-dependent diabetes mellitus (T1DM), insulin-independent diabetes mellitus (T2DM), and gestational diabetes mellitus (GDM). T1DM is an autoimmune disease in which the immune cells of the body kill the insulin-producing β -cells in the pancreas which result in the scarcity of insulin (Sobczak and Stewart, 2019). Currently, there is no therapy to prevent this. However, T1DM people can live normally with regular blood sugar monitoring, daily insulin treatment, education and support (IDF, 2019). Typical symptoms of T1DM includes polyphagia, polyuria, polydipsia, bedwetting, constant hunger and sudden weight loss. Both in T1DM and T2DM the end result is the development of hyperglycemia. The major consequence of T2DM is the insulin resistance, it may be due to the defects in insulin receptors (Cerf, 2013). In the initial stages of T2DM, the insulin secretion is impaired and this will develop hyperinsulinemia (HI) but during the disease progression the β -cells become damaged, leading to hypoinsulinemia (Cerf, 2013). The common occurrence of T2DM is in adults but due the counter play of obesity, physical inactivity and poor diet now it is commonly seen in children also. Both the T1DM and T2DM exhibit the same symptoms but in most of the cases the T2DM developed asymptotically and the tracing of its time of appearance is impossible. This is one of the main reasons for one third to one half of the people in the world population affected with T2DM, they are the victims of asymptomatic T2DM. The root causes of T2DM is not completely understood but it has an evident link with obesity and increasing age. As well as family history and ethnicity are the other main causative agents. T2DM can effectively be managed through education, adoption of healthy lifestyle and diet with medication. Evidence suggests that T2DM can be completely prevented and T2DM peoples can lead healthy and happy lives. Another common type of diabetes is GDM or diabetes in pregnancy (Hod et al., 2015). It is a condition in which the blood glucose level increases dramatically during the pregnancy. It may occur at any time during pregnancy more specifically in the first trimester (Immanuel and Simmons, 2017). Oral glucose tolerance test

(OGTT) is the main diagnostic parameter for GDM. Typically, it is a measurement of plasma glucose concentration in fasting and it is assessed one or two hrs after consuming 75 g of glucose (Metzger et al., 2010).

Diabetes estimates for every year show a typical increase in the prevalence of diabetes by age and lifestyle changes associated with rapid urbanization and westernization (Arise et al., 2014; IDF, 2019). World health organization (WHO) reported that diabetes will be the 7th leading cause of death in 2030 if we are not given deliberate attention (Oputa and Chinenye, 2012; Wild et al., 2004). Based on the latest IDF report, an estimated 463.0 million adults aged 20-79 years worldwide have diabetes and among these 79.4 % reside in low-and middle-income countries. According to 2019 estimates, by 2030 about 578.4 million, and by 2045, 700.2 million adults aged 20-79 years, will be livelihood with diabetes. In continuation with this data in 2019 currently 351.7 million people of age 20-64 years have diagnosed or undiagnosed diabetes. This number is expected to reach 417.3 million by 2030 and to 486.1 million by 2045. Coming to the country wise distribution of diabetes, China, India and the United States of America are the countries with the highest number of people with diabetes in 2019 (IDF, 2019).

Despite these statistics, the more dangerous situation faced in coming years is the development of diabetes in both children and in adolescents. In the European countries, most of the children and adolescents were affected with T1DM, but in other populations T2DM is more common than T1DM. Effect of diabetes in premature mortality and low quality life is also a major economic concern on countries and health systems (Largay, 2012; Ogle et al., 2016; Yang et al., 2012). Prevalence of T2DM has increased drastically across the world and it has spread to all regions of the earth. The main player behind this spreading is the sedentary lifestyle and increased consumption of unhealthy foods which develops obesity. According to the IDF 2019 report, females are more susceptible for the occurrence of T2DM compared with

all other groups. Around 60 % of the world diabetic population is suffering from the occurrence of T2DM. Prediabetes or non-diabetic hyperglycemia means there is an impairment in both glucose tolerance and fasting glucose level. It is an indicator of the future onset of T2DM (Heianza et al., 2011).

1.2 Insulin resistance and hyperinsulinemia

Insulin is an essential hormone in glucose metabolism and it affects almost all the organs in the body including adipose tissue, liver, brain, pancreas, kidney and muscle (Thomas et al., 2019). Insulin resistances is the main player in the metabolic disturbances associated with obesity and T2DM. It is a condition in which the cells reduce their response against the insulin concentration (Shanik et al., 2008). The most common symptom in insulin resistant diabetic people is the increased basal insulin levels (Fig: 1.1). Disturbances in insulin release, HI, and reduced insulin sensitivity are the main factors for the genesis of T2DM. Continuous exposure to high levels of insulin results in the genesis of insulin resistance. In order to create insulin resistance, numerous *in vivo* studies were conducted by using the administration of high insulin and it is confirmed that basal HI is the major independent factor for the development of insulin resistance (Matthews et al., 1983). Compared to the continuous and pulsate usage of insulin, continuous administration of insulin causes insulin resistance (Schmitz et al., 1986). Intermittent delivery of insulin is more effective to reduce blood glucose level than continuous release (Paolisso et al., 1988). So in order to maintain this, like other hormone sensitive pathways, insulin signaling pathway is also tightly regulated. The insulin receptor itself acts as a negative regulator of this pathway (De Meyts et al., 1973). Each receptor protein has two insulin binding sites in which one insulin molecule binds to the receptor with high affinity but the other binds with lower affinity (De Meyts et al., 1973). High concentration of insulin or its continuous exposure causes decreased binding affinity of the receptors and

reduced the number of receptors through the insulin occupied receptor degradation (Gavin et al., 1974; Seino and Bell, 1989). In addition to this, the insulin signaling pathway is regulated by a multiplicity of influences (e.g. tumor necrosis factor, free fatty acids etc) (Roth et al., 2004). The pathogenesis of insulin resistance is a highly complex network of metabolism which include both glucose, fats and inflammatory cascade (Singh and Saxena, 2010). Insulin resistance is the major clinical and biochemical determinant not only of diabetes but also of different other diseases like cardio vascular disease (CVD), obesity, hypertension and other metabolic diseases (Grundy et al., 2004). Resistance to insulin has been developed initially before the appearance of initial signs of diseases. So it is quite important to recognize and treat the insulin resistance in patients. Because it is difficult to diagnose HI for a longer period of time and it will increase the risk of development of many metabolic syndromes.

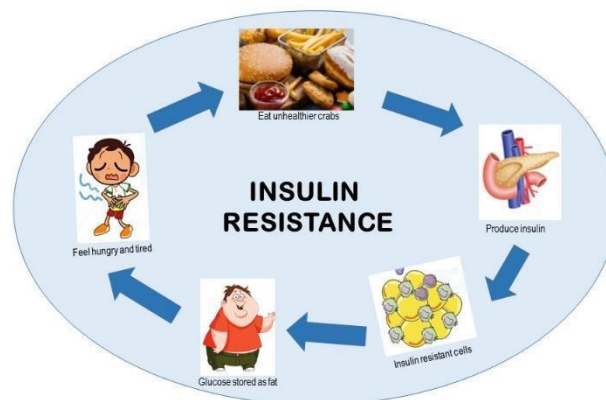


Figure 1.1: Insulin resistance and HI

HI is strongly linked with T2DM. Dysregulated insulin secretion or impairments in insulin clearance results in a huge increase in insulin level without creating hypoglycemia is referred as HI. Meanwhile insulin resistance is defined as, it is a condition in which decreased glucose uptake takes place in the cells. People with obesity and without diabetes or hypertension possess HI than the insulin resistance. Along with this finding many other reports confirmed that HI is one of the major factors which contribute to insulin resistance as well as

it is an independent health risk for the onset of many other diseases. In the relationship between insulin sensitivity and cardiovascular disease study (RISC), people suffering from HI tended to have worse lipid profile, high fat deposition and higher liver insulin resistance compared with other people (Hoi-Hansen et al., 2005). In addition to this, RISC study reported that pre-exposure of HI leads to an up-regulation in insulin induced secretory response than the insulin sensitivity (Kobayashi and Olefsky, 1978). So HI itself is a major contributor of many metabolic diseases and is likely a primary defect rather than a consequence of insulin resistance in the population (Hoi-Hansen et al., 2005). The initial symptom associated with non-diabetic patients is HI, impaired glucose tolerance and dyslipidemia which finally leads to the onset of T2DM (Olefsky and Saltiel, 2000). HI has been considered as an area of interest in the modern world, as it has so many effects on various diseases in the modern era (Singh and Saxena, 2010).

1.3 Diagnostic criteria for hyperinsulinemia and insulin resistance

Diagnosis of HI is a challenging one, because the results of HI and insulin resistance have been overlapped. Despite this, further disturbances are created when analysing the data from available reports (Crofts et al., 2015). Currently numerous methods are available for assessing the insulin sensitivity and insulin resistance directly or indirectly. Assessment of insulin resistance and HI are increased clinically and this calls for the existence of relatively simple methods. The diagnostic parameters measure the level or presence of a marker protein which will reflect the disease pathology and predict the future effects (Singh and Saxena, 2010). The application of these markers is a useful tool to diagnose HI and insulin resistance. They are the sensitive detectors of early organ damage. Basic science investigations have a great role in quantifying insulin resistance and insulin sensitivity in both humans and animal models (Singh and Saxena, 2010). These markers varied from invasive time-consuming

procedures to simple tests. Currently, WHO and international diabetes federation (IDF) recommend other diagnostic parameters for the assessment of β -cell function and insulin sensitivity. They include OGTT, insulin tolerance test (ITT), homeostatic model assessment insulin resistance (HOMA-IR), glycated hemoglobin (HbA1c), insulinogenic index (IGI) etc. Each has its own advantages and limitations (Shanik et al., 2008). Among the various diagnostic tools, the hyperinsulinemic-euglycemic clamp has been the reference standard for direct estimation of insulin resistance. OGTT, intravenous glucose tolerance test (IGTT), and HOMA-IR are indirect measurements (Singh et al., 2013). HOMA-IR and quantitative insulin sensitivity check index (QUICKI) are the best and more considerably validated markers that provide an approximate of glucose homeostasis.

1.3.1 Hyperinsulinemic-euglycemic clamp

The use of hyperinsulinemic-euglycemic clamp for HI is a golden standard to measure insulin secretion capacity in presence of glucose and also determine the insulin sensitivity (Singh and Saxena, 2010). It is a reference method for assessing the insulin sensitivity. Besides this, it has some logistic limitations and has some complications in large scale epidemiological studies. It is quite expensive to perform. This test assesses a 24 hrs urinary C-peptide excretion which is a reflection of insulin secretion and is negatively correlated with insulin sensitivity (Shanik et al., 2008). In addition to this, it is used to determine whole-body insulin clearance and liver insulin clearance (Shanik et al., 2008). Glucose clamp is difficult to apply in larger populations because it requires repeated blood sampling and insulin infusion. So there is a need for the development of simple accessible measures. Most of the tests quantify the fasting insulin level and most of them are derivative of the hyperinsulinemic-euglycemic clamp (Shanik et al., 2008).

1.3.2 Fasting insulin

Fasting insulin is an important parameter for diurnal insulin exposure and sensitivity. It is the most practical approach for the measurement of HI and insulin resistance (Thomas et al., 2000). The lack of standardization procedure of this insulin assay is the main constraint for the overlap between insulin resistance and normal. Using a reliable insulin assay, it is possible to detect the insulin resistance early, before the appearance of the clinical symptoms (Singh and Saxena, 2010). If the glucose levels change rapidly in the postprandial state, the fasting insulin test is done overnight fast. Insulin blood test is used to measure the amount of insulin in the body. It is commonly used to measure abnormal insulin levels and insulin resistance. Normal range of insulin in our body is an average of 2.6-24.9 mcIU/ML. In a healthy person, the level of insulin is equal to the level of blood glucose. The data obtained from fasting insulin test is interpreted that in fasting if the glucose level is below 40 mg/dl and the insulin, as well as C-peptide levels, are high which indicates the presence of insulinoma. The limitation of this test is, in the glucose intolerant peoples it does not cover the low insulin secretion in hyperglycemic conditions. Due to the lack of standardization it gives more false positive results.

1.3.3 Oral glucose tolerance test

According to literature survey the use of one-hour OGTT is considered as a very reliable method for assessing the fasting insulin and glucose levels. It is a commonly used easy test to detect the glucose intolerance and T2DM (Singh and Saxena, 2010). In this test the standard glucose load (75 g) is administered orally to discover how quickly it dissociates from the bloodstream. It indicates the capability of the body to make use of the glucose after a good meal. OGTT gives a perfect idea about glucose tolerance but not to insulin resistance (Dalla Man et al., 2005).

1.3.4 Homeostatic model assessment insulin resistance

HOMA-IR is a method used to quantify the β -cell function and insulin resistance. It is a mathematical model of the relationship of insulin and glucose dynamics. HOMA-IR provides the estimate of insulin resistance and β -cell function through an equation using the continuous measurement of fasting insulin and glucose (Singh and Saxena, 2010). HOMA-IR assesses the insulin sensitivity only based on the fasting insulin and glucose concentrations (Legro et al., 1998). The effect of pancreatic β -cells on the glucose levels and glucose concentrations are depending on insulin secretion. So deficiency in β -cell function will definitely affect the insulin secretion (Wallace et al., 2004). Likewise, development of insulin resistance is reflected by the decrease in the suppression of hepatic glucose production (HGP) by insulin. HOMA-IR is proved that it is a robust clinical and epidemiological tool for the assessment of insulin resistance. The usage of HOMA-IR in assessment of HI and insulin resistance have been validated in children and adolescents (Atabek and Pirgon, 2007) and consider the HOMA-IR value of 2.5 is an indicator of insulin resistance in adults but in children, the value is not been established due to the shortage of detailed studies (Singh et al., 2013).

HOMA describes the glucose-insulin homeostasis by using a simple equation derived from the use of glucose insulin product divided by a constant.

$$\text{HOMA-IR} = (\text{glucose} \times \text{insulin})/22.5$$

Glucose concentration represented in mmol/l and insulin concentration is represented in $\mu\text{U/l}$. While, 22.5 is a normalizing factor; i.e, the product of normal fasting plasma glucose (4.5 mmol/l), and the normal fasting plasma insulin (5 $\mu\text{U/ml}$).

In addition to this, the β -cell function is also calculated by using another equation

i.e; $\text{HOMA } \beta \text{ cell} = 20 \times \text{fasting plasma insulin } (\mu\text{U/ ml})/\text{FPG (mmol)}^{-3}$

1.3.5 Insulinogenic index

The IGI is a commonly used index for β -cell function (Goedecke et al., 2009). It is the ratio of change in insulin level to change in glucose level over the first 30 min after the food intake (Aono et al., 2018). IGI is an index of insulin secretion, derived from OGTT and it is widely used in clinical studies to detect early-phase insulin secretion (Hanefeld et al., 2003; Nishi et al., 2005). IGI has several advantages like less complex protocols, less cost and use of a physiological route of glucose administration (Pacini and Mari, 2003). The limitation of this index is that it is not extensively validated (Goedecke et al., 2009).

Many other simpler methods are used for the assessment of insulin secretion and all these are based on basal glucose and insulin concentration (Aono et al., 2018). HOMA-IR provides the information about the insulin secretion in fasting levels and does not give the data about the secretory ability of β -cell in response to glucose. Apart from plasma glucose, the IGI is a powerful predictor of T2DM

$$\text{IGI} = \delta \text{ insulin (0-30 min)} / \delta \text{ glucose (0-30 min)}$$

1.3.6 Quantitative insulin sensitivity check index

Compared with clamp-insulin resistance, the QUICKI is the first-rate index of the insulin resistance. It is derived from fasting plasma glucose and insulin levels (Mather et al., 2001). It is a mathematical transformation depending on fasting blood glucose and plasma insulin concentrations. These parameters provide precise information about insulin sensitivity with good predictive power (Chen et al., 2003; Chen et al., 2005). It is a variation of HOMA equations, here logarithms and reciprocal of the glucose-insulin product are considered. It has been shown that QUICKI have a linear correlation with glucose clamp in obese and diabetic peoples (Chen et al., 2003). QUICKI cannot be considered as a new model, because it is a simple log of HOMA-IR. In addition to this it has the same limitations as that of HOMA.

Compared with healthy people the QUICKI value has been observed to be lower in people having metabolic conditions like diabetes, glucose intolerance, hyperlipidemia associated with insulin resistance. If the patients having the QUICKI value is below 0.357 is considered as higher risk or frequently present with metabolic syndrome (Hrebíček et al., 2002).

$$\text{QUICKI} = 1/[\log (\text{Insulin } \mu\text{U/ml}) + \log (\text{Glucose mg/dl})]$$

1.3.7 Glucose effectiveness

Most of the methods checked the insulin-dependent glucose usage, but glucose itself has an ability to enhance its disposal; that property of glucose is technically called glucose effectiveness (Shanik et al., 2008). It accounts for about half of the glucose disposal so it is an important diagnostic parameter of HI. It can be assessed through glucose tolerance test (GTT) or by pancreatic clamps but both are very difficult to perform. Meanwhile, differentiation of whole body insulin clearance from hepatic insulin clearance is not possible in GTT (Shanik et al., 2008).

Furthermore, investigators search for more practical indices that assess insulin sensitivity easily as compared with hyperinsulinemic-euglycemic clamps. Some of such indices are stumvoll index, matsuda index, gutt index, avignon index etc. Currently many newer proteins are recognized as a marker for the assessment of insulin resistance. Some of them are C-reactive protein (CRP), soluble CD36, insulin growth factor binding protein-1 (IGFBP-1), adiponectin, glycosylated hemoglobin (HbA1c) and protein kinase C (PKC).

1.3.8 C-reactive protein

CRP is one of the major proteins seen in association with systemic inflammation, and it is the main predictor of future development of cardiovascular events (Singh and Saxena, 2010). It is a highly sensitive protein and during the prevalence of metabolic syndrome associated with insulin resistance, the CRP level has been found to be up-regulated with increased blood

pressure, decreased high density lipoprotein (HDL), increased fasting plasma glucose concentrations, and increased triglyceride (TG) levels (Pasceri et al., 2000). One of the recent studies reported that CRP level is associated with several measures of insulin resistance like fasting insulin, HOMA, QUICKI, the insulin:glucose ratio and the avignon index (Meng et al., 2007). It has many advantages like it's simplicity to perform, high-sensitivity and stability, CRP can be considered as a better clinical proceeding measure for recognizing the persons at risk for insulin resistance (Ridker et al., 2004).

1.3.9 Soluble CD36

CD36 is a pro-atherogenic protein, it reduces oxidized low-density lipoprotein through the formation of foam cells. Hyperglycemia and impaired insulin signaling in insulin resistance lead to increased expression of CD36 (Handberg et al., 2006). It has been reported that there is an increased level of soluble CD36 present in T2DM and insulin resistance patients (Handberg et al., 2006). It might represent a potential marker of insulin resistance and its complications.

1.3.10 Insulin growth factor binding protein-1

Recent reports recommend that IGFBP-1 is a possible marker to find out the insulin resistance (Motaghedi et al., 2007). It has a potent correlation with the analysis of insulin sensitivity, mainly in children younger than 10 years (Motaghedi et al., 2007). In the patients having obesity and insulin resistance, the levels of IGFBP-1 become decreased. In young people IGFBP-1 acts as a convenient and susceptible marker of insulin resistance.

1.3.11 Adiponectin

Adiponectin is a key molecule in the pathogenesis of metabolic syndrome. It exerts pleiotropic insulin-sensitizing effects (Matsuzawa et al., 2004; Ryo et al., 2004). The adiponectin levels

are increased in insulin resistance people (Higashiura et al., 2004) and it has a negative correlation with HOMA in individuals without metabolic syndrome (Hivert et al., 2008).

1.3.12 Glycated haemoglobin

HbA1c developed only when the glucose levels are high. The glucose reacts with the haemoglobin protein in the RBC and forms HbA1c. HbA1c is an important measure used to analyse the long term glycemic control in diabetes. Its role in patients with metabolic syndrome or insulin resistance is doubtful. The amount of HbA1c is directly proportional to the amount of blood sugar during that time. It can be an effective measurement of prediabetes and diabetic also. The normal value of HbA1c in healthy people is below 42 mM/mol or 6.00 %. In the case of prediabetes people, levels of HbA1c are in the range of 42-47 mM/mol (6.0-6.4 %), in diabetic people the value is 6.5 % and above. HbA1c is an important predictor of long term complications of diabetes. It cannot be taken as an important diagnostic tool for diabetes but it has been demonstrated that HbA1c represents both fasting and postprandial glycemic states (Monnier et al., 2003; Rohlfing et al., 2002; Yates and Laing, 2002) and can be considered a predictor of insulin resistance (Osei et al., 2003).

Besides this, studies discovered that patients with normal blood glucose levels actually need high insulin levels to maintain normoglycemia which gives a false sense of safety regarding metabolic health. It is necessary to understand the concepts and merits and demerits underlying each method for the interpretation of the data for measuring the insulin sensitivity.

1.3.13 Protein kinase C

Activation of the PKC during hyperglycemia acts as a potential marker for diabetic retinopathy and microangiopathy (Gerald and King, 2010). One of the studies revealed that PKC activation in mononuclear cells may act as a marker for diabetic microangiopathy (Gerald and King, 2010).

1.4 Causes and pathophysiology of hyperinsulinemia

Genetic, environmental, and socioeconomic factors all contribute to the development and progression of HI. One of the studies reported that it was impossible to differentiate if insulin resistance preceded or accompanied HI (Crofts et al., 2015). Differences in β -cell function and fat distribution in HI are associated with ethnic and racial differences. Dietary and environmental factors interact with hormones in the gastrointestinal tract and develop hyperinsulin secretion in fasting (Meeks et al., 2017) (Fig: 1.2). Some of the examples are air pollution, bisphenol A exposure etc. (Chen et al., 2016). Air pollution has been leading to disturbances in the membrane lipids and increased fasting glucose and insulin production as well as increased the body mass index. Bisphenol A is a chemical that has disrupted the endocrine and increased insulin and C-peptide production (Stahlhut et al., 2018).

HI is associated with race and ethnicity and it is mediated by differences in body composition. Studies reported that dietary differences are also a contributor to the HI in blacks. Blacks had a high fat as well as carbohydrate intake which increased the free fatty acids (FFAs) and resulted in reduced insulin sensitivity and clearance (Arslanian et al., 2002). Higher FFAs are responsible for the decline in insulin secretion and decreased glucose effectiveness (Johnston et al., 2018). Another study showed that compared with whites, black girls had higher fasting insulin, earlier puberty, and rapid fat deposition (Casazza et al., 2008).

HI attacks the body through five mechanisms. They are, increased production of reactive oxygen species (ROS) and advanced glycation end products (AGEs), increased fatty acid/triglyceride (TG) production, hyperglycemia, production of different hormones and cytokines (Crofts et al., 2015). ROS is a collective term used for the representation of highly reactive chemical molecules, one of the causes as well as the main pathophysiological agent of HI. Many of the studies reported that increased HI is due to increased ROS. When the β -cells

were exposed to excess lipids, it led to an increased mitochondria redox state and produced ROS (Saadeh et al., 2012). It can be reduced by supplementation with antioxidants like N-acetyl cysteine (NAC). In non-diabetic healthy black people, the level of FFA is increased and it will simultaneously increase protein carbonyls, which is a marker of oxidative stress (OS). Compared with whites, blacks are more susceptible to OS (Fisher et al., 2012). ROS are produced by many of the metabolic processes but a number of other factors contribute to the excess production of ROS (Bayir, 2005). When they are produced excessively, it affects many of the molecules in the body like lipids, protein and DNA (Crofts et al., 2015). Damage to DNA molecules is a crucial factor in the development of cancer (Crofts et al., 2015). In addition to this, polyunsaturated fatty acids are another important molecule susceptible to ROS attack and they initiate lipid peroxidation which finally resulted in the loss of cell membrane fluidity, permeability and integrity (Bayir, 2005). Among the amino acids cysteine and methionine are more prone to ROS attack which leads to the development of diseases like Alzheimer's disease (Eto et al., 2002).

Overnutrition is another factor responsible for the pathophysiology of the HI and it generates AGEs through glycation and glycol-oxidation. Defective release of AGEs were observed in diabetic nephropathy. Consumption of exogenous AGEs results in increased levels of plasma AGEs. These AGEs cause changes in the micro-vascular system and create inflammation (Chilelli et al., 2013). HI plays an important role in the production of TG and FFAs (Crofts et al., 2015). The main consequence of this is the development of fatty liver disease (Vanni et al., 2010). HI increases the FFA uptake as well as the *de novo* lipogenesis (DNL) in the liver. In addition to this, the increased TG and cholesterol levels were recognized as the key components of metabolic syndromes and fatty liver disease (Vanni et al., 2010).

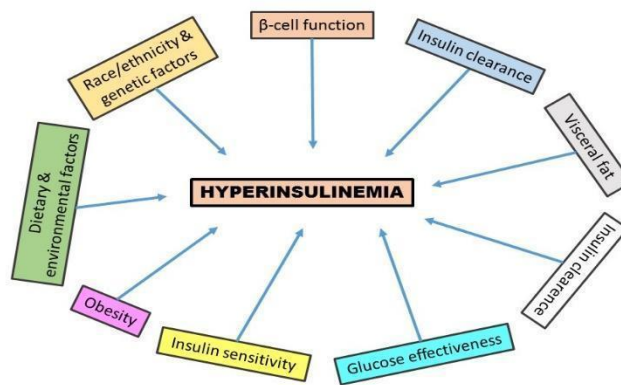


Figure. 1.2. Causes of hyperinsulinemia

Another factor involved in the pathophysiology of HI is hyperglycemia (Weir and Bonner-Weir, 2004). In order to enhance cell growth and proliferation, cancer cells show continuous glucose uptake (Giovannucci et al., 2010) but hyperglycemia augments this process. Hyperglycemia activates insulin growth factor-1 (IGF-1) to enhance vascular smooth muscle proliferation which is the main feature of atherosclerosis and cancer. It will increase blood coagulation also (Stegenga et al., 2006). The next factor is the hormones or cytokine production during HI. Through the increased production of TG and appetite, HI also plays a prominent role in increasing adiposity (Bugianesi et al., 2005). Adipose tissue is an endocrine organ that produces hormones and cytokines necessary for cellular communication. During hypertrophy, adipose tissue activates the stress and inflammatory pathways which increases the release of cytokines like leptin, tumor necrosis factor (TNF)- α and vascular endothelial growth factor (VEGF) and it simultaneously decreases adiponectin levels (Matafome et al., 2013). These impairments result in the development of insulin resistance and a reduced glucose and lipid uptake (Martin et al., 2008; Lustig et al., 2004). In addition to this another factor which contributes more for the pathophysiology of HI is IGF-1. Both IGF-1 and VEGF have a prominent role in the growth and division of many cells (Giovannucci et al., 2010).

Besides this HI also has an ability to elevate levels of plasminogen activator inhibitor type-1 (PAL-1), this increases the risk of thrombosis. Compared with the enhanced coagulation

problem from hyperglycemia, it is clear that more than 80 % of people died with thrombotic death, due to PAL activation (Stegenga et al., 2006). Continuation with this, bariatric surgery is also associated with the progression of HI. Bariatric surgery is prescribed for obese people with comorbid conditions. HI is the main factor that underlies the racial differences in bariatric surgical outcomes. Compared to whites, blacks attain more weight in the years following surgery (Thomas et al., 2019). Bariatric surgery has some metabolic and clinical benefits and it gives rapid relief from HI within one week of surgery (Thomas et al., 2019). Unlike this, after surgery, the insulin sensitivity was improved but glucose effectiveness remained constant (Purnell et al., 2018).

However, more research is needed to find out the effects of various genetic and environmental factors for the genesis of HI and to determine which plays a crucial role in metabolic disease.

1.5 Metabolic consequences of hyperinsulinemia

HI can be epidemiologically linked to metabolic syndrome, gestational and T2DM. So it increases the prevalence of other diseases like cardiovascular, obesity, cancer, and inflammation etc. (Ceriello and Motz, 2004; Weir and Bonner-Weir, 2004). It is an independent risk factor for the development of a vast array of diseases including osteoarthritis, certain cancers, especially breast and colon/rectum, and Alzheimer's disease and other dementias (Feng et al., 2013; Yan and Li, 2013; Mehran Arya et al., 2012). HI directly or indirectly affects almost all biological systems of our body. It affects the circulatory system, gastrointestinal system, endocrine system, nervous system, cancers, and skeletal system.

In the circulatory system, it develops diseases like atherosclerosis, cardiomyopathy, endothelial dysfunction and thrombosis through the generation of ROS, inflammation, and AGEs generation. In addition to this, HI creates gastrointestinal diseases like T2DM, GDM, hypertriglyceridemia, and nonalcoholic fatty liver disease (NAFLD). Inflammation and obesity

are diseases affected by the endocrine system and are caused by HI. Alzheimer's diseases and retinopathy are the diseases caused by HI and it affects the nervous system. Other disease conditions linked with HI include tinnitus, gout, autism and schizophrenia (Monzo et al., 2013; Meyer et al., 2011). However, more detailed investigations are necessary to confirm these findings.

1.5.1 Hyperinsulinemia and diabetes

Obese people showed a decrease in normal glucose tolerance in the first phase of insulin secretion which finally results in T2DM (Weiss et al., 2005). One of the major predictors of T2DM is fasting insulin levels, so HI is associated with T2DM incidents (Ghasemi et al., 2015). HI leads to T2DM through its effects on insulin resistance, fat storage, and direct effects on β -cells (Thomas et al., 2019).

1.5.2 Hyperinsulinemia and NAFLD

One of the studies reported that people without diabetes have a baseline HI and it was associated with NAFLD incidents (Rhee et al., 2011). Hepatic steatosis was linked with fasting insulin (Ardig et al., 2005). In addition to this, the levels of fasting insulin and insulin exposure were assessed by glucose tolerance test and found that it was positively correlated with intrahepatocellular lipids, which is the hallmark of NAFLD (Mehta et al., 2012).

In addition to this, the NAFLD patients have HI as well as a decreased hepatic insulin clearance (Bril et al., 2014). DNL was originally attributed to minor lipid contents in liver and adipose tissue (Thomas et al., 2019). However, some of the studies have been reported that DNL is increased during an increased fasting insulin levels (Hudgins et al., 2011).

1.5.3 Hyperinsulinemia and pregnancy

If the pregnant women possess a high level of blood glucose, then the fetus is exposed to high blood sugar. In response to this, the fetal pancreas is responsible for the production of more

insulin (Thomas et al., 2019). After birth also, the baby continues to face an excess level of insulin or HI that experiences a sudden decrease in blood sugar level and which leads to further dangerous complications.

1.5.4 Hyperinsulinemia and obesity

Strong evidence indicates that HI is an important precursor of obesity. Insulin activates the biochemical pathways that control lipolysis, lipid uptake and lipogenesis. So impairments in insulin levels are associated with obesity. Besides this, dietary and pharmacological interventions reduce insulin levels and also lead to weight loss. Obesity defines the expansion of white adipose tissue (WAT), increased adipocyte differentiation, adipocyte hypertrophy and hyperplasia (Berry et al., 2014; Lim et al., 2015). WAT is a type of adipose tissue that acts as an energy reserve (Berry et al., 2014) but brown adipose tissue (BAT) is responsible for the expenditure of energy through thermogenesis (Beranger et al., 2013). So one of the proposed treatment strategies for obesity is enhancing the activity of BAT (Chondronikola et al., 2016; Labbe et al., 2016). Some of the studies have shown that insulin has an important role in lipid accumulation in white adipocytes. This takes place mainly through decreased lipolysis, enhanced TG synthesis and increased fatty acid uptake (Czech et al., 2013; Kersten, 2001). Recently it has been reported that HI enhances adipocyte inflammation and reduces the DNL in WAT (Pedersen et al., 2015). Overall there were numerous studies reported that adipose tissue insulin signaling has an essential role in the onset and development of obesity.

1.5.5 Hyperinsulinemia associated mitochondrial dysfunctions and endoplasmic stress: role of mitochondria associated ER membrane

HI is one of the major factors for the development of insulin resistance and it is an independent factor for the genesis of metabolic syndrome including T2DM and obesity (Salvado et al., 2015). Recent studies established that the development of insulin resistance is mainly through

the abnormal handling of the lipid metabolites and increased levels of inflammatory cytokines which finally leads to the activation of many kinases and finally destroys the insulin signaling (Walter and Ron, 2011).

Endoplasmic reticulum (ER), a cell organelle plays a crucial role in the development of insulin resistance and progression to T2DM. It plays a predominant role in lipid metabolism and also membrane and secretory protein synthesis. More specifically ER participates in the biosynthesis of insulin receptors and insulin. So any disturbances in ER homeostasis results in the initiation of ER stress and activation of unfolded protein response (UPR) (Salvado et al., 2015) which leads to the development of insulin resistance. ER stress is linked to different processes like lipid accumulation, inflammation, β -cell apoptosis and insulin biosynthesis (Gregor et al., 2009). Many studies showed that ER stress marker expressions were up-regulated in the liver and adipose tissues of obese patients (Puri et al., 2008). UPR activation has played an important role in the genesis of low grade inflammation and all the three pathways are involved in the inflammation mediated activation (Gregor and Hotamisligil, 2011). The activated inositol-requiring transmembrane kinase/endoribonuclease 1 (IRE1) simultaneously activates nuclear factor kappa B (NF- κ B) and c-jun N-terminal kinase (JNK) that phosphorylate the insulin receptor substrate (IRS) 1 and inhibit insulin signaling (Hu et al., 2006). At the same time, NF- κ B activates both protein kinase RNA-like ER kinase (PERK) and activating transcription factor 6 (ATF6) branches of UPR (Deng et al., 2004; Wu et al., 2004). In the case of the liver, ER stress has acted as an important player in the genesis of hepatic insulin resistance. ER stress-activates insulin resistance through the activation of transcription factors and modifies the enzymes that participated in gluconeogenesis and lipogenesis. As a result, the abnormal activation of these pathways took place. ER stress also activates the production of stress proteins and disturbing insulin signaling. In continuation with this, ER stress enhances the lipid accumulation inside the hepatocytes (Flamment et al., 2012).

The overexpression of some ER chaperones or consumption of chaperone proteins results in the resolving of ER stress, inflammation and insulin resistance (Boden, 2009). Targeting the impairments of ER homeostasis might be a good therapeutic approach for the treatment of insulin resistance and T2DM which is the hot area for the development of new pharmacological targets for the treatment of these diseases (Salvado et al., 2015). In addition to this, some of the antidiabetic drugs have the ability to modulate ER stress. However, some of the major proteins involved in UPR might be beneficial in T2DM treatment. (Salvado et al., 2015).

Cellular metabolism is largely dependent on mitochondria. Mitochondria play an important role in energy homeostasis of the cell (Kim et al., 2008). Alterations in energy homeostasis leads to mitochondrial dysfunction (Frisard and Ravussin, 2006). Importantly it has been reported that insulin resistance is associated with mitochondrial dysfunctions in tissues like liver, pancreas, muscles, fat and heart (Ashrafian et al., 2007; Nisoli et al., 2007). Insulin resistance is the characteristic of many metabolic diseases like T2DM, obesity, cardiovascular diseases etc (Cooper et al., 2007). This has been caused by a number of factors like, HI, inflammation, increased caloric intake and glucocorticoid levels (Gregor and Hotamisligil, 2011). Insulin resistance influences the alterations in mitochondrial function including the accumulation of lipids (Koves et al., 2008), dysregulated mitochondrial dynamics and morphology (Jheng et al., 2012), decreased mitochondrial number, low level of mitochondrial oxidative enzymes, increased mitochondrial oxidants (Fazakerley et al., 2018; Paglialunga et al., 2015) and low level of energy synthesis (Ritov et al., 2005). Many of the studies showed that mitochondria have a major role in the pathogenesis of the insulin resistance. Same way mitochondrial alterations also result in the genesis of insulin resistance. Increased mitochondrial oxidants are the consistent marker of insulin resistance in both *in vitro* (Fazakerley et al., 2018; Hoehn et al., 2009) and *in vivo* (Fazakerley et al., 2018; Paglialunga et al., 2015). So the usage of pharmacological interventions to reduce the oxy-radicals is more

effective for resolving insulin resistance (Hoehn et al., 2009; Paglialunga et al., 2015). Most of the studies imply that there is a direct link between mitochondrial oxidants and insulin resistance (Lee et al., 2010; Lee et al., 2017). OS is the main player of insulin resistance and it is specific to the mitochondria which initiate mitochondria oxidants and induce insulin resistance. One of the reports showed that the increased expression of mitochondrial catalase in mice improved insulin sensitivity through the increased fatty acid oxidation (Lee et al., 2010). Elevated FFAs lead to intracellular lipid accumulation which finally leads to insulin resistance in muscle and liver (Petersen and Shulman, 2006). Insulin resistant metabolic tissues possess abnormal mitochondria with abnormal functions in oxidative phosphorylation and decreased mitochondrial gene expression which finally leads to the onset of both T2DM and NAFLD (Kim et al., 2008). Enhanced intracellular fat accumulation leads to a reduction in mitochondrial oxidative phosphorylation (Pessayre and Fromenty, 2005). One study reported that abnormal mitochondrial functions were observed in T2DM patients. The onset of T2DM could be a primary disorder of mitochondria because the mitochondrial function has been affected by ambient blood glucose concentration (Taylor, 2012). A study found that during normal blood glucose levels, no apparent mitochondrial dysfunction has been observed (Taylor, 2012).

1.6 Management and Pharmacotherapies of hyperinsulinemia

The management of hyperinsulinemic people can be extremely complicated, particularly in prolonged and persistent HI. They will require a comprehensive diet plan. It focuses on lifestyle changes including diet, exercise and weight loss. Treatment of HI includes medications. A healthful balanced diet has a significant impact on treating HI and insulin resistance. Diet that contains vegetables, fiber, fruits, and whole grains helps to control blood glucose levels. In addition to dietary changes exercise may improve the body tolerance against insulin and help to maintain a healthy weight. Aerobic exercise is more beneficial against HI.

It includes walking, jogging, light hiking etc. In one study using hyperinsulinemic-euglycemic clamp and arginine stimulation test, it is reported that male athletes have lower insulin secretion, lower fasting glucose, and increased insulin sensitivity and insulin clearance (Thomas et al., 2019). Exercise training gradually increases insulin sensitivity and glucose effectiveness through the decrease of insulin (Karstoft et al., 2017).

If the diet and exercise could not give a better relief then the medication is recommended (Erion and Corkey, 2017). HI and obesity are highly interlinked, so treating obesity with dietary changes, lifestyle modifications, pharmacotherapy, or surgery effectively decreases HI (Kolb et al., 2018). Furthermore, in most of the cases, medications similar to diabetes or a combination of drugs are used to treat HI. One of the most common antidiabetic drugs which can reduce both glucose and insulin level is metformin (Hostalek et al., 2015). It is the most common drug approved by the FDA for the treatment of both HI and metabolic syndrome or prediabetes (Hostalek et al., 2015). Liraglutide is another drug which decreases fasting insulin and increases weight loss (Pi-Sunyer et al., 2015). Several other medications can affect β -cell function and insulin sensitivity. Fenofibrate, a peroxisome proliferator-activated receptor (PPAR)- α agonist, increases fat oxidation and in mice, it decreases insulin secretion and improves insulin clearance (Ramakrishnan et al., 2016). Another drug, bezafibrate, a partial PPAR agonist, lowers both insulin and lipids (Thomas et al., 2019). Besides this, the combination therapy is the more effective medication that directly targets HI (Alemzadeh et al., 2004; Page and Johnson, 2018; Zdravkovic et al., 2005).

1.7 Natural products with antidiabetic activity

Current methodologies to reduce the effects of insulin resistance and T2DM are based on synthetic drugs. Almost all the drugs available in the market have some side effects (Coman et al., 2012). In order to reduce these issues, there is a continuous need to find new and better agents which are an alternative for the current treatment and management of these diseases

(Coman et al., 2012). Natural products such as bioactive compounds, plant extracts and microbial metabolites may be an attractive alternative against these synthetic drugs because they have antihyperglycemic effects (Rout et al., 2009). So therapies based on phytochemicals could develop a new pharmacological approach to treat these types of diseases. Furthermore, they can reduce the side effects and also have low cost, and they can be consumed with every day diet (Coman et al., 2012). Many plants have been reported to have antidiabetic properties. Some of them show very promising effects, which indicate that the dietary intake of these phytochemicals could be a promising strategy for diabetes prevention. *Galega officinalis* is a well-established antidiabetic plant, having anti hyperglycemic and insulin sensitizing potential (Bailey, 2017). The compounds isolated from these plants include a guanidine compound galegine and biguanide compound metformin. Guanidine compounds were toxic to the human body, despite this finding the plant *Galega officinalis* still have importance today because one of the most common and widely accepted drug metformin, was derived from this plant. Another plant species traditionally used for T2DM treatment is *Salacia reticulata* in countries like India and Sri Lanka. The α -glucosidase inhibitors like salacinol and kotalanol have been isolated from this plant. The inhibitory effects of these plants are similar to well-known α -glucosidase inhibitors as well as antidiabetic drugs acarbose and voglibose. *Morus alba* is the natural antidiabetic plant and it is enriched with α -glucosidase inhibitors. One of the studies reported that more than 15 bioactive molecules with α -glucosidase inhibitory potential were seen in leaf extract of this plant. Furthermore, so many other plants have been reported for their antidiabetic potential, it includes *Curcuma longa*, *Momordica charantia*, *Aegle marmelos*, *Urtica dioica* (Bnouham et al., 2003), *Tinospora cordifolia*, *Salvia officinalis* (Eidi et al., 2005), *Eucalyptus globules* (Ahlem et al., 2009) etc and numerous compounds were isolated from these plants and they showed better antidiabetic activity. Most of these compounds are coming under the categories of flavonoids, alkaloids, phenols, etc. (Soumyanath, 2005). In many studies very

little is understood about the mechanism of action of each compound. Recently, more and more research is being carried out to elucidate the mechanism of action of these plants and the compounds (Coman et al., 2012). One of the crucial factors for the genesis of T2DM is oxidative stress (OS). OS initiates abnormal production of ROS which results in the impairments in cellular metabolism. So any compound which has an antioxidant potential may act as a synergistic molecule by exerting its hypoglycemic as well as antioxidants potential. Polyphenolic compounds, more specifically flavonoids, have more ability to act as anti-diabetic molecules (Coman et al., 2012). They are well known for their anti-inflammatory, antioxidants and anti-carcinogenic potentials.

1.8 Vanillic acid

In our study we selected vanillic acid (VA) to check its potential against HI. VA is a widely used flavouring agent. It is a phenolic compound and a 4-hydroxy-3- methoxy benzoic acid derivative and an oxidized form of vanillin. Vanillin is a 4-hydroxy-3- methoxy benzaldehyde and a non-toxic food additive (Mirza and Panchal, 2020) (Fig: 1.3). In the liver the vanillin is converted into vanillic acid (Pacheco-Palencia et al., 2008). It is an intermediary compound formed during the conversion of ferulic acid to vanillin (Mirza and Panchal, 2020). It is present at high concentrations in vanilla beans, *Angelica sinensis* (Mirza and Panchal, 2020) and in vinegar. It has been used as a Chinese medicine also (Prabhakar and Doble, 2011).

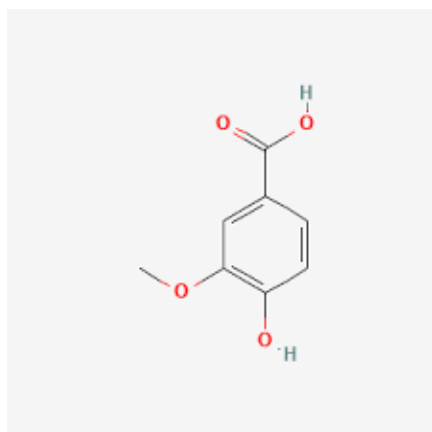


Figure. 1.3 Vanillic acid : A methoxybenzoic acid (C₈H₈O₄; Molecular weight- 168.15 g/mol).

VA has been found to have diverse pharmacological actions such as antioxidant (Chou et al., 2010; Tai et al., 2012), antidiabetic (Chang et al., 2015), anti-inflammatory (Calizto-Compos et al., 2015) and cardioprotective effects. In addition, the presence of VA was detected in cerebrospinal fluid (Alzweiri et al., 2013), it can inhibit the snake venom nucleotides (Alzweiri et al., 2013) and can inhibit carbonic anhydrase enzyme (Dhananjaya et al., 2009). It has been reported that VA shows a protective effect on liver toxicity (Itoh et al., 2010). Furthermore, it acts as a respiratory stimulant (Coman et al., 2012). Numerous clinical studies have been conducted based on the excretion of VA in urine and one study reported that VA is a metabolic byproduct of 4-hydroxy-3-methoxyphenylglycol and 4-hydroxy-3-methoxymandelic acid (Coman et al., 2012). In most of the studies, the VA was administered orally for a long duration to treat chronic diseases. Initially, acute toxicity studies were conducted as a preliminary study, and the details obtained from this study were used to conduct the subacute toxicity studies. It gives a better understanding of the effect of the continuous utilization of the medicines over a short period and provides a basis for conducting chronic toxicological studies (Hayes, 2007). From the acute toxicity studies of VA, in rats, VA shows LD₅₀ at 5020 mg/kg but in the case of mice, the value was at 2691 mg/kg (Coman et al., 2012). In the subacute toxicity studies, VA does not show any mortality or clinical toxic signs during the period of study and showed

a normal increase in body weight and internal organ weight (Coman et al., 2012). These studies ensure that VA is a reasonably safe molecule in experimental rats at selected dose (Coman et al., 2012). Hence VA could be developed as a lead molecule for diabetic complications. Although VA possesses antioxidant and hepatoprotective effects, the complete mechanism of action of VA in liver metabolism during HI has not been well established. In this study, we studied the adverse biochemical alterations during HI in hepatocytes and possible recovery with VA. We found the mechanism of action of VA in HepG2 cell's glucose and lipid metabolism during HI and the role of ER, mitochondria and mitochondria associated ER membrane (MAM) on it.

1.9 Hypothesis and Objectives

Alternative approaches with novel signaling pathways are needed to prevent and treat metabolic diseases such as T2DM and associated health issues. HI in association with insulin resistance is considered as an important independent health risk and it directly or indirectly contribute to the genesis of many diseases such as all inflammatory diseases, gestational and T2DM, all vascular diseases, NAFLD, certain cancers and obesity (Ceriello and Motz, 2004; Weir and Bonner-Weir, 2004). The onset of HI can have numerous harmful effects on the many tissues in the body. It also creates a group of disturbances such as impaired glucose tolerance, high levels of TG and cholesterol, increased production of IGF-1 (Giovannucci et al., 2010), high levels of AGEs and increased levels of ROS (Ceriello and Motz, 2004). Same time, there were only a few studies presented for standardizing the diagnostic process of HI (Crofts et al., 2015). Most of the research is done in the field of insulin resistance. Recent researches in the field of HI revealed that, the HI is not only involved in the aetiology of the all the symptoms of metabolic syndrome but also a risk factor for the onset of many other conditions such as Alzheimer's disease, dementia, retinopathy, nephropathy, osteoporosis, and some cancers (breast, liver, ovarian) (Feng et al., 2013; Pollak, 2008; Yan and Li, 2013). Due to the

increasing prevalence of these diseases in the world and the increasing global concerns about the epidemic of metabolic syndrome, more research on this field is very urgent. Earliest detection of a disease state is most important for the prevention and control of that disease. HI is precisely identified with dynamic glucose and insulin testing, and also has few (pharmaceutical) management options (Crofts et al., 2015). Non-pharmacological management with the utilization of herbal dietary products has been an option and in addition to this further work is needed in the search for culinary plants for prophylactic and therapeutic use. Considering the importance of natural product derived nutraceuticals, we can exclude the adverse side effects created by synthetic drugs as well as it can easily be included in our diet also. Furthermore, the T2DM and the complications of HI, can be effectively prevented by using a healthy diet and medication. So on the basis of this hypothesis, the present work aims to evaluate the adverse biochemical mechanisms created by HI in hepatocytes and study how it is related to mitochondrial alterations, ER stress and disturbances in MAM also.

The main aims of this present study are

- Standardization of the *in vitro* model of HI employing HepG2 cells.
- Investigation on alterations in redox status of the cell during insulin resistance via HI in HepG2 cells.
- Studies on glucose metabolism during HI in HepG2 cells and possible recovery with vanillic acid.
- Effect of HI on lipid metabolism in HepG2 cells - genesis of inflammation and progression of NAFLD.
- Studies on alterations in mitochondrial biology during HI and amelioration with vanillic acid.
- Calcium homeostasis in the initiation of ER stress and dysregulation of MAM during HI.

References

- Ahlem S, Khaled H, Wafa M, Sofiane B, Mohamed D, JeanClaude M, Abdelfattah EF. Oral administration of Eucalyptus globulus extract reduces the alloxan-induced oxidative stress in rats. *Chem Biol Int.* 2009; 181: 71-76.
- Alemzadeh R, Fledelius C, Bodvarsdottir T, Sturis J. Attenuation of hyperinsulinemia by NN414, a SUR1/Kir6.2 selective K1-adenosine triphosphate channel opener, improves glucose tolerance and lipid profile in obese Zucker rats. *Metab.* 2004; 53: 441-447.
- Alzweiri M, Al-Hiari Y. Evaluation of vanillic acid as inhibitor of carbonic anhydrase isozyme III by using a modified Hummel-Dreyer method: approach for drug discovery. *Biomed Chromatogr.* 2013; 27: 1157-1161.
- Aono D, Oka R, Kometani M, Takeda Y, Karashima S, Yoshimura K, Takeda Y, Yoneda T. Insulin secretion and risk for future diabetes in subjects with a nonpositive insulinogenic index. *J Diabetes Res.* 2018; 22: 1-9.
- Ardig`o D, Numeroso F, Valtueña S, Franzini L, Piatti PM, Monti L, Delsignore R, Reaven GM, Zavaroni I. Hyperinsulinemia predicts hepatic fat content in healthy individuals with normal transaminase concentrations. *Metab.* 2005; 54: 1566–1570.
- Arise RO, Ganiyu AI, Oguntibeju OO. Lipid profile, antidiabetic and antioxidant activity of Acacia ataxacantha bark extract in streptozotocin-induced diabetic rats. *Antioxidant-Antidiabetic Agents and Human Health.* 2014; 5: 3-24.
- Arslanian SA, Saad R, Lewy V, Danadian K, Janosky J. HI in African-American children: decreased insulin clearance and increased insulin secretion and its relationship to insulin sensitivity. *Diabetes.* 2002; 51: 3014-3019.
- Ashrafian H, Frenneaux MP, Opie LH. Metabolic mechanisms in heart failure. *Circulation* 2007; 116: 434-448.

Atabek ME, Pirgon O. Assessment of insulin sensitivity from measurements in fasting state and during an oral glucose tolerance test in obese children. *J Pediatr Endocrinol Metab.* 2007; 20: 187-195.

Ayepola OR, Brooks NL, Oguntibeju OO. Oxidative stress and diabetic complications: the role of antioxidant vitamins and flavonoids. *Antioxidant-antidiabetic agents and human health.* 2014; 5: 923-931.

Bailey CJ. Metformin: historical overview. *Diabetologia.* 2017; 60: 1566-1576.

Bayir H. Reactive oxygen species. *Crit Care Med.* 2005; 33: S498-S501.

Beranger GE, Karbiener M, Barquissau V, Pisani DF, Scheideler M, Langin D, et al. In vitro brown and "brite"/"beige" adipogenesis: human cellular models and molecular aspects. *Biochimica et biophysica acta.* 2013; 1831: 905-914.

Berry R, Jeffery E, Rodeheffer MS. Weighing in on adipocyte precursors. *Cell Metab.* 2014; 19: 8-20.

Bnouham M, Merhfour F-Z, Ziyat A, Mekhfi H, Aziz M, Legssyer A. Antihyperglycemic activity of the aqueous extract of *Urtica dioica*. *Fitoterapia.* 2003; 74: 677-681.

Boden G. Endoplasmic reticulum stress: another link between obesity and insulin resistance/inflammation?. *Diabetes.* 2009; 58: 518-519.

Bril F, Lomonaco R, Orsak B, Ortiz-Lopez C, Webb A, Tio F, Hecht J, Cusi K. Relationship between disease severity, hyperinsulinemia, and impaired insulin clearance in patients with nonalcoholic steatohepatitis. *Hepatology.* 2014; 59: 2178-2187.

Bugianesi E, McCullough AJ, Marchesini G. Insulin resistance: A metabolic pathway to chronic liver disease. *Hepatology.* 2005; 42: 987-1000.

Calizto-Compos C, Carvalho TT, Hohmann MSN, Pinho-Ribeiro FA, Fattori V, MAnchope MF, et al. Vanillic Acid Inhibits Inflammatory Pain by Inhibiting Neutrophil

Recruitment, Oxidative Stress, Cytokine Production, and NF κ B Activation in Mice. *J Nat Prod.* 2015; 78: 1799-1808.

Casazza K, Goran MI, Gower BA. Associations among insulin, estrogen, and fat mass gain over the pubertal transition in African-American and European-American girls. *J Clin Endocrinol Metab.* 2008; 93: 2610-2615.

Cerf ME. Beta cell dysfunction and insulin resistance. *Front Endocrinol.* 2013; 4: 1-12.

Ceriello A and Motz E. Is oxidative stress the pathogenic mechanism underlying insulin resistance, diabetes, and cardiovascular disease? The common soil hypothesis revisited. *Arterioscler Thromb Vasc Biol.* 2004; 24: 816-823.

Chang WC, WU JSB, Chen CW, Kuo PL, Chien HM, Wang YT, Shen SC. Protective Effect of Vanillic Acid against Hyperinsulinemia, Hyperglycemia and Hyperlipidemia via Alleviating Hepatic Insulin Resistance and Inflammation in High-Fat Diet (HFD)-Fed Rats. *Nutrients.* 2015; 7: 9946-9959.

Chen H, Sullivan G, Quon MJ. Assessing the predictive accuracy of QUICKI as a surrogate index for insulin sensitivity using a calibration model. *Diabetes.* 2005; 54: 1914-1925

Chen H, Sullivan G, Yue LQ, Katz A, Quon MJ. QUICKI is a useful index of insulin sensitivity in subjects with hypertension. *Am J Physiol Endocrinol Metab.* 2003; 284: E804-E812.

Chen Z, Salam MT, Toledo-Corral C, Watanabe RM, Xiang AH, Buchanan TA, Habre R, Bastain TM, Lurmann F, Wilson JP, Trigo E, Gilliland FD. Ambient air pollutants have adverse effects on insulin and glucose homeostasis in Mexican Americans. *Diabetes Care.* 2016; 39: 547–554.

Chilelli NC, Burlina S, Lapolla A. AGEs, rather than hyperglycemia, are responsible for microvascular complications in diabetes: A “glycooxidation-centric” point of view. *Nutr Metab Cardiovasc Dis.* 2013; 23: 913-919.

Chondronikola M, Volpi E, Borsheim E, Porter C, Saraf MK, Annamalai P, et al. Brown Adipose Tissue Activation Is Linked to Distinct Systemic Effects on Lipid Metabolism in Humans. *Cell Metab.* 2016; 23: 1200-1206.

Chou TH, Ding HY, Hung WJ, Liang CH. Antioxidative characteristics and inhibition of alpha-melanocyte-stimulating hormone-stimulated melanogenesis of vanillin and vanillic acid from *Origanum vulgare*. *Exp Dermatol.* 2010; 19: 742-750.

Coman C, Rugina OD, Socaciu C. Plants and natural compounds with antidiabetic action. *Not Bot Horti Agrobot Cluj Napoca.* 2012; 40: 314-325.

Cook MN, Girman CJ, Stein PP, Alexander CM, Holman RR. Glycemic control continues to deteriorate after sulfonylureas are added to metformin among patients with type 2 diabetes. *Diabetes care.* 2005; 28: 995-1000.

Cooper SA, Whaley-Connell A, Habibi J, Wei Y, Lastra G, Manrique CM, Stas S, Sowers JR. Renin-angiotensin-aldosterone system and oxidative stress in cardiovascular insulin resistance. *Am J Physiol Heart Circ Physiol.* 2007; 293: H2009–H2023.

Crofts CA, Zinn C, Wheldon M, Schofield G. Hyperinsulinemia: A unifying theory of chronic disease. *Diabetes.* 2015; 64: 34-43.

Czech MP, Tencerova M, Pedersen DJ, Aouadi M. Insulin signalling mechanisms for triacylglycerol storage. *Diabetologia.* 2013; 56: 949-964.

Dalla Man C, Campioni M, Polonsky KS, Basu R, Rizza RA, Toffolo G, Cobelli C. Two-hour seven-sample oral glucose tolerance test and meal protocol: minimal model assessment of beta-cell responsiveness and insulin sensitivity in nondiabetic individuals. *Diabetes.* 2005; 54: 3265-3273

De Meyts P, Roth J, Neville DM Jr, Gavin JR 3rd, Lesniak MA. Insulin interactions with its receptors: experimental evidence for negative cooperativity. *Biochem Biophys Res Commun.* 1973; 55: 154-161.

Deng J, Lu PD, Zhang Y, Scheuner D, Kaufman RJ, Sonenberg N, Harding HP, Ron D. Translational repression mediates activation of nuclear factor kappa B by phosphorylated translation initiation factor 2. *Mol Cell Biol.* 2004; 24: 10161-10168.

Dhananjaya BL, Nataraju A, Raghavendra Gowda CD, Sharath BK, D'Souza CJ. Vanillic acid as a novel specific inhibitor of snake venom 5'-nucleotidase: a pharmacological tool in evaluating the role of the enzyme in snake envenomation. *Biochemistry (Mosc).* 2009; 74: 1315-1319.

Eidi M, Eidi A, Zamanizadeh H. Effect of *Salvia officinalis* L. leaves on serum glucose and insulin in healthy and streptozotocin-induced diabetic rats. *J Ethnopharmacol.* 2005; 100: 310-313.

Erion K and Corkey B. Hyperinsulinemia: a Cause of Obesity?. *Curr Obes Rep.* 2017; 6:178-186.

Eto K, Asada T, Arima K, Makifuchi T, Kimura H. Brain hydrogen sulfide is severely decreased in Alzheimer's disease. *Biochem Biophys Res Commun.* 2002; 293: 1485-1488.

Fazakerley DJ, Chaudhuri R, Yang P, Maghzal GJ, Thomas KC, Krycer JR, et al. Mitochondrial CoQ deficiency is a common driver of mitochondrial oxidants and insulin resistance. *Elife.* 2018; 7: e32111

Fazakerley DJ, Minard AY, Krycer JR, Thomas KC, Stöckli J, Harney DJ, et al. Mitochondrial oxidative stress causes insulin resistance without disrupting oxidative phosphorylation. *Int J Biol Chem.* 2018; 293:7315-7328.

Feng L, Chong MS, Lim WS, Lee TS, Collinson SL, Yap P, et al. Metabolic syndrome and amnesic mild cognitive impairment: Singapore Longitudinal Ageing Study-2 findings. *J Alzheimer's Dis.* 2013; 34: 649-657.

Fisher G, Alvarez JA, Ellis AC, Granger WM, Ovalle F, Man CD, Cobelli C, Gower BA. Race differences in the association of oxidative stress with insulin sensitivity in African- and European- American women. *Obesity (Silver Spring)*. 2012; 20: 972–977.

Flamment M, Hajduch E, Ferré P, Fougère F. New insights into ER stress-induced insulin resistance. *Trends Endocrinol Metab*. 2012; 23: 381-390.

Fowler MJ. Microvascular and macrovascular complications of diabetes. *Clinical diabetes*. 2008; 26: 77-82.

Frisard M and Ravussin E. Energy metabolism and oxidative stress: impact on the metabolic syndrome and the aging process. *Endocrine*. 2006; 29: 27-32.

Gavin JR III, Roth J, Neville DM Jr, De Meyts P, Buell DN. Insulin-dependent regulation of insulin receptor concentrations: a direct demonstration in cell culture. *Proc Natl Acad Sci USA*. 1974; 71: 84–88.

Geraldes P, King GL. Activation of protein kinase C isoforms and its impact on diabetic complications. *Circ Res*. 2010; 106: 1319-1331.

Ghasemi A, Tohidi M, Derakhshan A, Hasheminia M, Azizi F, Hadaegh F. Cut-off points of homeostasis model assessment of insulin resistance, beta-cell function, and fasting serum insulin to identify future type 2 diabetes: Tehran Lipid and Glucose Study. *Acta Diabetol*. 2015; 52: 905-915.

Giovannucci E, Harlan DM, Archer MC, Bergenstal RM, Gapstur SM, Habel LA, et al. Diabetes and cancer: A consensus report. *Diabetes Care*. 2010; 33: 1674-1685.

Goedecke JH, Dave JA, Faulenbach MV, Utzschneider KM, Lambert EV, West S, et al. Insulin response in relation to insulin sensitivity: an appropriate beta-cell response in black South African women. *Diabetes Care*. 2009; 32: 860-865

Gregor MF and Hotamisligil GS. Inflammatory mechanisms in obesity. *Annu Rev Immunol*. 2011; 29: 415-445.

Gregor MF, Yang L, Fabbrini E, Mohammed BS, Eagon JC, Hotamisligil GS, Klein S. Endoplasmic reticulum stress is reduced in tissues of obese subjects after weight loss. *Diabetes*. 2009; 58: 693-700.

Grundy SM, Brewer HB Jr, Cleeman JI, Smith SC Jr, Lenfant C. Definition of metabolic syndrome: Report of the National Heart, Lung, and Blood Institute/American Heart Association conference on scientific issues related to definition. *Circulation*. 2004; 109: 433-438

Handberg A, Levin K, Hojlund K, Beck-Nielsen H. Identification of the oxidized low-density lipoprotein scavenger receptor CD36 in plasma: a novel marker of insulin resistance. *Circulation*. 2006; 114: 1169-1176

Hanefeld M, Koehler C, Fuecker K, et al. Insulin secretion and insulin sensitivity pattern is different in isolated impaired glucose tolerance and impaired fasting glucose: the risk factor in impaired glucose tolerance for atherosclerosis and diabetes study. *Diabetes Care*. 2003; 26: 868-874.

Hayes AW. *Principles and Methods of Toxicology* (5th ed). Boca Raton; CRC Press. 2007; 1223-1245.

Heianza Y, Hara S, Arase Y, Saito K, Fujiwara K, Tsuji H, et al. HbA1c 5.7-6.4% and impaired fasting plasma glucose for diagnosis of prediabetes and risk of progression to diabetes in Japan (TOPICS 3): a longitudinal cohort study. *Lancet*. 2011; 378: 147-155.

Higashiura K, Ura N, Ohata J, Togashi N, Takagi S, Saitoh S, et al. Correlations of adiponectin level with insulin resistance and atherosclerosis in Japanese male populations. *Clin Endocrinol (Oxf)*. 2004; 61: 753-759.

Hivert MF, Sullivan LM, Fox CS, Nathan DM, D'Agostino RB Sr, Wilson PW, Meigs JB. Associations of adiponectin, resistin, and tumor necrosis factor-alpha with insulin resistance. *J Clin Endocrinol Metab*. 2008; 93: 3165-3172

Hod M, Kapur A, Sacks DA, Hadar E, Agarwal M, Di Renzo GC, et al. The International Federation of Gynecology and Obstetrics (FIGO) Initiative on gestational diabetes mellitus: A pragmatic guide for diagnosis, management, and care. *Int J Gynaecol Obstet.* 2015; 131: S173-S211.

Hoehn KL, Salmon AB, Hohnen-Behrens C, Turner N, Hoy AJ, Maghzal GJ, et al. Insulin resistance is a cellular antioxidant defense mechanism. *Proc Natl Acad Sci. U.S.A.* 2009; 106: 17787-17792

Hoi-Hansen T, Pedersen-Bjergaard U, Thorsteinsson B. The Somogyi phenomenon revisited using continuous glucose monitoring in daily life. *Diabetologia.* 2005; 48: 2437-2438.

Hostalek U, Gwilt M, Hildemann S. Therapeutic Use of Metformin in Prediabetes and Diabetes Prevention. *Drugs.* 2015; 75: 1071-1094.

Hřebíček J, Janout V, Malincíková J, Horáková D, Cízek L. Detection of insulin resistance by simple quantitative insulin sensitivity check index QUICKI for epidemiological assessment and prevention. *J Clin Endocrinol Metab.* 2002; 87: 144-147

Hu P, Han Z, Couvillon AD, Kaufman RJ, Exton JH. Autocrine tumor necrosis factor alpha links endoplasmic reticulum stress to the membrane death receptor pathway through IRE1 α -mediated NF- κ B activation and down-regulation of TRAF2 expression. *Mol Cell Biol.* 2006; 26: 3071-3084.

Hudgins LC, Parker TS, Levine DM, Hellerstein MK. A dual sugar challenge test for lipogenic sensitivity to dietary fructose. *J Clin Endocrinol Metab.* 2011; 96: 861-868.

Immanuel J and Simmons D. Screening and treatment for early onset gestational diabetes mellitus: a systematic review and meta-analysis. *Curr Diab Rep.* 2017; 17: 1-11.

International Diabetes Federation. *IDF Diabetes Atlas.* Brussels, Belgium: International Diabetes Federation. 2019; 8: 1-147.

Itoh A, Isoda K, Kondoh M, Kawase M, Watari A, Kobayashi M, Tamesada M, Yagi K. Hepatoprotective effect of syringic acid and vanillic acid on CCl₄-induced liver injury. *Biol Pharm Bull.* 2010; 33: 983-987.

Jheng HF, Tsai PJ, Guo SM, Kuo LH, Chang CS, Su IJ, et al. Mitochondrial fission contributes to mitochondrial dysfunction and insulin resistance in skeletal muscle. *Mol Cell Biol.* 2012; 32: 309-319.

Johnston LW, Harris SB, Retnakaran R, Giacca A, Liu Z, Bazinet RP, Hanley AJ. Association of NEFA composition with insulin sensitivity and beta cell function in the Prospective Metabolism and Islet Cell Evaluation (PROMISE) cohort. *Diabetologia.* 2018; 61: 821-830.

Karstoft K, Clark MA, Jakobsen I, Knudsen SH, van Hall G, Pedersen BK, Solomon TPJ. Glucose effectiveness, but not insulin sensitivity, is improved after short-term interval training in individuals with type 2 diabetes mellitus: a controlled, randomised, crossover trial. *Diabetologia.* 2017; 60: 2432-2442.

Kersten S. Mechanisms of nutritional and hormonal regulation of lipogenesis. *EMBO Rep.* 2001; 2: 282-286.

Kim JA, Wei Y, Sowers JR. Role of mitochondrial dysfunction in insulin resistance. *Circ Res.* 2008; 102: 401-414.

Kobayashi M and Olefsky JM. Effect of experimental hyperinsulinemia on insulin binding and glucose transport in isolated rat adipocytes. *Am J Physiol Gastrointest Liver Physiol.* 1978; 235: E53-E62.

Kolb H, Stumvoll M, Kramer W, Kempf K, Martin S. Insulin translates unfavourable lifestyle into obesity. *BMC Med.* 2018; 16: 232.

Koves TR, Ussher JR, Noland RC, Slentz D, Mosedale M, Ilkayeva O, et al. Mitochondrial overload and incomplete fatty acid oxidation contribute to skeletal muscle insulin resistance. *Cell Metab.* 2008; 7: 45-56.

Labbe SM, Caron A, Chechi K, Laplante M, Lecomte R, Richard D. Metabolic activity of brown, "beige," and white adipose tissues in response to chronic adrenergic stimulation in male mice. *American journal of physiology. Endocrinol Metab.* 2016; 311: E260-E268.

Largay J. Case Study: New-onset diabetes: How to tell the difference between Type 1 and Type 2 Diabetes. *Clinical Diabetes.* 2012; 30: 25-26.

Lee HY, Choi CS, Birkenfeld AL, Alves TC, Jornayvaz FR, Jurczak MJ, et al. Targeted expression of catalase to mitochondria prevents age-associated reductions in mitochondrial function and insulin resistance. *Cell Metab.* 2010; 12: 668-674

Lee HY, Lee JS, Alves T, Ladiges W, Rabinovitch PS, Jurczak MJ, et al. Mitochondrial-targeted catalase protects against high-fat diet-induced muscle insulin resistance by decreasing intramuscular lipid accumulation. *Diabetes.* 2017; 66: 2072–2081

Legro RS, Finegood D, Dunaif A. A fasting glucose to insulin ratio is a useful measure of insulin sensitivity in women with polycystic ovary syndrome. *J Clin Endocrinol Metab.* 1998; 83: 2694-2698

Lewis EJ, Xu X. Abnormal Glomerular Permeability Characteristics in Diabetic Nephropathy: Implications for the therapeutic use of low-molecular weight heparin. *Diabet care.* 2008; 31: S202-S207.

Lim GE, Albrecht T, Piske M, Sarai K, Lee JT, Ramshaw HS, et al. 14-3-3zeta coordinates adipogenesis of visceral fat. *Nat Commun.* 2015; 6: 1-7.

Lustig RH, Sen S, Soberman JE, Velasquez-Mieyer PA. Obesity, leptin resistance, and the effects of insulin reduction. *Int J Obes Relat Metab Disord.* 2004; 28: 1344-1348.

Martin SS, Qasim A, Reilly MP. Leptin resistance: A possible interface of inflammation and metabolism in obesity-related cardiovascular disease. *J Am Coll Cardiol.* 2008; 52: 1201-1210.

Matafome P, Santos-Silva D, Sena CM, Seça R. Common mechanisms of dysfunctional adipose tissue and obesity-related cancer. *Diabetes Metab Res Rev.* 2013; 29: 285-295.

Mather KJ, Hunt AE, Steinberg HO, Paradisi G, Hook G, Katz A, Quon MJ, Baron AD. Repeatability characteristics of simple indices of insulin resistance: implications for research applications. *J Clin Endocrinol Metab.* 2001; 86: 5457-5464

Matsuzawa Y, Funahashi T, Kihara S, Shimomura I. Adiponectin and metabolic syndrome. *Arterioscler Thromb Vasc Biol.* 2004; 24: 29-33.

Matthews DR, Naylor BA, Jones RG, Ward GM, Turner RC: Pulsatile insulin has greater hypoglycemic effect than continuous delivery. *Diabetes.* 1983; 32: 617-621.

Meeks KA, Stronks K, Adeyemo A, Addo J, Bahendeka S, Beune E, et al. Peripheral insulin resistance rather than beta cell dysfunction accounts for geographical differences in impaired fasting blood glucose among sub-Saharan African individuals: findings from the RODAM study. *Diabetologia.* 2017; 60: 854-864.

Mehran Arya E, Templeman Nicole M, Brigidi GS, Lim Gareth E, Chu K-Y, Hu X, et al. Hyperinsulinemia drives diet-induced obesity independently of brain insulin production. *Cell Metab.* 2012; 16: 723-737.

Mehta SR, Godsland IF, Thomas EL, Pavitt DV, Morin SX, Bell JD, Taylor-Robinson SD, Johnston DG. Intrahepatic insulin exposure, intrahepatocellular lipid and regional body fat in nonalcoholic fatty liver disease. *J Clin Endocrinol Metab.* 2012; 97: 2151-2159.

Meng YX, Ford ES, Li C, Quarshie A, Al-Mahmoud AM, Giles W, Gibbons GH, Strayhorn G. Association of C-reactive protein with surrogate measures of insulin resistance among

nondiabetic US from National Health and Nutrition Examination Survey 1999-2002. Clin Chem. 2007; 53: 2152-2159

Metzger BE, Gabbe SG, Persson B, Buchanan TA, Catalano PA, Damm P, Dyer AR. International Association of Diabetes and Pregnancy Study Groups Consensus Panel International association of diabetes and pregnancy study groups recommendations on the diagnosis and classification of hyperglycemia in pregnancy. Diabetes Care. 2010; 33: 676-682.

Meyer U, Feldon J, Dammann O. Schizophrenia and autism: Both shared and disorder-specific pathogenesis via perinatal inflammation? Pediatr Res. 2011; 69: 1-15.

Mirza AC, Panchal SS. Safety assessment of vanillic acid: Subacute oral toxicity studies in wistar rats. Turk J Pharm Sci. 2020; 17: 432-439.

Monnier L, Lapinski H, Colette C. Contributions of fasting and postprandial plasma glucose increments to the overall diurnal hyperglycemia of type 2 diabetic patients: variations with increasing levels of HbA(1c). Diabetes Care. 2003; 26: 881-885

Monzo HJ, Park TI, Dieriks VB, Jansson D, Faull RL, Dragunow M, et al. Insulin and IGF1 modulate turnover of polysialylated neuronal cell adhesion molecule (PSANCAM) in a process involving specific extracellular matrix components. J Neurochem. 2013; 136: 758-770.

Motaghedi R, Gujral S, Sinha S, Sison C, Ten S, Maclaren NK. Insulin-like growth factor binding protein-1 to screen for insulin resistance in children. Diabetes Technol Ther. 2007; 9: 43-51

Nishi Y., Fukushima M., Suzuki H., et al. Insulin secretion and insulin sensitivity in Japanese subjects with impaired fasting glucose and isolated fasting hyperglycemia. Diabetes Res Clin Pract. 2005; 70: 46-52.

Nisoli E, Clementi E, Carruba MO, Moncada S. Defective mitochondrial biogenesis: a hallmark of the high cardiovascular risk in the metabolic syndrome? *Circ Res.* 2007; 100: 795–806.

Ogle GD, Middlehurst AC, Silink M. The IDF Life for a Child Program Index of diabetes care for children and youth. *Pediatr Diabetes.* 2016; 17: 374-384.

Olefsky JM and Saltiel AR. PPAR gamma and the treatment of insulin resistance. *Trends Endocrinol Metab.* 2000; 11: 362-368

Oputa RN and Chinenye S. Diabetes mellitus: A global epidemic with potential solution. *African J Diabetes Med.* 2012; 20: 33-35.

Osei K, Rhinesmith S, Gaillard T, Schuster D. Is glycosylated hemoglobin A1c a surrogate for metabolic syndrome in nondiabetic, first-degree relatives of African-American patients with type 2 diabetes? *J Clin Endocrinol Metab.* 2003; 88: 4596-4600.

Pacheco-Palencia LA, Mertens-Talcott S, Talcott ST. Chemical composition, antioxidant properties, and thermal stability of a phytochemical enriched oil from Acai (*Euterpe oleracea* Mart.). *J Agric Food Chem.* 2008; 56: 4631-4636.

Pacini G and Mari A. Methods for clinical assessment of insulin sensitivity and β -cell function. *Best Pract Res Clin Endocrinol Metab.* 2003; 17: 305-322.

Page MM, Johnson JD. Mild suppression of hyperinsulinemia to treat obesity and insulin resistance. *Trends Endocrinol Metab.* 2018; 29: 389-399.

Paglialunga S, Ludzki A, Root-McCaig J, Holloway GP. In adipose tissue, increased mitochondrial emission of reactive oxygen species is important for short-term high-fat diet-induced insulin resistance in mice. *Diabetologia.* 2015; 58: 1071-1080

Paolisso G, Sgambato S, Torella R, Varricchio M, Scheen A, D'Onofrio F, Lefebvre PJ. Pulsatile insulin delivery is more efficient than continuous infusion in modulating islet cell

function in normal subjects and patients with type 1 diabetes. *J Clin Endocrinol Metab.* 1988; 66: 1220–1226.

Pasceri V, Willerson JT, Yeh ET. Direct proinflammatory effect of C-reactive protein on human endothelial cells. *Circulation.* 2000; 102: 2165-2168

Pedersen DJ, Guilherme A, Danai LV, Heyda L, Matevossian A, Cohen J, et al. A major role of insulin in promoting obesity associated adipose tissue inflammation. *Mol Metab.* 2015; 4: 507-518.

Pessayre D and Fromenty B. NASH: a mitochondrial disease. *J Hepatol.* 2005; 42: 928-940.

Petersen KF, Shulman GI. Etiology of insulin resistance. *Am J Med.* 2006; 119: S10–S16.

Pi-Sunyer X, Astrup A, Fujioka K, Greenway F, Halpern A, Krempf M, Lau DC, Le Roux CW, Violante Ortiz R, Jensen CB, Wilding JP. A randomized, controlled trial of 3.0 mg of liraglutide in weight management. *N Engl J Med.* 2015; 373: 11-22.

Pollak M. Insulin and insulin-like growth factor signalling in neoplasia. *Nat Rev Cancer.* 2008; 8: 915-928.

Prabhakar PK, Doble M. Effect of Natural Products on Commercial Oral Antidiabetic Drugs in Enhancing 2-Deoxyglucose Uptake by 3T3-L1 Adipocytes. *Ther Adv Endocrinol Metab.* 2011; 2: 103-114.

Puri P, Mirshahi F, Cheung O, Natarajan R, Maher JW, Kellum JM, Sanyal AJ. Activation and dysregulation of the unfolded protein response in nonalcoholic fatty liver disease. *Gastroenterology.* 2008; 134: 568-576.

Purnell JQ, Johnson GS, Wahed AS, Dalla Man C, Piccinini F, Cobelli C, et al. Prospective evaluation of insulin and incretin dynamics in obese adults with and without diabetes for 2 years after Roux-en-Y gastric bypass. *Diabetologia.* 2018; 61: 1142-1154.

Ramakrishnan SK, Russo L, Ghanem SS, Patel PR, Oyarce AM, Heinrich G, Najjar SM. Fenofibrate decreases insulin clearance and insulin secretion to maintain insulin sensitivity. *J Biol Chem.* 2016; 291: 23915-23924.

Rhee EJ, Lee WY, Cho YK, Kim BI, Sung KC. HI and the development of nonalcoholic fatty liver disease in nondiabetic adults. *Am J Med.* 2011; 124: 69-76.

Ridker PM, Wilson PW, Grundy SM. Should C-reactive protein be added to metabolic syndrome and to assessment of global cardiovascular risk? *Circulation.* 2004; 109: 2818-2825

Ritov VB, Menshikova EV, He J, Ferrell RE, Goodpaster BH, Kelley DE. Deficiency of sub sarcolemmal mitochondria in obesity and type 2 diabetes. *Diabetes.* 2005; 54: 8-14.

Rohlfing CL, Wiedmeyer HM, Little RR, England JD, Tennill A, Goldstein DE. Defining the relationship between plasma glucose and HbA(1c): analysis of glucose profiles and HbA(1c) in the Diabetes Control and Complications Trial. *Diabetes Care.* 2002; 25: 275-288

Roth J, Qiang X, Marban SL, Redel H, Lowell BC. The obesity pandemic: Where have we been and where are we going? *Obes Res.* 2004; 12: 88S-101S.

Rout SP, Chowdary KA, Kar DM, Das L. Plants as source of novel anti-diabetic Drug: present scenario and future perspectives. *Curr Trends Biotechnol Pharm.* 2009; 3: 37-55.

Ryo M, Nakamura T, Kihara S, Kumada M, Shibazaki S, Takahashi M, et al. Adiponectin as a biomarker of the metabolic syndrome. *Circ J.* 2004; 68: 975-981

Saadeh M, Ferrante TC, Kane A, Shirihai O, Corkey BE, Deeney JT. Reactive oxygen species stimulate insulin secretion in rat pancreatic islets: studies using mono-oleoyl-glycerol. *PLoS One.* 2012; 7: 1-10.

Salvado L, Palomer X, Barroso E, Vázquez-Carrera M. Targeting endoplasmic reticulum stress in insulin resistance. *Trends Endocrinol Metab.* 2015; 26: 438-448.

Schmitz O, Arnfred J, Nielsen OH, Beck Nielsen H, Orskov H. Glucose uptake and pulsatile insulin infusion: euglycaemic clamp and [3-3H] glucose studies in healthy subjects. *Acta Endocrinol (Copenh)*. 1986; 113: 559-563.

Seino S and Bell GI. Alternative splicing of human insulin receptor messenger RNA. *Biochem Biophys Res Commun*. 1989; 159: 312-316.

Shanik MH, Xu Y, Škrha J, Dankner R, Zick Y, Roth J. Insulin resistance and hyperinsulinemia: is hyperinsulinemia the cart or the horse?. *Diabet Care*. 2008; 31: S262-S268.

Singh B and Saxena A. Surrogate markers of insulin resistance: A review. *World J Diabetes*. 2010; 1: 36-47.

Singh Y, Garg MK, Tandon N, Marwaha RK. A study of insulin resistance by HOMA-IR and its cut-off value to identify metabolic syndrome in urban Indian adolescents. *J Clin Res Pediatr Endocrinol*. 2013; 5: 245-251.

Sobczak AI and Stewart AJ. Coagulatory defects in type-1 and type-2 diabetes. *Int J Mol Sci*. 2019; 20: 1-27.

Soumyanath A, editor. *Traditional medicines for modern times: antidiabetic plants*. CRC press; 2005; chapter 2: 1-64.

Stahlhut RW, Myers JP, Taylor JA, Nadal A, Dyer JA, Vom Saal FS. Experimental BPA exposure and glucose-stimulated insulin response in adult men and women. *J Endocr Soc*. 2018; 2: 1173-1187.

Stegenga ME, van der Crabben SN, Levi M, de Vos AF, Tanck MW, Sauerwein HP, et al. Hyperglycemia stimulates coagulation, whereas hyperinsulinemia impairs fibrinolysis in healthy humans. *Diabetes*. 2006; 55: 1807-1812.

Tai A, Sawano T, Ito H. Antioxidative properties of vanillic acid esters in multiple antioxidant assays. *Biosci Biotechnol Biochem*. 2012; 76: 314-318.

Taylor R. Insulin resistance and type 2 diabetes. *Diabetes*. 2012; 61: 778-779.

Thomas DD, Anderson WA, Apovian CM, Hess DT, Yu L, Velazquez A, Carmine B, Istfan NW. Weight recidivism after Roux-en-Y gastric bypass surgery: an 11-year experience in a multiethnic medical center. *Obesity (Silver Spring)*. 2019; 27: 217-225.

Thomas DD, Corkey BE, Istfan NW, Apovian CM. Hyperinsulinemia: an early indicator of metabolic dysfunction. *J Endocr Soc*. 2019; 3: 1727-1747.

Thomas GN, Critchley JA, Tomlinson B, Anderson PJ, Lee ZS, Chan JC. Obesity, independent of insulin resistance, is a major determinant of blood pressure in normoglycemic Hong Kong Chinese. *Metabolism*. 2000; 49: 1523-1528.

Vanni E, Bugianesi E, Kotronen A, De Minicis S, Yki-Järvinen H, Svegliati-Baroni G. From the metabolic syndrome to NAFLD or vice versa? *Dig Liver Dis*. 2010; 42: 320-330.

Wallace TM, Levy JC, Matthews DR. Use and abuse of HOMA modeling. *Diabet Care* 2004; 27: 1487-1495

Walter P and Ron D. The unfolded protein response: from stress pathway to homeostatic regulation. *Science*. 2011; 334: 1081-1086.

Weir GC and Bonner-Weir S. Five stages of evolving beta cell dysfunction during progression to diabetes. *Diabetes*. 2004; 53: S16-S21.

Weiss R, Caprio S, Trombetta M, Taksali SE, Tamborlane WV, Bonadonna R. β -Cell function across the spectrum of glucose tolerance in obese youth. *Diabetes*. 2005; 54: 1735-1743.

Wild SG, Roglie A, Green R, Sicree E, King H. Global prevalence of diabetes. Estimates for the year 2000 and projections for 2030. *Diabet Care*. 2004; 27: 1047-1054.

Wu S, Tan M, Hu Y, Wang JL, Scheuner D, Kaufman RJ. Ultraviolet light activates NF- κ B through translational inhibition of I κ B α synthesis. *J Biol Chem*. 2004; 279: 34898-34902.

Yan W, Li X. Impact of diabetes and its treatments on skeletal diseases. *Front Med.* 2013; 7: 81-90

Yang W, Zhao W, Xiao J, Li R, Zhang P, Kissimova-Skarbek K, et al. Medical care and payment for diabetes in China: enormous threat and great opportunity. *PLoS One.* 2012; 7: e39513-e39513.

Yates AP, Laing I. Age-related increase in haemoglobin A1c and fasting plasma glucose is accompanied by a decrease in beta cell function without change in insulin sensitivity: evidence from a cross-sectional study of hospital personnel. *Diabet Med.* 2002; 19: 254-258

Zdravkovic M, Kruse M, Rost KL, Møss J, Kecskes A, Dyrberg T. The effects of NN414, a SUR1/Kir6.2 selective potassium channel opener, in healthy male subjects. *J Clin Pharmacol.* 2005; 45: 763-772.

Chapter 2

Establishment of hyperinsulinemia induced insulin resistance in HepG2 cells and effect of vanillic acid (VA)

2.1 Introduction

The global prevalence of diabetes is increasing day by day and it is characterized by constant hyperglycemia (Engwa et al., 2018). According to IDF statistics 2019, about 82 million people with the disease are of type 2 diabetes in South East Asian regions including India (IDF, 2019). T2DM is the most common form of diabetes and it is characterized by insulin resistance. Insulin resistance is a condition in which the insulin induced glucose utilization is disturbed in insulin sensitive tissues like muscle, liver and adipocytes. Insulin is an essential hormone responsible for the regulation of glucose metabolism in almost all the tissues of the body (Wilcox, 2005). The major factors contributing to the development of insulin resistance are fasting hyperglycemia and HI, increased HbA1c, hyperlipidemia, impaired glucose tolerance, an increase in HGP etc. (Ye, 2013). The common factor behind the development of insulin resistance associated with T2DM in most patients is an increase in insulin levels from basal levels (Shanik et al., 2008). During the early stages of insulin resistance, under hyperglycemic conditions, the pancreas increases insulin secretion in order to compensate for the decreased insulin response; however, the end result is the development of HI to maintain the stable plasma glucose. This later decreases β -cells function and finally results in β -cell loss and leads to insulin resistance and T2DM (Zhang et al., 2010). So HI is the root cause of insulin resistance and diabetes (Corkey, 2012). In human studies also, it has been reported that the inhibition of HI with certain agents would result in the reduction of insulin resistance without affecting

glucose tolerance (Reed et al., 2011). It has been suggested that insulin resistance and subsequent compensatory HI develops earlier than the β -cell dysfunction. This is because the insulin secretion in insulin resistance, non-diabetic persons is increased in proportion to the severity of the insulin resistance even though glucose tolerance remains normal. Thus, early identification of individuals with insulin resistance may be a way to guide earlier intervention strategies to prevent or delay diabetes onset and related chronic diseases.

There are reports that high insulin could alter redox status (Kim et al., 2008). But there is no detailed study on the liver. One of the major organs responsible for the detoxification process in our body is the liver and it also has a prominent role in maintaining normal glucose homeostasis (Leclercq et al., 2007). Liver is the major organ that participates in the energy metabolism of the body and the target site of insulin. So it is more susceptible to hyperglycemia-induced OS, which may lead to liver tissue injury (Mohamed et al., 2016). OS is a condition in which the oxidant to antioxidant ratio is increased (Palsamy et al., 2010). The central players behind the hepatic injury are the increased levels of oxidants like superoxide anions, hydroxyl radicals etc. produced by Kupffer cells of the liver (Wei et al., 2010). Abnormal production of ROS results in the genesis of numerous life-threatening events like irreversible modifications of proteins, carbohydrates and membrane lipids (Leung and Nieto, 2013). The most important covalent modification of proteins is the protein alkylation and it is caused either by ROS or by reaction with the byproducts of OS. In both cases, the end result is the changes in the structure and function of the proteins (Ahmed et al., 2004). The increased levels of unwanted proteins inside the cells lead to certain deleterious effects like inhibition of both binding and enzymatic activities, increased the chances of aggregation, altered uptake of the cells etc (Ahmed, 2005; Yagmur et al., 2006). As a result, it results in apoptosis in the liver cells and also initiates the inflammation cascade which leads to massive liver tissue destruction (Wei et al., 2010). However, in order to cope up with this, the liver is enriched with several

potent antioxidants like superoxide dismutase (SOD), catalase (CAT), glutathione peroxidase (GPx) and glutathione reductase (GSH) (Parveen et al., 2010). These antioxidants protect the liver cells from oxidative damage and also reduce the free radicals. In diabetic conditions, the liver is resistant to insulin which results in abnormal HGP (McKillop et al., 2002) and an increase in gluconeogenesis (Lindsay et al., 2003). Increased HGP plays a vital role in the development of postprandial hyperglycemia, one of the noticeable symptoms of T2DM (Brownlee, 2000). Here I report the effects of high insulin in HepG2 cells, a representative of the *in vitro* model of liver.

Many synthetic diabetic drugs are available in the market and they can significantly down regulate the diabetic complications and improve insulin sensitivity but most of them are associated with some adverse effects such as liver problems, lactic acidosis and diarrhea (Sanchez-Rangel and Inzucchi, 2017). Considering this, there is a need to design and implement a cost-effective and safer ligand to face this public health problem. So natural product based molecules could be attractive for the development of a complementary therapy for diabetes and insulin resistance (Guzmán and Gurrola-Díaz, 2019). Biological activity of plants is based on their chemical constituents, so plants are believed to be the real chemist and are beneficial to human health (Mamun-or-Rashid et al., 2014). These natural compounds can be used to improve insulin sensitivity, reduce the complications and alleviate the long term pathological effects of the disease. Vanillic acid (VA) is a plant derived phenolic compound, widely used as a flavoring agent and a nutritionally beneficial component in the food manufacturing industry (Karmakar et al., 2000). VA does not show any toxicity concern about its intake as a flavoring agent in the food industry. So this is found to be an ideal agent for research for its therapeutic activity against various metabolic disorders. So I have taken this compound for detailed evaluation of its beneficial activities against HI. Moreover there is not

much report available on the effect of VA on HI induced OS and altered redox status in HepG2 cells.

2.2 Materials and methods

2.2.1 Chemicals and reagents

Dulbecco's modified eagle's medium (DMEM), fetal bovine serum (FBS), pencillin-streptomycin antibiotics and 0.5% trypsin–ethylene diamine tetra acetic acid (EDTA) were from Gibco-BRL Life Technologies, (Waltham, MA, USA). 3-(4,5-dimethyl-thiazol-2-yl)-2,5-diphenyl tetrazolium bromide (MTT), radioimmunoprecipitation assay buffer (RIPA buffer), dimethylsulfoxide (DMSO), 2, 7-dichlorodihydrofluorescein diacetate (DCFH-DA), protease inhibitor cocktail, and vanillic acid (VA) were purchased from Sigma Aldrich (St Louis, MO, USA). Superoxide dismutase 1 (SOD1), superoxide dismutase 2 (SOD2), β -actin and rabbit secondary antibodies were from Santa Cruz (Dallas, TX, USA). Metformin, N-acetyl- cysteine (NAC), glycine and Triton-x100 were from SRL (Mumbai, India). Recombinant human insulin, dipotassium phosphate (K_2HPO_4), potassium dihydrogen phosphate (KH_2PO_4), disodium hydrogen phosphate (Na_2HPO_4), potassium phosphate (K_2PO_4) and methanol were from Merck (Kenilworth, NJ, USA). All other chemicals used were of analytical grade.

2.2.2 Cell culture

Human hepatocellular carcinoma (HepG2) cell lines were purchased from NCCS, Pune and were maintained in DMEM supplemented with 10 % FBS and antibiotics (100 U/ml of pencillin & 100 μ g/ml streptomycin) in a humidified atmosphere with 5 % CO_2 and 37 $^{\circ}C$ temperature.

2.2.3 Establishment of insulin resistance through HI in HepG2 cells

The insulin resistant HepG2 cell model was established according to the method of Jung et al. (2017) with little modifications. Briefly, HepG2 cells were seeded in 96-well plates at a density of 2×10^4 cells/well counted using a haemocytometer (Merck) and grown for 24 hrs to reach 80 % confluence. Then cells were incubated with or without of three different concentrations (50 or 100 nM or 1 μ M) of insulin and parameters relevant to insulin resistance (glucose uptake, insulin receptor substrate (IRS) 2, glucose transporter 2 (Glut2)) were studied to confirm the development of HI mediated insulin resistance in HepG2 cells.

Experimental groups:

C - Control

IR - HI created insulin resistance (1 μ M human recombinant insulin)

VA1 - IR + 5 μ M vanillic acid

VA2 - IR + 10 μ M vanillic acid

M - IR + metformin (1 mM)

The VA or metformin were co-treated with HI induced insulin resistance for 24 hrs in the experimental groups.

2.2.3.1 Cell viability determination

Cell viability was measured by MTT assay. Briefly after 60 % confluence, the cells were incubated with three concentrations (50 or 100 nM or 1 μ M) of human recombinant insulin (MERK, USA) for 24 hrs. Then precisely, 100 μ l of MTT solution was added into 96 well plates at a final concentration of 0.5 mg/ml and incubated for 3-4 hrs at 37 °C. After that the medium was discarded and the formazan crystals were dissolved in 100 μ l of DMSO. Then the

purple colour was read after 20 min at an absorbance of 570 nm (BioTek Synergy 4US). Finally, the percentage cell viability was tabulated.

2.2.3.2 Glucose uptake assay

2.2.3.2.1 Glucose uptake assay (colorimetric)

Briefly, the cells were incubated with various concentrations of insulin for 24 hrs. Then glucose uptake was assessed using a glucose uptake colorimetric assay kit (Abcam, UK). The control and hyperinsulinemic group were incubated in 4-(2-hydroxyethyl)-1-piperazineethanesulfonic acid (HEPES) buffered saline (20 mM) containing 10 μ M 2-deoxy-D-glucose (2-DG) at room temperature (RT, 22 to 28 °C) for 5 min. After two washes the cells were trypsinized by adding 100 μ l of 10X trypsin-EDTA and centrifuged at 20,000 x g (AG-716 rotor, model 7780 high speed refrigerated centrifuge, Kubota Laboratory Centrifuges Co., Tokyo, Japan) for 15 min at 4 °C. The pellets were dissolved in a neutralizing buffer (10 μ l), centrifuged at 20,000 x g for 15 min at 4 °C. The supernatant was collected. Reaction mix A (10 μ l) was mixed with 50 μ l supernatant and incubated for 1 h at RT. Extraction buffer (90 μ l) was added and heated to 90 °C for 40 min. Finally, 12 μ l of neutralizing buffer and 38 μ l of reaction mix B were added. Then the absorbance was measured every 2-3 min at 412 nm (BioTek Synergy 4, BioTek Instruments Corp., Winooski, VT, USA).

2.2.3.2.2 Analysis of glucose uptake by flow cytometry

Briefly, the cells were treated with three different concentrations of insulin for 24 hrs. Then intracellular glucose uptake was assessed using flow cytometry. The control and hyperinsulinemic groups were incubated in phosphate buffered saline (PBS) (20 mM) containing 10 μ M 2-[N-(7-nitrobenz-2-oxa-1,3-diazol-4-yl) amino]-2-deoxy-D-glucose (2-NBDG), at RT for 5 min. 2-NBDG is a fluorescent probe and D-glucose derivative. After two washes the cells were trypsinized by adding 100 μ l of 10X trypsin-EDTA and centrifuged at

20,000 x g (AG-716 rotor, model 7780 high speed refrigerated centrifuge, Kubota Laboratory Centrifuges Co., Tokyo, Japan) for 15 min at 4 °C. The pellets were resuspended in PBS and again centrifuged at 20,000 x g for 15 min at 4 °C. The pellet was collected and mixed with PBS and filtered the content using a cell strainer. Then the cells are analyzed on flow cytometer FACS Aria™ II (BD Biosciences).

2.2.3.3 Analysis of major proteins in insulin signaling pathway

The major proteins in the insulin signaling pathway are IRS2 and Glut2. The expression of these proteins were visualized using western blotting (for details please see section 2.2.14).

2.2.4 Cytotoxicity assay of VA

The cell viability was determined by MTT assay. Briefly, 2×10^4 HepG2 cells were seeded in 96-well plates and incubated in a 5 % CO₂ incubator at 37 °C. After cell attachment to the wells and reaching 80 % confluency, they were treated with different concentrations (5 μM, 10 μM, 20 μM, 30 μM, 40 μM, 50 μM, 100 μM, 500 μM) of VA. Then the cells were incubated with MTT solution (100 μl) of concentration (5 mg/ml) at 37 °C for 4 hrs. The viable cells convert the MTT to purple coloured formazan crystals. Then the formazan crystals were dissolved by adding 100 μl DMSO. The purple colour developed in the plate after 20 min of incubation at RT was read using a microplate reader at absorbance of 570 nm (BioTek Synergy 4US). Then the percentage of cell viability was calculated.

2.2.5 Cell viability of VA in hyperinsulinemic condition

Briefly, cells were seeded in 96-well plates and incubated in a 5 % CO₂ incubator at 37 °C. After reaching 80 % confluency, they were co-treated with 1 μM of human recombinant insulin and different concentrations (5 μM & 10 μM) of VA or metformin (1 mM) for 24 hrs. Then 100 μl of MTT solution was added to each well and incubated for 3-4 hrs at 37 °C. After that

the medium was discarded and 100 µl of DMSO was added. Then absorbance was read at 570 nm (BioTek Synergy 4US) and calculated the cell viability.

2.2.6 Estimation of intracellular ROS

Intracellular ROS levels were determined by using DCFH-DA. It is a cell permeable probe, during ROS generation, oxidized by intracellular non specific esterases and converted into fluorescent 2,7 dichlorofluorescein (DCF). Briefly, after treatments the cells were incubated with the DCFH-DA (20 µM) at 37 °C for 20 min. After that the cells were washed three times with PBS and the fluorescence was measured at an excitation of 488 nm and emission of 525 nm using a fluorescence microplate reader (BioTek Synergy 4). Fluorescent imaging was done using a bioimager system (BD pathway™ Bioimager, BD Biosciences, San Jose, CA, USA).

2.2.7 Superoxide dismutase (SOD) assay

SODs are the metalloenzymes and they are the crucial factor of the antioxidant defense system. Total SOD (cytosolic and mitochondrial SOD) activity was assayed spectrophotometrically using an assay kit (Cayman, USA). The kit utilizes the tetrazolium salt for detection of superoxide radicals generated by xanthine oxidase and hypoxanthine. For this, after respective treatments the cells were collected and homogenized with a homogenizer in a 20 mM cold HEPES buffer (1 mM EGTA, 210 mM mannitol, 70 mM Sucrose). Then the cells were centrifuged at 1500 x g for 5 min at 4 °C and collected the supernatant. After that 10 µl of sample and standards (bovine-erythrocyte SOD) were added to each well containing 200 µl of radical detector. In order to initiate the reaction, 20 µl of xanthine oxidase were added and incubated for 30 min. The absorbance was read at 450 nm.

2.2.8 Expression of SOD1 and SOD2

The protein expression of both cytosolic SOD (SOD1) and mitochondrial SOD (SOD2) were analyzed using western blotting (please refer section 2.2.14 for further details).

2.2.9 Glutathione peroxidase assay

This assay indirectly measures the GPx activity by coupled reaction with glutathione reductase. Briefly, 3×10^5 cells were seeded in a 6-well plate. After respective treatments the cells were collected and homogenized in a cold buffer containing 50 mM tris HCl (pH 5.5), 5 mM ethylenediaminetetraacetic acid (EDTA) and 1 mM dithiothreitol (DTT). It was then centrifuged at 10,000 x g for 15 min at 4 °C. The supernatant was collected and used for assay. Then 20 µl of sample, assay buffer (100 µl) and co-substrate mix (50 µl) were added to respective wells. Then 20 µl of cumene hydroperoxide were added to start the reaction. The absorbance was read at 340 nm using a microplate reader.

2.2.10 Glutathione assay

Reduced glutathione (GSH) activity was assayed colorimetrically according to manufacturer's instructions (Cayman, USA). The kit uses the glutathione reductase for the detection of GSH. GSH reacts with 5, 5'-dithio-bis-2- (nitrobenzoic acid), Ellman's reagent (DTNB) and produces a yellow coloured TNB, which was measured. Briefly, after respective treatments the cells were collected and dissolved in 2 ml of sample buffer and centrifuged at 10,000 x g for 15 min at 4 °C. Collected supernatants were deproteinized. After that 50 µl of sample and standard were added to corresponding wells. Then 150 µl of assay cocktail (MES buffer, reconstituted cofactor mixture, reconstituted enzyme mixture, water and DTNB) were added and kept the plate in the dark. Then absorbance was measured every 2-3 min at 407 nm for 30 min using the microplate reader.

2.2.11 Glucose-6-phosphate dehydrogenase activity assay

Glucose-6-phosphate dehydrogenase (G6PDH) activity was measured by assay kit (Biovision). G6PDH activities were measured as the rate of reduction of NADP to NADPH. Here oxidized product of G6PDH was utilized to convert a colourless product to intensely coloured product. In this assay we used NADH as standard. In brief, the cells after treatment were collected and homogenized with PBS. Then 50 μ l of samples were added to the respective well contained 50 μ l of reaction mix. Reaction mix possesses G6PDH assay buffer, G6PDH substrate and G6PDH developer. Then the absorbance was measured at 450 nm.

2.2.12 Estimation of protein carbonyl content

Protein carbonyl content assay was based on the fact that DNPH reacts with protein carbonyls from schiff's base which produces hydrazone. It was then quantified at 360 nm. After appropriate treatments, the cell pellets were homogenized in a cold buffer (50 mM phosphate buffer pH 6.7, 1mM EDTA). After centrifugation the supernatant was used for assay. 200 μ l of sample was added to both control tube and sample tube. To that 800 μ l of DNPH was added to the sample tube and 800 μ l of 2.5 M HCl was added to the control tube. All the tubes were kept in the dark at RT for 1 hr. 1 ml of 20 % TCA was added with 5 min incubation in ice. Then it was centrifuged at 10,000 x g for 10 min and discarded the supernatant. Then the pellet was dissolved in 1 ml of (1:1) ethyl acetate/ethanol mixture and centrifuged at 10,000 x g for 10 min at 4 °C. Then the collected pellet was dissolved in 500 μ l of guanidine hydrochloride. Again it was centrifuged and 220 μ l of supernatant was taken and read the absorbance at 360 nm using a multimode plate reader.

2.2.13 Lipid peroxidation assay

Lipid peroxidation was assayed with TBARS assay kit (Cayman, USA). After treatments, the cells were collected and sonicated for 5 seconds. 100 µl of sample and standard were added to respective tubes containing 100 µl of sodium dodecyl sulfate (SDS). Then 4 ml of colouring reagents were added to each well. All the tubes were boiled for 1 hr and were placed in ice for 10 min to stop the reaction. After incubation it was centrifuged for 10 min at 1600 x g at 4 °C. Then 150 µl of samples were transferred into the 96 well plate and the absorbance was read at 530 nm.

2.2.14 Western blot

Cells were cultured in T-25 flasks containing 5 ml DMEM medium and did the respective treatments. After that the cells were collected and lysed in a lysis buffer with protease inhibitor cocktail and Tween 20. Then the lysate was centrifuged at 20,000 x g for 15 min at 4 °C. Then the supernatant was collected and protein concentration was measured using Pierce BCA method. Samples of 25 µl were loaded into each well and the samples were run on 10 % SDS-PAGE at 55 V. Then it was transferred at 25 V into polyvinylidene difluoride (PVDF) membrane using transblot Turbo (BioRad, USA). Equal protein loading was assured by ponceau S staining. After transferring, the membrane was blocked with BSA in tris buffered saline-Tween 20 (TBST) for 1 hr at RT. Then after washing with TBST, the membrane was probed with primary antibody (1:1000), in TBST with a gentle shaking at 4 °C overnight. Then the membrane was washed three times with TBST for 10 min. HRP-Conjugated secondary antibody (1:1000) in TBST was added for 90 min at RT with agitation. After three TBST washes, membranes were developed using enhanced chemiluminescence substrate (ECL substrate) kit (Abcam, UK) and the proportional thickness of bands were measured using Image Lab software in the ChemiDoc system (ChemiDoc MP Imaging System, Bio-Rad).

2.2.15 Statistical analysis

All analyses of data were carried out with sextuplicates and data are shown as mean \pm standard error of the mean (SEM) for control and treated cells. The normality of the variables were tested using the Kolmogorov Smirnov Z test and the variables were found to be approximately normally distributed. Hence the significance difference between the groups were tested using one-way analysis of variance (ANOVA) and further significantly different pairs ($p \leq 0.05$) were identified using Duncan's multiple comparison test. All calculations were done using the Statistical Package for the Social Sciences for Windows standard version 20 (SPSS Inc., USA).

2.3 Results

2.3.1 High insulin induced cell death in HepG2 cells

In order to detect the cytotoxicity of high insulin in HepG2 cells, I have selected three concentrations of insulin (50, 100 nM and 1 μ M) and evaluated the cell viability for 24 and 48 hrs (Fig: 2.1A & Fig: 2.1B). Insulin of 50 nM (IN1) and 100 nM (IN2) showed cell viability of 95.6 % and 92.6 % respectively but insulin of 1 μ M (IN3) showed 78 % cell viability ($p \leq 0.05$) compared to control (Fig: 2.1A).

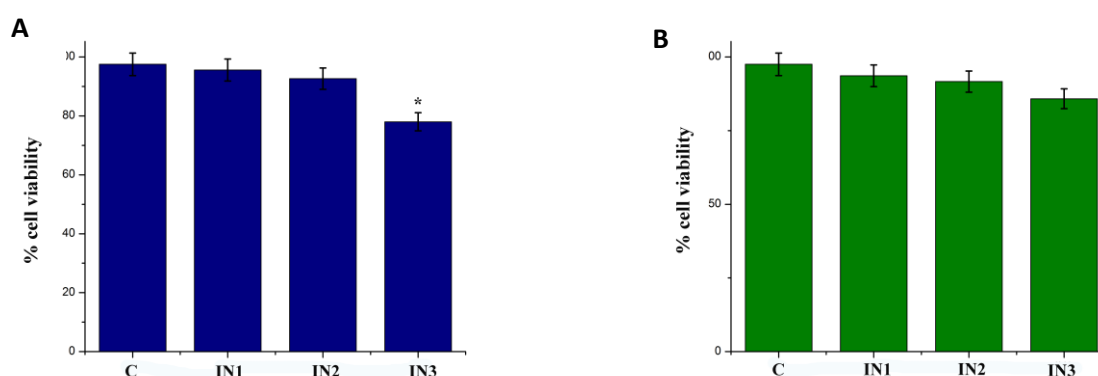
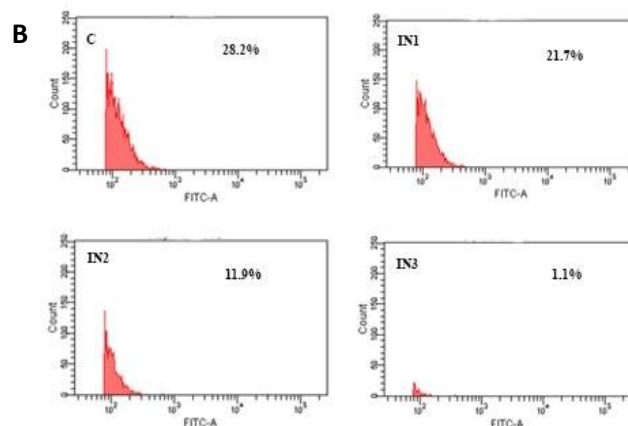
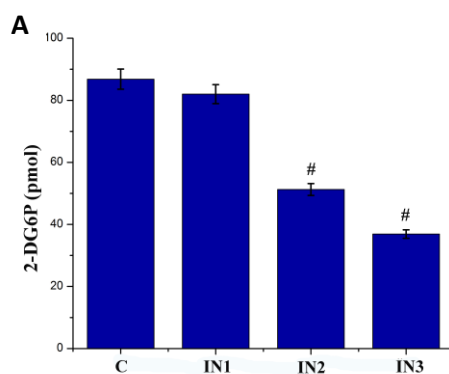


Figure. 2.1 Cell viability of high insulin. (A) Cell viability of high insulin for 24 hrs. (B) Cell viability of high insulin for 48 hrs. C - control cells; IN1 - 50 nM insulin; IN2 - 100 nM insulin; IN3 - 1 μ M insulin. Values are expressed as mean \pm SEM where n=6. * indicates that the mean value was significantly different from control cells ($p \leq 0.05$).

2.3.2 Induction of insulin resistance through hyperinsulinemic shock in HepG2 cells

The results of the glucose uptake with three different concentrations of insulin treated HepG2 cells are shown in Fig: 2.2A. The intracellular uptake of 2-DG with three concentrations of insulin (50, 100 nM and 1 μ M; IN1, IN2 and IN3 respectively) treated cells was reduced by 5.5, 35.4 and 51.9 %, respectively, as compared with control cells. Among these, 100 nM and 1 μ M (IN2 & IN3) concentrations of insulin showed a noticeable ($p \leq 0.05$) decrease in glucose uptake compared to control cells (Fig: 2.2A). This was also confirmed with flow cytometry data which quantify the number of cells which absorbed the 2-NBDG (Fig: 2.2B). The data showed that intracellular uptake of 2-NBDG in IN1, IN2 and IN3 were 21.7 %, 11.9 % and 1.1 % respectively (Fig: 2.2B). Compared with other two concentrations (IN1 & IN2), IN3 (1 μ M insulin) showed a significant decrease ($p \leq 0.05$) in the glucose uptake compared with control cells (Fig: 2.2B).

The expression levels of major proteins in the insulin signaling pathway, IRS2 and Glut2 were significantly down regulated with 1 μ M insulin compared to normal (Fig: 2.2C) suggesting that IN3 (1 μ M insulin) significantly ($p \leq 0.05$) affected glucose uptake, insulin sensitivity and developing insulin resistance. Based on these data, 1 μ M insulin concentration was chosen to induce hyperinsulinemic shock in subsequent experiments (Fig: 2.2C).



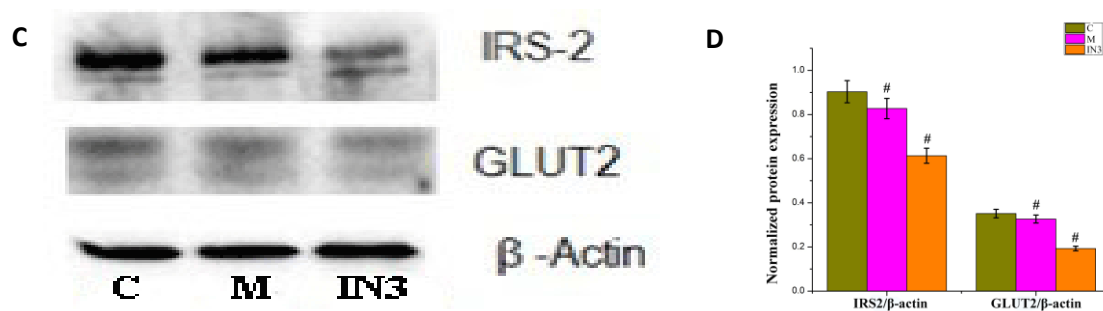


Figure. 2.2. Induction of IR through hyperinsulinemic shock in HepG2 cells. (A) Glucose uptake (calorimetric). (B) Glucose uptake using flow cytometry. HepG2 cells were incubated in normal medium and different concentrations of insulin for 24 hrs. (C) Western blot analysis of insulin receptor substrate (IRS) 2 and glucose transporter (GLUT) 2. (D) Densitometric analysis of IRS2 and GLUT2. C - control; M - 1 mM metformin; IN1 - 50 nM insulin; IN2 - 100 nM insulin; IN3 - 1 μM insulin. Protein quantification was carried out using densitometric analysis, normalized using an internal control of β-actin. Values are expressed as mean ± SEM where n=6. # indicates that the mean value was significantly different from control cells ($p \leq 0.05$).

2.3.3 Cytotoxicity of VA

In order to check the cytotoxicity and to select suitable concentrations of the compound (VA) for further *in vitro* study, I have determined the cell viability using various concentrations of VA (5 μM, 10 μM, 20 μM, 30 μM, 40 μM, 50 μM, 100 μM, and 500 μM) for 24 hrs. VA of 500 μM (VA8) showed a significant cytotoxicity compared with all other concentrations ($p \leq 0.05$) (Fig: 2.3). With this data I have selected 5 μM and 10 μM concentrations of VA for *in vitro* studies (Fig: 2.3).

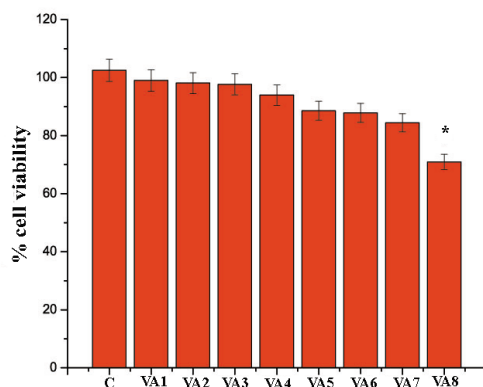


Figure. 2.3 Cell viability of VA. Cell viability of HepG2 cells incubated in DMEM with 1 % FBS and different concentrations of vanillic acid for 24 hrs. C - control; VA1 - 5 μ M vanillic acid; VA2 - 10 μ M vanillic acid; VA3 - 20 μ M vanillic acid; VA4 - 30 μ M vanillic acid; VA5 - 40 μ M vanillic acid; VA6 - 50 μ M vanillic acid; VA7 - 100 μ M vanillic acid; VA8 - 500 μ M vanillic acid. Values are expressed as mean \pm SEM where n=6. * indicates that the mean value was significantly different from control cells ($p \leq 0.05$).

2.3.4 Cell viability of VA during HI created insulin resistance in HepG2 cells

Incubation of HepG2 cells with 1 μ M of insulin (HI created insulin resistance) for 24 hrs caused a significant cell death (19.2 %; $p \leq 0.05$) compared to control (Fig: 2.4). Co-treatment with VA of 5 μ M and 10 μ M concentrations reduced the cell death (7.2 % and 14.2 % respectively) compared to IR cells (Fig: 2.4). Positive control metformin also showed a noticeable decrease in the cytotoxicity (9.2 %) compared to IR cells (Fig: 2.4).

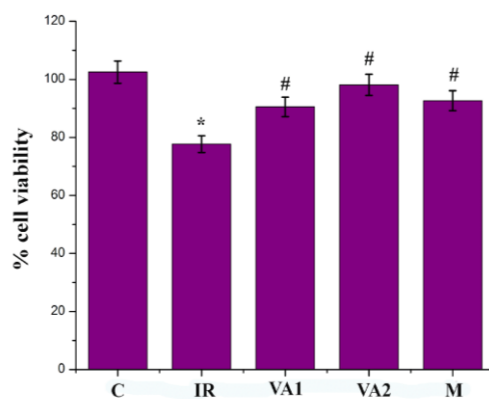
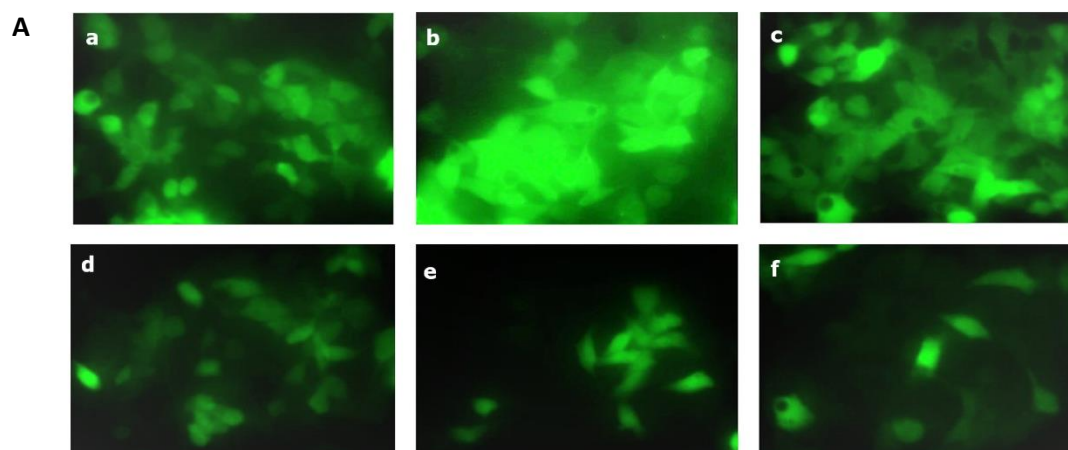


Figure. 2.4. Cell viability of VA during HI. Cell viability of 5 and 10 μM vanillic acid and metformin on hyperinsulinemia created insulin resistant models (IR). C - control cells; IR - hyperinsulinemia created insulin resistant cells; VA1 - IR + 5 μM vanillic acid; VA2 - IR + 10 μM vanillic acid; M - IR + metformin (1 mM). Values are expressed as mean \pm SEM where $n=6$. * indicates that the mean value was significantly different from control cells ($p \leq 0.05$). # indicates the mean value was significantly different from IR cells ($p \leq 0.05$).

2.3.5 Effect of VA on ROS generation

Evaluation of reactive oxygen species by fluorescent microscopy revealed surplus generation of ROS during IR. The IR group showed a noticeable increase in ROS levels (68.2 %) compared to control (Fig: 2.5A & Fig: 2.5B). Co-treatment with VA (5 μM and 10 μM) was noticeably ($p \leq 0.05$) effective for preventing ROS generation by 88.2 and 99.6 % respectively when compared with the IR group (Fig: 2.5A & Fig: 2.5B). Treatment with metformin and NAC also significantly reduced the ROS generation by 96 and 108 %, respectively (Fig: 2.5A & Fig: 2.5B).



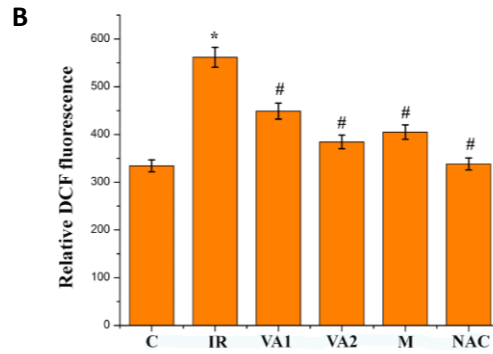


Figure. 2.5 Intracellular reactive oxygen species generation determined using DCFDA. (A) Fluorescent microscopic images of HepG2 cells stained with DCFDA. (B) Relative fluorescence intensity of DCFDA uptake. a - control cells; b - hyperinsulinemia created insulin resistant cells; c - IR + 5 μ M vanillic acid; d - IR + 10 μ M vanillic acid; e - IR + metformin (1 mM); f - IR + N-acetyl cysteine (1 mM). Values are expressed as mean \pm SEM where n=6. * indicates that the mean value was significantly different from control cells ($p \leq 0.05$). # indicates the mean value was significantly different from IR cells ($p \leq 0.05$).

2.3.6 Effect of HI created insulin resistance on SOD levels

Alteration in SOD levels in the cells during HI was analyzed. Compared to control cells, the SOD activity was significantly ($p \leq 0.05$) increased in IR cells (75.1 %). Co-treatment with VA (5 μ M and 10 μ M) decreased the SOD activity by 9.5 and 66.6 % ($p \leq 0.05$) respectively, compared to IR (Fig: 2.6A). But treatment with metformin significantly ($p \leq 0.05$) increased the SOD activity by 14.8 % respectively. This data was also confirmed with protein expression analysis of both SOD1 and SOD2 enzymes. IR cells showed a significant increase in the levels of SOD1 (91.2 %) and SOD2 (52.2 %) compared with control cells (Fig: 2.6B & Fig: 2.6C). VA of 5 and 10 μ M concentrations showed a significant decrease in the expression of both SOD1 by 50.5 and 86.9 % and SOD2 by 33.8 and 49.1 % respectively (Fig: 2.6B & Fig: 2.6C). Co-treatment with metformin also down-regulated the SOD1 by 64.5 % and SOD2 by 93.9 % compared to IR cells.

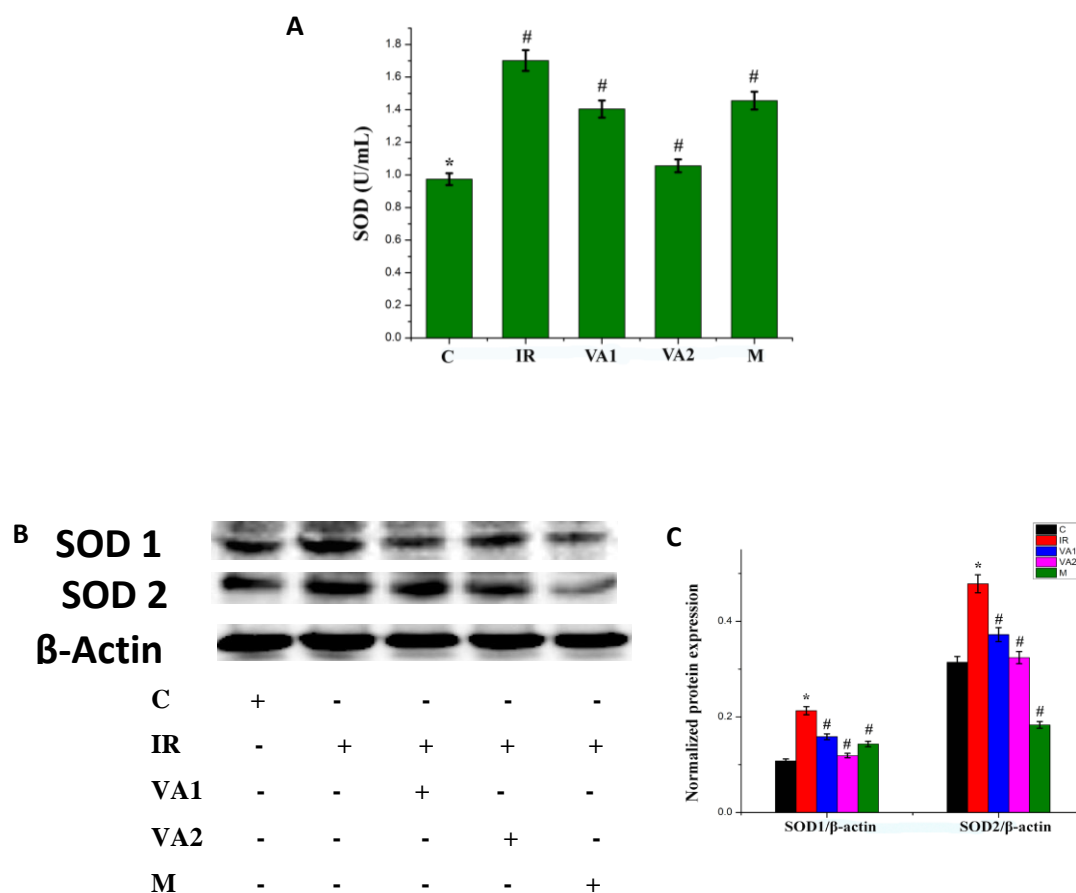


Figure. 2.6 Activity of SOD during hyperinsulinemia. (A) SOD activity. **(B)** Western blot analysis of both SOD1 and SOD2. **(C)** Densitometric analysis of SOD1 and SOD2. C - control cells; IR - hyperinsulinemia created insulin resistant cells; VA1 - IR + 5 μ M vanillic acid; VA2 - IR + 10 μ M vanillic acid; M - IR + metformin (1 mM). Protein quantification was carried out using densitometric analysis, normalized using an internal control of β -actin. Values are expressed as mean \pm SEM where n=6. * indicates that the mean value was significantly different from control cells ($p \leq 0.05$). # indicates the mean value was significantly different from IR cells ($p \leq 0.05$).

2.3.7 VA increases the GPx levels

It catalyzes the peroxidation of H_2O_2 in the presence of GSH to form water and oxidized glutathione. Thus as a H_2O_2 scavenger GPx has a prominent importance. Here also, GPx activity was decreased in high insulin treated insulin resistant cells by 19.1 % compared to control. But co-treatment with VA significantly ($p \leq 0.05$) improved the GPx activity by 29.3 % (5 μ M) and 35.8 % (10 μ M) compared to IR (Fig: 2.7). Metformin increased the GPx levels by 42.9 % respectively compared to IR cells.

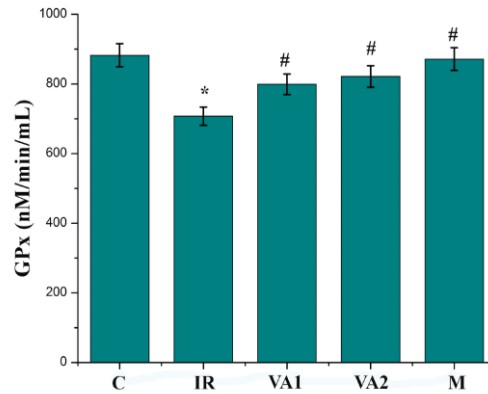


Figure. 2.7 Glutathione peroxidase (GPx) activity. C - control cells; IR - hyperinsulinemia created insulin resistant cells; VA1 - IR + 5 μM vanillic acid; VA2 - IR + 10 μM vanillic acid; M - IR + metformin (1 mM). Values are expressed as mean \pm SEM where n=6. * indicates that the mean value was significantly different from control cells ($p \leq 0.05$). # indicates the mean value was significantly different from IR cells ($p \leq 0.05$).

2.3.8 Hyperinsulinemia reduced the GSH and G6PDH activity

Compared to control, IR cells caused a significant ($p \leq 0.05$) decrease in GSH level by 31.4 %. Here also, VA co-treatment at both concentrations (5 μM and 10 μM) showed a significant ($p \leq 0.05$) increase in GSH levels by 58 and 65.3 % respectively (Fig: 2.8A). Metformin significantly improved GSH level by 34 % (Fig: 2.8A). In addition to this, the activity of G6PDH was significantly ($p \leq 0.05$) lowered in IR cells by 54.5 % compared to the control group. VA (5 μM and 10 μM) increased the G6PDH activity by 16 % and 39.2 % respectively (Fig: 2.8B). Treatment with metformin at 1 mM also improved the G6PDH activity by 48.1 % compared to the IR group (Fig: 2.8B).

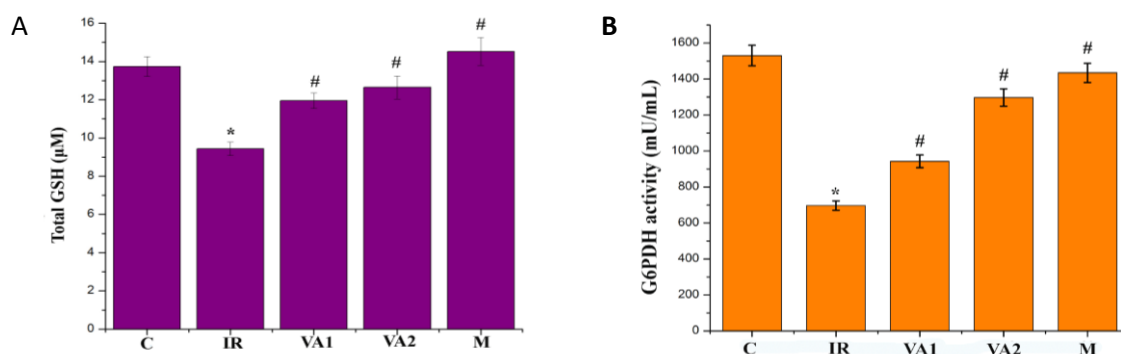


Figure. 2.8 (A) Total glutathione (GSH) levels. (B) G6PDH activity. C - control cells; IR - hyperinsulinemia created insulin resistant cells; VA1 - IR + 5 µM vanillic acid; VA2 - IR + 10 µM vanillic acid; M - IR + metformin (1 mM). Values are expressed as mean ± SEM where n=6. * indicates that the mean value was significantly different from control cells ($p \leq 0.05$). # indicates the mean value was significantly different from IR cells ($p \leq 0.05$).

2.3.9 Hyperinsulinemia induces damage to cellular lipids and proteins

Lipid peroxidation was also significantly increased ($p \leq 0.05$) in IR cells (52.8 %) compared to control (Fig: 2.9A). Treatment with VA at 5 µM and 10 µM, or metformin (1mM) lowered MDA levels by 22.6, 39.6 and 47.3 % respectively, compared to IR (Fig: 2.9A).

Protein carbonyls are the end products of protein oxidation and the common markers of protein oxidation. The concentration of protein carbonyls also was significantly higher (47.9 %) in IR cells (Fig: 2.9B) as compared to normal. Co-treatment with VA at both concentrations significantly reduced ($p \leq 0.05$) the protein carbonyl concentrations by 38.2 % and 50.2 % at 5 µM and 10 µM respectively (Fig: 2.9B). Metformin treatment decreased the protein oxidation by 43 %.

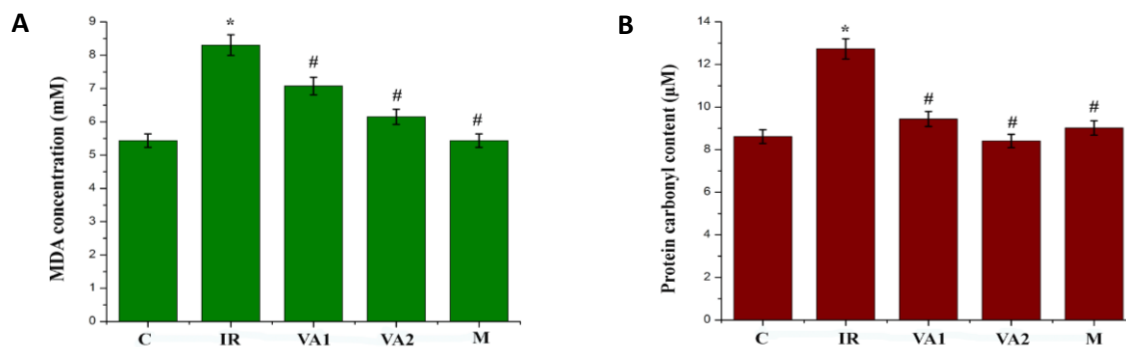


Figure. 2.9 Estimation of Lipid peroxidation product and protein carbonyl content. (A) Estimation of malondialdehyde (MDA) formation in different groups. (B) Quantification of protein carbonyl content. C - control cells; IR - hyperinsulinemia created insulin resistant cells; VA1 - IR + 5 µM vanillic acid; VA2 - IR + 10 µM vanillic acid; M - IR + metformin (1 mM). Values are expressed as mean ± SEM where n=6. * indicates that the mean value was significantly different from control cells ($p \leq 0.05$). # indicates the mean value was significantly different from IR cells ($p \leq 0.05$).

2.4 Discussion

T2DM is the most common type of diabetes and insulin resistance is one of the hallmarks of T2DM (American diabetes association, 2010). Treatment of insulin resistance is a critical strategy in the prevention and management of T2DM and related complications. HI is known to be present prior to the development of diabetes and has been recognized as a risk factor for insulin resistance (Schofield and Sutherland, 2012). HI is not an end result of insulin resistance, but it is an independent driver of many metabolic consequences and insulin resistance is one of them (Shanik et al., 2008).

The human liver possesses an important role in glucose metabolism as well as it is the major site of insulin clearance. The major contributors to the genesis of HI and associated insulin resistance is the enormous production of insulin and reduced insulin clearance which finally result in an increase in basal insulin level (Michael et al., 2000). All these consequences lead to the development of both hyperglycemia and insulin resistance which results in liver dysfunction and hyperplasia. The liver has a crucial role in the pathogenesis of T2DM in relation to glucose and lipid metabolism. In my study, I have focused on the alterations in the antioxidant system of the cells during OS which is induced by HI.

Here, first I developed a cell model for HI created insulin resistance. Cells with HI created insulin resistance are a good model to study T2DM related complications (Yan et al., 2017). There are several methods of inducing insulin resistance in HepG2 cells. Different investigators have published various protocols using various inducers (TNF α , high glucose, high insulin, high glucose and high insulin, palmitate) with different concentrations and lengths of incubation (Liu et al., 2017). Here I selected three concentrations of insulin (50 nM, 100 nM and 1 μ M) for mimicking HI and insulin resistance in HepG2 cells and checked the effects of these three concentrations of insulin on cell viability and glucose uptake. Consistent with

previous reports insulin (1 μM) treatment (hyperinsulinemia) for 24 hrs induced the insulin resistance in HepG2 cells (Duraisamy et al., 2003; Jung et al., 2017). HI created insulin resistance was confirmed with the significant reduction of glucose uptake and predominant inhibition of the insulin signaling pathway at 1 μM insulin. For example, high insulin treatment decreased the IRS2, and GLUT2 expressions in HepG2 cells as compared to normal. VA is a well-known food additive; it does not show any cytotoxicity. HI created insulin resistance showed a significant cytotoxicity in HepG2 cells but co-treatment with VA and metformin reduced the cytotoxicity significantly. Meanwhile, the results clearly confirmed that insulin at 1 μM concentration showed a decrease in both glucose uptake as well as in cell viability during all incubation periods but it showed a tremendous decrease in glucose uptake only at 24 hrs. So I confirmed the time period for induction of insulin resistance to be 24 hrs.

HI also creates OS by producing enormous amount of ROS. OS is a condition that occurs only when the ROS production exceeds and it creates disturbances in the antioxidant system (Pizzino et al., 2017). The effect of HI created insulin resistance on the redox status of HepG2 cells, which is essential for maintaining the normal functional status of cells, was the primary focus. Meanwhile, the potential of VA to restores the redox status during hyperinsulinemic shock was also analyzed. It is well known that OS is associated with multiple alterations of cell structure and function (Birben et al., 2012). During insulin resistance and diabetes, the initial symptom is the breakdown of the redox homeostasis through the generation of oxyradicals. OS is created by a group of free radicals such as superoxide anion, hydroxyl radicals, H_2O_2 and singlet oxygen (Pizzino et al., 2017) etc. Alterations in the innate antioxidant system were seen with insulin resistance. Antioxidants are the molecules that delays or inhibit the oxidation of substrates and have the capacity to capture the free radicals (Birben et al., 2012). Compounds involved in the innate antioxidant system such as superoxide dismutase (SOD), glutathione peroxidase (GPx), reduced glutathione (GSH) were studied. SOD is the

first line of defense against these oxyradicals. It catalyses the self-reaction of superoxides to form H_2O_2 which later detoxified by glutathione peroxidase with the help of GSH. The role of HI in the induction of OS in animals had been well studied by Crofts et al (2015). But no detailed investigation dealing with various compounds involved in the innate antioxidant system, lipid peroxidation and protein carbonyl were found. In the present study, HI created insulin resistance significantly increased the SOD and decreased GPx and GSH levels in HepG2 cells. They are the main enzymes responsible for the removal of oxyradicals (Ochiai et al., 2008). The increase in SOD during OS might be a compensatory regulatory response in the liver (Li et al., 2015) and its overexpression might lead to accumulation of H_2O_2 (Fukai and Ushio-Fukai, 2011). GPx is an antioxidant protein that has an important role in the reduction of H_2O_2 (Espinoza et al., 2015). The accumulation of increased levels of peroxides inactivates the GPx and increases OS (Miyamoto et al., 2003). There was a significant decrease in the levels of GPx in HI created insulin resistant cells. GSH is another antioxidant, abundantly seen in the liver and an important determinant of redox signalling (Lu, 2013). Normally the liver is protected from OS by the capacity of the hepatocytes to produce GSH. But when a pathological condition occurs the GSH homeostasis is altered (Chen et al., 2013). Hepatic glutathione depletion generates chronic mitochondrial dysfunction and develops many liver diseases including T2DM (Chen et al., 2013). During OS, the level of GSH was reduced by decreasing the levels of H_2O_2 and lipid peroxides (Yin et al., 2017). However, I have noted the levels of other antioxidant enzymes like GSH and GPx in HepG2 cell lines, and they were decreased during HI (Fig: 2.8A & Fig: 2.7) whereas VA of 5 μ M and 10 μ M of concentrations showed an increase in the level of GPx, as well as in GSH level. Metformin also increased the levels of both GPx and GSH. Alterations in antioxidant status resulting from OS is commonly considered as an initial stimulus for down-regulation of HMP shunt. Here I have found that impaired antioxidant enzymes have a critical role in the silencing of G6PDH, an enzyme

involved in the first step of the pentose phosphate pathway. One study demonstrated that G6PDH activity in cardiac myocytes was rapidly increased in OS (Jain et al., 2003). In this study I have demonstrated that during HI created insulin resistance conditions the levels of G6PDH was decreased in hepatocytes. That means that the HMP shunt was silenced. Decreased pentose phosphate pathway definitely reduces the levels of reducing equivalents like NADPH and this will affect the regeneration of antioxidants like glutathione and declines the other antioxidants level. Meanwhile our compound VA effectively up-regulated the enzyme and activated the pathway.

Besides this, increased ROS also attack the cellular proteins, DNA and membrane lipids which results in the formation of protein carbonyls, create several crucial mutations and undergo lipid peroxidation which finally results in cellular dysfunction (Matteucci and Giampietro, 2000). Lipid peroxidation has a significant role in the progression of insulin resistance and diabetes. During the HI condition, lipid peroxidation is increased. Increased lipid peroxidation products will definitely attack the membrane lipids and lose membrane fluidity which results in alteration in cellular signaling. The OS markers like MDA and protein carbonyl were found to be drastically increased in insulin resistant cells. MDA, a marker of lipid peroxidation and it participates in the transcriptional regulation of innate antioxidant enzymes and decreases their production (Kuehne et al., 2015). Over all, HI created insulin resistance, decreased GPx and GSH activities, and increased the SOD activity which then changed the antioxidant balance and an induction of MDA and lipid peroxides, but VA increased all the enzyme activities except SOD. During the initial stages of OS the SOD levels become increased due to the increased production of ROS and it is a protective mechanism seen in the liver. Here the treatment period of HI created insulin resistance is 24 hrs. During this period the SOD level was increased due to the initiation of OS but VA has been dose dependently decreased the ROS production simultaneously reduced the SOD activity. One of the studies reported the

antioxidant potential of VA so it can reduce the OS (Kumar et al., 2011). Through this way, it eliminates the superoxide radicals in HepG2 cells.

Antioxidant therapy is a more promising therapy for diabetics and other metabolic diseases (Palsamy et al., 2010). Increasing the antioxidant levels in diabetes mellitus patients with liver damage may hopefully reduce the effects of OS and thereby decrease the severity of diabetic complications (Seven et al., 2004). A few phytochemicals have been investigated to protect against or possibly reverse liver damage caused by OS. Vitamin E and betaine are the antioxidants which have shown good clinical results in the reduction of liver disease severity and the protection of the liver from diabetes mellitus-induced damage (Mohamed et al., 2016). Here also, VA showed its potential as a potent antioxidant agent by reducing the ROS levels and restoring the antioxidants to normal in HepG2 cells. VA is an FDA approved food additive and it has so many pharmacological properties (Gitzinger et al., 2011). Furthermore, VA does not show any toxic effects in HepG2 cells that make it an attractive compound for using as a functional drug. Apart from this detailed clinical and preclinical investigations are necessary for exploring the other properties of VA as well as usage of this compound in humans.

References

Ahmed N, Thornalley PJ, Lüthen R, Häussinger D, Sebekova K, Schinzel R, et al. Processing of protein glycation, oxidation and nitrosation adducts in the liver and the effect of cirrhosis. *J Hepatol.* 2004; 41: 913-919.

Ahmed N. Advanced glycation endproducts: Role in pathology of diabetic complications. *Diabetes Res Clin Pract.* 2005; 67: 3-21.

American Diabetes Association. Diagnosis and classification of diabetes mellitus. *Diabet Care.* 2010; 33: S62-S69.

Birben E, Sahiner UM, Sackesen C, Erzurum S, Kalayci O. Oxidative stress and antioxidant defense. *World Allergy Organ J.* 2012; 5: 9-19.

Brownlee M. Negative consequences of glycation. *Metab.* 2000; 49: 9-13.

Chen Y, Dong H, Thompson DC, Shertzer HG, Nebert DW, Vasiliou V. Glutathione defense mechanism in liver injury: insights from animal models. *Food Chem Toxicol.* 2013; 60: 38-44.

Corkey BE. Banting lecture 2011: hyperinsulinemia: cause or consequence?. *Diabetes.* 2012; 61: 4-13.

Crofts CAP, Zinn C, Wheldon M, Schofield G. Hyperinsulinemia: A unifying theory of chronic disease. *Diabetesity.* 2015; 1: 34-43.

Duraisamy Y, Gaffney J, Slevin M, Smith CA, Williamson K, Ahmed N. Aminosalicic acid reduces the antiproliferative effect of hyperglycaemia, advanced glycation end products and glycated basic fibroblast growth factor in cultured bovine aortic endothelial cells: Comparison with aminoguanidine. *Vascular Biochemistry.* 2003; 246: 143-153.

Engwa GA, Nwalo FN, Chibuzor GE, Ejiagha EC, Abonyi MC, Ugwu TE, et al. Relationship between Type 2 Diabetes and Glucose-6 Phosphate Dehydrogenase (G6PD) Deficiency and Their Effect on Oxidative Stress. *Diabetes Metab J.* 2018; 9: 1-8.

Espinosa-Diez C, Miguel V, Mennerich D, Kietzmann T, Sánchez-Pérez P, Cadenas S, Lamas S. Antioxidant responses and cellular adjustments to oxidative stress. *Redox Biol.* 2015; 6: 183-197.

Fukai T and Ushio-Fukai M. Superoxide dismutases: Role in redox signaling, vascular function, and diseases. *Antioxid Redox Signal.* 2011; 15: 1583-1606.

Gitzinger M, Kemmer C, Fluri DA, Daoud El-Baba M, Weber W, Fussenegger M. The food additive vanillic acid controls transgene expression in mammalian cells and mice. *Nucleic Acids Res.* 2011; 40: e37-e37.

Guzmán TJ and Gurrola-Díaz CM. Glucokinase activation as antidiabetic therapy: effect of nutraceuticals and phytochemicals on glucokinase gene expression and enzymatic activity. *Arch Physiol Biochem.* 2019; 1-12.

International Diabetes Federation. *IDF diabetes atlas.* Brussels, Belgium: International Diabetes Federation. 2019; 8: 1-147.

Jain M, Brenner DA, Cui L, Lim CC, Wang B, Pimentel DR. Glucose-6-phosphate dehydrogenase modulates cytosolic redox status and contractile phenotype in adult cardiomyocytes. *Circ Res.* 2003; 93: e9-e16.

Jung HA, Ali MY, Bhakta HK, Min BS, Choi JS. Prunin is a highly potent flavonoid from *Prunus davidiana* stems that inhibits protein tyrosine phosphatase 1B and stimulates glucose uptake in insulin-resistant HepG2 cells. *Arch Pharm Res.* 2017; 40: 37-48

Karmakar B, Vohra RM, Nandanwar H, Sharma P, Gupta KG, Sobti RC. Rapid degradation of ferulic acid via 4-vinylguaiacol and vanillin by a newly isolated strain of *Bacillus coagulans*. *J Biotechnol*. 2000; 80: 195-202.

Kim JA, Wei, Y, Sowers, JR. Role of mitochondrial dysfunction in insulin resistance. *Circ Res*. 2008; 102(4), 401-414.

Kuehne A, Emmert H, Soehle J, Winnefeld M, Fischer F, Wenck H. Acute activation of oxidative pentose phosphate pathway as first-line response to oxidative stress in human skin cells. *Mol Cell*. 2015; 59: 359-371.

Kumar S, Prahalathan P, Raja B. Antihypertensive and antioxidant potential of vanillic acid, a phenolic compound in L-NAME-induced hypertensive rats: a dose-dependence study. *Redox Rep*. 2011; 16: 208-215.

Leclercq IA, Morais ADS, Schroyen B, Van Hul N, Geerts A. Insulin resistance in hepatocytes and sinusoidal liver cells: mechanisms and consequences. *J Hepatol*. 2007; 47: 142-156.

Leung TM and Nieto N. CYP2E1 and oxidant stress in alcoholic and non-alcoholic fatty liver disease. *J Hepatol*. 2013; 58: 395-398.

Li W, Cao L, Han L, Xu Q, Ma Q. Superoxide dismutase promotes the epithelial-mesenchymal transition of pancreatic cancer cells via activation of the H₂O₂/ERK/NF- κ B axis. *Int J Oncol*. 2015; 46: 2613-2620.

Lindsay JR, McKillop AM, Mooney MH, O'harte FPM, Bell PM, Flatt PR. Demonstration of increased concentrations of circulating glycosylated insulin in human Type 2 diabetes using a novel and specific radioimmunoassay. *Diabetologia*. 2003; 46: 475-478.

Liu L, Zhang X, Chen F, Hu J, Zeng B. The establishment of insulin resistance model. InBIO Web of Conferences. EDP Sciences. 2017; 8: 1-7.

Lu SC. Glutathione synthesis. *Biochim Biophys Acta Gen Subj*. 2013; 1830: 3143-3153.

Mamun-or-Rashid ANM, Hossain MS, Hassan N, Dash BK, Sapon A, Sen MK. A review on medicinal plants with antidiabetic activity. *J pharmacogn Phytochem*. 2014; 3: 149-159.

Matteucci E and Giampietro O. Oxidative stress in families of type 1 diabetic patients. *Diabet. Care*. 2000; 23: 1182-1186.

McKillop AM, Abdel-Wahab YH, Mooney MH, O'Harte FP, Flatt PR. Secretion of glycated insulin from pancreatic beta-cells in diabetes represents a novel aspect of beta-cell dysfunction and glucose toxicity. *Diabetes Metab J*. 2002; 28: 3S61-3S69.

Michael MD, Kulkarni RN, Postic C, Previs SF, Shulman G.I, Magnuson MA, Kahn CR. Loss of insulin signaling in hepatocytes leads to severe insulin resistance and progressive hepatic dysfunction. *Mol Cell*. 2000; 6: 87-97.

Miyamoto Y, Koh YH, Park YS, Fujiwara N, Sakiyama H, Misonou, Y, et al. Oxidative stress caused by inactivation of glutathione peroxidase and adaptive responses. *Biol Chem*. 2003; 384: 567-574.

Mohamed J, Nafizah AN, Zariyantey AH, Budin S. Mechanisms of diabetes-induced liver damage: the role of oxidative stress and inflammation. *Sultan Qaboos Univ Med J*. 2016; 16: e132-e141.

Ochiai Y, Kaburagi S, Okano Y, Masaki H, Ichihashi M, Funasaka Y, Sakurai H. A Zn (II)-glycine complex suppresses UVB-induced melanin production by stimulating metallothionein expression. *Int J Cosmet Sci*. 2008; 30: 105-112.

Palsamy P, Sivakumar S, Subramanian S. Resveratrol attenuates hyperglycemia-mediated oxidative stress, proinflammatory cytokines and protects hepatocytes ultrastructure in streptozotocin–nicotinamide-induced experimental diabetic rats. *Chem Biol Interact.* 2010; 186: 200-210.

Parveen K, Khan MR, Mujeeb M, Siddiqui WA. Protective effects of Pycnogenol® on hyperglycemia-induced oxidative damage in the liver of type 2 diabetic rats. *Chem Biol Interact.* 2010; 186: 219-227.

Pizzino G, Irrera N, Cucinotta M, Pallio G, Mannino F, Arcoraci V., et al. Oxidative stress: harms and benefits for human health. *Oxid Med Cell Longev.* 2017; 2017: 1-13.

Reed MA, Pories WJ, Chapman W, Pender J, Bowden R, Barakat H, et al. Roux-en-Y gastric bypass corrects hyperinsulinemia implications for the remission of type 2 diabetes. *J Clin Endocrinol Metab.* 2011; 96: 2525-2531.

Sanchez-Rangel E and Inzucchi SE. Metformin: clinical use in type 2 diabetes. *Diabetologia.* 2017; 60: 1586-1593.

Schofield CJ and Sutherland C. Disordered insulin secretion in the development of insulin resistance and Type 2 diabetes. *Diabetic Med.* 2012; 29: 972-979.

Seven A, Guzel S, Seymen O, Civelek S, Bolayirli M, Uncu M, et al. Effects of vitamin E supplementation on oxidative stress in streptozotocin induced diabetic rats: Investigation of liver and plasma. *Yonsei Med J.* 2004; 45: 703-710.

Shanik MH, Xu Y, Škrha J, Dankner R, Zick Y, Roth J. Insulin resistance and hyperinsulinemia: is hyperinsulinemia the cart or the horse?. *Diabet Care.* 2008; 31: S262-S268.

Wei Y, Chen P, de Bruyn M, Zhang W, Bremer E, Helfrich W. Carbon monoxide-releasing molecule-2 (CORM-2) attenuates acute hepatic ischemia reperfusion injury in rats. *BMC Gastroenterol.* 2010; 10: 1-9.

Wilcox G. Insulin and insulin resistance. *Clin Biochem Rev.* 2005; 26:19-39.

Yagmur E, Tacke F, Weiss C, Lahme B, Manns MP, Keifer P, et al. Elevation of Nepsilon-(carboxymethyl)lysine-modified advanced glycation end products in chronic liver disease is an indicator of liver cirrhosis. *Clin Biochem.* 2006; 39: 39-45.

Yan F, Chen Y, Azat R, Zheng X. Mulberry anthocyanin extract ameliorates oxidative damage in HepG2 cells and prolongs the lifespan of *Caenorhabditis elegans* through MAPK and Nrf2 pathways. *Oxid Med Cell Longev.* 2017; 2017: 1-12.

Ye J. Mechanisms of insulin resistance in obesity. *Front Med.* 2013; 7:14-24.

Yin L, Mano JI, Tanaka K, Wang S, Zhang M, Deng X, Zhang S. High level of reduced glutathione contributes to detoxification of lipid peroxide-derived reactive carbonyl species in transgenic *Arabidopsis* overexpressing glutathione reductase under aluminum stress. *Physiol Plant.* 2017; 161: 211-223.

Zhang Z, Liew CW, Handy DE, Zhang Y, Leopold JA, Hu J, et al. High glucose inhibits glucose-6-phosphate dehydrogenase, leading to increased oxidative stress and β -cell apoptosis. *FASEB J.* 2010; 24: 1497-1505.

Chapter 3

Consequences of hyperinsulinemia in glucose metabolism in HepG2 cells and amelioration with VA

3.1 Introduction

Recently, it is well known that the insulin resistance is recognized as the main predictor of many metabolic diseases like diabetes (Crofts et al., 2015). Briefly at the early stages, there is a minute increase in the resistance to the insulin stimulated glucose uptake, it results in the increased production of insulin from the β -cells to maintain the normoglycemia (Porte et al., 2002). But with time, the insulin resistance progresses and it will create a stress on the insulin production, up to a point they are unable to produce insulin. That time the patient enters into the impaired glucose tolerance state from normal glucose tolerance (Lustig et al., 2004). This finally results in the complete failure of β -cells and the glycemic control will be lost; it leads to the development of T2DM (Taylor et al., 2007). During the whole period before the development of T2DM and even for some time after T2DM the plasma insulin levels are very high and that condition is referred to as HI. HI by meaning is the excessive insulin production that results in insulin resistance (Rufino et al., 2017). The major consequences of HI created insulin resistance is increased HGP, reduced insulin receptor binding and up-regulated TG production in the liver; it will definitely affect hepatic glucose metabolism and insulin release (Farese et al., 2012). Liver is the only organ responsible for the glucose generation through the gluconeogenesis and also it is the main storage site of glycogen. So understanding about hepatic glucose metabolism may help to predict the pathogenic mechanisms underlying obesity and diabetes mellitus (Adeva-Andany et al., 2016). In order to study hepatic glucose metabolism I

have selected HepG2 cells because it is the most widely used cell line for many toxicity studies in the liver and also it is considered as normal cell lines. Furthermore, the liver is the main site of action of insulin and insulin has so many diverse functions in the liver such as activation of glycogen synthesis, lipogenesis and inhibition of gluconeogenesis enzymes (Gribble, 2005). So insulin has a prominent role in hepatic growth and regeneration. But during HI, HGP is increased even if the blood glucose levels are high (Schett et al., 2013). This generates hyperglycemia conditions associated with insulin resistance. The release of insulin is tightly controlled by glucose metabolism within the β -cell. During the well-fed state after digestion glucose, fatty acids and amino acids were released (Rui, 2014) and the pancreas is ready to produce insulin which facilitates the glucose uptake into the cells. In the liver, the excess glucose is either stored as glycogen or converted into fatty acids and amino acids (Rui, 2014) (Fig: 3.1). The liver is enriched with both IRS 1 and 2. When insulin interacts with these proteins they undergo autophosphorylation and activate the downstream molecule phosphatidylinositol-3-kinase (PI3K), protein kinase B (AKT) and finally leads to the increased expression of GLUT2 proteins on the membrane surface (Taniguchi et al., 2006; Thirone et al., 2006) and it results in increased glucose uptake.

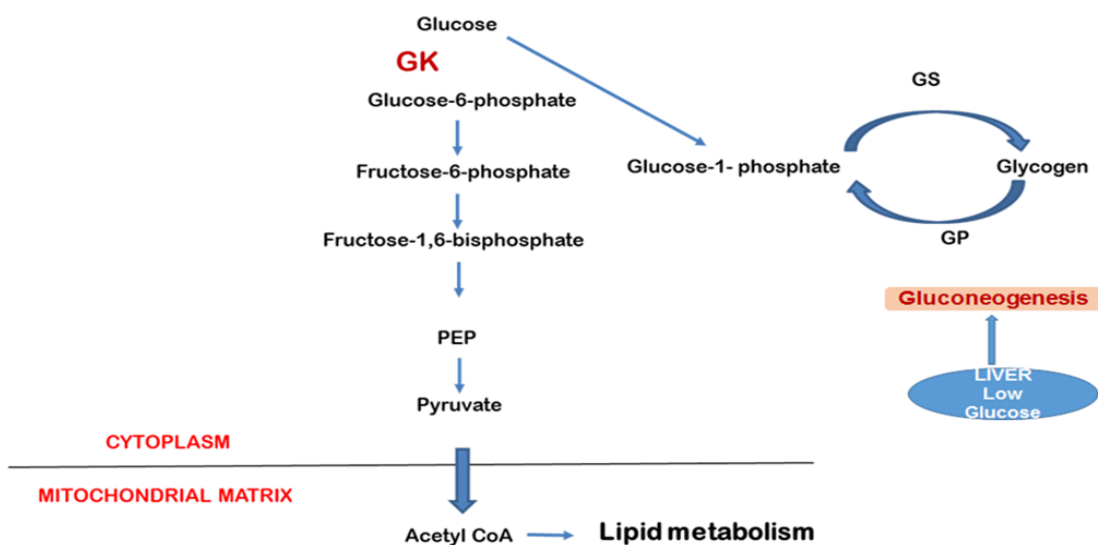


Figure. 3.1 Hepatic glucose metabolism

A previous study reported that the inhibition of both the insulin receptors in hepatocytes resulted in reduced hepatic lipogenesis and up-regulated gluconeogenesis. This condition is referred to as total insulin resistance (Dong et al., 2008; Kubota et al., 2008). In addition to this selective insulin resistance is a condition commonly seen in the liver in which the expression of IRS2 is completely inhibited whereas IRS1 expression is not altered (Kubota et al., 2016). Recent studies revealed that selective insulin resistance is the crucial underlying factor observed in the genesis of T2DM and obesity (Farese et al., 2010; Kubota et al., 2016; Shimomura et al., 2000). In this condition, the action of insulin on lipogenesis becomes unaltered or it becomes exaggerated at the same time the level of gluconeogenesis would be altered.

Despite glucose metabolism, the liver is the major site for insulin degradation (Duckworth et al., 1998). In addition to this, both kidneys and other tissues have also participated in the removal of insulin (Villa-Pérez et al., 2018). Insulin degrading enzyme (IDE) is the main protein that is responsible for the degradation of insulin. It is a zinc metalloendopeptidase and is named based on its high affinity for insulin and its removal (Villa-Pérez et al., 2018). About 50 % of circulatory insulin is degraded by the liver when they pass across the liver. The molecular mechanism behind insulin removal is receptor-mediated (Bevan, 2001).

In this chapter, I have tried to study the establishment of selective insulin resistance during HI in HepG2 cells and also I have revealed the other consequences of HI on hepatic glucose metabolism. I have focused my study on the role of HI in glycogenesis, gluconeogenesis and glycolysis in relation to the importance of GK. Also, I have attempted to check the other glucose utilizing pathways like glycation and sorbitol pathways during hyperglycemia. Furthermore, here I have studied the role of IDE in the progression of HI

created insulin resistance in HepG2 cells. Overall in this chapter, I have shown that the HI created alterations in hepatic glucose metabolism and the potential of VA against this.

3.2 Materials and methods

3.2.1 Chemicals and reagents

Dimethyl sulfoxide (DMSO), RIPA buffer, vanillic acid (VA) and metformin were purchased from Sigma Aldrich (St Louis, USA). Amino guanidine was from SRL (Mumbai, India). Dulbecco's modified eagle's medium (DMEM), fetal bovine serum (FBS), 0.5 % trypsin - ethylene diamine tetra acetic acid (Trypsin-EDTA) and pencillin- streptomycin antibiotics were from Gibco-BRL Life Technologies, USA. Glucokinase (GK), glucokinase regulatory protein (GKRP), insulin receptor substrate 1 and 2 (IRS1 & IRS2), glucose transporter 2 (GLUT 2), phosphatidyl inositol-3-kinase (PI3K), protein kinase B (AKT), phosphorylated protein kinase B (p-AKT) and phosphorylated Bcl-2 associated death receptor (p-BAD) antibodies were obtained from Santa Cruz Biotechnology (Dallas, USA). Glycogen synthase (GS), glycogen synthase kinase-3 β (GSK3 β), insulin degrading enzyme (IDE), β -actin and all other secondary antibodies were purchased from Cell Signaling Technology (Beverly, USA). Phosphoenol pyruvate carboxykinase (PEPCK), 2-[N-(7-nitrobenz-2-oxa-1,3-diazol-4-yl) amino]-2-deoxy-D-glucose (2-NBDG), receptor for advanced glycation end products (RAGE), dolichyl-diphospho-oligosaccharide-protein glycosyltransferase non-catalytic subunit (DDOST) and glucose-6-phosphatase (G-6-P) were from Abcam (UK). Recombinant human insulin was from Merck (USA). The remaining chemicals used were of analytical grade unless or otherwise mentioned.

3.2.2 Cell culture and induction of hyperinsulinemia created insulin resistance

HepG2 cells (NCCS, Pune) were cultured in DMEM supplemented with 10 % FBS, 100 U/ml penicillin and 100 µg/ml streptomycin at 5 % CO₂ and 37 °C in an incubator. The HI created insulin resistance was induced according to the previous method (Jung et al., 2017). Briefly, when the HepG2 cells reached 80 % confluence, the cells were treated with 1 µM human insulin for 24 hrs to induce insulin resistance, and the cells were co-treated with VA and metformin in 1 % serum-containing media.

Experimental groups:

C - Control

IR - HI created insulin resistance (1 µM human recombinant insulin)

VA1 - IR + 5 µM VA

VA2 - IR + 10 µM VA

M - IR + Metformin (1 mM)

The VA or metformin were co-treated with HI induced insulin resistance for 24 hrs in the experimental groups.

3.2.3 Glucose uptake using 2-NBDG

Glucose uptake was measured using fluorescent glucose analogue 2-[N-(7-nitrobenz-2-oxa-1,3-diazol-4-yl) amino]-2-deoxy-D-glucose (2-NBDG). Briefly, after respective treatments the cell culture medium was removed and washed with PBS. Cells were then incubated in the presence of a low glucose medium and simultaneously the cells are treated with VA and metformin for 3 hrs. Cells were stimulated with insulin (100 nM) for 10 min and treated with

100 μ M NBDG for 1hr. After two washes with PBS the cells were trypsinized by adding 100 μ L of 10X trypsin-EDTA and concentrated the cells by centrifuging at 20,000 x g for 15 min at 4 °C. The pellets were resuspended in PBS and again centrifuged at 20,000 x g for 15 min at 4 °C for collecting the cells. Then the pellet was mixed with PBS and filtered the content using a cell strainer. Cells are then ready to be analyzed on flow cytometer FACS Aria™ II (BD Biosciences, USA). Then intracellular glucose uptake was assessed using flow cytometry.

3.2.4 Analysis of insulin signaling pathway

The HI created insulin resistance was evaluated by the insulin signaling pathway. The major protein candidates of this pathway like IRS1, IRS2, GLUT2, PI3K, AKT/p-AKT and IDE were analyzed by western blot (for details, please refer to section 3.2.14). The expression levels of these proteins were analyzed from the densitometric data calculated using Image J software.

3.2.5 GK activity

The activity of GK was detected and quantified calorimetrically (ELISA; MyBiosource, San Deigo, USA). A microtiter plate pre-coated with an antibody specific to GK provided in the kit was used. In order to perform this assay, the cells after respective treatments, were harvested. Then both standard and 100 μ l of the sample were added into the respective wells of a microtiter plate. After 2 hrs of incubation at 37 °C the wells were washed. Then, 100 μ l of avidin conjugated horseradish peroxidase (HRP) was added to all the wells and incubated for 1hr at 37 °C. Then the wells were washed and added 90 μ l of TMB substrate solution to the wells. Then incubated for 25 min at 37 °C. Then 50 μ l of stop solution was added to terminate the reaction and immediately measured the colour change at 450 nm.

The amount of GKRP protein was quantified calorimetrically according to an ELISA method. In this assay, a 96- well plate was coated with nuclear protein samples of 50 μ l and incubated at 4 °C overnight. After this, the plate was washed five times with PBST. Then 100 μ l of GKRP

antibody (1:1000) was added and incubated for 1 hr followed by five times wash with PBST. Then added the anti-rabbit secondary antibody (1:2000) which is HRP conjugated and incubated for 1 hr. Then it was washed with PBST followed by the addition of 50 μ l of substrate solution and incubated for 20 min. After that, 50 μ l of stop solution was added to terminate the reaction and immediately read the colour change at 450 nm.

3.2.6 GK and p-BAD expression

The expression level of GK and p-BAD proteins during insulin resistance conditions were analyzed by western blotting (for details, please refer to section 3.2.14).

3.2.7 Molecular docking

Autodock v4.2 and auto dock tools were used to analyze the interaction between the GK ligand-binding domain and VA. These docking softwares were used to find the most populated cluster with the lowest binding energy, which was deemed as the most stable conformation. The 3D model of GK was taken from Brookhaven protein data bank, and the structure of VA was downloaded from Chemspider and converted to PDB format using Chem-3D Pro 10. The docking fitness of the VA to GK and the amino acids of GK involved in the interaction was predicted by using iGEMDOCK. The binding energy of VA-GK was analyzed using the software Autodock v4.2.

3.2.8 Glycogen assay and glycogenesis

The glycogen level was assayed using a kit from Abcam, UK. For this assay, the cells were seeded in a 24-well plate. After respective treatments, the cells were homogenized for 10 min on ice followed by boiling of homogenates for 10 min to inactivate the enzymes. After centrifugation the supernatant was collected. 50 μ l of supernatants (samples) and standards were added into the 96-well plate. Then 2 μ l of hydrolysis buffer (provided by the kit) was

added to all the wells and incubated for 30 min. After that, 48 μ l of reaction mix was added. Then it was incubated for 30 min at RT and the OD was measured at 450 nm. The expression levels of proteins involved in glycogen metabolism; GS and GSK-3 β were analyzed by western blotting (for details, please refer to section 2.8).

3.2.9 Studies on gluconeogenesis

The expression levels of major proteins in hepatic gluconeogenesis like PEPCK and G-6-P were evaluated at protein levels by western blotting (for details, please refer to section 3.2.14).

3.2.10 Sorbitol assay

The sorbitol levels were quantified using a kit from Biovision, USA. Briefly the cells were cultured and treated with respective treatments. Initially in order to prepare the standard curve, the working solutions of sorbitol standards were prepared by serial dilution using the stock solution (1.0 mM) provided in the kit. The sorbitol standard was diluted by taking 10 μ l of stock with 990 μ l of dH₂O. Then 0, 2, 4, 6, 8, 10 μ l of standards were added to each wells in a 96-well plate and adjusted the volume in each well with a 50 μ l assay buffer. Then 50 μ l of samples were added into the wells. Then 50 μ l of reaction mixture (assay buffer, enzyme mix, developer and probe) was added to all the wells including sample, blank and standard wells. Then it is incubated at 37 ^oC for 30 min. Then the absorbance was read at 560 nm.

3.2.11 Antiglycation activity assay

The method of Riya et al. (2015) was used to measure bovine serum albumin (BSA) derived advanced glycation end products (AGEs) with slight modifications. VA of different concentrations was added to BSA (10 mg/mL) and glucose (500 mM). Fluorescence of AGE at an excitation/emission wavelength of 370/440 nm was obtained after 24 hrs and 7 days using

the fluorescence microplate reader. The two results were compared and the percentage inhibition with VA against glycation was measured.

3.2.12 Analysis of AGE with hyperinsulinemia

The method of Rani et al. (2018) was used to analyze the AGE. Cell samples and a standard (provided with the kit) were added to the AGE conjugate coated ELISA plate provided with the kit. After 10 min incubation at RT, 50 µl of anti-AGE polyclonal antibody was added and incubated for 1 hr. The plate was washed with 250 µl 1X wash buffer. HRP conjugated secondary antibody (100 µl) was added to the wells and incubated for 1hr at RT. Substrate solution (100 µl) was added which was followed by the addition of 100 µl of stop solution and measured immediately at 450 nm using the microplate reader.

3.2.13 Analysis of glycation pathway

The major proteins involved in this pathway such as RAGE and DDOST were analyzed by western blot (for details, please refer to section 3.2.14). The expression levels of these proteins were analyzed from the densitometric data calculated using Image J software.

3.2.14. Western blot

Expression of various proteins of pharmacological and functional importance in glucose transport, insulin signaling pathway, glucose storage, glucose generation and glycation such as IRS1, IRS2, GLUT2, PI3K, AKT, p-AKT, IDE, GK, p-BAD, GS, GSK3β, PEPCK, G-6-P, RAGE and DDOST were studied using western blotting. Cells were cultured in T-25 flasks containing 5 ml DMEM medium and the respective treatments with VA were done as described above. After that the cells were harvested and lysed in a lysis buffer with a protease inhibitor cocktail and Triton X 100. Then the lysate was centrifuged at 20,000 x g for 15 min at 4 °C. The supernatant was collected and protein content was measured and normalized using a Pierce

BCA protein assay kit (Thermo Fisher Scientific Co., Waltham, MA, USA) using bovine serum albumin (BSA) as a standard and expressing the results as BSA equivalents. Samples were then run on an SDS-PAGE gel (10 %) (BioRad, Hercules, CA, USA), transferred at 25 V for 15 min to PVDF membrane (a non-reactive thermoplastic fluoropolymer produced using the polymerization of vinylidene difluoride) (Merck) using a trans blot apparatus (BioRad). The samples (25 μ l) were loaded into each well. After transfer, the PVDF membrane was blocked with 3 % BSA in tris buffered saline-Tween 20 (TBST, pH=8) for 1 hr at RT. After washing with TBST, the membrane was probed with primary antibodies (IRS1, IRS2, GLUT2, PI3K, AKT, p-AKT, IDE, GK, p-BAD, GS, GSK3 β , PEPCK, G-6-P, RAGE and DDOST, 1:1000 dilution) in TBST and incubated for 2 hrs at RT with moderate shaking. The membrane was washed three times with TBST for 10 min. HRP-conjugated secondary antibody (1:2000) was added and agitated for 90 min at RT. After three TBST washes, membranes were incubated with ECL substrate (BioRad) and the proportional thickness of bands were measured using Image Lab software in the Chemi Doc system (ChemiDoc MP Imaging System, Bio-Rad) assuming all bands were in the Beer-Lambert law region.

3.2.15 Statistical analysis

All analyses were carried out with sextuplicates and data are shown as mean \pm SEM for control and treated cells. The normality of the variables were tested using the Kolmogorov Smirnov Z test and the variables were found to be approximately normally distributed. Hence the significance difference between the groups were tested using ANOVA and further significantly different pairs ($p \leq 0.05$) were identified using Duncan's multiple comparison test. All calculations were done using the Statistical Package for the Social Sciences for Windows standard version 20 (SPSS Inc., USA).

3.3 Results

3.3.1 Flow cytometric analysis of glucose uptake

Flow cytometry results showed that in control cells the NBDG uptake was 45 %. In HI treated cells, the glucose uptake was decreased to 1.9 % compared to control cells. Here more than 40 % decrease was seen in the hyperinsulinemic group which showed the development of insulin resistance ($p \leq 0.05$). The cellular uptake of NBDG with VA of 5 μM and 10 μM concentrations showed an increased glucose uptake of 18 % and 26 % respectively. Metformin of 1 mM concentration significantly increased the glucose uptake by 40 % compared with HI created insulin-resistant cells ($p \leq 0.05$; Fig: 3.2).

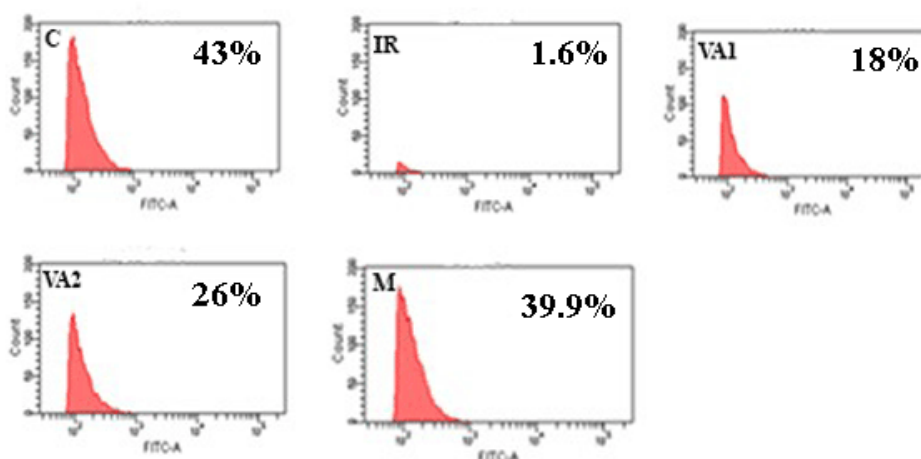


Figure. 3.2 Glucose uptake using 2-NBDG. Effect of vanillic acid on the glucose uptake using 2-NBDG in hyperinsulinemia created insulin resistant HepG2 cells using flow cytometry. C - control cells; IR - hyperinsulinemia created insulin resistant cells; VA1 - IR + 5 μM vanillic acid; VA2 - IR + 10 μM vanillic acid; M - IR + metformin (1 mM). Values are expressed as mean \pm SEM where $n=6$. * indicates that the mean value was significantly different from control cells ($p \leq 0.05$). # indicates the mean value was significantly different from IR cells ($p \leq 0.05$).

3.3.2 Effect of hyperinsulinemia created insulin resistance on the insulin signaling pathway

To evaluate the mechanism by which the defects created during HI in insulin signaling, I examined the major proteins involved in the insulin signaling pathway. Western blot data showed that the protein level expression of IRS1 does not have any alterations in the hyperinsulinemic condition compared with control cells. Also VA and metformin treatments during hyperinsulinemia created insulin resistance (IR) do not show any changes in the expression of IRS1. Meanwhile, HI down-regulated the IRS2 (36.4 %) expression compared to control. Treatment of HepG2 cells with different concentrations of VA (5 μ M and 10 μ M) and metformin significantly increased the IRS2 expression ($p \leq 0.05$; Fig: 3.3A & Fig: 3.3B) by 19.6 %, 25.4 % and 45.8 % respectively. Furthermore, IR down-regulated the expressions of other proteins in the insulin signaling pathway like GLUT2, PI3K and p-AKT by 64.8, 55.1 and 74.8 % respectively. This reveals that HI induced insulin resistance by inhibiting the insulin signaling pathway. At the same time, VA treatment increased these protein levels in a dose-dependent manner which was comparable to IR treatment. GLUT2 expression was increased significantly ($p \leq 0.05$) to 45.4, 84.3 and 137.2 % for 5 μ M and 10 μ M of VA and 1mM of metformin respectively, compared to the IR group. On treatment with different concentrations of VA and metformin, PI3K expression was up-regulated by 73.3, 73.7 and 74.5 % for 5 μ M and 10 μ M of VA and 1mM of metformin respectively (Fig: 3.3A & Fig: 3.3B). Meanwhile, VA and metformin treatment increased the protein levels of p-AKT/AKT ratio to 66.0, 77.2 and 66.3 % compared to IR groups for 5 μ M and 10 μ M of VA and 1mM of metformin respectively (Fig: 3.3A & Fig: 3.3B). Furthermore, HI inhibits the expression of IDE by 46.4 % compared with control. VA treatment of 5 μ M and 10 μ M concentrations dose-dependently increased the expression level of IDE by 64.9 and 121.6 % respectively. Metformin of 1mM concentration also up-regulated the level of IDE by 112.3 %. Over all data indicates that HI

induce the insulin resistance in HepG2 cells by inhibiting the insulin signaling pathway and down-regulating the IDE levels in hepatocytes but treatment with VA noticeably reversed the effects of HI by up regulating the levels of these proteins and this was comparable with the metformin (Fig: 3.3A & Fig: 3.3B).

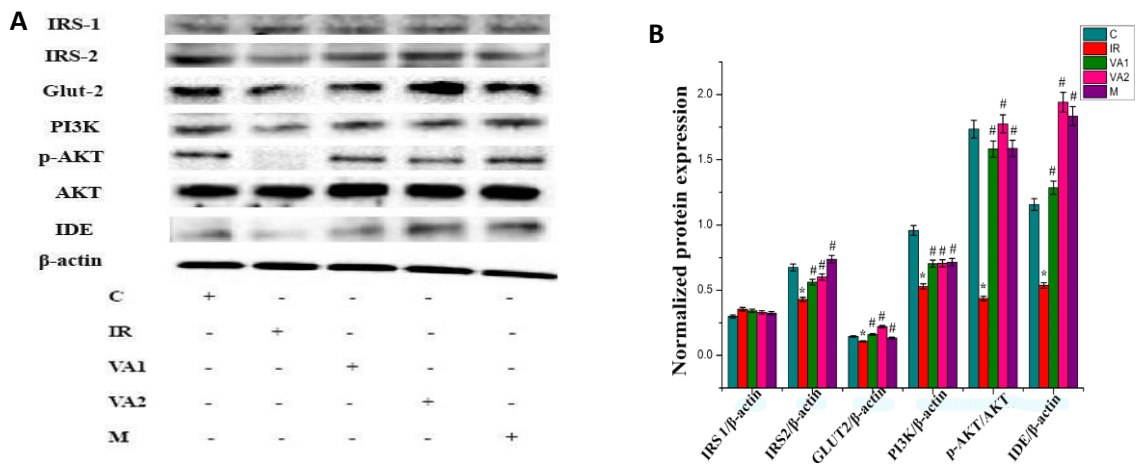


Figure 3.3 Analysis of insulin signaling pathway. (A) After VA co-treatment the cells were lysed, IRS-1, IRS-2, GLUT2, PI3K, AKT, p-AKT, IDE and β-actin expression were analyzed by western blotting. (B) Densitometric quantification of IRS-1, IRS-2, GLUT2, PI3K, AKT, p-AKT, IDE normalized to β-actin. C - control cells; IR - hyperinsulinemia created insulin resistant cells; VA1 - IR + 5 μM vanillic acid; VA2 - IR + 10 μM vanillic acid; M - IR + metformin (1 mM). Each value represents the mean ± SEM where n=6. * indicates that the mean value was significantly different from control cells ($p \leq 0.05$). # indicates the mean value was significantly different from IR cells ($p \leq 0.05$).

3.3.3 Effect of hyperinsulinemia created insulin resistance on glycolysis via the regulation of GK

GK is the rate-limiting enzyme in hepatic glycolysis. Analysis of GK activity showed a significant ($p \leq 0.05$) decrease (20 %) in IR cells compared to control cells (Fig: 3.4A). While with VA co-treatment, the level of GK was increased significantly ($p \leq 0.05$) by 15 % and 16.7 % for 5 and 10 μM concentrations compared to IR cells. Metformin caused a significant increase of the GK levels by 20 % (Fig: 3.4A). To determine how the GK is down-regulated in IR cells, the levels of GKRP were analyzed. Here I have found that in IR cells the levels of GKRP were increased (41.1 %) significantly ($p \leq 0.05$) compared to control cells. VA of both

concentrations (5 and 10 μM) significantly reduced the activity of GKRP by 21.6 % and 46.4 % respectively (Fig: 3.4B). Metformin also reduced the activity of GKRP by 41.8 % as compared to IR. Here compared with metformin VA of 10 μM concentration showed a better result (Fig: 3.4B).

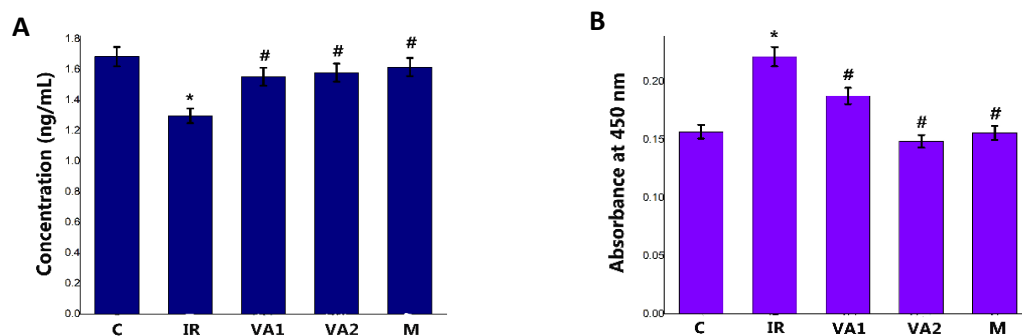


Figure. 3.4 Effect of hyperinsulinemia on glycolysis. (A) GK activity is analyzed by GK activity assay. (B) GKRP activity is analyzed by indirect ELISA. C - control cells; IR - hyperinsulinemia created insulin resistant cells; VA1 - IR + 5 μM vanillic acid; VA2 - IR + 10 μM vanillic acid; M - IR + metformin (1 mM). Data are presented as mean \pm SEM where n=6. * indicates that the mean value was significantly different from control cells ($p \leq 0.05$). # indicates the mean value was significantly different from IR cells ($p \leq 0.05$).

3.3.4 Docking of VA to GK

To determine the putative binding mode and potential ligand-target interactions of VA, it was docked to human GK using Autodock v4.2. The VA is bound to GK with a binding energy of -4.94 kcal/mol showing a stable binding affinity into the active site of GK (Fig: 3.5). The amino acid residues of GK interacting with VA are given in Figure 3.4. The result of Autodock v4.2 showed the amino acid residues in the close proximity of affinity pocket leveraged binding of VA to GK through hydrophobic as well as electrostatic interactions (Fig: 3.5). The amino acid residues of GK involved in the interactions with VA were Glu17, Leu20, Phe23, Gln24, Leu25, Gln26, Arg369, Glu372, Ser373, Val374, Thr376, Arg377 and His380 (Fig: 3.5). VA was found to form a hydrogen bond with residue Arg369 in the binding pocket of GK.

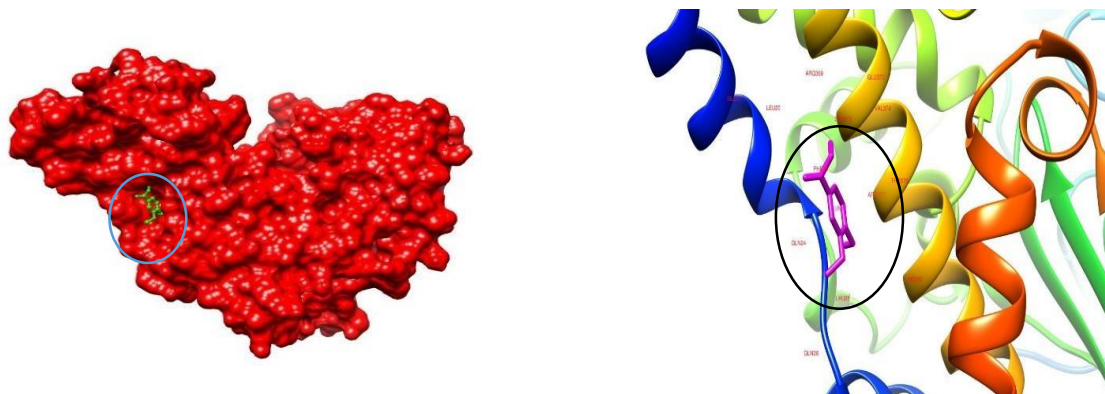


Figure. 3.5 Molecular docking. The docking model predicted interaction details between VA and GK. Hydrophobicity surface representation of human glucokinase-vanillic acid complex (Green stick: vanillic acid) and interacting amino acid residues of glucokinase with vanillic acid.

3.3.5 GK activation is linked with the hepatic p-BAD expression

Western blot analysis was performed for GK and p-BAD proteins expression analysis (Fig: 3.6A & Fig: 3.6B). IR caused a significant reduction in expression of GK (69.7 %) compared to control cells. VA co-treatment significantly up-regulated the GK expression (62.7 and 108.7 % for 5 and 10 μ M respectively; $p \leq 0.05$) compared to IR cells. Metformin group noticeably enhanced (101.2 %) the GK levels compared to IR. During IR conditions, there was a significant down-regulation in the expression of mitochondrial protein p-BAD by 58.6 % ($p \leq 0.05$) as compared to control. VA co-treatment at 5 and 10 μ M significantly ($p \leq 0.05$) up-regulated the expression of p-BAD by 58 % and 115.5 % respectively compared to IR cells. Also, metformin treatment significantly ($p \leq 0.05$) increased the p-BAD protein by 110.6 % compared to IR cells (Fig: 3.6A & Fig: 3.6B).

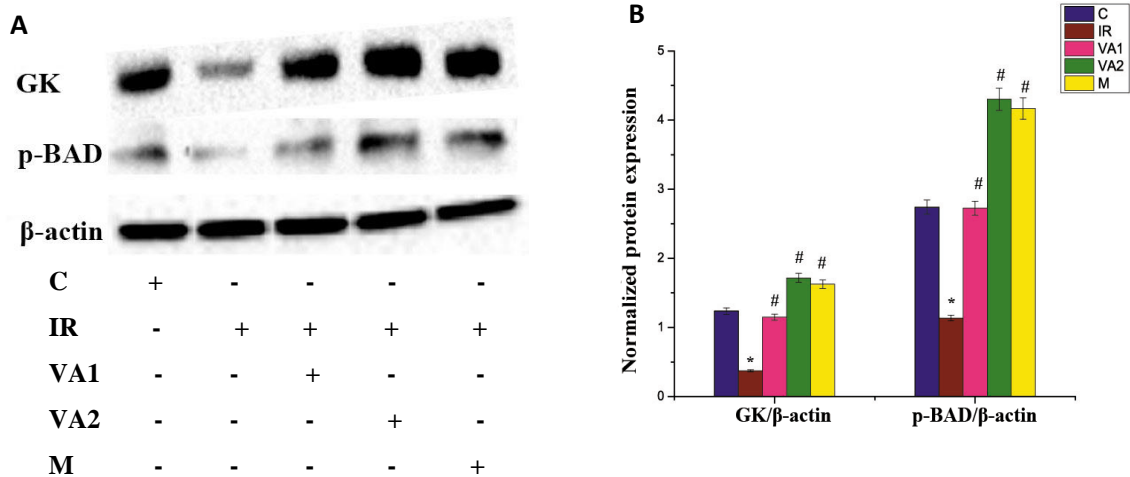


Figure 3.6 Effect of VA on GK and p-BAD. (A) After treatment with VA, the cells were lysed, and GK, p-BAD and β -actin expression were analyzed by western blotting. (B) Densitometric quantification of GK and p-BAD normalized to β -actin. C - control cells; IR - hyperinsulinemia created insulin resistant cells; VA1 - IR + 5 μ M vanillic acid; VA2 - IR + 10 μ M vanillic acid; M - IR + metformin (1 mM). The protein contents were normalized by β -actin. Each value represents the mean \pm SEM where n=6. * indicates that the mean value was significantly different from control cells ($p \leq 0.05$). # indicates the mean value was significantly different from IR cells ($p \leq 0.05$).

3.3.6 Hyperinsulinemia enhances the glycogenesis in the liver

During hyperinsulinemia created insulin resistance conditions, the glycogen level was decreased drastically (46.6 %) as compared to control cells (Fig: 3.7A & Fig: 3.7B). While with VA, the level of glycogen was increased significantly by 30.7 % and 41.9 % ($p \leq 0.05$) for 5 and 10 μ M concentrations respectively compared to IR cells (Fig: 3.7A & Fig: 3.7B). Metformin also significantly enhanced the glycogen content of IR cells by 42.2 % as compared to IR cells. This was also confirmed by western blot data. Here I have checked the expression of both GS and GSK-3 β (Fig: 3.7A & Fig: 3.7B). The result showed that there was a significant reduction in the GS enzyme by 38.7 % ($p \leq 0.05$) and up-regulation of GSK-3 β by 123.5 % ($p \leq 0.05$; Fig: 3.7A & Fig: 3.7B) in IR cells. The co-treatment of VA (5 and 10 μ M) caused 29.7 % and 84.1 % increase in GS activity and 85.7 % and 94.7 % decrease in GSK-3 β compared to IR cells respectively. Metformin co-treatment also significantly increased the GS enzyme

by 85.2 % and decreased the GSK-3 β by 79.1 % compared to the IR cells (Fig: 3.7A & Fig: 3.7B)

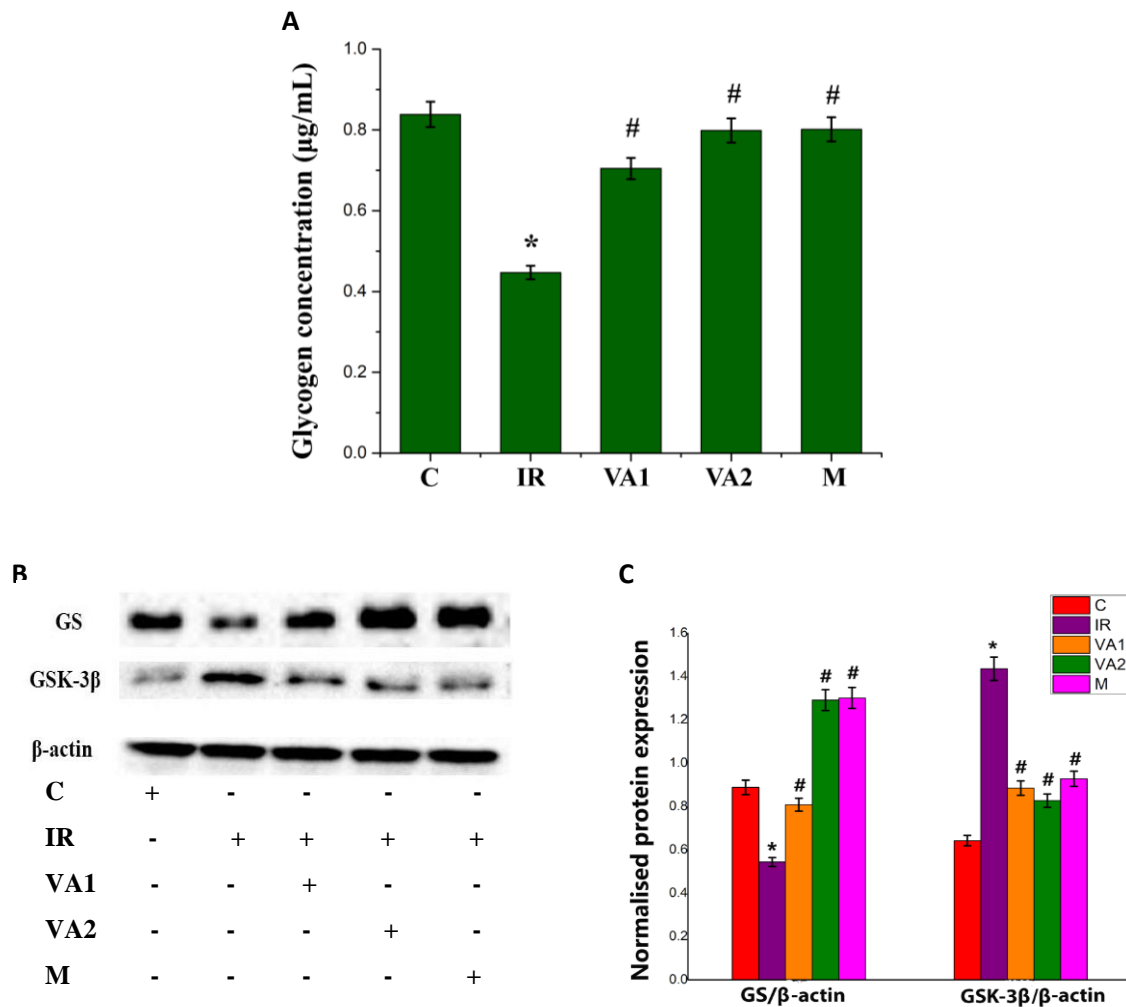


Figure 3.7 Hyperinsulinemia and glycogenesis. (A) Glycogen assay (B) After VA co-treatment the cells were lysed, and GS, GSK-3 β and β -actin expression were analyzed by western blotting. (C) Densitometric quantification of GS and GSK-3 β were normalized to β -actin. C - control cells; IR - hyperinsulinemia created insulin resistant cells; VA1 - IR + 5 μ M vanillic acid; VA2 - IR + 10 μ M vanillic acid; M - IR + metformin (1 mM). Each value represents the mean \pm SEM where n=6. * indicates that the mean value was significantly different from control cells ($p \leq 0.05$). # indicates the mean value was significantly different from IR cells ($p \leq 0.05$).

3.3.7 Effect of hyperinsulinemia on hepatic gluconeogenesis

Here, I have found that during IR, the expression of PEPCK and G-6-P were significantly increased; 58.7 % and 101.7 % respectively as compared to control. VA co-treatment down-regulated the expression of PEPCK by 45.4 % at 5 μ M and by 80.5 % at 10 μ M ($p \leq 0.05$)

compared with IR (Fig: 3.8A & Fig: 3.8B). Also VA dose-dependently decreased G-6-P expression by 9 % at 5 μ M and by 49 % at 10 μ M concentrations as compared to IR cells (Fig: 3.8A & Fig: 3.8B). Metformin significantly reduced the expression of both PEPCK and G-6-P by 132.2 % and 110.5 % respectively when compared to IR.

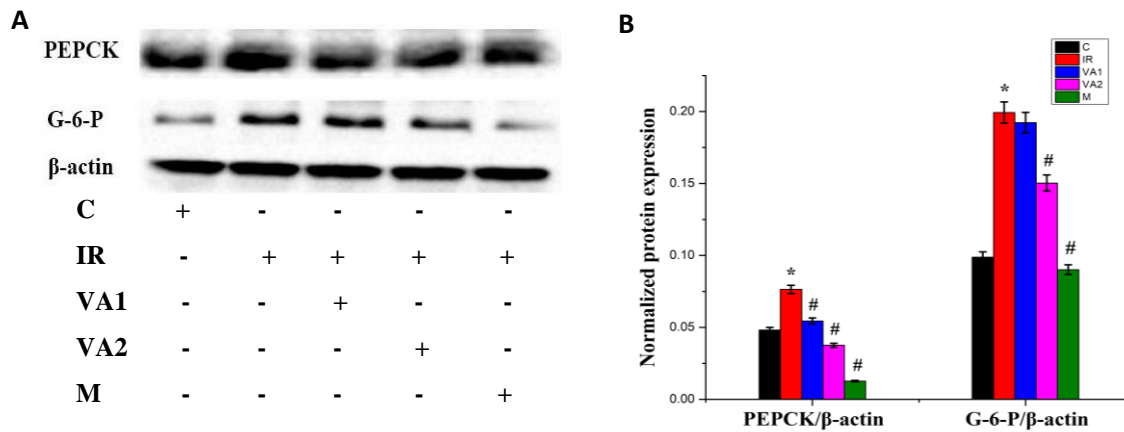


Figure 3.8 Effect of hyperinsulinemia in gluconeogenesis. (A) After VA co-treatment the cells were lysed, and PEPCK, G-6-P and β -actin expression were analyzed by western blotting. (B) Densitometric quantification of PEPCK and G-6-P were normalized to β -actin. C - control cells; IR - hyperinsulinemia created insulin resistant cells; VA1 - IR + 5 μ M vanillic acid; VA2 - IR + 10 μ M vanillic acid; M - IR + metformin (1 mM). Each value represents the mean \pm SEM where n=6. * indicates that the mean value was significantly different from control cells ($p \leq 0.05$). # indicates the mean value was significantly different from IR cells ($p \leq 0.05$).

3.3.8 Sorbitol assay

During hyperglycemic conditions, the glucose enters into the polyol pathway and produces sorbitol. Sorbitol accumulation was also determined in the IR cells and found that the IR cells showed a significant increase in sorbitol accumulation (220 %) as compared with control (Fig: 3.9). VA caused a significant decrease ($p \leq 0.05$) in the sorbitol level by 96.0, and 149.5 % with 5 μ M and 10 μ M doses of VA respectively (Fig: 3.9). Metformin of 1mM concentration significantly increased the sorbitol level by 165.1 % compared with IR.

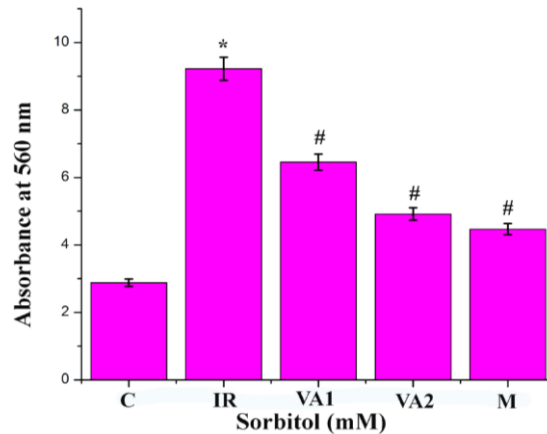


Figure. 3.9 Effect of VA on polyol pathway. C - control cells; IR - hyperinsulinemia created insulin resistant cells; VA1 - IR + 5 μ M vanillic acid; VA2 - IR + 10 μ M vanillic acid; M - IR + metformin (1 mM). Each value represents the mean \pm SEM where n=6. * indicates that the mean value was significantly different from control cells ($p \leq 0.05$). # indicates the mean value was significantly different from IR cells ($p \leq 0.05$).

3.3.9 Antiglycation capacity of VA

VA showed a dose-response inhibition of glycation (IC₅₀; 397 μ M). The half maximal inhibitory concentration (IC₅₀) is a measure of the potency of a substance in inhibiting a specific biological or biochemical function. The effect of VA was better than that of the aminoguanidine, as the positive control (IC₅₀; 500 μ M; Fig: 3.10).

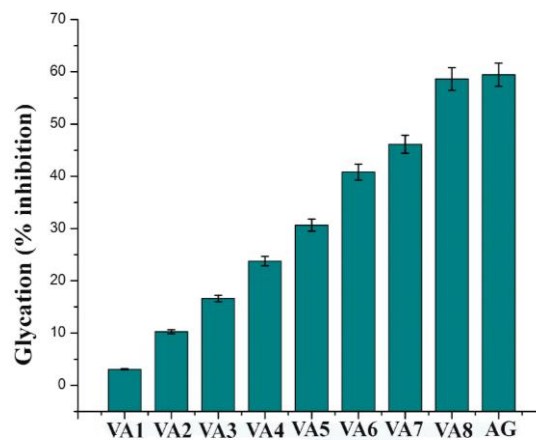


Figure. 3.10 Antiglycation capacity of VA. Evaluation of antiglycation effect of VA; Ex λ 370 nm, Em λ 440 nm. Different concentrations of vanillic acid (VA1 - 5 μ M, VA2 - 10 μ M, VA3 - 50 μ M, VA4 - 100 μ M, VA5 - 150

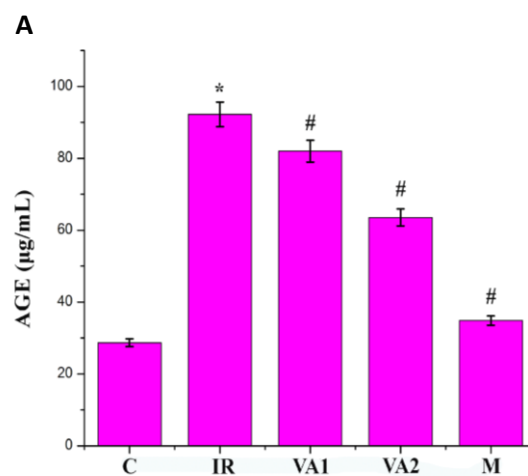
μM , VA6 - 200 μM , VA7 - 250 μM , VA8 - 500 μM) were used, IC50 -397 $\mu\text{M}/\text{ml}$. Amino guanidine (AG) was used as a reference (IC50 - 500 μM). Values are expressed as mean \pm SEM where $n=6$.

3.3.10 Production of AGE during high insulin

IR showed an increased level of AGE (221 %) as compared to control. While with VA, the formation of AGE was reduced by 232 and 252 % for 5 and 10 μM , respectively, with IR. Metformin significantly reduced the AGE levels by 283 % (Fig: 3.11A).

Western blotting was done for DDOST and RAGE proteins. IR caused a significant increase in the expression of RAGE (120 %) compared to control. VA co-treatment significantly decreased the expression of RAGE (147 and 165 % for 5 and 10 μM ; $p \leq 0.05$) compared to the IR group (Fig: 3.11B & Fig: 3.11C).

Metformin significantly ($p \leq 0.05$) decreased RAGE levels by 168 %. Expression of DDOST was reduced by 34.5 % in IR cells compared to control cells. But VA co-treatment at 5 and 10 μM concentrations significantly ($p \leq 0.05$) increased the DDOST protein levels by 56.1 and 63.3 %, respectively, compared to IR. Metformin also increased the DDOST levels by 68.9 % compared to IR cells (Fig: 3.11B & Fig: 3.11C).



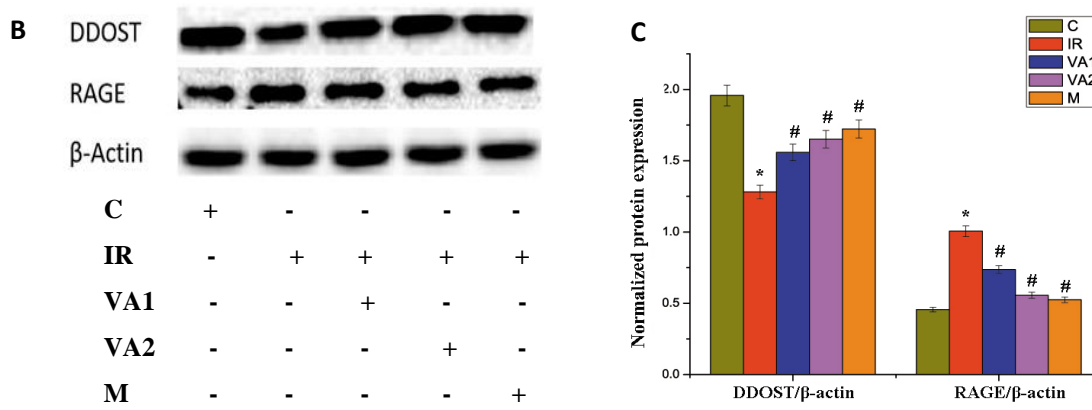


Figure. 3.11 Hyperinsulinemia and glycation. (A) Quantification of advanced glycation end products (AGEs) content. (B) After VA co-treatment the cells were lysed, DDOST (Dolichyl-diphospho oligosaccharide-protein glycosyltransferase), RAGE (Receptor for advanced glycation end products) and β -actin expression were analyzed by western blotting. (C) Densitometric analysis of protein expression of RAGE and DDOST, normalized to β -actin. C - control cells; IR - hyperinsulinemia created insulin resistant cells; VA1 - IR + 5 μ M vanillic acid; VA2 - IR + 10 μ M vanillic acid; M - IR + metformin (1 mM). Values are expressed as mean \pm SEM where n=6. * indicates that the mean value was significantly different from control cells ($p \leq 0.05$). # indicates the mean value was significantly different from IR cells ($p \leq 0.05$).

3.4 Discussion

Increased endogenous glucose production via hepatic glucose output is one of the major characteristics of T2DM. In this chapter, I focused on both the hepatic glucose metabolism in relation with the mitochondrial dysfunction in HI. The basic knowledge about hepatic glucose metabolism helps to reduce the occurrence of metabolic alterations like T2DM, fatty liver diseases and obesity. Here I examined both the expressions of the vital proteins in the insulin signaling pathway and the role of IDE in HI. In addition to this, I have studied hepatic glucose metabolism by analyzing glycolysis, glycogenesis, and gluconeogenesis. Furthermore, I analyzed the other utilization ways of glucose in HI such as the polyol pathway and the glycation. In addition to this, I have also analyzed the effects of VA and metformin in the hyperinsulinemic HepG2 cells. Impairments in glucose metabolism are the crucial player behind the genesis of many of the diseases (Adeva-Andany et al., 2016).

The liver is the central organ responsible for glucose homeostasis. Glucose enters into the liver through a portal vein and stores the glucose as glycogen and triglycerides. During fasting conditions, the glucose is released into the blood through gluconeogenesis or glycogenolysis and maintains normoglycemia. Furthermore, the liver is the main target site of insulin. Here insulin stimulates glucose uptake and activates glycogen synthesis meanwhile it inhibits gluconeogenesis and glycogenolysis. The liver is enriched with both IRS1 and IRS2 because they are the exclusive players for the regulation of insulin receptor signaling (Kubota et al., 2008). Both the receptors interact with the downstream molecules and maintain the normal metabolism of the cell. The impaired insulin signaling pathway is a hallmark of the development of hepatic insulin resistance. Many reports revealed that in insulin resistance, the insulin signaling pathway is fully inhibited by the total failure of insulin receptors (Farese et al., 2012). This condition is referred to as total insulin resistance and under this condition,

gluconeogenesis is increased and lipogenesis is decreased. In selective insulin resistance, these two conditions were coexisting in the liver (Dong et al., 2008, Kubota et al., 2008). Selective insulin resistance is the pathogenic paradox underlying the development of T2DM and obesity. As a result, the action of insulin on the hepatic gluconeogenesis is altered but the hepatic lipogenic pathway is intact or it becomes up-regulated (Farese et al., 2010) which leads to the development of both hyperglycemia and steatosis in liver (Brown and Goldstein, 2008). Recent reports suggested that mice lacking hepatic IRS2 expression but having unaltered IRS1 expression resulted in the development of selective insulin resistance, meanwhile, in total insulin resistance, both IRS1 and IRS2 expression were decreased (Kubota et al., 2016). Similarly, our study also observed that the IRS1 expression is unaltered in HI treated groups while the IRS2 expression was decreased. This data suggests the possibility of the occurrence of selective insulin resistance rather than total insulin resistance in HI treated cells. One of the studies discovered that in the liver of T2DM patients the IRS2 mediated signaling is impaired and the IRS1 expression remains unaltered. Besides this, the liver biopsy data obtained from NAFLD patients have been showing an intact or increased IRS1 expression and a reduced IRS2 expression (Kubota et al., 2016).

Normal insulin signaling is essential for maintaining glucose homeostasis. So in this study, I have checked the expression levels of the components of the insulin signaling pathway such as PI3K and AKT. Here, I have found that in hyperinsulinemic conditions both the PI3K levels and the p-AKT expressions were reduced significantly. The decreased levels of these proteins are expected to be a responsible factor for the inhibition of the insulin signaling pathway under the condition of selective insulin resistance. While considering the glucose uptake, insulin stimulates the glucose entry inside the liver. The glucose entering inside the hepatocytes is through glucose transporters and its entry is depending on the concentration gradient (Adeva-Andany et al., 2016). One of the major glucose transporters in hepatocytes is

GLUT2, it facilitates the bidirectional flow of glucose across the membrane (Takeda et al., 1993). In our result also the glucose uptake is significantly decreased in HI-created insulin-resistant groups and this is because of the decreased expression of GLUT2 on the hepatocytes cell membrane. So HI has a role in the decreased expression of GLUT2 and thereby reduced the glucose uptake in HepG2 cells. HI caused a decrease of glucose uptake of more than 40 % as compared with control cells. HI is related to obesity and is a major risk factor for insulin resistance. One of the crucial factors for the development of HI is the reduction of insulin clearance and increased insulin secretion (Corkey, 2012; Ye, 2013).

Constant insulin degradation in our body appears to be an essential component in the normal metabolic regulation in the liver. IDE is the major protein participating in hepatic insulin clearance because of its high affinity towards insulin (Villa-Pérez et al., 2018). IDE is one of the potential targets in the regulation of T2DM and it controls the circulating insulin in a degradation dependent mechanism (Wei et al., 2014). The liver is the primary clearance site of insulin. Inside the liver the insulin degradation is receptor-mediated and about 50 % of insulin is degraded by this enzyme (Bevan, 2001). Consistent with the functional role of IDE in insulin clearance the mice lacking the IDE gene showed chronic HI due to reduced insulin clearance (Abdul-Hay et al., 2011). In mice, IDE inactivation using a gene knockout mechanism develops HI and insulin resistance (Farris et al., 2003). Here also I have observed a decreased expression of IDE in the HI treated group which indicates the development of HI and insulin resistance. VA treatment improves insulin resistance by activating the major proteins in the insulin signaling pathway and which would be expected to ameliorate HI. VA restores the IRS2 and GLUT2 expressions thereby improving blood glucose levels. Furthermore, VA significantly up-regulates the IDE levels in hyperinsulinemic cells this will further decrease the circulating levels of insulin which would result in normal glucose homeostasis.

When the glucose is entering inside the hepatocytes it undergoes glycolysis and generates energy for the normal metabolism of the cell. Within the cells, the major enzyme which trapped the glucose by forming glucose-6-phosphate (G6P) is GK (Adeva-Andany et al., 2016). GK is the predominant hexokinase expressed in the liver, it has a major role in hepatic glucose disposal and glucose output (Agius, 2009). The generation of G6P is an energy-dependent process (Ahn et al., 2009) and the enzyme GK has a low affinity towards glucose (Adeva-Andany et al., 2016). There are reports to argue that GK therapy is a more effective preventive measure in T2DM because it is especially important for glucose homeostasis (Agius, 2009). GK in the liver is activated during the hyperglycemic condition. Activated GK suddenly triggers the disposal of postprandial blood glucose (Agius, 2009). In fact, a decrease in GK activity has been reported in patients with T2DM (Roach, 2002). In my study, I have revealed the alterations in GK activity during HI in HepG2 cells and amelioration with VA. According to the data, the GK activity was down-regulated in the HI treated cells as compared with the control cells which result in hyperglycemia. So that hyperglycemia will be developed. But VA treatment dose-dependently increases the GK activity and reduces hyperglycemia. GK is the rate-limiting enzyme of glycolysis. VA up-regulates the GK level in HI treated cells and activates glycolysis through which reduced hyperglycemia. Animal studies showed that even a small mutation in GK protein level has a noticeable effect on blood glucose homeostasis (Roach, 2002). There are reports in diabetic patients that the liver GK activity has been reduced which suggest that hepatic GK may have a role in T2DM (Hariharan et al., 1997). Regulation of GK is carried out by the activity of glucokinase regulatory protein (GKRP). In the liver, GKRP is the best-characterized interaction partner of GK. GKRP acts as a predominant competitor of the glucose molecule and an inhibitor of GK (Kamata et al., 2004). Dissociation of both GK and GKRP is carried out only at high glucose concentrations (Ueta et al., 2014). In this study, the GKRP levels become increased in the HI treated group as compared with the

control. HI decreased the GK activity through the up-regulation of GKRP. VA dose-dependently reversed the condition by increasing the activity of GK and decreased the GKRP activity.

GK is situated in mitochondria and forms a hetero pentameric complex on the mitochondrial membrane. Among these members, BAD is the main critical component of the complex and it integrates glycolysis and apoptosis via interaction with GK (Giménez-Cassina et al., 2014). The hepatic loss of p-BAD is linked to reduced glycolysis and enhanced gluconeogenesis. When the phosphorylated BAD level increases it activates GK and promotes glycolysis, and when the p-BAD level is diminished, it will down-regulate the glycolysis and enhances the gluconeogenesis (Giménez-Cassina et al., 2014). p-BAD activates the GK and enhances the glucose metabolism in the liver and pancreas (Danial et al., 2008). So I checked the expression level of p-BAD in HI treated cells and the effect of VA on it. In HI treated cells the p-BAD level was decreased significantly as compared to control cells. VA reversed this condition by increased expression of p-BAD and through this way it up-regulated the GK levels. From our data, it is evident that VA is an activator of GK via BAD. This was confirmed with my docking data too. According to our docking results, the binding of VA to GK is through hydrophobic and electrostatic interactions. In addition to this, the binding energy for this interaction is -4.94 kcal/mol. This means VA was stably placed in the active site of GK and promotes glucose consumption in hepatocytes. Meanwhile, docking results also revealed that VA formed a hydrogen bond with Arg369 residue in the binding pocket of GK. From these results, it was suggested that VA could promote the activation of GK and up-regulate the GK level in HI treated cells.

In the human liver, the major quantitative pathway for glucose utilization is glycogen synthesis (Adeva-Andany et al., 2016). G6P is the precursor for glycogen synthesis and is supplied by GK. During insulin resistance conditions, the amount of glycogen becomes down-

regulated by the inhibition of the GS enzyme (Irimia et al., 2017). I have also reported the same result that during hyperinsulinemia created insulin resistance condition in the HepG2 cells, the glycogen level was decreased. Increased G6P allosterically activates GS protein (McDevitt et al., 2001). Impairment of GK during T2DM decreases the G6P level and subsequently reduces glycogenesis (Roach, 2002). Another enzyme that takes part in the glycogen synthesis is glycogen synthase kinase-3 β (GSK-3 β), which inactivates GS and the decreased glycogen stores in the liver (Mitro et al., 2007). It is a negative regulator of glycogenesis. During diabetic conditions the GSK-3 β level increases (Han et al., 2016). From this data, it is evident that during hyperinsulinemia created insulin resistance conditions, the level of GSK-3 β is high, which decreases GS enzyme and decreases glycogenesis. VA treatment inhibits the GSK-3 β expression thereby increasing glycogen synthesis.

In addition to glucose utilization, the human liver releases glucose to the bloodstream either through glycogenolysis or from gluconeogenesis (Adina-Zada et al., 2012; Adkins et al., 2003). The unique ability of this organ to control glucose production and storage is important for maintaining normal blood glucose during fasting or starvation (Hariharan et al., 1997). In patients with T2DM, gluconeogenesis has been identified as the primary source of glucose production, while glycogenolysis was found not to contribute (Petersen et al., 2017). So next, I have investigated the contributors of the HGP during hyperinsulinemia created insulin resistance in HepG2 cells. Gluconeogenesis is the *de novo* synthesis of glucose, initiated in the mitochondria from pyruvate, and finally, glucose is generated in the cytosol (Rizza, 2010). Increased HGP is mainly due to the overexpression of PEPCK and glucose-6-phosphatase (G-6-P) (Rui, 2011). PEPCK is the rate regulator of gluconeogenesis (Rizza, 2010) and after several reverse steps of glycolysis, G-6-P is involved in the final step of glucose generation in the liver. Proteins involved in gluconeogenesis and GK action are acted in the opposite direction, so a coordinated regulation is essential to control the hepatic glucose input and

output. I have found that hyperinsulinemia created insulin resistance increased gluconeogenesis through the increased expression of G-6-P and PEPCK levels while VA decreased gluconeogenesis and increased glycolysis and glycogenesis.

Furthermore, glucose acts as an initial factor for the activation of the polyol pathway and a precursor molecule for glycosylation reactions (Qiu et al., 2012). The polyol pathway is the glucose utilization pathway and the major enzymes that participated in this pathway include aldose reductase and sorbitol dehydrogenase (Qiu et al., 2012). Sorbitol is the primary product of this pathway and was produced by the action of aldose reductase (Qiu et al., 2012). One of the studies reported that the sorbitol pathway can play an important role in the progression of T2DM complications (Yabe-Nishimura, 1998). It has been reported that in diabetic patients the increased level of sorbitol was observed (Yoshii et al., 2001). In this investigation, I demonstrated that HI up-regulated the sorbitol levels in HepG2 cells were down-regulated by the action of VA. I have found an abnormal accumulation of sorbitol in HI treated cells. Sorbitol level in the HI treated group was 220.3 % higher than in the control.

Hyperglycemia is the main inducer of the non-enzymatic glycation of proteins which result in the production of AGEs (Bierhaus et al., 2005). Glycation is one among various pathological complications of diabetes; it has a significant role in the induction of micro-and macro-vascular complications (Brownlee, 2000). The liver is not only the main target site of AGEs but also a site for clearing circulating AGEs (Tang and Chen, 2014). Effects of AGEs are dependent on the membrane receptors like RAGE and AGE receptor-1 (AGE-R1) (Tang and Chen, 2014). RAGE-AGE axis is the main contributor to hepatic insulin resistance in diabetic patients (Yamagishi et al., 2015). Glycation probably acts as an amplifier in the case of insulin resistance. In diabetes, almost all proteins undergo glycation and produce AGEs (Ahmed, 2005). Insulin is the major protein subjected to glycation and it produces impaired insulin (Song and Schmidt, 2012). Increased levels of AGEs and up-regulated expression of

RAGE confirmed the induction of severe glycation in the hyperinsulinemic group. Overexpression of AGE alters innate antioxidant defense status (Nowotny et al., 2015). Therefore, the enzymes become ineffective in neutralizing the reactive radicals and accelerate the OS observed (Maritim et al., 2003). In the previous chapter, I observed that in HI treated cells the OS is ameliorated and here I suggested that one of the reasons for the progression of OS is glycation. Furthermore, this data showed a significant decrease in the expression of DDOST in the hyperinsulinemic group that means the progression of glycation. In the second chapter, I have shown that VA reduced the OS. This is consistent with the current study. Here VA decreased the glycation by down-regulating the level of RAGE. So the antiglycation property of VA will have a significant role in the development of VA-based nutraceuticals.

Reference

Abdul-Hay SO, Kang D, McBride M, Li L, Zhao J, Leissring MA. Deletion of insulin-degrading enzyme elicits antipodal, age-dependent effects on glucose and insulin tolerance. *PloS One*. 2011; 6: 1-6.

Adeva-Andany MM, Pérez-Felpete N, Fernández-Fernández C, Donapetry-García C, Pazos-García C. Liver glucose metabolism in humans. *Biosci Rep*. 2016; 36: 1-15.

Adina-Zada A, Zeczycki TN, Attwood PV. Regulation of the structure and activity of pyruvate carboxylase by acetyl CoA. *Arch Biochem Biophys*. 2012; 519: 118-130.

Adkins A, Basu R, Persson M, Dicke B, Shah P, Vella A, et al. Higher insulin concentrations are required to suppress gluconeogenesis than glycogenolysis in nondiabetic humans. *Diabetes*. 2003; 52: 2213-2220.

Agius L. Targeting hepatic glucokinase in type 2 diabetes: weighing the benefits and risks. *Diabetes*. 2009; 58:18-20.

Ahmed N. Advanced glycation end product-Role in pathology of diabetic complications. *Diabetes Res Clin Pract*. 2005; 67: 3-21.

Ahn KJ, Kim J, Yun M, Park JH, Lee JD. Enzymatic properties of the N- and C-terminal halves of human hexokinase II. *BMB Rep*. 2009; 42: 350-355

Bevan P. Insulin signalling. *J Cell Sci*. 2001; 114: 1429-1430.

Bierhaus A, Humpert PM, Morcos M, Wendt T, Chavakis T, Arnold B, et al. Understanding RAGE, the receptor for advanced glycation end products. *J Mol Med*. 2005; 83: 876-886.

Brown MS and Goldstein JL. Selective versus total insulin resistance: a pathogenic paradox. *Cell Metab.* 2008; 7: 95-96.

Brownlee, M. Negative consequences of glycation. *Metab.* 2000; 49: 9-13.

Corkey BE. Banting lecture 2011: hyperinsulinemia: cause or consequence? *Diabetes.* 2012; 61: 4-13.

Crofts CAP, Zinn C, Wheldon M, Schofield G. Hyperinsulinemia: A unifying theory of chronic disease. *Diabetes.* 2015; 1: 34-43.

Daniel NN, Walensky LD, Zhang CY, Choi CS, Fisher JK, Molina AJA, et al. Dual role of proapoptotic BAD in insulin secretion and beta cell survival. *Nat Med.* 2008; 14: 144-153.

Dong XC, Copps KD, Guo S, Li Y, Kollipara R, DePinho RA, et al. Inactivation of hepatic Foxo1 by insulin signaling is required for adaptive nutrient homeostasis and endocrine growth regulation. *Cell Metab.* 2008; 8: 65-76.

Duckworth WC, Bennett RG, Hamel FG. Insulin degradation: progress and potential. *Endocr Rev.* 1998; 19: 608-624.

Farese RV and Sajan MP. Metabolic functions of atypical protein kinase C: “good” and “bad” as defined by nutritional status. *Am J Physiol Endocrinol Metab.* 2010; 298: E385-E394.

Farese RV, Zechner R, Newgard CB, Walther TC. The problem of establishing relationships between hepatic steatosis and hepatic insulin resistance. *Cell Metab.* 2012; 15: 570-573.

Farris W, Mansourian S, Chang Y, Lindsley L, Eckman EA, Frosch MP, et al. Insulin-degrading enzyme regulates the levels of insulin, amyloid β -protein, and the β -amyloid precursor protein intracellular domain in vivo. *Proc Natl Acad Sci U.S.A.* 2003; 100: 4162-4167.

Giménez-Cassina A, Garcia-Haro L, Choi CS, Osundiji MA, Lane EA, Huang H, et al. Regulation of hepatic energy metabolism and gluconeogenesis by BAD. *Cell Metab.* 2014; 19: 272-284.

Gribble FM. A higher power for insulin. *Nature.* 2005; 434: 965-966.

Han HS, Kang G, Kim JS, Choi BH, Koo SH. Regulation of glucose metabolism from a liver-centric perspective. *Exp Mol Med.* 2016; 48: 1-10.

Hariharan N, Farrelly D, Hagan D, Hillyer D, Arbeeny C, Sabrah T, et al. Expression of human hepatic glucokinase in transgenic mice liver results in decreased glucose levels and reduced body weight. *Diabetes.* 1997; 46:11-16.

Irimia JM, Meyer CM, Segvich DM, Surendran S, DePaoli-Roach AA, Morral N, et al. Lack of liver glycogen causes hepatic insulin resistance and steatosis in mice. *J Biol Chem.* 2017; 292: 10455-10464.

Jung HA, Ali MY, Bhakta HK, Min BS, Choi JS. Prunin is a highly potent flavonoid from *Prunus davidiana* stems that inhibits protein tyrosine phosphatase 1B and stimulates glucose uptake in insulin-resistant HepG2 cells. *Arch Pharm Res.* 2017; 40: 37-48.

Kamata K, Mitsuya M, Nishimura T, Eiki J, Nagata Y. Structural basis for allosteric regulation of the monomeric allosteric enzyme human glucokinase. *Structure.* 2004; 12: 429-438

Kubota N, Kubota T, Itoh S, Kumagai H, Kozono H, Takamoto I, et al. Dynamic functional relay between insulin receptor substrate 1 and 2 in hepatic insulin signaling during fasting and feeding. *Cell Metab.* 2008; 8: 49-64.

Kubota N, Kubota T, Kajiwara E, Iwamura T, Kumagai H, Watanabe T, et al. Differential hepatic distribution of insulin receptor substrates causes selective insulin resistance in diabetes and obesity. *Nat Commun.* 2016; 7: 1-16.

Lustig RH, Sen S, Soberman JE, Velasquez-Mieyer PA. Obesity, leptin resistance, and the effects of insulin reduction. *Int J Obes.* 2004; 28: 1344-1348.

Maritim AC, Sanders A, Watkins Iii JB. Diabetes, oxidative stress, and antioxidants: A review. *J Biochem Mol Toxicol.* 2003; 17: 24-38.

McDevitt RM, Bott SJ, Harding M, Coward WA, Bluck LJ, Prentice AM. De novo lipogenesis during controlled overfeeding with sucrose or glucose in lean and obese women. *Am J Clin Nutr.* 2001; 74: 737-746.

Mitro N, Mak PA, Vargas L, Godio C, Hampton E, Molteni V, et al. The nuclear receptor LXR is a glucose sensor. *Nature.* 2007; 445: 219-223.

Nowotny K, Jung T, Höhn A, Weber D, Grune T. Advanced glycation end products and oxidative stress in type 2 diabetes mellitus. *Biomolecules.* 2015; 5: 194-222.

Petersen MC, Vatner DF, Shulman GI. Regulation of hepatic glucose metabolism in health and disease. *Nat Rev Endocrinol.* 2017; 13: 572-587.

Porte Jr D, Baskin DG, Schwartz MW. Leptin and insulin action in the central nervous system. *Nutrition reviews.* 2002; 60: S20-S29.

Qiu L, Lin J, Xu F, Gao Y, Zhang C, Liu Y, et al. Inhibition of Aldose Reductase Activates Hepatic Peroxisome Proliferator-Activated Receptor and Ameliorates Hepatosteatosis in Diabetic db/db Mice. *Exp Diabetes Res.* 2012; 2012: 1-8.

Rani MP, Anupama N, Sreelekshmi M, Raghu KG. Chlorogenic acid attenuates glucotoxicity in H9c2 cells via inhibition of glycation and PKC α up-regulation and safeguarding innate antioxidant status. *Biomed Pharmacother.* 2018; 100: 467-477.

Riya MP, Antu KA, Pal S, Chandrakanth KC, Anilkumar KS, Tamrakar AK, et al. Antidiabetic property of *Aerva lanata* (L.) Juss. ex Schult. is mediated by inhibition of alpha glucosidase, protein glycation and stimulation of adipogenesis. *J Diabetes.* 2015; 7: 548-561.

Rizza RA. Pathogenesis of fasting and postprandial hyperglycemia in type 2 diabetes: implications for therapy. *Diabetes.* 2010; 59: 2697-2707.

Roach PJ. Glycogen and its metabolism. *Curr Mol Med.* 2002; 2:101-120.

Rufino AT, Ribeiro M, Pinto Ferreira J, Judas F, Mendes AF. Hyperglycemia and hyperinsulinemia-like conditions independently induce inflammatory responses in human chondrocytes. *J Funct Morphol Kinesiol.* 2017; 2: 1-10.

Rui L. Energy metabolism in the liver. *Compr Physiol.* 2014; 4: 177-197.

Schett G, Kleyer A, Perricone C, Sahinbegovic E, Iagnocco A, Zwerina J, et al. Diabetes is an independent predictor for severe osteoarthritis: results from a longitudinal cohort study. *Diabet Care.* 2013; 36: 403-409.

Shimomura I, Matsuda M, Hammer RE, Bashmakov Y, Brown MS, Goldstein JL. Decreased IRS-2 and increased SREBP-1c lead to mixed insulin resistance and sensitivity in livers of lipodystrophic and ob/ob mice. *Mol Cell*. 2000; 6: 77-86.

Song F and Schmidt AM. Glycation and insulin resistance: Novel mechanisms and unique targets? *Arterioscler Thromb Vasc Biol*. 2012; 32: 1760-1765.

Takeda J, Kayano T, Fukumoto H, Bell GI. Organization of the human GLUT2 (pancreatic beta-cell and hepatocyte) glucose transporter gene. *Diabetes*. 1993; 42: 773-777.

Tang Y and Chen A. Curcumin eliminates the effect of advanced glycation end-products (AGEs) on the divergent regulation of gene expression of receptors of AGEs by interrupting leptin signaling. *Lab Investig*. 2014; 94: 503-516.

Taniguchi CM, Emanuelli B, Kahn CR. Critical nodes in signalling pathways: insights into insulin action. *Nat Rev Mol Cell Biol*. 2006; 7: 85-96.

Taylor DM, Barnes TR, Young AH. The Maudsley prescribing guidelines in psychiatry. John Wiley & Sons; 2021; 13: 340-346.

Thirone AC, Huang C, Klip A. Tissue-specific roles of IRS proteins in insulin signaling and glucose transport. *Trends Endocrinol Metab*. 2006; 17: 72-78.

Ueta K, O'Brien TP, McCoy GA, Kim K, Healey EC, Farmer TD, et al. Glucotoxicity targets hepatic glucokinase in Zucker diabetic fatty rats, a model of type 2 diabetes associated with obesity. *American Journal of Physiology. Endocrinol Metab*. 2014; 306: e1225- e1238.

Villa-Pérez P, Merino B, Fernández-Díaz CM, Ciudad P, Lobatón CD, Moreno A, et al. Liver-specific ablation of insulin-degrading enzyme causes hepatic insulin resistance and glucose intolerance, without affecting insulin clearance in mice. *Metab*. 2018; 88: 1-11.

Wei X, Ke B, Zhao Z, Ye X, Gao Z, Ye J. Regulation of insulin degrading enzyme activity by obesity-associated factors and pioglitazone in liver of diet-induced obese mice. *PLoS One*. 2014; 9: 1-7.

Yabe-Nishimura C. Aldose reductase in glucose toxicity: a potential target for the prevention of diabetic complications. *Pharmacol Rev*. 1998; 50: 21-33.

Yamagishi SI and Matsui T. Role of receptor for advanced glycation end products (RAGE) in liver disease. *Eur J Med Res*. 2015; 20: 1-7.

Ye J. Mechanisms of insulin resistance in obesity. *Front Med*. 2013; 7: 14-24

Yoshii H, Uchino H, Ohmura C, Watanabe K, Tanaka Y, Kawamori R. Clinical usefulness of measuring urinary polyol excretion by gas-chromatography/mass-spectrometry in type 2 diabetes to assess polyol pathway activity. *Diabetes Res Clin Pract*. 2001; 51: 115-123.

Chapter 4

Hyperinsulinemia mediated alteration in lipid metabolism and inflammation in HepG2 creates an ambience for NAFLD and amelioration with VA

4.1 Introduction

The pervasiveness of obesity and metabolic syndromes is increasing day by day (Bechmann et al., 2012). The rapid progression of obesity is closely associated with the prevalence of NAFLD (Feldstein, 2010). Liver is the major organ that maintains the lipid homeostasis by controlling the lipid uptake, *de novo* synthesis of lipids and the delivery of lipids in the form of VLDL (Browning and Horton, 2004). Meanwhile, adipose tissue is the main organ responsible for lipid storage. However, the liver plays a specific role to regulate lipid homeostasis in normal conditions (Lee et al., 2018). Therefore, under pathological conditions like obesity and diabetes, the lipid flux becomes altered which will result in the accumulation of fats in the liver. Also, insulin resistance is the chief pathologic determinant for the development of both diabetes and obesity (Loria et al., 2013). Accumulation of excessive amount of lipids in hepatocytes is the initial step for the development of many serious liver diseases like NAFLD includes non-alcoholic steatohepatitis (NASH), cirrhosis, fibrosis and liver cancer (Loria et al., 2013). Among these, nowadays NAFLD is one of the crucial epidemic problems worldwide. Liver lipid accumulation takes place only when the rate of fatty acid input increases and the rate of fatty acid output decreases. This results in the alterations in lipid metabolism of the body like fatty acid metabolism and its transport. Clinical data suggested that T2DM has an important

role in the development of liver diseases (Loria et al., 2013). One of the crucial factors for reduced life expectancy in T2DM patients is the development of fatty liver disease (Trombetta et al., 2005). In this chapter, I have aimed to point out the alterations in the hepatic lipid metabolism during HI and its role in the prevalence of NAFLD. I also aimed to study the HI created inflammation in HepG2 cells. Furthermore, I also observed the DPP4 inhibition potential of VA and also discussed the role of DPP4 in NAFLD.

Fatty acid uptake and *de novo* synthesis of fatty acids in the liver contribute to the excessive production of TG whereas major pathways involved in the removal of TG involves formation of very low density lipoprotein (VLDL) and fatty acid β oxidation (Wang et al., 2010). The major source for the entry of fatty acids into the circulation is the lipolysis that takes place in adipose tissue during fasting conditions and insulin inhibits this mechanism in normal conditions (Arner, 2005). But in insulin resistance states like obesity and diabetic, the adipocyte lipolysis was up-regulated which resulted in increased fatty acids in circulation (Delarue and Magnan, 2007). These fatty acids are then taken up by the liver and it is mediated by the proteins like fatty acid transport proteins (FATPs), cluster of differentiation 36 (CD36), and calveolins (Koo, 2013). All these proteins are located on the hepatocyte's plasma membrane and involved in fatty acid uptake but they have diverse functions. FATPs are responsible for fatty acid uptake and convert them to fatty acyl CoA. Silencing of FATP in mice resulted in the reduction in hepatic TG content and a decreased fatty acid uptake (Doege et al., 2008). CD36 is a fatty acid translocase and involved in the transport of long chain fatty acids. CD36 is regulated by the peroxisome proliferator-activated receptor γ (PPAR γ) (Silverstein and Febbraio, 2009). Calveolins represent a family of proteins which are responsible for lipid trafficking and formation of lipid droplets (Koo, 2013). During the fatty acid uptake due to the hydrophobicity of the fatty acids they do not diffuse freely in the cytoplasm so they target fatty acid binding protein (FABP) in cytoplasm. FABP also affects the other proteins in the liver

such as PPAR α and PPAR γ and increased lipid levels inside the liver. In obese patients the FABP levels are overexpressed (Charlton et al., 2009).

De novo lipogenesis (DNL) is another major pathway involved in hepatic lipid metabolism. It enables the liver to produce the lipids from acetyl CoA. The first step of DNL is the conversion of acetyl CoA to the malonyl CoA and the enzyme responsible for this conversion is acetyl CoA carboxylase (ACC). Malonyl CoA is then converted from palmitate by the action of fatty acid synthase (FAS). The newly formed fatty acid undergoes a series of modifications and finally it is either stored as TG or transported as VLDL (Ipsen et al., 2018). The increased DNL leads to hypertriglyceridemia and the formation of saturated fatty acids like palmitate; it can act as a precursor for the initiation of inflammation and apoptosis (Listenberger et al., 2003). The central player of the genesis of fat accumulation and fatty liver disease is the uncontrolled DNL. The transcription factors involved in the regulation of DNL are sterol regulatory element binding protein 1c (SREBP1c) and carbohydrate regulatory element binding protein (ChREBP). SREBP1c is activated by insulin while ChREBP is activated by carbohydrates (Sanders and Griffin, 2016). One of the studies reported that the TG levels were increased by the overexpression of SREBP1c (Kohjima et al., 2007). Furthermore, SREBP1c contributes to the development of insulin resistance through the increased production of harmful lipids like diacylglycerol, it causes the inhibitory effects on insulin signaling and also increases the lipogenesis. After the entry of fatty acid into the liver it either enters into the TG synthesis or is stored or it undergoes β -oxidation and produces energy (Bechmann et al., 2012). Fatty acids and their metabolites are the active participants in the lipotoxicity and which activates ROS production in hepatocytes.

TGs are the storage form of lipids in the liver and are also processed to form VLDL (Neuschwander-Tetri, 2010). The major enzymes involved in the synthesis of TG are mitochondrial glycerol-3-phosphate-acyltransferase (mtGPAT) and diacylglycerol acyl

transferase (DGAT) (Coleman and Lee, 2004). This is controlled by SREBP1c and ChREBP which link lipid and glucose metabolism (Postic and Girard, 2008). DGAT has two isoforms in mammals and it forms TG from diacylglycerol (Wang et al., 2010). The expression of DGAT2 is very high in the liver while DGAT1 is dominantly expressed in adipocytes and intestine (Cases et al., 2001). One of the studies reported that patients with fatty liver possess an increased level of DGAT2 but an unaltered level of DGAT1 expression. This data indicates the importance of DGAT2 in the development of fatty liver diseases (Wang et al., 2010). Meanwhile fatty acid oxidation is the one of the catabolism of fatty acids and it generates energy. Acetyl CoA synthase is the enzyme responsible for the production of the initial molecule of this pathway. Acetyl CoA is the activated form of fatty acids and it then enters into the oxidation process. The prime organelle for the β -oxidation is the mitochondria and the protein responsible for its transport is carnitine palmitoyltransferase 1(CPT1). During the fed state the fatty acid oxidation is reduced and the DNL is up-regulated (Akkaoui et al., 2009) (Fig: 4.1). 3-hydroxy-3-methylglutaryl-coenzyme A (HMG-CoA) is the major enzyme involved in cholesterol biosynthesis. Furthermore, the liver is the major tissue in which the FGF-21 is abundantly expressed. It functions as a hormone, it is activated during fasting conditions and regulates lipid and carbohydrate metabolism (Ding et al., 2012). FGF-21 enhances the fatty acid oxidation in the liver and also increases the rate of TCA cycle (Markan et al., 2014). It also enhances the hepatic insulin sensitivity and thereby increases the hepatic glucose disposal (Badman et al., 2009). Through this way it maintains a glucose homeostasis.

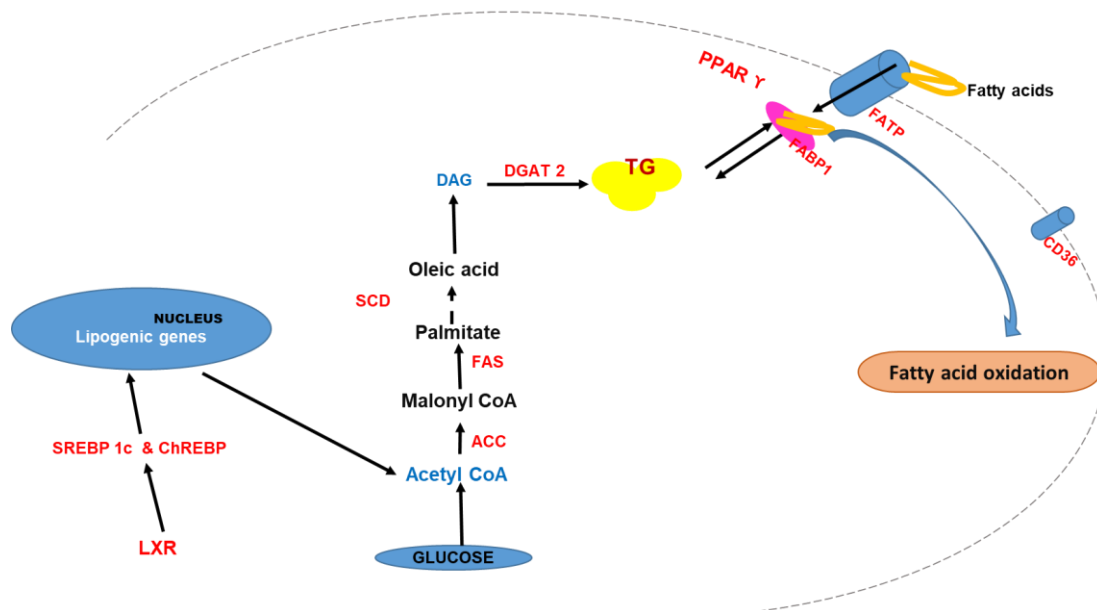


Figure. 4.1 Effect of hyperinsulinemia on hepatic lipid metabolism

Furthermore, dipeptidyl peptidase- 4 (DPP4) is one of the interesting target therapies in both diabetes and liver disease. As compared to other tissues, the DPP4 expression is very high in hepatocytes (Kawaguchi et al., 2011). The function of this enzyme is the inhibition of the incretin hormones like glucagon-like peptide-1 (GLP-1) and glucose-dependent insulinotropic polypeptide (GIP) (Lovshin and Drucker, 2009). GLP-1 reduces body weight and increases insulin secretion (Mudaliar and Henry, 2010). DPP4 is also called CD24. One of the studies reported that in HepG2 cells during high glucose concentrations, the level of DPP4 increases (Pazhanivel and Jayanthi, 2010). So inhibitors of DPP4 is an effective strategy to reduce diabetic complications such as hyperglycemia (Lovshin and Drucker, 2009; Kawaguchi et al., 2011). These inhibitors are more specific for DPP4 and it causes a noticeable decrease in DPP4 levels thereby increasing the incretin levels. Through this way, DPP4 inhibitors stimulate insulin secretion (Mulvihill, 2018) and can reduce hepatic glucose production by producing glucagon (Trzaskalski et al., 2020). DPP4 inhibitors relatively reduced the risk of hypoglycemia and facilitates the glucose dependent incretin based insulin release. Furthermore, recent studies proved that DPP4 is a novel biomarker of NAFLD. Several reports suggested

that the circulating levels of DPP4 are directly proportional to the occurrence of NAFLD (Itou et al., 2013). In addition to this, DPP4 initiates inflammation in the liver through the activation of several cytokines and chemokines (Klemann et al., 2016).

Hepatic inflammation is another major factor for development of liver diseases. Low grade inflammation is one of the common factors for the pathogenesis of many metabolic diseases like diabetes, obesity and NAFLD. In low-grade inflammation, the level of cytokines such as TNF- α and interleukin (IL)-6 were significantly increased which will increase the ROS production. In addition to this, development of chronic low grade hepatic inflammation could result in the genesis of insulin resistance in the liver (Hsieh and Hsieh, 2011). Furthermore, increased fat accumulation inside the liver leads to hepatocyte damage and activating inflammatory response (Del Campo et al., 2018). Activated inflammation aggravates the disease progression and also acts as feedback for the further activation of inflammation.

4.2 Materials and methods

4.2.1 Chemicals

Vanillic acid, metformin, DMSO, RIPA buffer, protease inhibitor and Oil Red O stain were purchased from Sigma Aldrich (St Louis, USA). Isopropanol and formaldehyde were from SRL (Mumbai, India). Dulbecco's modified eagle's medium (DMEM), fetal bovine serum (FBS), 0.5% trypsin - ethylene diamine tetra acetic acid (Trypsin-EDTA) and penicillin-streptomycin antibiotics were from Gibco-BRL Life Technologies (Grand Island, USA). FABP, PPAR γ , PKC, ACC, p-ACC, FAS, SCD1, HMG CoA reductase and β -actin antibodies were obtained from Santa Cruz Biotechnology (Dallas, USA). SREBP1c, FGF-21 and all other secondary antibodies were purchased from Cell Signaling Technology (Beverly, MA, USA). Recombinant human insulin was from Merck (USA). The remaining chemicals used were of analytical grade.

4.2.2 Cell culture and induction of hyperinsulinemia created insulin resistance

HepG2 cells (NCCS, Pune) were maintained in DMEM supplemented with 10 % FBS, 100 U/ml penicillin and 100 µg/ml streptomycin at 5 % CO₂ and 37 °C in an incubator. The HI created insulin resistance was induced according to the previous method (Jung et al., 2017). Briefly, when the cells reached the 80 % confluence, the cultures were exposed to 1 µM human insulin for 24 hrs to induce insulin resistance, simultaneously the cells were subjected to corresponding treatments with 1 % serum-containing media.

Experimental groups:

C - Control

IR - Hyperinsulinemia created insulin resistance (1 µM human recombinant insulin)

VA1 - IR + 5 µM VA

VA2 - IR + 10 µM VA

M - IR + Metformin (1 mM)

The VA and metformin were co-treated with HI induced insulin resistance for 24 hrs in the experimental groups.

4.2.3 Oil Red O staining

Briefly, after respective treatments the cells were washed with PBS and fixed with the fixing solution for 1 hr at RT. After fixing, the remaining fixing solution was aspirated off and the cells were washed with the distilled water. Then the permeabilization solution was added and kept for 5 min at RT. Stock solution of oil Red O staining solution is prepared before the initiation of the experiment. For the preparation of the stock of stain, 30 mg of the same was mixed with 10 ml of dH₂O and incubated overnight at 37 °C. From this, the working solution

was prepared in 3:2 ratios by adding 3 ml of stock solution into the 2 ml of distilled water. This solution is kept for 10 min at RT and filtered using a Whatman No.1 filter paper. After the removal of permeabilization solution, the cells are then subjected to appropriate volume of staining solution and incubated for 5 min at RT. Then the cells were washed with distilled water for 3 times and observed under a microscope. The lipid accumulation was quantified by extracting the absorbed dye using 100 % isopropanol. The absorbance was measured at 500 nm using isopropanol as blank.

4.2.4 Analysis of hepatic fatty acid uptake

The hepatic fatty acid uptake during HI created insulin resistance conditions were evaluated by analyzing the expression levels of main proteins involved in the fatty acid uptake. The major proteins involved in this pathway like FABP, PPAR γ and PKC were analyzed by western blot. The expression levels of these proteins were analyzed from the densitometric data calculated using Image J software (for details, please refer to section 4.2.11).

4.2.5 Analysis of hepatic *de novo* lipogenesis cholesterol biosynthesis

The expression level of ACC, p-ACC, FAS, SCD1, SREBP1c, HMG CoA reductase and FGF-21 proteins during insulin resistance condition were analyzed by western blotting (for details, please refer to section 4.2.11).

4.2.6 Triglyceride accumulation assay

TG was estimated by Cayman triglyceride estimation kit (Cayman chemicals, MI, USA). The kit utilizes the action of lipase, which breaks down the TG into fatty acid and glycerol. The glycerol undergoes several reactions and finally produces a purple colored product. For this, after treatment the cells were washed and lysed by sonication with the diluted standard diluent in the kit. Then 10 μ l of cell lysate and standards were added to respective wells for both

standard and samples. Then it was mixed with 150 μ l of enzyme buffer and mixed well. After that the plate was incubated for 30 min at 37 $^{\circ}$ C. Then the absorbance was measured at 540 nm

4.2.7 Diacylglycerol-O-Acyltransferase Homolog 2 activity assay

The DGAT-2 activity was measured by using the human diacylglycerol-O-acyltransferase homolog 2 ELISA kit (Mybiosource, USA). It is a sandwich enzyme immunoassay used for the *in vitro* quantitative measurement of DGAT-2 in human tissue, cell lysate or other biological fluids. Briefly, for this assay the cells were cultured in a 6-well plate. After respective treatment the cells were washed with PBS and the cells were made to detach by adding 1 ml of 10X trypsin to each well. Then the cells were collected by centrifugation (1500 x g for 10 min at 4 $^{\circ}$ C) and washed 3 times with PBS. Then the cells were dissolved in ice cold PBS and subjected to ultra-sonication for 4 times. After that the cell supernatants were collected. Then 2.0 ml of standard diluent was added to the standard solution (10 ng/ml; provided in the kit) and diluted the standard. Then the seven concentrations of standard (10 ng/ml, 5 ng/ml, 2.5 ng/ml, 1.25 ng/ml, 0.625 ng/ml, 0.312 ng/ml, 0.156 ng/ml, and 0 ng/ml) were prepared. Then 100 μ l of each diluted standard and samples were added to respective pre-coated wells provided in the kit. Then the plate was incubated for 90 min at 37 $^{\circ}$ C. After incubation, the retaining solution was removed from each well and 100 μ l of detection solution was added to each well. Then it was incubated for 45 min at 37 $^{\circ}$ C. Then a 300 μ l wash buffer (provided in the kit) was added to each well. After 1-2 min, the solution was removed and tapped the plate on an absorbent paper. Then 100 μ l of detection solution B was added to each well and incubated for 45 min at 37 $^{\circ}$ C and repeated the wash procedure described above for 4 times. Then 90 μ l of substrate solution was added to each well and incubated for 25 min at 37 $^{\circ}$ C. Finally, 50 μ l of stop solution was added to each well and the colour was turned yellow. The absorbance was measured at 450 nm using a microplate reader.

4.2.8 DPP4 inhibition assay

Screening of DPP4 was carried out by using the DPP4 inhibitor screening assay kit from Abcam, UK. It is a fluorescent based method for screening the DPP4 inhibitors. For this assay the sample (compound; VA) was dissolved in DMSO and added different concentrations of sample to each well with a final volume of 10 μ l. Then wells in the plate were classified as 100 % activity wells, background wells, sitagliptin positive control wells, and sample wells as per the instructions from the manufacturer. Then 30 μ l of assay buffer, 10 μ l of diluted DPP4, and 10 μ l of solvent were added to the three 100 % activity wells. Then 40 μ l of assay buffer and 10 μ l of solvent (DMSO) were added to the background wells and the 30 μ l of diluted assay buffer and 10 μ l of diluted DPP4 and 10 μ l of sitagliptin were added to the positive control well. 30 μ l of assay buffer, 10 μ l of diluted DPP4, and 10 μ l of different concentrations of sample were added to each sample well. Then 50 μ l of diluted substrate solution was added to all the wells to initiate the reaction. The plate was covered with the plate cover and incubated for 30 min at 37 $^{\circ}$ C. Then the fluorescence was read using an excitation wavelength of 350 nm and an emission wavelength of 450 nm.

4.2.9 Estimation of inflammatory cytokines

Inflammatory cytokines such as IL6 and TNF- α were estimated in conditioned media using indirect ELISA method. For this after treatments the culture media was collected. Then 100 μ l of culture media was added to the ELISA plates and incubated for overnight at 4 $^{\circ}$ C. Then the solution was removed carefully and the wells were washed 3 times with PBS. Then 200 μ l of blocking buffer (5 % nonfat milk) was added to the wells and incubated for 1hr at RT. After washing 3 times with PBS, then 100 μ l of specific primary antibodies (1:1000) for IL6 or TNF α were incubated for 2 hrs at RT. The plates were washed 3 times with PBS and treated with HRP-conjugated secondary antibodies (1:1000). Then 100 μ l of TMB substrate solution was

added and incubated for 30 min at RT on the shaker in the dark. Then 100 μ l of stop solution was added and read the absorbance at 450 nm in a multimode reader.

4.2.10 NF- κ B (p65) transcription factor activity assay

NF- κ B transcription factor activity was determined by using Cayman NF- κ B (p65) transcription factor assay kit (Cayman chemicals, USA). It is a sensitive and non-radioactive method used for detecting specific DNA binding activity of NF- κ B in nuclear extracts. This kit is based on an ELISA method and an ideal way to measure NF- κ B transcription activity assay but is not cross reactive with p50. In this assay, the microplate provided in the kit is immobilized with a specific double stranded DNA sequence containing NF- κ B response element and detect the NF- κ B by the addition of specific primary antibody. After treatment the cells were collected by centrifugation at 12000 x g for 20 min. The cytoplasmic and nuclear fractions were separated using a nuclear extraction kit (Cayman chemicals, USA). Then the nuclear fractions containing NF- κ B of 10 μ l were added to respective wells and incubated overnight at 4 $^{\circ}$ C. Then all the wells were washed with 100 μ l of wash buffer. After that all the wells except blank were added with 100 μ l of NF- κ B (p65) primary antibody and incubated for 1hr at RT. Then the wells were washed with a wash buffer and added 100 μ l of HRP-conjugated goat anti-rabbit secondary antibody to each well except blank. Then the plate was incubated for 1hr at RT. The wells were again washed with a wash buffer and added 100 μ l of developing solution to all the wells. After that the plate was incubated for 30 min at RT with gentle agitation. Next, 100 μ l of stop solution was added to all the wells. Then the absorbance was read at 450 nm in the microplate reader. The absorbance indicates the NF- κ B (p65) concentration in nuclear extracts.

4.2.11 Western blot

Expression of various proteins involved in hepatic lipid metabolism such as FABP, PPAR γ , PKC, ACC, p-ACC, FAS, SCD1, SREBP1c, HMG CoA reductase, and FGF-21 were studied using western blotting. Cells were cultured in T-25 flask and after the respective treatments with VA, protein was extracted from the cell lysate using cold RIPA buffer with protease inhibitor cocktail (Sigma Aldrich, USA). After complete lysis of the cells, the cell suspension was centrifuged at 12000 rpm for 15 min at 4⁰C and collected the supernatant. The protein concentration of the supernatant was quantified using bicinchoniniacid (BCA) protein assay (Pierce, Rockford, IL, USA) and normalized the protein content. The protein samples (25 μ l) were then run on an SDS-PAGE gel (10 %) (BioRad, Hercules, CA, USA), transferred at 25 V for 15 min to PVDF membrane (Merck) using a trans blot apparatus (BioRad). After transfer, the PVDF membrane was blocked with 3 % BSA in TBST for 1 hr at RT. Then it was washed for 3 times with TBST for 10 min each and the membrane was probed with primary antibodies against FABP, PPAR γ , PKC, ACC, p-ACC, FAS, SCD1, SREBP1c, HMG CoA reductase, and FGF-21 (1:1000 dilution) in TBST and incubated for 2 hrs at RT with moderate shaking. The membrane was washed thrice with TBST for 10 min. HRP-conjugated secondary antibody (1:2000) was added and agitated for 90 min at RT. After three TBST washes, the membrane was developed using ECL substrate (BioRad). The proportional thickness of bands was measured using Image Lab software in the ChemiDoc system (ChemiDoc MP Imaging System, Bio-Rad) assuming all bands were in the Beer-Lambert law region.

4.2.12 Statistical analysis

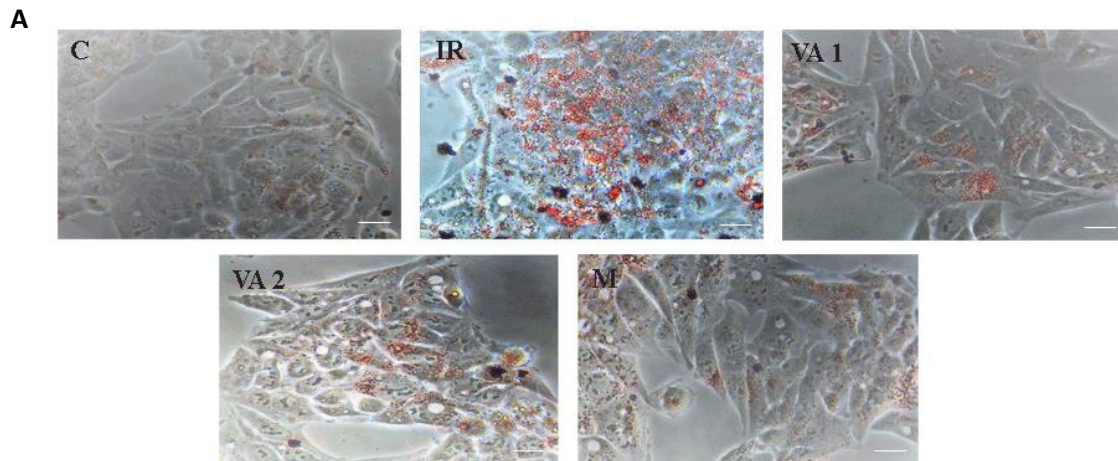
All analyses were carried out with sextuplicates and data are presented as mean \pm SEM for control and treated cells. Data were subjected to ANOVA and further significantly different pairs ($p \leq 0.05$) were identified using Duncan's multiple comparison test. The normality of the variables was tested using the Kolmogorov Smirnov Z test and the variables were found to be

approximately normally distributed. The significance was accepted at $p \leq 0.05$. All calculations were done using the Statistical Package for the Social Sciences for Windows standard version 20 (SPSS Inc., USA).

4.3 Results

4.3.1 Hyperinsulinemia enhanced the lipid droplet accumulation in HepG2 cells

During HI created insulin resistance, the lipid droplet accumulation was significantly ($p \leq 0.05$) increased by 19.8 % compared to control. While VA of 5 μM and 10 μM concentrations showed a noticeable decrease in lipid droplet formation by 11.6 % and 16.7 % respectively compared with the HI treated group (Fig: 4.2A & Fig: 4.2B). It was less in metformin treated cells as compared to IR cells. In metformin treated cells the eluted Oil red O concentration was decreased significantly ($p \leq 0.05$) to 23 % compared to IR cells (Fig: 4.2 & Fig: 4.2B).



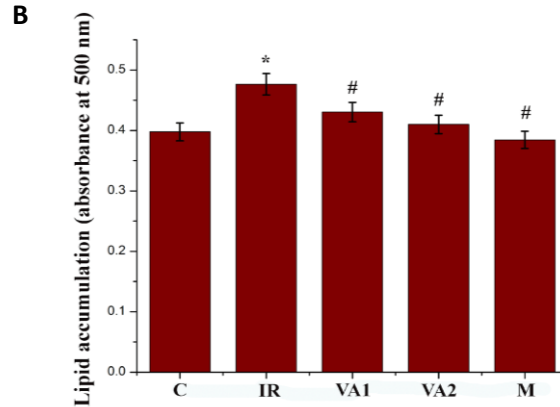


Figure. 4.2 Lipid droplet accumulation. (A) Oil Red O staining assay. (B) Quantification of lipid accumulation. C - control cells; IR - hyperinsulinemia created insulin resistant cells; VA1 - IR + 5 μ M vanillic acid; VA2 - IR + 10 μ M vanillic acid; M - IR + metformin (1 mM). Values are expressed as mean \pm SEM where n=6. * indicates that the mean value was significantly different from control cells ($p \leq 0.05$). # indicates the mean value was significantly different from IR cells ($p \leq 0.05$). Scale bar correspondence to 50 μ m.

4.3.2 Effect of hyperinsulinemia on fatty acid uptake

There was also a significant increase in the expression of major proteins involved in hepatic fatty acid uptake. The main proteins in this pathway like FABP, PPAR γ and PKC were up-regulated by 58.6 %, 142.4 % and 173.8 % ($p \leq 0.05$) respectively in the IR group compared to control cells (Fig: 4.3A & Fig: 4.3B). Treatment with VA of both concentrations like 5 μ M and 10 μ M significantly ($p \leq 0.05$) down-regulated the expression of these proteins. VA decreased the expression of FABP by 44.4 % and 79.8 % respectively. Meanwhile VA dose dependently reduced the expression of PPAR γ by 49.9 % and 86 % respectively (Fig: 4.3A & Fig: 4.3B). Simultaneously, 5 μ M and 10 μ M concentrations of VA decreased the expression of PKC by 17.3 % and 32.2 % respectively. Metformin treatment also significantly reduced the expression of FABP and PPAR γ by 130.2 % and 71.9 % ($p \leq 0.05$) respectively and also down-regulated the expression of PKC by 62.5 % (Fig: 4.3A & Fig: 4.3B).

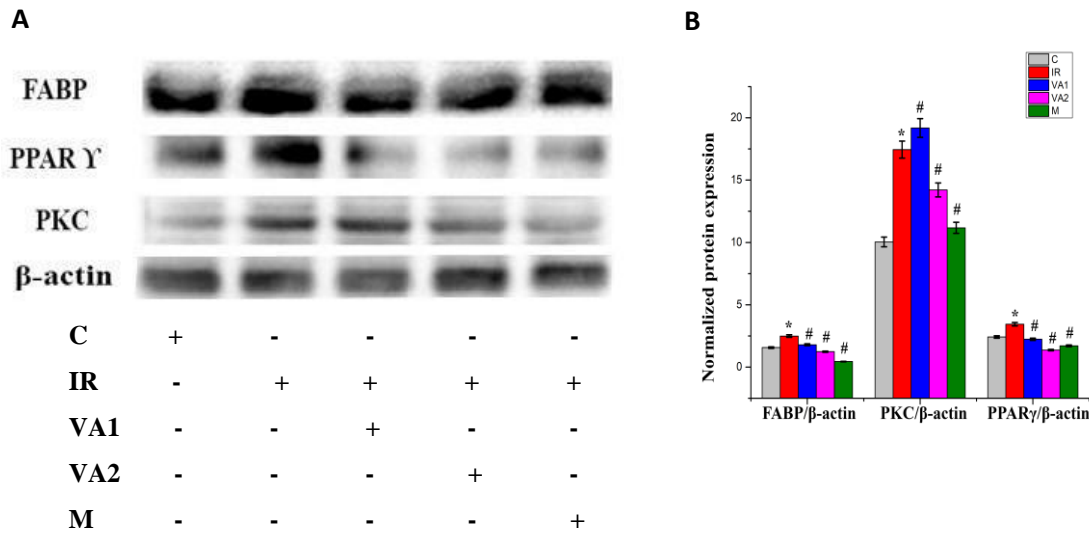


Figure. 4.3 Effect of insulin resistance in free fatty acid uptake. (A) After VA co-treatment the cells were lysed, FABP, PPAR- γ , PKC and β -actin expression were analyzed by western blotting. **(B)** Densitometric quantification of FABP, PPAR- γ , PKC normalized to β -actin. C - control cells; IR - hyperinsulinemia created insulin resistant cells; VA1 - IR + 5 μ M vanillic acid; VA2 - IR + 10 μ M vanillic acid; M - IR + metformin (1 mM). Each value represents the mean \pm SEM where n=6. * indicates that the mean value was significantly different from control cells ($p \leq 0.05$). # indicates the mean value was significantly different from IR cells ($p \leq 0.05$).

4.3.3 Hyperinsulinemia created insulin resistance up-regulates the hepatic lipogenesis

To evaluate the effect of HI on DNL as well as cholesterol biosynthesis, I studied the proteins involved in these pathways in the liver. Western blot data indicated that during HI created insulin resistance the expression levels of all major proteins in DNL such as p-ACC, FAS, SCD1 and SREBP1c levels were significantly increased compared to control. The level of p-ACC, FAS, SCD1 and SREBP1c were up-regulated significantly ($p \leq 0.05$) in HI conditions by 40.5 %, 132.5 %, 138.9 % and 33.7 % respectively compared to control (Fig: 4.4A & Fig: 4.4B). VA and metformin treatments also down-regulated the enzyme expression significantly compared to IR group. The increased expression of p-ACC during hyperinsulinemic condition was significantly decreased by VA of both concentrations (5 μ M; 27.6 % and 10 μ M; 27.9 %; $p \leq 0.05$) (Fig: 4.4A & Fig: 4.4B). Meanwhile, treatment of cells with two concentrations of

VA (5 μ M and 10 μ M) significantly reduced the FAS expression ($p \leq 0.05$; Fig: 4.4A & Fig: 4.4B) by 60.2 % and 93.3 % respectively. Furthermore, the increased levels of both SCD1 and SREBP1c in HI conditions were reversed by VA with decreased expression of these proteins. VA dose dependently reduced the SCD1 expression by 37.4 % for 5 μ M and 38.9 % for 10 μ M respectively. Simultaneously, VA of 5 μ M and 10 μ M concentrations significantly ($p \leq 0.05$) decreased the level of SREBP1c by 30.6 % and 71.4 % respectively (Fig: 4.4A & Fig: 4.4B). While metformin (1 mM) treatment significantly ($p \leq 0.05$) reduced the expression of all the proteins in the DNL such as p-ACC, FAS, SCD1 and SREBP1c by 27.9 %, 69.6 %, 42.4 %, 47.7 % compared to IR group (Fig: 4.4A & Fig: 4.4B).

Furthermore, the expression of the major enzyme responsible for the cholesterol synthesis is also studied. HI significantly ($p \leq 0.05$) increased the expression of HMG CoA reductase by 128.4 % compared to control (Fig: 4.4A & Fig: 4.4B). Also VA (5 μ M and 10 μ M concentrations) and metformin (1mM) treatments significantly ($p \leq 0.05$) down-regulated the level of HMG CoA reductase by 12.7 %, 57.5 % and 122 % respectively. Next I checked the protein level expression of FGF-21 in HI created insulin resistant cells and found that during HI the expression levels of FGF-21 was decreased by 40.7 % compared to control (Fig: 4.4A & Fig: 4.4B). At the same time, the VA treatment significantly ($p \leq 0.05$) increased the expression of FGF-21 to 23.6 % and 24.3 % for 5 μ M and 10 μ M of VA. Metformin treatment also significantly ($p \leq 0.05$) increased the FGF-21 levels by 13.9 % compared to the IR group.

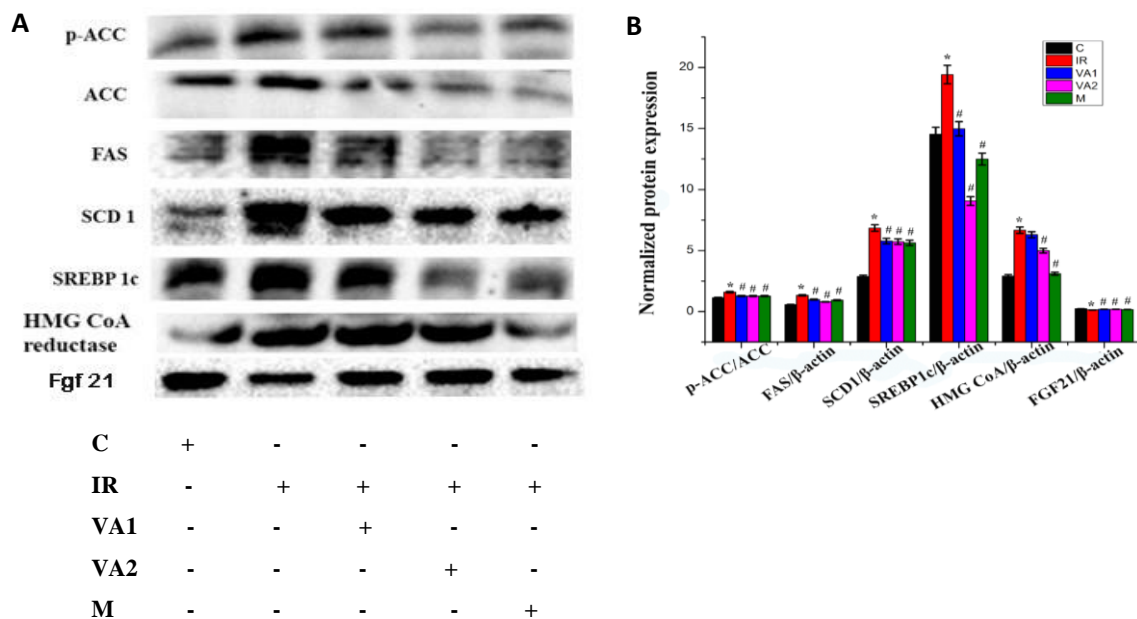


Figure. 4.4 Hepatic lipogenesis. (A) After VA co-treatment the cells were lysed, p-ACC, ACC, FAS, SCD-1, SREBP1c, HMG CoA reductase, FGF-21 and β -actin expression were analyzed by western blotting. (B) Densitometric quantification of p-ACC, ACC, FAS, SCD-1, SREBP 1c, HMG CoA reductase, FGF-21 normalized to β - actin. C - control cells; IR - hyperinsulinemia created insulin resistant cells; VA1 - IR + 5 μ M vanillic acid; VA2 - IR + 10 μ M vanillic acid; M - IR + metformin (1 mM). Each value represents the mean \pm SEM where n=6. * indicates that the mean value was significantly different from control cells ($p \leq 0.05$). # indicates the mean value was significantly different from IR cells ($p \leq 0.05$).

4.3.4 Hyperinsulinemia enhanced the triglyceride accumulation and DGAT-2 activity in hepatocytes

During HI conditions the TG accumulation was increased drastically (163.4 %) as compared to control cells. Meanwhile, with VA, the level of TG was reduced significantly ($p \leq 0.05$) by 98.3 % and 147.2 % for 5 μ M and 10 μ M concentrations respectively compared to IR cells (Fig: 4.5A). Metformin treatment also significantly ($p \leq 0.05$) decreased the TG accumulation by 263.4 % compared to IR cells.

Furthermore, HI up-regulated the activity of DGAT-2 by 23.6 % compared to control. VA caused a significant ($p \leq 0.05$) decrease in the DGAT-2 activity by 18.8 % and 21.8 % with 5 μ M and 10 μ M concentrations of VA respectively (Fig: 4.5B). Metformin treatment also significantly ($p \leq 0.05$) reduced the DGAT-2 activity by 22.8 % compared with IR.

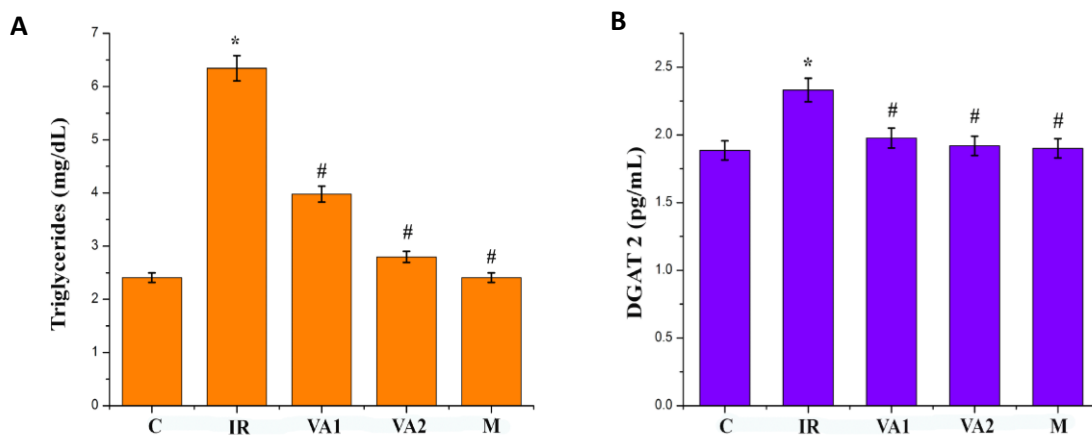


Figure. 4.5 Effect of hyperinsulinemia on TG accumulation & DGAT2 levels. (A) Estimation of triglycerides in different groups. (B) DGAT-2 activity is analysed by DGAT-2 activity assay. C-control cells; IR - hyperinsulinemia created insulin resistant cells; VA1 - IR + 5 μ M vanillic acid; VA2 - IR + 10 μ M vanillic acid; M - IR + metformin (1 mM). Values are expressed as mean \pm SEM where n=6. * indicates that the mean value was significantly different from control cells ($p \leq 0.05$). # indicates the mean value was significantly different from IR cells ($p \leq 0.05$).

4.3.5 Effect of hyperinsulinemia on DPP4 inhibition

The increased concentrations of VA showed a significant ($p \leq 0.05$) increase in the DPP4 inhibition (Fig: 4.6). VA showed a dose dependent inhibition of DPP4 activity. The positive control used in this assay showed an inhibition of 202.6 % with a concentration of 100 μ M (Fig: 4.6). Same time, the VA of 100 μ M concentration showed an inhibition of DPP4 activity by 143.17 %.

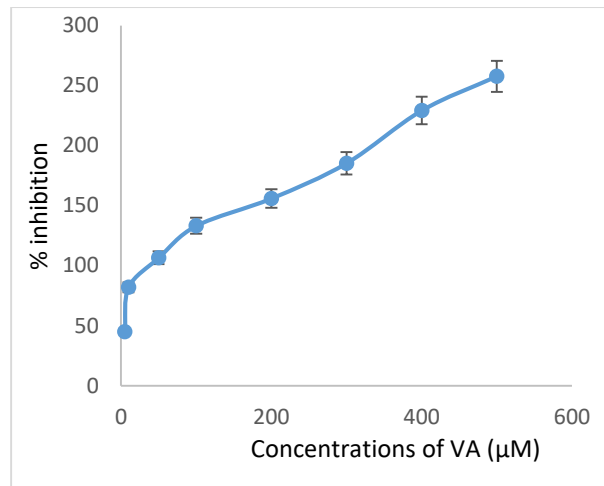


Figure. 4.6 Determination of DPP4 inhibition. DPP4 inhibition capacity of VA. Evaluation of DPP4 inhibition of VA. Different concentrations of vanillic acid (VA1-5 μM vanillic acid, VA2-10 μM vanillic acid, VA3-50 μM vanillic acid, VA4-100 μM vanillic acid, VA5-200 μM vanillic acid, VA6-300 μM vanillic acid, VA7-400 μM vanillic acid & VA8-500 μM vanillic acid) were used.

4.3.6 Effect of hyperinsulinemia in NF-κB transcription activity

The nuclear activity of NF-κB p65 was studied by ELISA (Fig: 4.7). In the HI treated group the nuclear activity of NF-κB showed a significant increase (20.5 %). In VA treated groups, the nuclear activity was decreased significantly ($p \leq 0.05$) in a dose dependent manner by 16.7 % and 27.7 % for 5 μM and 10 μM concentrations of VA compared to IR groups. The metformin treated group also showed a significant ($p \leq 0.05$) decrease in the NF-κB by 31.5 % compared with the IR group.

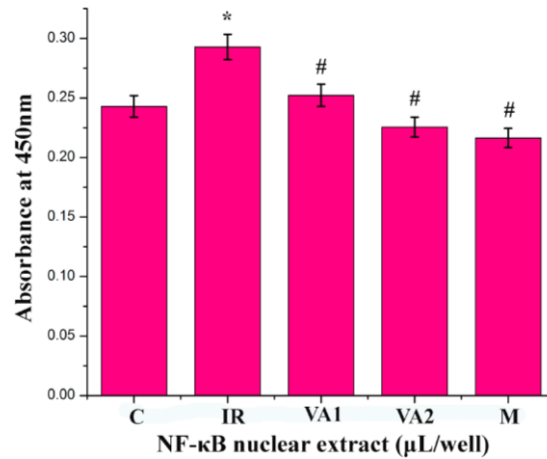


Figure. 4.7 NF-κB translocation during hyperinsulinemia. NF-κB translocation is analyzed by NF-κB translocation assay kit. C - control cells; IR - hyperinsulinemia created insulin resistant cells; VA1 - IR + 5 μM vanillic acid; VA2 - IR + 10 μM vanillic acid; M - IR + metformin (1 mM). Each value represents the mean ± SEM where n=6. * indicates that the mean value was significantly different from control cells ($p \leq 0.05$). # indicates the mean value was significantly different from IR cells ($p \leq 0.05$).

4.3.7 Hyperinsulinemia potentiate the progression of inflammation

HI induced the release of pro-inflammatory cytokines such as TNF- α and IL6 significantly ($p \leq 0.05$) and treatment with VA and metformin decreased the secretion of cytokines. IL6 levels were significantly increased (161 %; $p \leq 0.05$) in the IR cells compared to control (Fig: 4.8A). On treatment with VA, the IL6 levels were found to decrease significantly ($p \leq 0.05$) by 22 % and 45.8 % for 5 μM and 10 μM concentrations of VA respectively compared with the IR group. Metformin showed a significant ($p \leq 0.05$) decrease of IL6 levels by 55.9 % compared with IR cells (Fig: 4.8A).

In IR group the levels of the inflammatory cytokine TNF- α was increased significantly ($p \leq 0.05$) by compared with control cells and on treatment with 5 μM and 10 μM concentrations of VA and 1mM of metformin the level of TNF- α was decreased significantly ($p \leq 0.05$) by 32.6 %, 48.7 % and 55.5 % respectively (Fig: 4.8B).

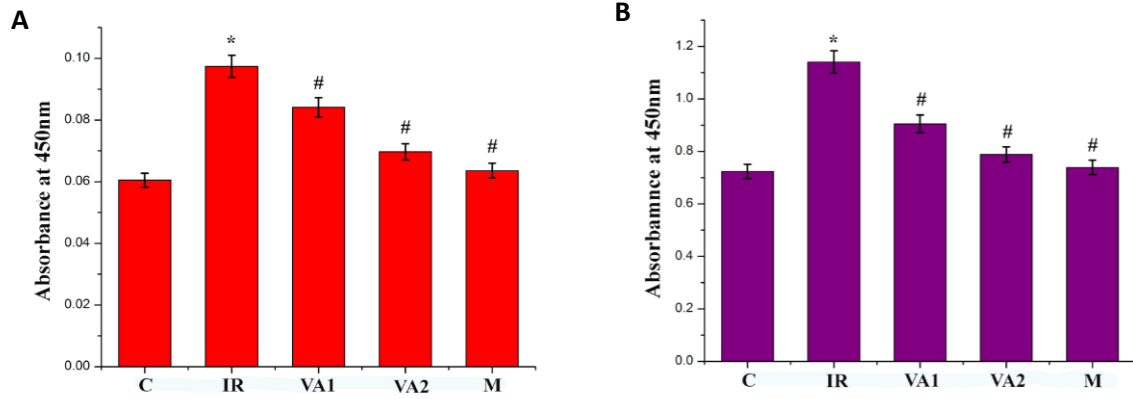


Figure. 4.8 Hyperinsulinemia & inflammation. (A) IL6 activity is analysed by ELISA. (B) TNF α activity is analysed by ELISA. C - control cells; IR - hyperinsulinemia created insulin resistant cells; VA1 - IR + 5 μ M vanillic acid; VA2 - IR + 10 μ M vanillic acid; M - IR + metformin (1 mM). Each value represents the mean \pm SEM where n=6. * indicates that the mean value was significantly different from control cells ($p \leq 0.05$). # indicates mean value was significantly different from IR cells ($p \leq 0.05$).

4.4 Discussion

One of the essential organs necessary for the regulation of whole body lipid homeostasis is liver (Ipsen et al., 2018). Meanwhile the adipose tissue is considered as the main organ participating in the extra fat storage (Lee et al., 2018). Liver controls the synthesis of new fatty acids, fatty acid exports and their redistribution to the various tissues as well as have a prominent role in the utilization of fatty acids as energy source (Younossi et al., 2016). With the help of various receptors, hormones, nuclear receptors and transcription factors, the liver maintains a regulated lipid metabolism (Bechmann et al., 2012). Disturbances in any one of these pathways resulted in the hepatic fat accumulation which finally results in the development of fatty liver and obesity (Ipsen et al., 2018). Obesity is the main risk factor for the development of many of the lipid metabolism disorders like hypertension, atherosclerosis, fatty liver disease, as well as metabolic disease like insulin resistance and diabetes (Kawasaki et al., 2012).

Fatty liver condition develops only when an imbalance between the fatty acid uptake and its disposal will take place. Four major pathways are involved in the regulation of these processes (Ipsen et al., 2018). They are the circulating lipid uptake pathway, fatty acid oxidation pathway, DNL, and export of lipids via VLDL formation (Ipsen et al., 2018). But the molecular mechanism responsible for the excess fat accumulation in the liver is not fully revealed. So in this chapter I have tried to explore the current insights to the major pathways, protein expressions and exaggerated inflammatory cytokines during the HI created insulin resistance. Also discussed the molecular mechanisms involved in the progression of NAFLD in relation with hepatic lipid accumulation. In addition I also discussed the role of DPP4 on the prevalence of NAFLD and also revealed the DPP4 inhibition potential of VA.

In the liver the fatty acid uptake takes place mainly through the fatty acid transporter proteins (FATP) while a small amount of fatty acids were entered into the liver through passive diffusion (Mashek, 2013). In hepatocytes, the major proteins involved in fatty acid transport

are FATP, CD36 and caveolins (Koo, 2013). FATP has six isoforms in mammals. Among these the predominant FATPs in hepatocytes are FATP2 and FATP5 (Doerge et al., 2008). The silencing of FATP2 in the liver resulted in the reduced uptake of fatty acid and decreased the prevalence of hepatic steatosis. Recent reports suggest that overexpression of CD36 leads to the increased hepatic fatty acid uptake and fatty acid accumulation which resulted in hepatic steatosis. While silencing of the CD36 resulted in the reduced hepatic lipid accumulation. These results revealed the importance of CD36 on hepatic lipid metabolism and its role in the prevalence of NAFLD (Greco et al., 2008; Koonen et al., 2007; Wilson et al., 2016). Same time, caveolins are mainly involved in both lipid uptake and formation of lipid droplets in the liver (Koo, 2013). From our data it is clear that during HI created insulin resistance the lipid accumulation inside the hepatocytes increased noticeably. HI created insulin resistant cells showed a significant increase in the lipid droplet formation while our compound VA dose dependently decreased the lipid droplet formation in hepatocytes and reduced lipid accumulation. When the fatty acids enter inside the liver, it goes and binds to the FABPs. Attachment of fatty acids to FABPs is necessary for the shuttling of the lipids across the cell organelles, because of the hydrophobic nature of lipids (Wang et al., 2015). In addition to this, FABPs are also involved in the nuclear transport of PPARs. So concentrations of FABPs are correlated with the activities of PPARs in hepatocytes (Wolfrum et al., 2001). One of the studies reported that in NAFLD patients the level of FABP is increased and its level indicates the increased deposition of fat in the liver (Higuchi et al., 2011). The obese peoples also have the increased levels of FABPs (Charlton et al., 2009). I found that during HI created insulin resistance conditions the expression of FABP were up-regulated significantly. This indicates the severity of fat accumulation inside the liver. While the compound, VA dose dependently decreased the FABP levels and reduced the fat accumulation in the HepG2 cells. Metformin treatment also reduced the lipid storage in the liver by down-regulating the FABP expression.

Hepatic protein kinase C helps to develop hepatic insulin resistance through the down-regulation of insulin signaling (Loria et al., 2013). One of the studies revealed that the antisense nucleotides against PKC noticeably reduced the clinical symptoms of metabolic syndromes such as increased hepatic insulin resistance, increased hepatic TGs and up-regulated fasting insulin levels. Here antisense nucleotides reduced the PKC expression by the activation of IRS2 activity through the phosphorylation (Samuel et al., 2007). In addition to this, one of the studies reported that the diacyl glycerol content in the hepatic lipid droplets are strongly associated with the activation of PKC in the liver (Samuel et al., 2007). Here also, in our data it is clear that in HI created insulin resistance condition the PKC expression was increased. With this data I suggested that this is one of the reasons for the inhibition of the insulin signaling pathway during HI condition and also develops the insulin resistance in HepG2 cells. It also increased TG accumulation in the liver. It has been proved that free fatty acids are the inducers of the insulin resistance and activation of PKC is the main contributor for the genesis of insulin resistance in the liver (Dey et al., 2006; Roden, 2006).

Furthermore, DNL is another major fatty acid uptake pathway found in the liver. It is the lipid synthesis pathway of the liver in which the liver releases the lipids into the bloodstream. The initial molecule entering into DNL is the acetyl CoA, it undergoes numerous chemical reactions carried out by different enzymes such as ACC, p-ACC, FAS and SCD1. The first step of DNL is carried out by the enzyme ACC which condenses acetyl CoA to malonyl CoA (Goedeke et al., 2018). ACC have two isoforms in the mammals in which ACC1 is abundantly seen in the lipogenic tissues like liver, adipose tissue and lactating mammary glands (Goedeke et al., 2018). ACC1 is located on the cytoplasm of the hepatocytes and it is responsible for the first committed step of DNL. In contrast, the function of mitochondrial ACC2 is the decreased fatty acid oxidation (Goedeke et al., 2018).

Genetic and pharmacological studies revealed that inhibition of the ACC results in the lowering of liver TGs through the increased fatty acid oxidation (Tong et al., 2006). Here I also found that the p-ACC 1 levels are up-regulated in HI and it increases TG synthesis in hepatocytes. But the compound VA could significantly reduce the expression of p-ACC1. In hepatic insulin resistance conditions, the lowering the expression of ACC1 using antisense technology results in the noticeable reductions in hepatic TG levels, hypertriglyceridemia and reversal of hepatic insulin resistance (Savage et al., 2006).

Furthermore, I have performed a set of western blots analyses to assess the expression levels of major proteins in the DNL as well as fatty acid uptake. The data obtained from these analyses demonstrated that in HI treated insulin resistant cells both the fatty acid uptake and the DNL were increased noticeably. The main contributor to fat accumulation in NAFLD patients is the increased rate of hepatic DNL (Donnelly et al., 2005). Here I also analyzed the proteins such as ACC/p-ACC, FAS, SCD1, SREBP1c, PKC and PPAR γ and I found that the inhibition of these proteins by the treatment with VA significantly reduced the TG synthesis and lipid accumulation. Through this way VA will decrease hepatic insulin resistance and fat accumulation in HepG2 cells. With these findings I found that VA has a potential to inhibit hepatic lipid accumulation. ACC1 enzyme catalyzed the rate limiting step of the DNL so pharmacological inhibition of ACC1 is an effective treatment for both the NAFLD and obesity. It is carried out mainly through the inhibition of DNL and activation of fatty acid oxidation. In addition to this, inhibition of hepatic ACC also has an effective therapeutic benefit for the treatment of hyperglycemia in diabetes and NAFLD (Goedeke et al., 2018). The key components for the development of hepatic insulin resistance are the excess TG storage and increased FFA uptake (Loria et al., 2013). The end result of the alterations in the whole body lipid homeostasis are the HI, hyperglycemia and failure of adipose tissue to store the FFAs. Paradoxically this results in the release of FFA into the circulation and the liver starts to

increase the gluconeogenesis and DNL (Loria et al., 2013). Our data is consistent with the above findings that, in HI created insulin resistant HepG2 cells, the TG accumulation was increased significantly and simultaneously the level of DGAT2 enzyme is also up-regulated. DGAT2 is the final protein involved in the conversion of diacylglycerol to triacylglycerol. So the amount of TG is directly proportional to the amount of DGAT2 enzyme. In our study also both the levels of TG and DGAT2 were increased in HI created insulin resistance cells while VA treatment dose dependently reversed the condition by down-regulating DGAT2 and which reduced TG production.

Not only in the lipid metabolism but also in the synthesis of DPP4 liver have a prominent role. DPP4 is an endopeptidase and a well characterized inhibitor of gastrointestinal peptides (Deacon, 2019; Mulvihill and Drucker, 2014). So inhibition of DPP4 is necessary for the increased release of hormones from islets of Langerhans and also it is an effective treatment for hyperglycemia in T2DM patients (Nauck and Meier, 2019). In addition to this, increased levels of DPP4 has a positive role in the genesis of both obesity and NAFLD (Itou et al., 2013). One of the studies reported that in NAFLD patients the level of DPP4 is increased and it has a strong correlation with liver fat content (Baumeier et al., 2017). DPP4 activates several cytokines and chemokines which have a noticeable impact on the genesis of inflammation (Klemann et al., 2016). It has been reported that the levels of IL6 and TNF- α were reduced in livers of DPP4 deficient mice (Varin et al., 2019). Evidence suggests that DPP4 activates NF- κ B through the interaction with caveolins-1 (Trzaskalski et al., 2020). Furthermore, the main mediators of insulin resistance are the IL6, TNF- α , and NF- κ B (Ipsen et al., 2018). IL6 is a major pro-inflammatory cytokine and its expression was increased drastically in NAFLD patients which results in systemic insulin resistance (Samuel et al., 2007). One of the studies reported that the expression levels of IL6 in hepatocytes is selectively induced by the increased FFAs and it is linked to the hepatic inflammatory response (Yamaguchi et al., 2007). Here I

found that HI causes the genesis of inflammation through the drastically increased release of the levels of pro-inflammatory cytokines such as TNF- α , IL6 and NF- κ B. This indicates the initiation of the inflammation process. VA treatment significantly reduced the levels of all these pro-inflammatory cytokines and protected the cells from inflammation created in obesity during HI. Recent research revealed that the down-regulation of inflammation results in the reduced dyslipidemia, insulin resistance, obesity and fatty liver diseases (Trzaskalski et al., 2020). The occurrence of obesity is the prime factor for the development of inflammation as well as obesity is the chronic inflammation disease (Kawasaki et al., 2012). One of the studies reported that the DPP4 inhibitor treated mice showed a decreased liver fat content, reduced the markers of inflammation and it also improved the glycemic parameters. Besides this, DPP4 has a positive correlation with the plasma glucose concentration and HbA1c levels (Ryskjaer et al., 2006). So the regulation of DPP4 using inhibitors is approved for the treatment of hyperglycemia and associated complications in T2DM. Also, the potential of DPP4 inhibitor substrates may have beneficial effects on liver metabolism (Gallwitz, 2012) while it also reduced risk of development of hypoglycemia (Trzaskalski et al., 2020). With these findings here I have screened VA for DPP4 inhibition activity. From cell free screening analysis data, it is evident that VA has a prominent potential for inhibiting the DPP4. These findings solidify the need for further evaluation of DPP4 inhibitory potential of compound in cell based assay.

There are pathways leading from T2DM to NAFLD and returning from NAFLD to progression of T2DM (Loria et al., 2013). Fatty liver is the major determinant of the progression of T2DM however once the T2DM is developed not only it will contribute to fatty liver disease but also helps for the progression of other severe liver damages like NASH, cirrhosis and hepatocellular carcinoma (Loria et al., 2013). Although the incidence of obesity increases day by day and the current treatment against obesity and its related diseases remain limited (Cao, 2010). So there is an urgent need to understand the molecular mechanism behind

the development of obesity related problems in the liver. While considering the emerging problem, our study provides some interesting findings that HI increased the DNL and fatty acid uptake in HepG2 cells. Furthermore, I also found that they were the key determinants for the progression of both obesity and obesity related problems like NAFLD and inflammation.

References

Akkaoui M, Cohen I, Esnous C, Lenoir V, Sournac M, Girard J, et al. Modulation of the hepatic malonyl-CoA-carnitine palmitoyltransferase 1A partnership creates a metabolic switch allowing oxidation of de novo fatty acids. *Biochem J.* 2009; 420: 429-438.

Arner P. Human fat cell lipolysis: biochemistry, regulation and clinical role. *Best Pract Res Clin Endocrinol Metab.* 2005; 19: 471-482

Badman MK, Koester A, Flier JS, Kharitonov A, Maratos-Flier E. Fibroblast growth factor 21-deficient mice demonstrate impaired adaptation to ketosis. *Endocrinol.* 2009; 150: 4931-4940.

Baumeier C, Schlüter L, Saussenthaler S, Laeger T, Rödiger M, Alaze SA, et al. Elevated hepatic DPP4 activity promotes insulin resistance and non-alcoholic fatty liver disease. *Mole Metab.* 2017; 6: 1254-1263.

Bechmann LP, Hannivoort RA, Gerken G, Hotamisligil GS, Trauner M, Canbay A. The interaction of hepatic lipid and glucose metabolism in liver diseases. *J Hepatol.* 2012; 56: 952-964.

Browning JD, Horton JD. Molecular mediators of hepatic steatosis and liver injury. *J Clin Investig.* 2004; 114: 147-152.

Cao Y. Adipose tissue angiogenesis as a therapeutic target for obesity and metabolic diseases. *Nat Rev Drug Discov.* 2010; 9: 107-115.

Cases S, Stone SJ, Zhou P, Yen E, Tow B, Lardizabal KD, et al. Cloning of DGAT2, a second mammalian diacylglycerol acyltransferase, and related family members. *J Biol Chem.* 2001; 276: 38870-38876.

Charlton M, Viker K, Krishnan A, Sanderson S, Veldt B, et al. Differential expression of lumican and fatty acid binding protein-1: new insights into the histologic spectrum of nonalcoholic fatty liver disease. *Hepatology*. 2009; 49: 1375-1384.

Coleman RA and Lee DP. Enzymes of triacylglycerol synthesis and their regulation. *Prog Lipid Res*. 2004; 43: 134-176.

Deacon CF. Physiology and pharmacology of DPP-4 in glucose homeostasis and the treatment of type 2 diabetes. *Front Endocrinol*. 2019; 10: 1-14.

Del Campo JA, Gallego P and Grande L. Role of inflammatory response in liver diseases: Therapeutic strategies. *World J Hepatol*. 2018; 10: 1-7.

Delarue J and Magnan C. Free fatty acids and insulin resistance. *Curr Opin Clin Nutr Metab Care* 2007; 10: 142-148.

Dey D, Basu D, Roy SS, Bandyopadhyay A, Bhattacharya S. Involvement of novel PKC isoforms in FFA induced defects in insulin signaling. *Mol Cell Endocrinol*. 2006; 246: 60-64.

Ding X, Boney-Montoya J, Owen BM, Bookout AL, Coate KC, Mangelsdorf DJ, Kliewer SA. β Klotho is required for fibroblast growth factor 21 effects on growth and metabolism. *Cell metab*. 2012; 16: 387-393.

Doege H, Grimm D, Falcon A, Tsang B, Storm TA, Xu H, et al. Silencing of hepatic fatty acid transporter protein 5 in vivo reverses diet-induced non-alcoholic fatty liver disease and improves hyperglycemia. *J Biol Chem*. 2008; 283: 22186-22192.

Donnelly KL, Smith CI, Schwarzenberg SJ, Jessurun J, Boldt MD, Parks EJ. Sources of fatty acids stored in liver and secreted via lipoproteins in patients with nonalcoholic fatty liver disease. *J Clin Investig*. 2005; 115: 1343-1351.

Feldstein AE. Novel insights into the pathophysiology of nonalcoholic fatty liver disease. *Semin Liver Dis.* 2010; 30: 391-401

Gallwitz B. Linagliptin--A Novel Dipeptidyl Peptidase Inhibitor for Type 2 Diabetes Therapy. *Clinical Clin Med Insights Endocrinol Diabetes.* 2012; 5: 1-11.

Goedeke L, Bates J, Vatner DF, Perry RJ, Wang T, Ramirez R, et al. Acetyl-CoA Carboxylase Inhibition Reverses NAFLD and Hepatic Insulin Resistance but Promotes Hypertriglyceridemia in Rodents. *Hepatology.* 2018; 68: 2197-2211.

Greco D, Kotronen A, Westerbacka J, Puig O, Arkkila P, Kiviluoto T, et al. Gene expression in human NAFLD. *Am J Physiol Gastrointest Liver Physiol.* 2008; 294: G1281-G1287.

Higuchi N, Kato M, Tanaka M, Miyazaki M, Takao S, Kohjima M, et al. Effects of insulin resistance and hepatic lipid accumulation on hepatic mRNA expression levels of apoB, MTP and L-FABP in non-alcoholic fatty liver disease. *Exp Ther Med.* 2011; 2: 1077-1081.

Hsieh PS and Hsieh YJ. Impact of liver diseases on the development of type 2 diabetes mellitus. *World J Gastroenterol.* 2011; 17: 5240-5245.

Ipsen DH, Lykkesfeldt J, Tveden-Nyborg P. Molecular mechanisms of hepatic lipid accumulation in non-alcoholic fatty liver disease. *Cell Mol Life Sci.* 2018; 75: 3313-3327.

Itou M, Kawaguchi T, Taniguchi E, Sata M. Dipeptidyl peptidase-4: a key player in chronic liver disease. *World J Gastroenterol.* 2013; 19: 2298-2306.

Jung HA, Ali MY, Bhakta HK, Min BS, Choi JS. Prunin is a highly potent flavonoid from *Prunus davidiana* stems that inhibits protein tyrosine phosphatase 1B and stimulates glucose uptake in insulin-resistant HepG2 cells. *Arch Pharm Res.* 2017; 40: 37-48.

Kawaguchi T, Taniguchi E, Itou M, Sakata M, Sumie S, Sata M. Insulin resistance and chronic liver disease. *World J Hepatol.* 2011; 3: 99-107.

Kawasaki N, Asada R, Saito A, Kanemoto S, Imaizumi K. Obesity-induced endoplasmic reticulum stress causes chronic inflammation in adipose tissue. *Sci Rep.* 2012; 2: 1-7.

Klemann C, Wagner L, Stephan M and von Hörsten S. Cut to the chase: a review of CD26/dipeptidyl peptidase-4's (DPP4) entanglement in the immune system. *Clin Exp Immunol.* 2016; 185: 1-21.

Kohjima M, Enjoji M, Higuchi N, Kato M, Kotoh K, Yoshimoto T, et al. Re-evaluation of fatty acid metabolism-related gene expression in nonalcoholic fatty liver disease. *Int J Mol Med.* 2007; 20: 351-358.

Koo SH. Nonalcoholic fatty liver disease: molecular mechanisms for the hepatic steatosis. *Clin Mol Hepatol.* 2013; 19: 210-215.

Koonen DP, Jacobs RL, Febbraio M, Young ME, Soltys CLM, Ong H, et al. Increased hepatic CD36 expression contributes to dyslipidemia associated with diet-induced obesity. *Diabetes.* 2007; 56: 2863-2871.

Lee YK, Park JE, Lee M, Hardwick JP. Hepatic lipid homeostasis by peroxisome proliferator-activated receptor gamma 2. *Liver Res.* 2018; 2: 209-215.

Listenberger LL, Han X, Lewis SE, Cases S, Farese RV, Ory DS, Schaffer JE. Triglyceride accumulation protects against fatty acid-induced lipotoxicity. *Proc Natl Acad Sci. U.S.A.* 2003; 100: 3077-3082.

Loria P, Lonardo A, Anania F. Liver and diabetes. A vicious circle. *Hepatol Res.* 2013; 43: 51-64.

Lovshin JA and Drucker DJ. Incretin-based therapies for type 2 diabetes mellitus. *Nat Rev Endocrinol.* 2009; 5: 262-269.

Markan KR, Naber MC, Ameka MK, Anderegg MD, Mangelsdorf DJ, Kliewer SA, et al. Circulating FGF21 is liver derived and enhances glucose uptake during refeeding and overfeeding. *Diabetes*. 2014; 63: 4057-4063.

Mashek DG. Hepatic fatty acid trafficking: multiple forks in the road. *Adv Nutr*. 2013; 4: 697-710.

Mudaliar S and Henry RR. Effects of incretin hormones on β -cell mass and function, body weight, and hepatic and myocardial function. *Am J Med*. 2010; 123: S19-S27.

Mulvihill EE and Drucker DJ. Pharmacology, physiology, and mechanisms of action of dipeptidyl peptidase-4 inhibitors. *Endocr Rev*. 2014; 35: 992-1019.

Mulvihill EE. Dipeptidyl peptidase inhibitor therapy in type 2 diabetes: control of the incretin axis and regulation of postprandial glucose and lipid metabolism. *Peptides*. 2018; 100: 158-164.

Nauck MA and Meier JJ. GIP and GLP-1: stepsiblings rather than monozygotic twins within the incretin family. *Diabetes*. 2019; 68: 897-900.

Neuschwander-Tetri BA. Hepatic lipotoxicity and the pathogenesis of nonalcoholic steatohepatitis: the central role of nontriglyceride fatty acid metabolites. *Hepatology (Baltimore, Md)* 2010; 52: 774-788.

Pazhanivel M and Jayanthi V. Diabetes mellitus and cirrhosis liver. *Minerva Gastroenterol Dietol*. 2010; 56: 7-11.

Postic C and Girard J. The role of the lipogenic pathway in the development of hepatic steatosis. *Diabetes Metab*. 2008; 34: 643-648.

Roden M. Mechanisms of disease: hepatic steatosis in type 2 diabetes – pathogenesis and clinical relevance. *Nat Clin Pract Endocrinol Metab*. 2006; 2: 335-348.

Ryskjaer J, Deacon CF, Carr RD, Krarup T, Madsbad S, Holst J, Vilsboll T. Plasma dipeptidyl peptidase-IV activity in patients with type-2 diabetes mellitus correlates positively with HbA1c levels, but is not acutely affected by food intake. *Eur J Endocrinol.* 2006; 155: 485-493.

Samuel VT, Liu ZX, Wang A, Beddow SA, Geisler JG, Kahn M, et al. Inhibition of protein kinase C ϵ prevents hepatic insulin resistance in nonalcoholic fatty liver disease. *J Clin Investig.* 2007; 117: 739-745.

Sanders FW and Griffin JL. De novo lipogenesis in the liver in health and disease: more than just a shunting yard for glucose. *Biol Rev.* 2016; 91: 452-468.

Savage DB, Choi CS, Samuel VT, Liu ZX, Zhang D, Wang A, et al. Reversal of diet-induced hepatic steatosis and hepatic insulin resistance by antisense oligonucleotide inhibitors of acetyl-CoA carboxylases 1 and 2. *J Clin Investig.* 2006; 116: 817-824.

Silverstein RL and Febbraio M. CD36, a scavenger receptor involved in immunity, metabolism, angiogenesis, and behavior. *Sci Signal.* 2009; 2: 1-16.

Tong L and Harwood Jr HJ. Acetyl-coenzyme A carboxylases: versatile targets for drug discovery. *J Cell Biochem.* 2006; 99: 1476-1488.

Trombetta M, Spiazzi G, Zoppini G, Muggeo M. type 2 diabetes and chronic liver disease in the Verona diabetes study. *Aliment Pharmacol Ther.* 2005; 22: 24-27.

Trzaskalski NA, Fadzeyeva E, Mulvihill EE. Dipeptidyl peptidase-4 at the interface between inflammation and metabolism. *Clin Med Insights: Endocrinol Diabetes.* 2020; 13: 1-10

Varin EM, Mulvihill EE, Beaudry JL, Pujadas G, Fuchs S, Tanti JF, et al. Circulating levels of soluble dipeptidyl peptidase-4 are dissociated from inflammation and induced by enzymatic DPP4 inhibition. *Cell Metab.* 2019; 29: 320-334.

Wang G, Bonkovsky HL, de Lemos A, Burczynski FJ. Recent insights into the biological functions of liver fatty acid binding protein 1. *J Lipid Res.* 2015; 56: 2238-2247.

Wang Z, Yao T, Song Z. Involvement and mechanism of DGAT2 upregulation in the pathogenesis of alcoholic fatty liver disease. *J Lipid Res.* 2010; 51: 3158-3165.

Wilson CG, Tran JL, Erion DM, Vera NB, Febbraio M, Weiss EJ. Hepatocyte-specific disruption of CD36 attenuates fatty liver and improves insulin sensitivity in HFD-fed mice. *Endocrinology.* 2016; 157: 570-585.

Wolfrum C, Borrmann CM, Borchers T, Spener F. Fatty acids and hypolipidemic drugs regulate peroxisome proliferator-activated receptors α - and γ -mediated gene expression via liver fatty acid binding protein: a signaling path to the nucleus. *Proc Natl Acad Sci. U.S.A.* 2001; 98: 2323-2328.

Yamaguchi K, Yang L, McCall S, Huang J, Yu XX, Pandey SK, et al. Inhibiting triglyceride synthesis improves hepatic steatosis but exacerbates liver damage and fibrosis in obese mice with nonalcoholic steatohepatitis. *Hepatology.* 2007; 45: 1366-1374.

Younossi ZM, Koenig AB, Abdelatif D, Fazel Y, Henry L, Wymer M. Global epidemiology of nonalcoholic fatty liver disease—meta-analytic assessment of prevalence, incidence, and outcomes. *Hepatology.* 2016; 64: 73-84.

Chapter 5

Repercussion of hyperinsulinemia on mitochondria and ER- mitochondria calcium signaling in HepG2 cells

5.1 Introduction

Obesity, T2DM and prediabetes partially, are the major insulin resistant states. During hepatic insulin resistance, the glucose production and lipid synthesis is increased (Bazotte et al., 2014). The end result of increased glucose production is the genesis of hyperglycemia (Barrena et al., 2014). Insulin has different metabolic actions in different tissues such as liver, skeletal muscle, adipose tissue etc (Kim et al., 2008). This explains the importance of insulin resistance in the prevalence of many metabolic diseases (Kim et al., 2008). Liver plays an inevitable role in both glucose and lipid metabolism (Kim et al., 2008). The hepatocytes are enriched with mitochondria and hepatic mitochondria have some uniqueness compared with other organ's mitochondria (Degli Esposti et al., 2012). Hepatic mitochondria act as a hub for the integration of lipid, carbohydrate and protein metabolism. The primary need of each cell in our body is energy and the glucose is the main energy providing substrate in our body. So both glucose and lipid metabolism is largely depending on the mitochondria (Kim et al., 2008). Mitochondria is the energy manufacturing factory of cells. The metabolic regulation of cells depends on the mitochondria, which produce energy in the form of ATP by metabolizing the nutrients. The metabolic pathways exclusively taking place inside the mitochondria include Krebs cycle and β -oxidation (Kim et al., 2008). However, mitochondria are the center for the calcium (Ca^{2+}) homeostasis also. Apart from this, mitochondria are not only the energy reservoir of all the cells but also determine the life span of the cells by regulating the apoptosis. The main decision

making part of the mitochondria for the transition from survival to death is its membrane permeabilization. The compartmentalization of mitochondria is carried out by the presence of outer and inner mitochondrial membranes. The location of electron transport chain (ETC) is in the inner mitochondrial membrane. Glycolysis and Krebs cycle or β -oxidation are the major pathways that provide reducing equivalents and give electrons for the synthesis of ATP. The proton gradient across the membrane is the driving force for the synthesis of ATP. So mitochondrial dysfunctions are the initiating event for many of the pathological conditions (Mantena et al., 2007). Furthermore, it has been reported that mitochondrial dysfunctions are closely associated with the insulin resistance in many of the tissues such as muscles, liver, fat, heart and pancreas (Fabbrini et al., 2010; Green et al., 2011). So both insulin resistance and mitochondrial dysfunctions are the main players behind the genesis of many metabolic diseases. Many of the liver diseases are initiated due to the excess accumulation of damaged mitochondria. One of the cell organelle normally produces ROS in smaller amounts as a result of oxidative phosphorylation is the mitochondria. When the cells are exposed to excess nutrients like glucose and lipids the mitochondrial substrates level becomes increased and results in excess ETC activity (Degli Esposti et al., 2012). Greater ETC results in the excessive electron leakage and the electrons partially oxidize the oxygen (Hamanaka and Chandel, 2010; Nohl et al., 2005). The end result of this mechanism is the enormous superoxide production. In continuation with chapter 2, during hyperglycemic conditions the OS is initiated as a result of HI. I have already found in my first chapter that, in HI the OS increases the lipid peroxidation and protein alkylation. The increased ROS will definitely affect the antioxidant system of the cells. Apart from this, increased ROS affect the mitochondria by down-regulating the MnSOD levels, aconitase, decreased glutathione levels and alterations in respiratory chain complexes. Furthermore, mitochondria have an essential role in both glucose and lipid metabolism. The last step of glycolysis is carried out by the enzyme pyruvate dehydrogenase and the location of

this protein is in the mitochondria. The end product of this reaction is the formation of acetyl CoA and CO₂. Role of mitochondria in lipid metabolism is the presence of certain proteins involved in both lipid catabolism and anabolism. The enzymes like carnitine palmityl transferase I and II (CPT I and II) are seen in the mitochondrial outer and inner membrane. In the liver they are responsible for the transport of acyl CoA (Degli Esposti et al., 2012). Liver mitochondria is also involved in protein metabolism. All the proteins involved in the detoxification of both ammonia and urea synthesis are exclusively present in the liver mitochondria (Degli Esposti et al., 2012). Many reports revealed that excess amount of structurally and functionally abnormal mitochondria like mega mitochondria were present in diabetic, obese and fatty liver patients (Begrache et al., 2006). In order to overcome these pathologies and maintain the mitochondrial integrity the hepatocyte mitochondria adopted some mechanisms. These mechanisms include removal of damaged mitochondria, increased mitochondrial biosynthesis, regulation of energy metabolism and decreased inflammation and cell death. The major regulator of mitochondrial biogenesis is the peroxisome proliferator-activated receptor-γ coactivator (PGC)-1α (Scarpulla, 2011). In addition to biogenesis PGC-1α is also involved in most of the metabolic pathways in the liver such as gluconeogenesis, fatty acid oxidation and ketogenesis (Handschin et al., 2005; Puigserver et al., 2003). AMP-activated protein kinase (AMPK) and sirtuin 1 (SIRT1) are the other main participant proteins in the biogenesis of mitochondria.

Apart from this, the liver is involved in the important metabolic secretory and excretory functions in the body to maintain the whole body homeostasis. Hepatocytes are the major cells in the liver responsible for VLDL formation for the synthesis and maintenance of plasma proteins such as albumin, coagulation factors etc. However, they are also involved in the processes like cholesterol synthesis, lipogenesis, Ca²⁺ homeostasis, glucose and xenobiotic metabolism. In order to perform these wide range of functions, the hepatocytes are enriched

with both rough and smooth ER (Wang and Kaufman, 2016). It has been revealed that the mitochondrial dysfunction and the ER stress are independently interrelated and it is developed due to the loss of insulin signaling and unwanted lipid synthesis (Rieusset, 2017). Each organ has independent function and each organelle stress has a prominent role in the prevalence of various metabolic diseases such as obesity, T2DM and fatty liver disease like NAFLD (Rieusset, 2017). Mitochondrial dysfunction affects the insulin signaling and its secretion via the activation of OS or imbalanced lipid metabolism (Rieusset, 2017). Likewise, the ER stress creates many adverse effects through the initiation of UPR. Meanwhile, both organelles stresses are able to start the inflammation pathways (Hummasti and Hotamisligil, 2010). Like the uniqueness of hepatic mitochondria, hepatic ER also shows an amazing capacity to adapt the intracellular and extracellular alterations and preserve the vital hepatic metabolism. Meanwhile, ER is involved in the UPR pathway for maintaining lipid as well as protein homeostasis (Walter and Ron, 2011). UPR is engaged to decrease the protein load, improves the protein folding and increases the protein quality through the activation of protein clearance by an enhanced ER-associated degradation process (ERAD). During the activation of UPR the three arms of UPR are activated; (i) inositol requiring enzyme 1 (IRE-1 α), (ii) activating transcription factor 6 (ATF6), and (iii) PKR-like ER kinase (PERK). In normal condition all these transmembrane ER proteins were attached into a chaperone glucose regulatory protein 78 (GRP78) and become inactive. When the accumulation of misfolded protein increases, GRP78 is detached from these stress sensors and becomes active. In addition, a combination of factors are involved in the UPR activation such as protein disulfide isomerase (PDI), numerous chaperones, heat shock proteins etc. Upon activation, the IRE-1 α activates its target protein XBP1 which activates the components of ERAD, heat shock protein and increases the phospholipid synthesis (Mohan et al., 2019). This finally results in the ER membrane expansion, a major characteristic of UPR activation (Mohan et al., 2019). Meanwhile the

activated XBP1 reduces the entry of proteins into the ER by degrading them using its RNase activity. The activated IRE-1 α and XBP1 simultaneously activate the TG synthesis and up regulate the hepatic lipid synthesis (Mohan et al., 2019). ATF6 is a membrane protein and it has two isoforms; ATF6 α and ATF6 β . During activation of ATF6, it enters into Golgi bodies and undergo cleavage by proteases. The cleaved fragment is then targeted to the nucleus and it regulates the gene expression (Nadanaka et al., 2004; Shen et al., 2002). The activated ATF6 also regulates the proteins involved in ERAD and activates the XBP1 also (Yoshida et al., 2001). The third arm PERK is activated during the accumulation of misfolded proteins and the activated PERK activates the eIF2 α , it inhibits the mRNA translation (Blais et al., 2004). PERK trans activates the ATF4 and is involved in the regulation of amino acid metabolism, autophagy, and apoptosis (Cullinan et al., 2003; Harding et al., 2003). If the adaptive UPR response is replaced by the chronic ER stress it becomes switched to cell death (Hetz et al., 2015) through excessive production of pro-apoptotic Bcl2 proteins or increased Ca²⁺ release (Urrea et al., 2013). Hepatic ER have a dominant role in lipid metabolism also. DNL in the liver is controlled by ER localized transcription factor, SREBP1c. In addition to this, the enzyme responsible for the TG synthesis (DGAT2) is also an ER localized protein. Furthermore, the VLDL assembly takes place inside the ER before it is localized into Golgi. ER homeostasis is essential for controlling hepatic and plasma lipid homeostasis and maintaining a membrane lipid composition. Furthermore, the hepatic lipids have a crucial role in the Ca²⁺ homeostasis in initiating the ER stress. Ca²⁺ is a versatile secondary messenger participating in numerous cellular processes (Gao et al., 2018). The important cell organelle responsible for the storage of Ca²⁺ is the ER (Berridge et al., 2003). Studies revealed that the excess amount of Ca²⁺ release not only develops the mitochondrial dysfunctions and the ER stress but also creates hepatic lipotoxicity (Egnatchik et al., 2014). One of the major pump responsible for the transport of

Ca²⁺ from cytoplasm to ER is sarcoplasmic/endoplasmic reticulum calcium ATPase (SERCA) and it is located in ER (Lai et al., 2017; Zhang et al., 2014).

It is important that both ER and mitochondria are not considered as individual organelles (Rieusset, 2017) because they are structurally and functionally interconnected and transport the molecules across the ER and mitochondria. These contact sites are referred to as mitochondria associated ER membranes (MAMs) (Giorgi et al., 2015; Marchi et al., 2014). MAMs are involved in many important functions like lipid transport, apoptosis, Ca²⁺ signaling and energy metabolism (Tubbs et al., 2014). The physical interaction in MAM is mainly due to the presence of certain connector proteins. Voltage-dependent anion channel (VDAC) is the mitochondrial protein (situated in the outer mitochondrial membrane), it interacts with the ER protein inositol 1,4,5-trisphosphate receptor (IP3R), (situated on the ER membrane) and to form MAM. GRP78 is the connector protein which connects the VDAC with IP3R. Furthermore, the transport of Ca²⁺ from ER to mitochondria takes place through MAM (Szabadkai et al., 2006). In addition to this numerous proteins has been identified in the MAM junction, they are mammalian target of rapamycin 2 (mTORC2), AKT, protein phosphatase 2A (PP2A) and phosphatase and tensin homolog (PTEN) etc. (Betz et al., 2013; Tubbs et al. 2014). Recent report suggested that the various proteins in the insulin signaling pathways were also identified in the membrane of MAM (Tubbs et al., 2014). It was shown that the insulin could modulate the IP3R action in the ER (Wang et al. 2012). One of the data revealed that the specific silencing of MFN2 in hepatocytes is associated with hepatic insulin resistance. This indicated that both the ER and mitochondria are the main actors for the energy metabolism and their alterations lead to the development of hepatic insulin resistance (Vial et al., 2011).

It has been proved that ER- mitochondria miscommunication is one of the crucial factors for the development of all metabolic diseases by promoting ER stress, mitochondrial dysfunction,

altered Ca^{2+} homeostasis and lipid accumulation (Rieusset, 2017). So the understanding about the importance of MAM in metabolic diseases and the targeting of MAM structure and function might be an emerging area and it creates a new interesting way to improve the glucose and lipid homeostasis in metabolic syndrome (Tubbs et al., 2014). MAM also has an important role in UPR signaling. One of the studies reported that inhibition of MAM protein PACS2 destroyed the MAM integrity and also created severe ER stress (Simmen et al., 2005). In addition to this the loss of other MAM proteins such as sigma-1 receptor (SigR1), mitofusin2 (MFN2) and cyclophilin D (CypD) can also initiate the ER stress (Rieusset et al., 2016; Sebastian et al., 2012). Recently there is little knowledge about the mitochondrial dysfunction, altered Ca^{2+} homeostasis and ER stress associated with altered insulin signaling. In addition to this, the implication of MAM dysfunctions in insulin resistance are also unknown. So in this chapter I have discussed the role of mitochondria and ER in the pathogenesis of HI created insulin resistance. Here I focused on the role of Ca^{2+} in the progression of HI created insulin resistance. While I also attempted to study about the MAM and the involvement of MAM in the pathogenesis of HI.

5.2 Materials and methods

5.2.1 Chemicals

Dimethylsulfoxide (DMSO), radioimmunoprecipitation assay buffer (RIPA buffer), and VA were from Sigma Aldrich Chemical Co. (St. Louis, MO, USA). JC1 dye, MitoSox, Mitotracker Deep Red FM, Fura 2AM and Calcein AM were purchased from Invitrogen™ Fisher Scientific (USA). Penicillin-streptomycin antibiotics, Dulbecco's modified eagle's medium (DMEM), fetal bovine serum (FBS), and 0.5% trypsin-ethylenediaminetetraacetic acid (trypsin-EDTA) were from Gibco-BRL Life Technologies (Waltham, MA, USA). Adenosine monophosphate activated kinase (AMPK), phospho-AMPK (p-AMPK), peroxisome proliferator activated

receptor γ coactivator-1 α (PGC-1 α), sirtuin 1 (Sirt 1), fission 1 protein (FIS 1), optic atrophy 1 (OPA 1) were purchased from Santa Cruz Biotechnology (Dallas, TX, USA). mTORC, PTEN, MFN 2, GRP75, CYPD, VDAC, p-IRE1, ATF6, p-PERK, p-eIF2 α , CHOP, XBP1, p-CAMII, InsP3R, SERCA, JNK, GRP78, β -actin and all other secondary antibodies were from cell signaling technology. Metformin was from SRL (Mumbai, India). Recombinant human insulin and methanol were from Merck (Kenilworth, NJ, USA). The remaining chemicals used were of analytical grade from SRL (Mumbai).

5.2.2 Cell culture

HepG2 cells from NCCS, Pune, were cultured in Dulbecco's modified eagle's medium (DMEM) along with fetal bovine serum (FBS; 10 %) and antibiotics at 37 °C in a CO₂ incubator with 5 % CO₂ and 95 % air. Cells were allowed to reach 80 % confluency. Then the cells were co-treated with high insulin (1 μ M) in the presence and absence of different concentrations of VA (5 μ M and 10 μ M) and metformin (1mM, positive control) in 1 % serum containing media.

5.2.3 Detection of mitochondrial superoxide

Mitochondrial superoxide production was evaluated with a MitoSox™ (Merck, USA) kit. The cells were treated with 5 mM mitosox and incubated for 20 min. After three washes with HBSS, the bioimages were visualized using the bioimager system at 514 and 580 nm. Fluorescence was measured with excitation at 514 nm and emission at 580 nm using the microplate reader.

5.2.4 Mitochondrial content

Estimation of mitochondrial content was determined by using a dye Mitotracker Deep Red FM. Briefly after treatment the cells were incubated with 5 μ M of Mitotracker Deep Red stain in PBS at 37 °C for 30 min. Then the cells were subjected to washing with PBS for 3 times. Then

it was visualised by fluorescent microscope (Nikon, Melville, NY) and measured the fluorescent intensity at an excitation and emission wavelengths of 644 and 665 nm respectively.

5.2.5 Analysis of aconitase activity

After treatments, cells were subjected to trypsinization using 1 ml of 10X trypsin-EDTA as previously and centrifuged at 800 x g for 10 min at 4 °C and the pellet was collected. The cell pellet was resuspended in a 1 ml assay buffer. The cell suspension was centrifuged at 20,000 x g for 10 min at 4 °C. Sample (cell supernatant) of 50 µl was added to the respective wells. Then aconitase nicotinamide adenine dinucleotide phosphate (aconitase NADP) (50 µl) reagent and aconitase isocitrate dehydrogenase solution (50 µl) were added along with 50 µl of substrate. The absorbance was measured at 340 nm for 30 min at 37 °C. The change in absorbance/min was determined and reaction rate was calculated.

5.2.6 Mitochondrial membrane potential ($\Delta\psi_m$)

After treatments with VA, the medium was changed and the cells were stained with JC-1 stain (Merck, USA) for 20 min at 37 °C. In normal cells, the JC-1 dye accumulates inside the mitochondria and forms JC-1 aggregates and gives a red fluorescence. Distortion of the $\Delta\psi_m$ prevents the dye entry into the mitochondria, as a result JC-1 monomers were formed and produced green fluorescence. The shift of fluorescence was visualized and fluorescence intensity was measured using the fluorescence microplate reader with an excitation 490 and emission wavelength of 530 nm for JC-1 monomers, and the excitation 525 and emission wavelength 590 nm for aggregates.

5.2.7 Mitochondrial biogenesis

The expression of proteins like AMPK, p-AMPK, Sirt1 and PGC-1 α were analysed with western blotting (for details please see section 5.2.15).

5.2.8 Mitochondrial dynamics

The expression levels of fission and fusion proteins were evaluated using western blotting (for details please see section 5.2.15).

5.2.9 Mitochondrial bioenergetics

ATP levels were measured using the ATP determination assay kit. After treatment with VA the cells were homogenized as previously described with ATP assay buffer. Then 100 µl of 1X somatic cell ATP releasing agent, and 50 µl of ultrapure water provided in the kit were added into 50 µl of sample. Then A 100 µl aliquot was transferred to the reaction vial with 100 µl of ATP assay mix and kept at RT for 3 min. The amount of light emitted at 560 nm was measured using the microplate reader.

The oxygen consumption rate was assessed by using an oxygen consumption assay kit. This kit uses a phosphorescent oxygen probe to check oxygen consumption rate. Blank wells were filled with only culture mediums. After treatments with VA, the spent medium was replaced with fresh medium. MitoXpress xtra solution (10 µl) was added to all the wells except the blank. Then 100 µl of HS mineral oil (provided with the kit) was added over each well. After that the fluorescence was read at 380 nm (excitation) and 650 nm (emission) kinetically for 150 min using the microplate reader.

5.2.10 Detection of total calcium and intracellular calcium levels by

Fura 2 AM

The total Ca²⁺ concentration was determined using the Ca²⁺ assay kit provided by Cayman chemicals (USA). This assay utilizes a variant of o-Cresolphthalein-Ca²⁺ reaction. In the presence of Ca²⁺ it forms a purple coloured complex. Briefly, the cells were seeded at a density of 5 × 10⁶ cells in 96-plates and subjected to treatments. After treatments the cells were collected and the cell pellets were dissolved in a 600 µl cold buffer consisting of 100 mM Tris

at a pH of 7.5. Then the content was centrifuged at $10,000 \times g$ for 15 min at 4°C . The supernatant was collected and stored. $10 \mu\text{l}$ of supernatant (samples) and standards were added into designated wells in the plate. Then the working detector of $200 \mu\text{l}$ was added to all the wells being used. The plate was shaken for 25 sec and incubated at RT for 5 min. Finally, I measured the absorbance at 580 nm.

The intracellular Ca^{2+} levels were detected using a fluorescent dye Fura2 AM. Briefly, the cells were seeded in 96-well plates and after incubation time they were subjected to respective treatments. Then the cell culture medium was removed and the cells were stained with the intracellular Ca^{2+} indicator dye Fura 2AM in PBS. Then the cells were incubated at 37°C for 20 min. Cells were then washed with PBS for 3 times and the images were visualized under Nikon Eclipse TS 100 fluorescence microscope at an excitation and emission wavelengths of 340 nm and 510 nm respectively.

5.2.11 Mitochondrial permeability transition pore

The mPTP opening was assessed by using a fluorescent dye calcein AM in the presence of cobalt chloride (Bonora et al., 2016). For this assay the cells were seeded in a 96-well plate and after respective treatments the cell culture medium was removed and washed with KRB. Then 1 ml of calcein AM working solution ($1 \mu\text{M}$ calcein AM and 2mM cobalt chloride in KRB) was added into all the wells. Then the plate was incubated for 37°C in a CO_2 incubator for 15 min. Then the plate was washed 3 times with KRB and images were taken under fluorescent microscope (Nikon, Melville, NY). Then fluorescent intensity was measured at an excitation wavelength of 488 nm and an emission wavelength of 525 nm.

5.2.12 Calcium dysregulation and role of ER

Ca²⁺ homeostasis was determined by analyzing the expression of various proteins involved in this mechanism. The expression of proteins such as p-CAMKII, InsP3R, SERCA, JNK and GRP78 were analyzed by using western blotting (for details, please refer to section 5.2.15).

5.2.13 Hyperinsulinemia and ER stress

ER stress was evaluated by studying the UPR pathway. The major proteins involved in the three arms of UPR such as p-IRE1, ATF6, p-PERK, p-eIF2, CHOP and XBP1 were assessed using western blotting. Band intensity was measured using Image J Software (for details, please refer to section 5.2.15).

5.2.14 Effect of hyperinsulinemia on mitochondria associated ER membrane

The major proteins involved in the mitochondria associated ER membrane (MAM) such as VDAC, Cyp D, GRP75, MFN2, PTEN and mTORC were analyzed by using western blotting (for details please refer section 5.2.15). All these proteins are presented on the surface of ER and mitochondria. Band intensity was measured using Image J Software.

5.2.15 Western blot

Cells were cultured in T-25 flasks containing DMEM medium and the respective treatments with VA were done. After the treatments, the total protein was isolated with a RIPA buffer. Then quantified the protein concentration and normalized the protein content using the Pierce BCA protein assay kit (Thermo Fisher Scientific Co., Waltham, MA, USA). Equal amounts of protein were added into the wells of 10 % SDS-PAGE gel and were separated. Then transferred the proteins into the PVDF membranes using the Trans-Blot Turbo TM transfer system (Bio-Rad, USA). The membranes were blocked with 3 % BSA in TBST for 1 hr at RT. Then the membranes were subjected to washing with TBST for 3 times. The membrane was incubated

at 4 °C overnight with primary antibodies of the membrane was incubated at 4 °C overnight with primary antibodies of AMPK, p-AMPK, PGC-1 α , Sirt 1, FIS1 and OPA1, p-CAMKII, InsP3R, SERCA, JNK, GRP78, p-IRE-1 α , ATF6, p-PERK, p-eIF2 α , CHOP, XBP1, VDAC, Cyp D, GRP75, MFN2, PTEN, mTORC and β -actin of 1:1000 dilution. Then the membrane was washed three times with TBST for 10 min each and incubated with HRP-conjugated secondary antibody (1:2000) for 90 min at RT. Then the membrane was washed 3 times with TBST and developed the membrane with ECL substrate (BioRad). Then the proportional thickness of bands were analyzed using Image Lab software in the Chemi Doc system (ChemiDoc MP Imaging System, Bio-Rad) and assuming all bands were in the Beer-Lambert law region.

5.2.16 Statistics

All analyses were done with sextuplicates and results are shown as mean \pm SEM for the control and the experimental groups. The normality of the variables was tested using the Kolmogorov Smirnov Z test and the variables were found to be approximately normally distributed. The data were tested using ANOVA. All the statistical analyses were done using the Statistical Package for the Social Sciences for Windows standard version 20 (SPSS Inc., USA) and the further significantly different pairs ($p \leq 0.05$) were identified using Duncan's multiple comparison test.

5.3 Results

5.3.1 Effect of VA on mitochondrial superoxide production

Surplus generation of ROS was observed in IR groups (Fig: 5.1A & Fig: 5.1B) compared to control. Fluorescence detection also showed an increment of fluorescence in IR cells (143 %). VA of both concentrations (5 and 10 μ M) reduced superoxide by 161 and 193 %, respectively

(Fig: 5.1A & Fig: 5.1B). Compared with metformin (187 %) 10 μ M of VA showed better results (Fig: 5.1A & Fig: 5.1B).

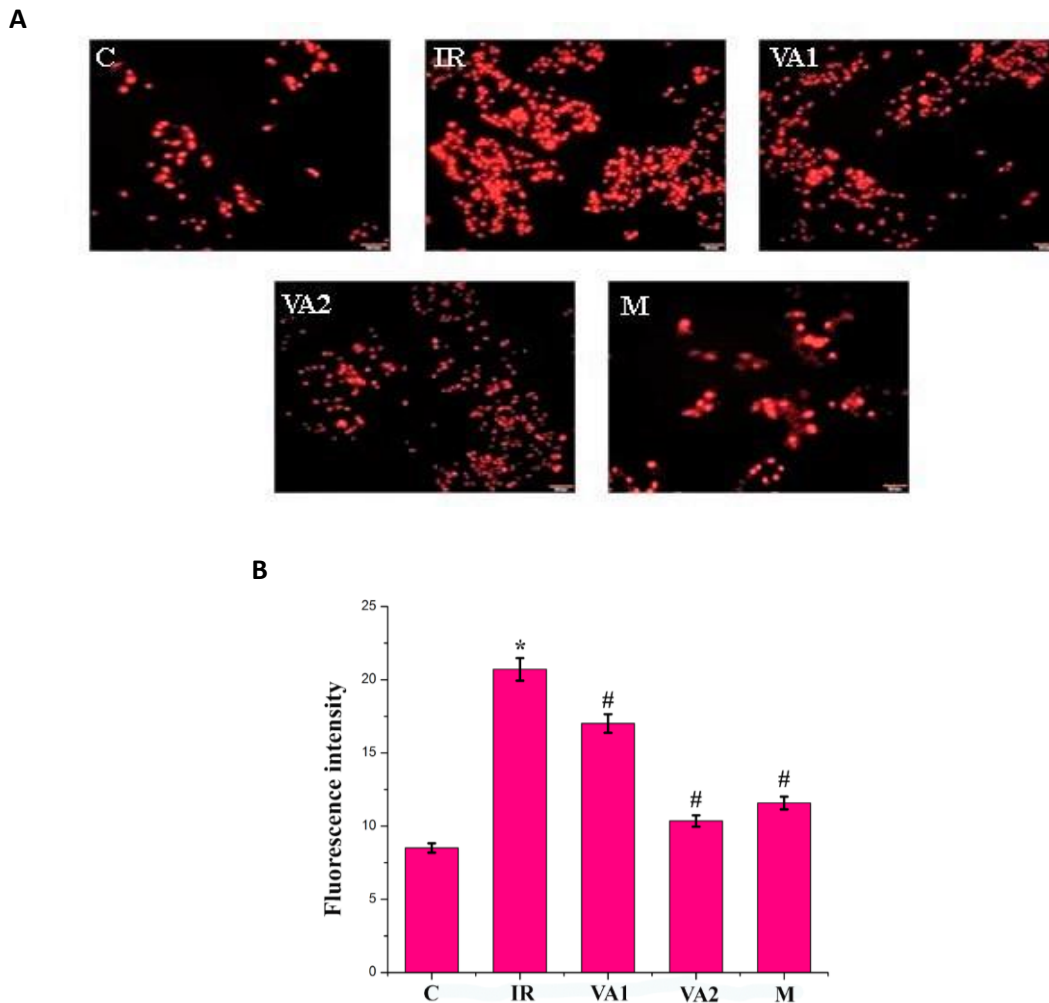


Figure. 5.1 Hyperinsulinemia and mitochondrial superoxide. (A) Effect of VA on mitochondrial superoxide generation using MitoSOX™ Red indicator (original magnification 40x). (B) Relative fluorescent intensity of the fluorescent images C - control cells; IR - hyperinsulinemia created insulin resistant cells; VA1 - IR + 5 μ M vanillic acid; VA2 - IR + 10 μ M vanillic acid; M - IR + metformin (1 mM). Values are expressed as mean \pm SEM where n=6. * indicates that the mean value was significantly different from control cells ($p \leq 0.05$). # indicates the mean value was significantly different from IR cells ($p \leq 0.05$). Scale 50 μ m

5.3.2 Mitochondrial content

Mitochondrial content was analyzed using the dye Mitotracker Deep red. HI causes a significant reduction in the mitochondrial density as compared with the control (40 % reduction; $p \leq 0.05$). In VA treated cells the mitochondrial content was restored significantly

in a dose dependent manner compared with HI treated cells. (10.9 and 22.8 % increase with 5 μ M and 10 μ M of VA respectively than the HI treated cells; $p \leq 0.05$). Metformin treatment also restored the mitochondrial content significantly by 17.2 % compared with HI treated cells ($p \leq 0.05$; Fig: 5.2A & Fig: 5.2B).

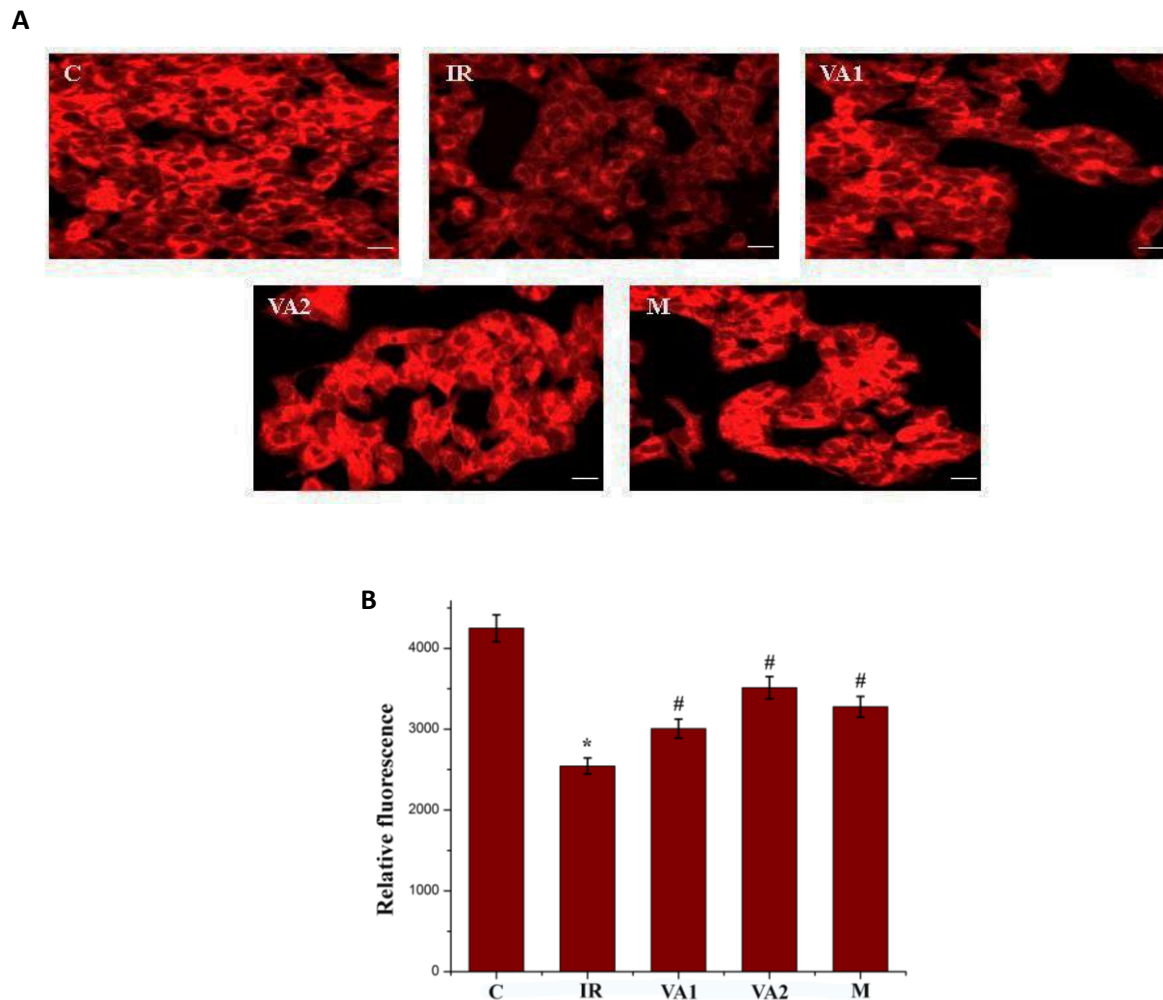


Figure 5.2 Effect of hyperinsulinemia in mitochondrial content. (A) Effect of VA on mitochondrial content using Mitotracker (original magnification 20x). (B) Relative fluorescent intensity of the fluorescent images. C - control cells; IR - hyperinsulinemia created insulin resistant cells; VA1 - IR + 5 μ M vanillic acid; VA2 - IR + 10 μ M vanillic acid; M - IR + metformin (1 mM). Values are expressed as mean \pm SEM where n=6. * indicates that the mean value was significantly different from control cells ($p \leq 0.05$). # indicates the mean value was significantly different from IR cells ($p \leq 0.05$). Scale 50 μ m

5.3.3 Aconitase activity

The aconitase activity was significantly decreased in IR (34 %) groups compared to the control. VA (5 and 10 μM) in a dose dependent manner showed a tendency to increase the enzyme level by 24.2 and 36.6 % compared to IR. Co-treatment with metformin significantly ($p \leq 0.05$) increased the aconitase levels by 56.5 % compared to IR (Fig: 5.3).

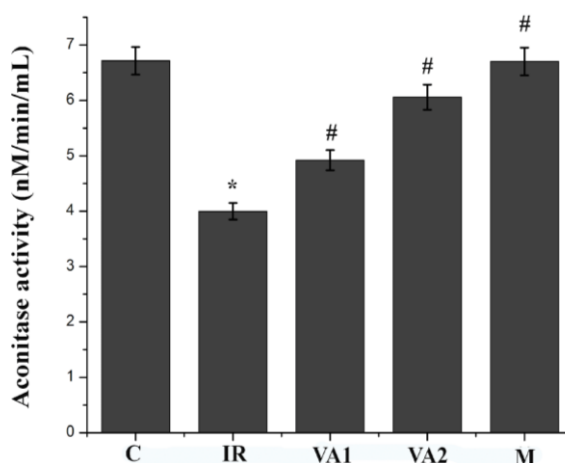


Figure. 5.3 Effect of hyperinsulinemia in aconitase activity. C - control cells; IR - hyperinsulinemia created insulin resistant cells; VA1 - IR + 5 μM vanillic acid; VA2 - IR + 10 μM vanillic acid; M - IR + metformin (1 mM). Values are expressed as mean \pm SEM where $n=6$. * indicates that the mean value was significantly different from control cells ($p \leq 0.05$). # indicates the mean value was significantly different from IR cells ($p \leq 0.05$).

5.3.4 Effect of vanillic acid on membrane potential

Analysis of the $\Delta\psi\text{m}$ of mitochondria during IR showed significant distortion of $\Delta\psi\text{m}$ compared with control (Fig: 5.4A & Fig: 5.4B). In control cells, the JC-1 dye forms aggregate inside the mitochondrial matrix and emits a red fluorescence due to the potential gradient. Alteration in $\Delta\psi\text{m}$ resulted in the prevention of entry of JC-1 in the mitochondria and resulted in green fluorescence (JC-1 monomers). IR cells showed depolarized $\Delta\psi\text{m}$ as can be seen in Fig: 5.4A, which had a higher amount of green fluorescence (103 %) compared to that of control. VA co-treatment with IR prevented the alteration of $\Delta\psi\text{m}$ which was evident from the significant increase ($p \leq 0.05$) of red fluorescence by 79.9 and 93.9 %, respectively, for 5 and

10 μM of VA compared to IR. The quantity of red fluorescence (aggregates) with metformin was improved, and the green fluorescence decreased by 116 % compared to IR (Fig: 5.4B). Valinomycin was the negative control, and it caused a decrease of the red fluorescence by 40.4 % and improved the green fluorescence by 108 % compared to control.

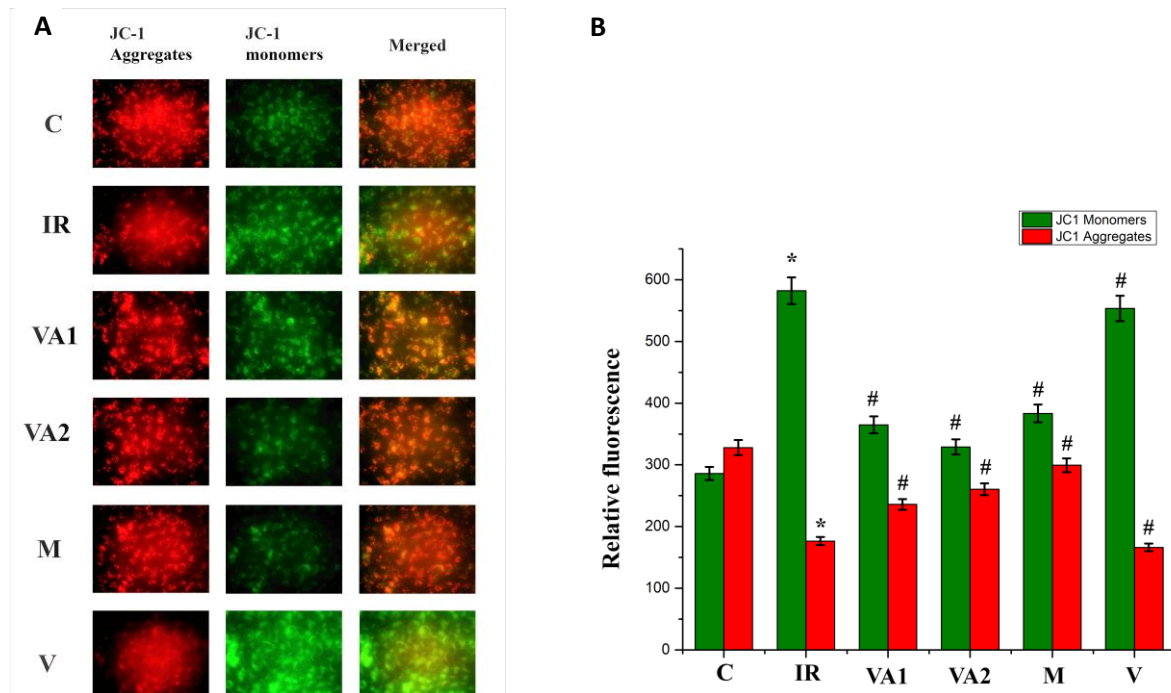


Figure. 5.4 Mitochondrial transmembrane potential ($\Delta\psi\text{m}$) determined using JC1 staining. (A) Alteration in membrane potential in various groups. (B) Relative fluorescent intensity of the fluorescent images. C - control cells; IR - hyperinsulinemia created insulin resistant cells; VA1 - IR + 5 μM vanillic acid; VA2 - IR + 10 μM vanillic acid; M - IR + metformin (1 mM); V - IR + valinomycin. Values are expressed as mean \pm SEM where $n=6$. * indicates that the mean value was significantly different from control cells ($p \leq 0.05$). # indicates the mean value was significantly different from IR cells ($p \leq 0.05$).

5.3.5 Mitochondrial biogenesis regulated by VA

AMPK, PGC-1 α and SIRT1 are the major proteins responsible for mitochondrial biogenesis. The active form of AMPK was determined in various groups using the ratio of p-AMPK to total AMPK. During IR, the expression of p-AMPK/AMPK was decreased significantly by 62.3 % compared to control cells whereas VA in a dose dependent manner increased the ratio significantly (193 and 185 % for 5 and 10 μM , respectively) (Fig: 5.5A & Fig: 5.5B). Also,

VA (5 and 10 μM) significantly ($p \leq 0.05$) increased the level of PGC-1 α by 50.4 and 71.3 %, respectively, compared to the IR group (Fig: 5.5A & Fig: 5.5C). In IR the level of PGC-1 α was reduced to 29.5 % compared to control as well as there was also a significant decrease in SIRT1 expression in IR cells (31.5 %). On the other hand, VA co-treatment at 5 and 10 μM increased the expression of SIRT1 by 115 and 119 %, respectively (Fig: 5.5A & Fig: 5.5C). Metformin significantly ($p \leq 0.05$) increased all three proteins (p-AMPK/AMPK, PGC-1 α and SIRT1) involved in mitochondrial biogenesis by 300, 80.6 and 113 %, respectively, compared to IR cells (Fig: 5.5A- Fig: 5.5C).

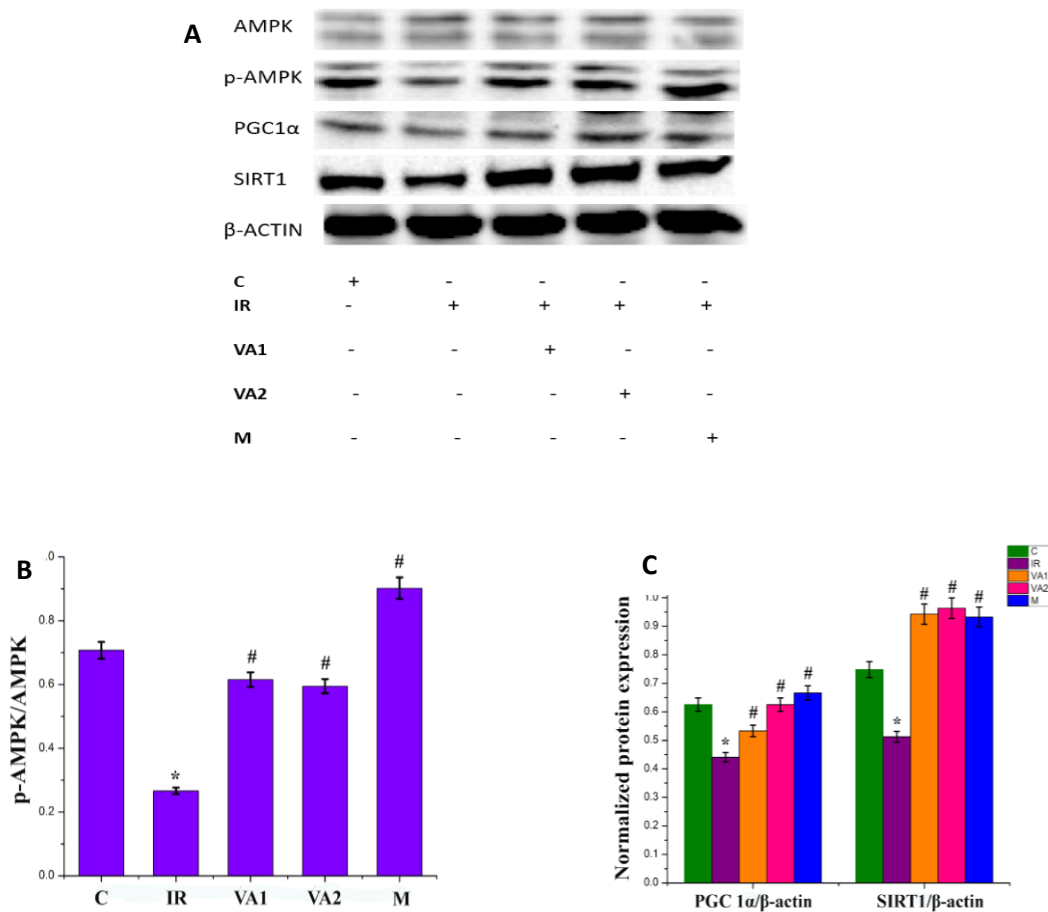


Figure. 5.5 Immunoblot analysis of proteins involved in mitochondrial biogenesis. (A) AMPK, p-AMPK, PGC-1 α , SIRT1 were analyzed using western blotting. (B) Densitometric determination of relative expression of p-AMPK/AMPK. (C) Densitometric analysis PGC-1 α and SIRT1 normalized to β -actin. C - control cells; IR - hyperinsulinemia created insulin resistant cells; VA1 - IR + 5 μM vanillic acid; VA2 - IR + 10 μM vanillic acid; M - IR + metformin (1 mM). Values are expressed as mean \pm SEM where n=6. * indicates that the mean value

was significantly different from control cells ($p \leq 0.05$). # indicates the mean value was significantly different from IR cells ($p \leq 0.05$). Protein quantification was carried out by densitometric analysis, normalized using internal control β -actin.

5.3.6 Mitochondrial fission and fusion proteins

During IR conditions there was a noticeable decrease in the levels of mitochondrial fusion protein OPA1 by 33.7 % ($p \leq 0.05$; Fig: 5.6A & Fig: 5.6B) and an up-regulation of fission protein FIS1 by 24.2 % (Fig: 5.6A & Fig: 5.6B). VA co-treatment at 5 and 10 μ M significantly ($p \leq 0.05$) increased the expression of OPA1 by 52.2 and 60.6 %, respectively, and in a dose dependent manner decreased the FIS1 by 92.3 and 109 % compared to the IR group. Metformin co-treatment also significantly ($p \leq 0.05$) increased the fusion protein by 58.1 % and reduced the fission protein 'FIS1' by 81.6 % compared to the IR group (Fig: 5.6A & Fig: 5.6B).

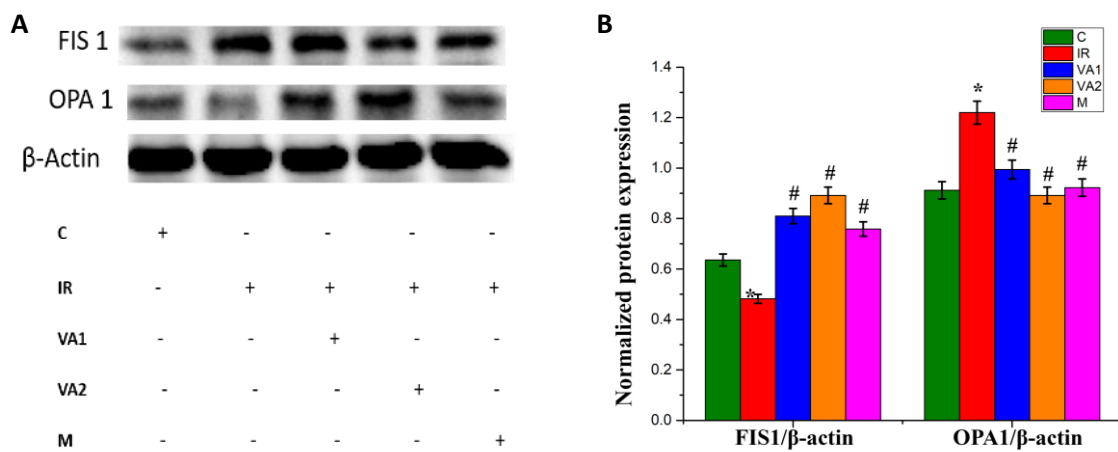


Figure 5.6 Analysis of proteins involved in mitochondrial dynamics. (A) Immunoblot analysis of proteins involved in mitochondrial fission and fusion (OPA1 and FIS1). (B) Densitometric quantification of OPA1 and FIS1 normalized to β -actin. C - control cells; IR - hyperinsulinemia created insulin resistant cells; VA1 - IR + 5 μ M vanillic acid; VA2 - IR + 10 μ M vanillic acid; M - IR + metformin (1 mM). Values are expressed as mean \pm SEM where n=6. * indicates that the mean value was significantly different from control cells ($p \leq 0.05$). # indicates the mean value was significantly different from IR cells ($p \leq 0.05$). Protein quantification was carried out by densitometric analysis, normalized using internal control β -actin.

5.3.7 ATP levels and oxygen consumption

There was a significant decrease in ATP levels ($p \leq 0.05$, 35.6 %; Fig: 5.7A) in IR cells compared to control cells. Co-treatment with VA at both concentrations (5 and 10 μM) significantly ($p \leq 0.05$) increased the ATP levels by 56.3 and 71.9 %, respectively, compared to IR. Metformin also significantly increased the ATP levels by 133 % compared with IR.

Oxygen consumption in cells was evaluated by calculating the change in fluorescence for two and a half hour. More changes in fluorescence represent more usage of oxygen by cells. This, in turn, represented the good metabolic status of cells. With the IR group oxygen consumption rate was reduced (25 %) as compared to control. Co-treatment with VA at 5 and 10 μM significantly ($p \leq 0.05$) improved the oxygen consumption rate by 13.1 and 26.2 % compared with the IR group (Fig: 5.7B). VA with better oxygen utilization seems to be effective against mitochondrial dysfunction in IR. Metformin also increased the oxygen consumption rate by 29.6 % compared to IR.

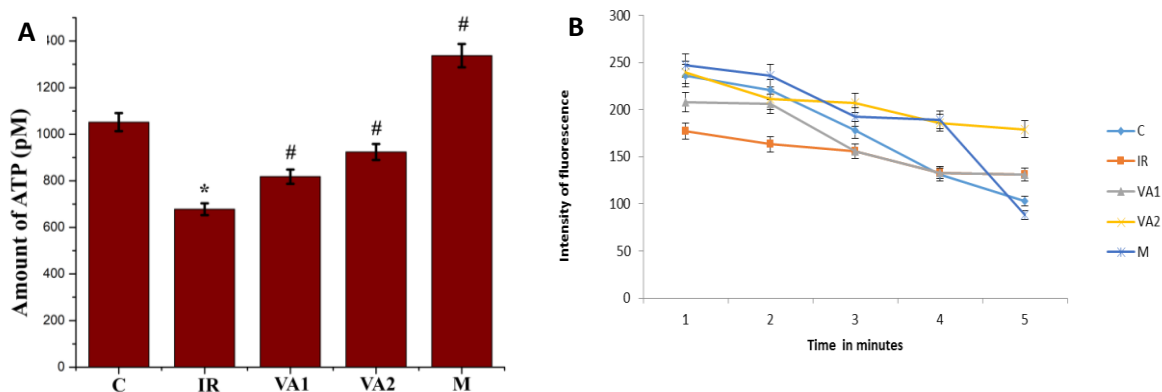
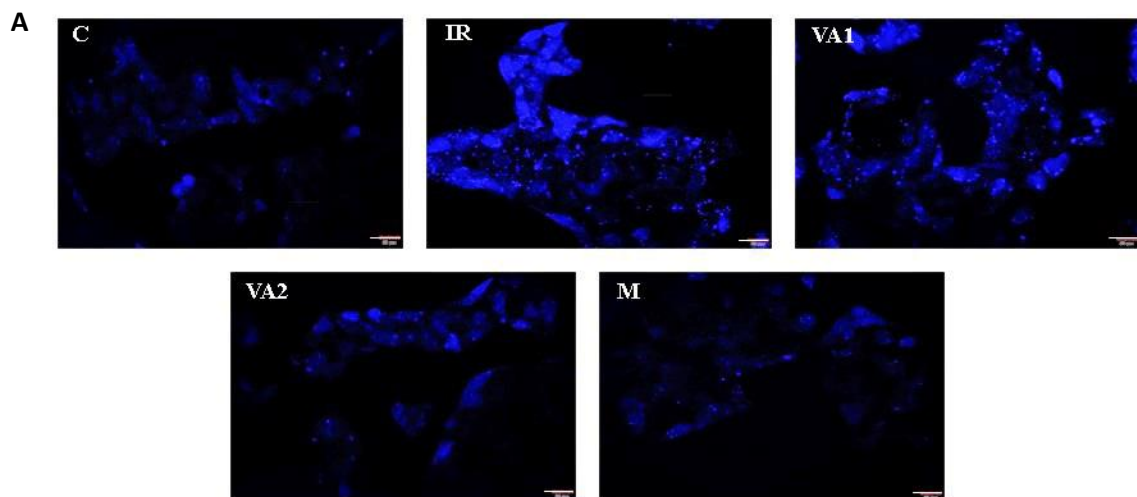


Figure. 5.7 Mitochondrial bioenergetics. (A) Level of ATP content in different groups. (B) Oxygen consumption rate in different groups. C - control cells; IR - hyperinsulinemia created insulin resistant cells; VA1 - IR + 5 μM vanillic acid; VA2 - IR + 10 μM vanillic acid; M - IR + metformin (1 mM). Values are expressed as mean \pm SEM where $n=6$. * indicates that the mean value was significantly different from control (cells ($p \leq 0.05$)). # indicates the mean value was significantly different from IR cells ($p \leq 0.05$).

5.3.8 Hyperinsulinemia induced intracellular calcium overload

HI caused an increase in intracellular Ca^{2+} overload (39.9 %) in HepG2 cells, which was proved from increased blue fluorescence of Fura -2AM compared to control cells. The treatment with VA of 5 μM and 10 μM concentrations and metformin of 1mM concentration showed a significant ($p \leq 0.05$) decrease in the Ca^{2+} accumulation by 19.1 %, 38.1 % and 38.6 % respectively (Fig: 5.8A & Fig: 5.8B). VA dose dependently reduced the Ca^{2+} overload by decreasing the blue fluorescence compared to HI treated cells. This was further confirmed by the result obtained from total Ca^{2+} assay. It was found that HI treated cells showed an 80 % increase in the total Ca^{2+} compared to control cells. The VA treatment decreased Ca^{2+} accumulation (20 % and 48 % with 5 μM and 10 μM respectively; Fig: 5.8C) compared to HI treated cells. Metformin treatment also significantly ($p \leq 0.05$) reduced the Ca^{2+} levels by 100 % compared to HI treated cells. These results suggest the efficacy of VA in maintaining the Ca^{2+} homeostasis in HI treated HepG2 cells.



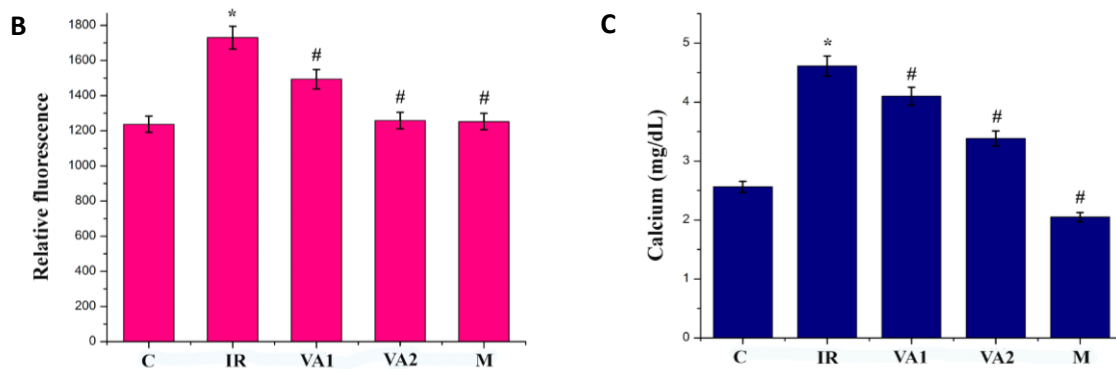


Figure. 5.8 Effect of hyperinsulinemia in calcium dysregulation. (A) Effect of VA on intracellular calcium generation using Fura 2AM (original magnification 20x). (B) Relative fluorescent intensity of the fluorescent images. (C) Intracellular calcium assay. C - control cells; IR - hyperinsulinemia created insulin resistant cells; VA1 - IR + 5 μM vanillic acid; VA2 - IR + 10 μM vanillic acid; M - IR + metformin (1 mM). Values are expressed as mean ± SEM where n=6. * indicates that the mean value was significantly different from control cells ($p \leq 0.05$). # indicates the mean value was significantly different from IR cells ($p \leq 0.05$). Scale bar corresponds to 20μm.

5.3.9 Effect of VA on mPTP opening

Here, I have assessed the mPTP opening by using a calcein-AM dye. The HI treated cells showed a significant decrease (24.6 %; $p \leq 0.05$) in the green fluorescence compared to control which indicates the continuous opening of the mPTP (Fig: 5.9A & Fig: 5.9B). The co-treatment with VA showed a dose-dependent increase in the fluorescence (12.1 and 20.8 % for 5 μM and 10 μM respectively; $p \leq 0.05$) by restoring the membrane potential and maintaining membrane integrity. It was further confirmed with the analysis of fluorescence intensity. The metformin treatment also showed an increased fluorescent intensity by 32.9 % compared to the HI group (Fig: 5.9A & Fig: 5.9B). These results revealed the beneficial effect of VA against the mitochondrial dysfunction caused by HI.

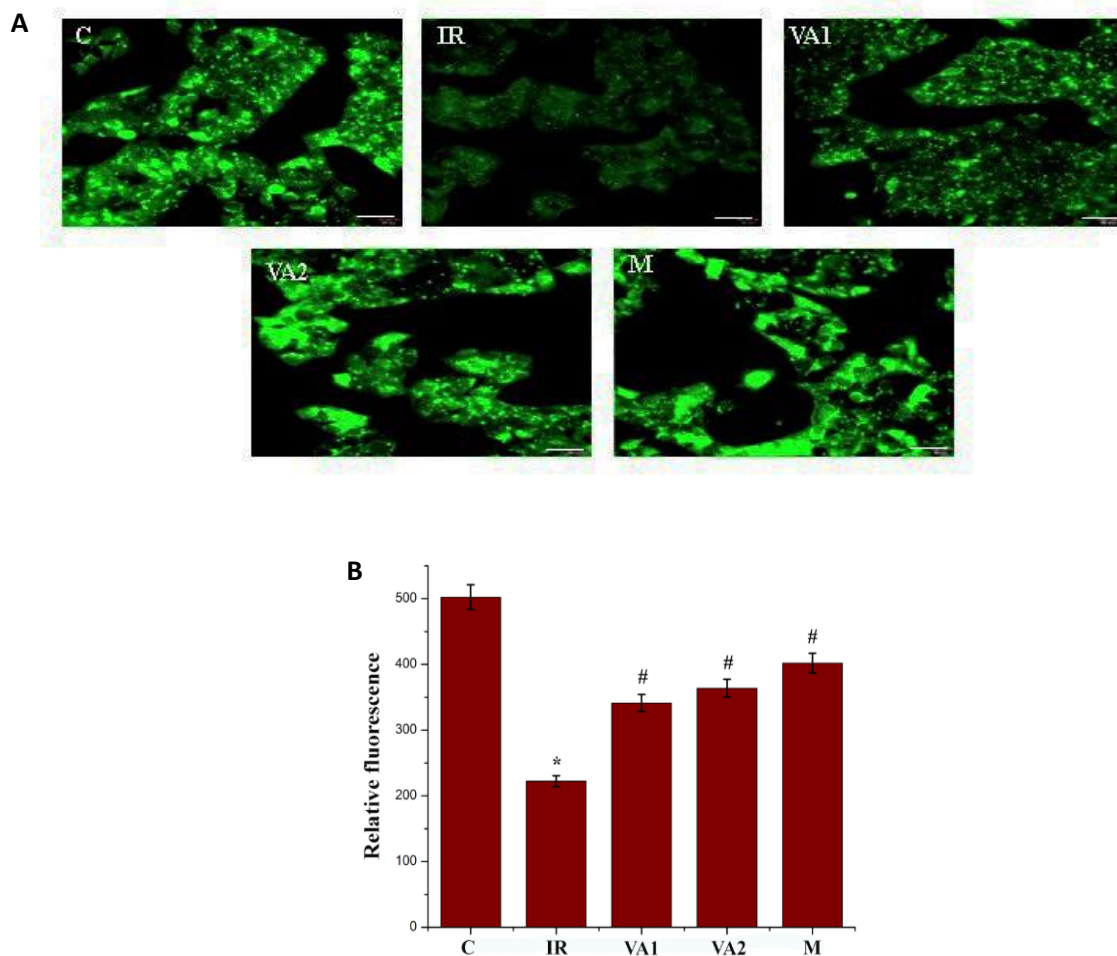


Figure 5.9 Insulin resistance & mPTP opening. (A) Effect of VA on mPTP opening using Calcein and cobalt chloride (original magnification 20x). (B) Relative fluorescent intensity of the fluorescent images. (C) Intracellular calcium assay. C - control cells; IR - hyperinsulinemia created insulin resistant cells; VA1 - IR + 5 μ M vanillic acid; VA2 - IR + 10 μ M vanillic acid; M - IR + metformin (1 mM). Values are expressed as mean \pm SEM where n=6. * indicates that the mean value was significantly different from control cells ($p \leq 0.05$). # indicates the mean value was significantly different from IR cells ($p \leq 0.05$). Scale bar corresponds to 20 μ m

5.3.10 Hyperinsulinemia and calcium dysregulation

The effect of HI on Ca^{2+} dysregulation was analysed by evaluating the expressions of various critical proteins involved in the Ca^{2+} homeostasis. In particular, the expression of proteins such as p-CAMKII, InsP3R, SERCA, JNK and GRP78 were analyzed. HI caused the increased expression of p-CaMKII, IP3R, JNK and GRP78 significantly by 135.1 %, 33.5 %, 172 % and 43 % respectively compared to control cells (Fig: 5.10A & Fig: 5.10B). Same time it down-

regulated the expression of SERCA by 46.8 %. p-CaMKII is the active form of cytoplasmic Ca²⁺ sensor that significantly decreased ($p \leq 0.05$) in the VA treated cells by 24.8 % and 83.9 % at 5 μM and 10 μM concentrations respectively compared to HI treated cells. Likewise, VA at 5 μM and 10 μM concentrations significantly ($p \leq 0.05$) down-regulated the IP3R levels by 41.2 % and 52 % respectively (Fig: 5.10A & Fig: 5.10B). JNK and GRP78 are the proteins involved in both Ca²⁺ homeostasis and stress conditions. VA noticeably reduced the JNK levels in HI treated cells by 143.5 % and 106.8 % and also decreased the GRP78 levels by 13.7 % and 88 % at 5 μM and 10 μM respectively compared to HI treated cells. Metformin treatment significantly down-regulated the expression of proteins like p-CaMKII, IP3R, JNK and GRP78 by 80.2 %, 39.1 %, 78.5 % and 92.3 % respectively (Fig: 5.10A & Fig: 5.10B). SERCA, an ER Ca²⁺ pump, has been noticeably decreased in the HI treated cells by 53.2 % whereas VA treated cells showed a significant ($p \leq 0.05$) increase in the SERCA levels by 33.2 % and 57.7 % respectively compared to HI treated cells. Metformin treatment also decreased the SERCA expression by 65.5 % compared to HI treated cells (Fig: 5.10A & Fig: 5.10B).

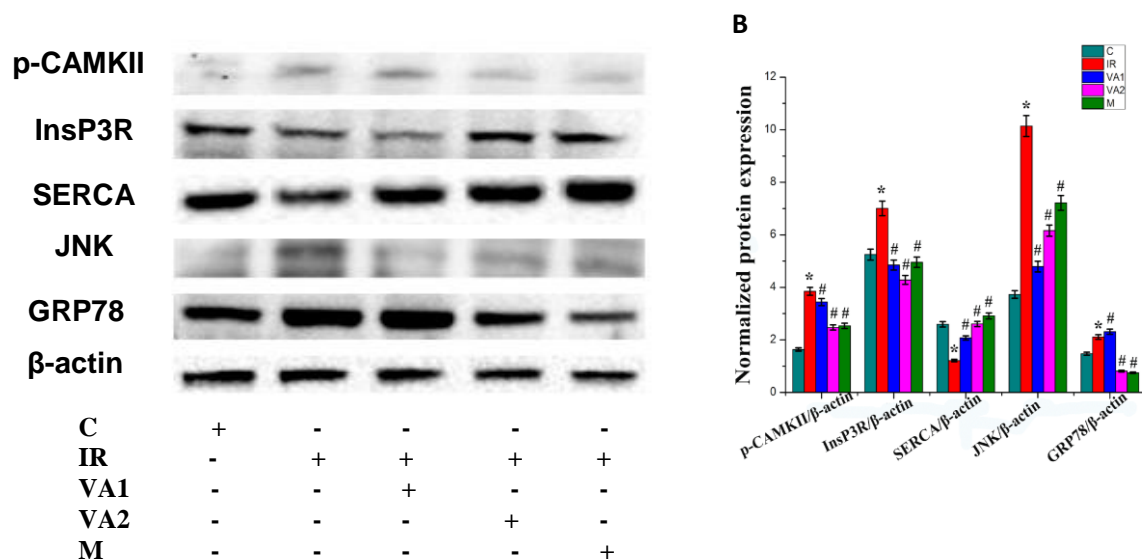


Figure. 5.10 ER & calcium. (A) Immunoblot analysis of proteins involved in calcium metabolism. (B) Densitometric quantification of CaMKII, InsP3R, SERCA, JNK and GRP78 normalized to β -actin. C - control cells; IR - hyperinsulinemia created insulin resistant cells; VA1 - IR + 5 μM vanillic acid; VA2 - IR + 10 μM vanillic acid; M - IR + metformin (1 mM). Values are expressed as mean \pm SEM where $n=6$. * indicates that the

mean value was significantly different from control cells ($p \leq 0.05$). # indicates the mean value was significantly different from IR cells ($p \leq 0.05$).

5.3.11 Hyperinsulinemia causes ER stress

The levels of ER stress markers p-IRE1 α , XBP1, p-PERK, p-eIF2 α and CHOP were increased significantly by 84.9 %, 52.3 %, 135.1 %, 104.1 % and 67.5 % respectively and the expression of ATF6 was down regulated noticeably by 51.4 % in the HI treated cells compared to control cells (Fig: 5.11A & Fig: 5.11B). Treatment with VA reduced the expression of the proteins significantly ($p \leq 0.05$) by 26.3 % and 56.1 % (p-IRE1 α); 60.8 % and 145 % (XBP1); 20.9 % and 93.5 % (p-PERK); 40.7 % and 55.8 % (p-eIF2 α); 21.3% and 38.5 % (CHOP) and increased the levels of AFT6 by 18.7 % and 35.1 % at 5 μ M and 10 μ M concentrations of VA (Fig: 5.11A & Fig: 5.11B). Metformin treatment also significantly ($p \leq 0.05$) down-regulated the levels of ER stress proteins by 67.4 % , 145.7 % , 99.3 % , 45.8 % , 63.5 % and up-regulated the levels of ATF6 by 76.1 % at 1mM concentration compared to HI treated cells (Fig: 5.11A & Fig: 5.11B).

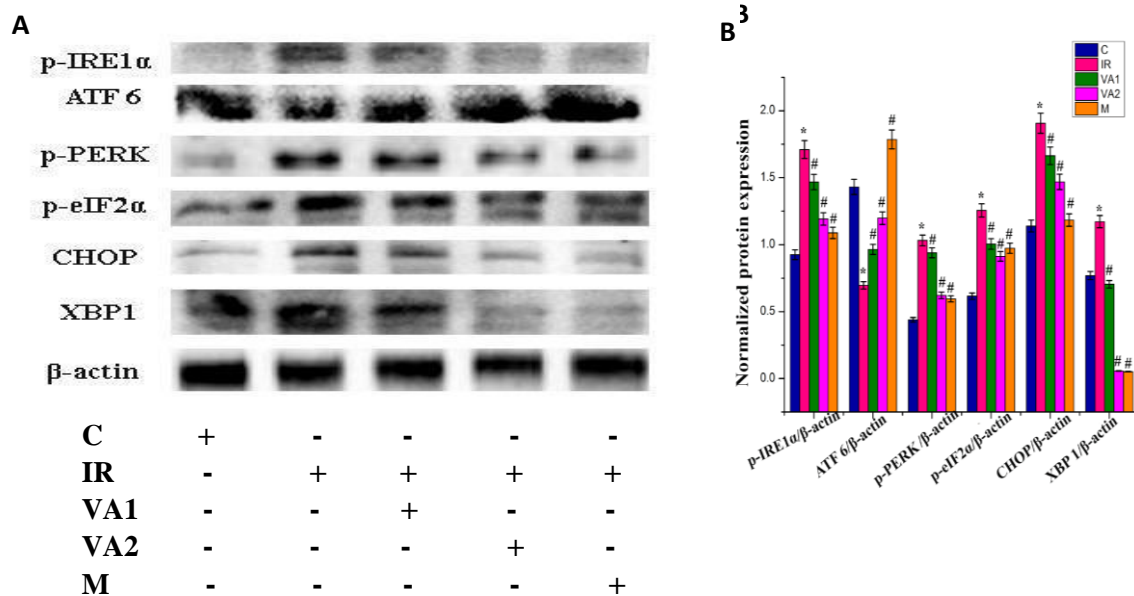


Figure. 5.11 Effect of hyperinsulinemia on ER stress. (A) Immunoblot analysis of proteins involved in ER stress. (B) Densitometric quantification of p-IRE1 α , ATF6, p-PERK, p-eIF2 α , CHOP and XBP1 normalized to β -actin. C - control cells; IR - high insulin treated insulin resistant cells; VA1 - IR + 5 μ M vanillic acid; VA2 - IR + 10 μ M vanillic acid; M - IR + metformin (1 mM). Values are expressed as mean \pm SEM where n=6. * indicates

that the mean value was significantly different from control cells ($p \leq 0.05$). # indicates the mean value was significantly different from IR cells ($p \leq 0.05$).

5.3.12 VA reduced the dysregulations in MAM during hyperinsulinemia

To identify the mechanism by which the HI induced alterations in the MAM, I evaluated the expression of major proteins involved in the formation of MAM. The western blot data showed that there was a significant decrease in the proteins like VDAC, CypD, GRP75, MFN2, and mTORC. VDAC is the mitochondrial component which creates an association with ER protein and forms MAM. There was a significant ($p \leq 0.05$) down-regulation in VDAC expression in the hyperinsulinemic group (69 %) when compared to control cells. While treatment with VA or metformin noticeably increased their levels by 52 %, 51 % and 35.8 % at 5 μ M, 10 μ M and 1 mM respectively compared to HI treated cells (Fig: 5.12A & Fig: 5.12B). GRP75 is the connecting protein situated between ER and mitochondria has been significantly ($p \leq 0.05$) decreased in the hyperinsulinemic group by 74.2 % whereas in VA treated cells the GRP78 levels were increased in a dose dependent manner by 60.7 % and 45.6 % respectively compared to HI treated cells (Fig: 5.12A & Fig: 5.12B). Metformin treatment also increased their levels by 56.7 % (Fig: 5.12A & Fig: 5.12B). Likewise, MFN2 and CypD are the major proteins seen in the ER-mitochondria junctions, and were also found to be down-regulated in the HI treated cells by 17.1 % and 43 % respectively. Meanwhile VA treatment of both concentrations (5 μ M and 10 μ M) and metformin significantly ($p \leq 0.05$) up-regulated the MFN2 levels by 22.7 %, 62.4 % and 35 % respectively (Fig: 5.12A & Fig: 5.12B). PTEN and mTORC are the other two proteins that have a prominent role in glucose metabolism and are also found in the MAM regions. It was found that in HI treated cells the expression of PTEN was increased significantly ($p \leq 0.05$) by 26.7 % compared to control. While VA treatment of 5 μ M and 10 μ M concentrations significantly ($p \leq 0.05$) reduced the levels of PTEN by 23.5 % and 52.2 % respectively. Metformin treatment also decreased the expression of PTEN by 29.4 % compared

to HI treated cells (Fig: 5.12A & Fig: 5.12B). In addition to this there was a significant ($p \leq 0.05$) decrease in the expression levels of mTORC by 56 % in HI treated cells compared to control cells whereas in VA treated cells the mTORC levels were decreased in a dose dependent manner by 102.4 % and 122.8 % respectively (Fig: 5.12A & Fig: 5.12B). Metformin also reduced the expression levels of mTORC by 133 %.

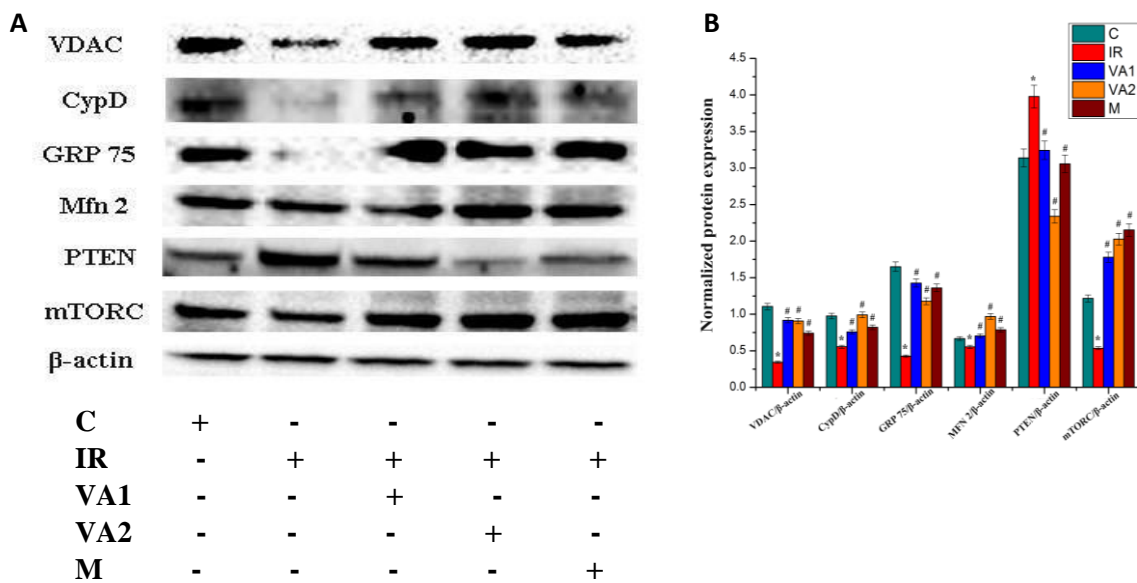


Figure. 5.12 Hyperinsulinemia & MAM. (A) Immunoblot analysis of proteins involved in MAM. (B) Densitometric quantification of VDAC, CypD, GRP75, MFN2, PTEN and mTORC normalized to β -actin. C - control cells; IR - hyperinsulinemia created insulin resistant cells; VA1 - IR + 5 μ M vanillic acid; VA2 - IR + 10 μ M vanillic acid; M - IR + metformin (1 mM). Values are expressed as mean \pm SEM where n=6. * indicates that the mean value was significantly different from control cells ($p \leq 0.05$). # indicates the mean value was significantly different from IR cells ($p \leq 0.05$).

5.4 Discussion

In insulin resistance conditions like T2DM, obesity, NAFLD and prediabetes both the hepatic glucose and lipids were increased. Similarly, excessive production of glucose and abnormal lipid accumulation were observed in the liver of both diabetic and obese peoples. In the previous chapters I had discussed the role of HI in hepatic glucose and lipid metabolism. Here I have discussed the role of mitochondria and ER in liver pathophysiology, especially those linked to alterations in glucose and lipid metabolism and also discussed the role of MAM on it. In addition to this, I also studied the role of cellular Ca^{2+} homeostasis as a critical mechanism for the development of insulin resistance and associated complications in metabolically active cells like HepG2 cells. Furthermore, I have discussed how the mitochondria, ER and MAM could provide a promising target for the treatment of metabolic disease like T2DM, obesity and NAFLD.

Liver is one of the organs that possesses a larger number of mitochondria than any other tissues in our body. So most of the liver diseases are initiated due to the increased accumulation of damaged mitochondria and ER (Finck and Kelly, 2006). Hepatic mitochondria have some unique properties because they are the hub that controls the hepatic metabolism of both glucose, amino acids and lipids (Degli Esposti et al., 2012). Depending on the demand of energy the mitochondrial content varies in each tissue (Degli Esposti et al., 2012). The number of mitochondria in the liver are about 500 to 4000 in each hepatocyte (Chatterjee et al., 2011). Meanwhile, mitochondria are the prominent organelle for maintaining the redox status of cells and the epicenter of ROS production also it is the prime energy production area of the cell. Most of the liver diseases were associated with the generation and accumulation of damaged mitochondria due to the production of ROS. Similarly, mitochondrial dysfunctions are the early step in the development of various pathological conditions in organs like the liver. The

integrity, dynamics, mitochondrial transition pore, bioenergetics and biogenesis, which are the critical functional indicators of mitochondria were studied in this chapter. When the intracellular ROS increases, it will up-regulate the mitochondrial ROS generation. Increased ROS inside the mitochondria resulted in the reduced number of functional mitochondria. Therefore, mitochondrial superoxide generation and aconitase enzyme levels were analyzed. Compared to normal cells, hyperinsulinemic insulin resistant HepG2 cells had increased superoxide generation (Fig: 5.1) and decreased aconitase level (Fig: 5.3). Aconitase is a mitochondrial protein sensitive to OS (Indo et al., 2007; Tan et al., 2015) and it detoxifies the superoxides through a suicidal inhibition (Green et al., 2004). The significant reduction of aconitase with insulin resistance was expected to cause alteration in the redox status in the cells. This results in alterations of the $\Delta\psi_m$ (Skulachev, 1998). $\Delta\psi_m$ is the major participant involved in the regulation of ROS production (Rauscher et al., 2001) and an important marker of mitochondrial integrity (Mathur et al., 2000). When the electrochemical potential difference generated by the proton gradient across the inner mitochondrial membrane is high, the lifetime of superoxide generating intermediates is increased (Korshunov et al., 1997; Zorov et al., 2014). In the present study compared to normal cells, the hyperinsulinemic model had an altered $\Delta\psi_m$. Distortion of mitochondrial dynamics towards fission along with an increase in fission proteins and dissipation of $\Delta\psi_m$ indicated poor mitochondrial health. The loss of $\Delta\psi_m$ leads to proteolysis and degradation of mitochondrial fusion proteins (Youle and Narendra, 2011) and also increased the fission rates (Van der Blik et al., 2013). HI results in an overexpression of fission proteins such as FIS1 and down-regulation of fusion proteins such as OPA1 leading to enhanced mitochondrial fission. Reduced expression of OPA1 was linked to the distortion of mitochondrial function (Tang, 2016) and up-regulation of FIS1 resulted in mitochondrial fragmentation (Mao et al., 2018). This results in nonfunctional fragmented mitochondria in the cytoplasm. Balanced mitochondrial dynamics is important for the normal

functioning of mitochondria and energy generation (Mao et al., 2018), and it is controlled by the fission and fusion balance (Rovira-Llopis et al., 2017). The increase of mitochondrial oxidants could lead to severe insulin resistance developing in most of the tissues and decreased the mitochondrial content (Fazakerley et al., 2018). It has also been reported that insulin resistance is associated with the reduced mitochondrial content, decreased levels of mitochondrial enzymes and its abnormal morphology which is observed in both *in vitro* and *in vivo* experiments (Kim et al., 2008). In this study also I have shown that in HI the levels of mitochondrial content decreased significantly which indicates the increased mitochondrial dysfunctions in insulin resistant HepG2 cells. In addition, $\Delta\psi_m$ provides the driving force for ATP synthesis in mitochondria. When the mitochondria lose their $\Delta\psi_m$, the ATP production also decreases. (Van der Blik et al., 2013). The current study showed a significant decrease in mitochondrial content and ATP generation in hyperinsulinemic HepG2 cells. To check respiration in mitochondria, basal oxygen consumption rates have been measured (Hartman et al., 2014). Ailing cells with mitochondrial dysfunction showed a decreased rate of oxygen utilization. A reduced oxygen consumption rate was observed in hyperinsulinemia created insulin resistant HepG2 cells. Imbalanced redox status and defective mitochondrial dynamics affected the mitochondrial biogenesis (Handy and Loscalzo, 2012). Therefore, the alterations of the important proteins in mitochondrial biogenesis were measured. The genes responsible for the regulation of mitochondrial biogenesis are AMPK, SIRT1 and PGC-1 α . AMPK is a protein kinase and it has an important role in the improvement of insulin sensitivity in insulin-resistant individuals (Jeon, 2016; Zhao et al., 2016) by stimulation of downstream genes like SIRT1 and PGC-1 α (Austin et al., 2011). SIRT1 is a member of the family of sirtuins and an upstream activator of PGC-1 α through AMPK activation (Austin et al., 2011; Zhu et al., 2010). PGC-1 α is considered as the master controller of mitochondrial biogenesis and the antioxidant defense system (Valle et al., 2005). Hyperinsulinemia created insulin resistant cells had a

decreased ratio of phosphorylated to total AMPK, decreased PGC-1 α , and SIRT1. These showed imbalances in mitochondrial biogenesis in the HI treated cells and that began the process of insulin resistance development. Insulin resistance decreased the SIRT1, AMPK and PGC-1 α expression and altered the mitochondrial homeostasis and enhanced OS (Choi et al., 2014). Furthermore, mitochondria controls both carbohydrates and lipid metabolism in the liver. So any defects in the mitochondria will result in the alterations in the both glucose and lipid metabolism and affect the whole body homeostasis (Kim et al., 2008). Intracellular lipid accumulation in the liver causes the decreased mitochondrial oxidation in T2DM patients. The increased lipids in the liver activates the PKC that increases the phosphorylation of IRS proteins leading to the decreased insulin signaling and develops insulin resistance (Kim et al., 2008). Meanwhile numerous mitochondrial abnormalities are found in the NAFLD patients also. So the lipid induced mitochondrial abnormalities inhibits the insulin signaling through the formation of excess ROS (Kim et al., 2008).

Ca²⁺ is a ubiquitous and most abundant ion in the body. It is a secondary messenger and it controls a variety of cellular processes such as hormone release, muscle contraction, organelle communication, neuronal transmission and cell growth and also it is a necessary factor for liver function (Berridge, 2012; Clapham, 2007). Due to these diverse functions and critical roles, the Ca²⁺ is tightly regulated and any changes in the Ca²⁺ homeostasis will result in the genesis of many of the pathological conditions (Guerrero-Hernandez and Verkhatsky, 2014; Luo and Anderson, 2013). However the Ca²⁺ levels are essential for the release of hormones like insulin and glucagon for maintaining a normal blood sugar. So alterations in the cytosolic and organelle Ca²⁺ level definitely affects the processes such as glucose, fatty acids and amino acid metabolism; xenobiotics; cell cycle and proliferation; bile formation and excretion etc. (Amaya and Nathanson, 2013; Bollen et al., 1987; Nathanson et al., 1992). In addition to these, the cytoplasmic Ca²⁺ also controls the glucose metabolism through the

gluconeogenesis and glycogenolysis activation (Amaya and Nathanson, 2013). The cytoplasmic Ca^{2+} affects the insulin by activating the AKT (Marchi et al., 2012). The increased gluconeogenesis and glycogenolysis results in hyperglycemia. In addition to this the increased cytoplasmic Ca^{2+} increased the DNL in the liver (Fu et al., 2012). The key organelles which are responsible for maintaining the Ca^{2+} homeostasis in the liver are mitochondria and ER. So the dysfunctions of these organelles are the crucial factors in the development of insulin resistance and metabolic alterations in the liver (Mantena et al., 2008; Ozcan et al., 2004). The Ca^{2+} levels in both cytosol and in cell organelles were controlled by numerous proteins. These proteins pump the Ca^{2+} from the cytosol to intracellular stores like ER and mitochondria or it pumps the Ca^{2+} to extracellular space. In mitochondria the Ca^{2+} uptake is necessary for their function and also it is the way to control the cytoplasmic Ca^{2+} concentrations. The Ca^{2+} enters inside the mitochondria through the channel proteins like VDAC and the driving force behind this transport is the electrochemical gradient. Inside the mitochondria the Ca^{2+} regulates the activity of TCA cycle and also activates the ATP synthesis (Rizzuto et al., 2012). So the mitochondrial Ca^{2+} levels are essential for aerobic metabolism. Meanwhile the excess concentration of Ca^{2+} results in the genesis of mitochondrial ROS and leads to mitochondrial dysfunction (Baines et al., 2005). However the increased mitochondrial Ca^{2+} will result in the continuous opening of the mPTP (Peng and Jou, 2010). Opening of the mPTP leads to the distortion of $\Delta\psi_m$ and mitochondrial swelling which results in the cell death (Kowaltowski et al., 2009). In our study, the increased mPTP opening in HI treated HepG2 cells revealed the excess accumulation of Ca^{2+} inside the mitochondria. The continuous opening of the mPTP leads to the release of the Ca^{2+} into the cytosol and it results in the increased cytosolic Ca^{2+} . It has been reported that the increased cytoplasmic Ca^{2+} levels during HI created insulin resistance results in increased HGP. The increased Ca^{2+} levels were detected by the increased expression of a Ca^{2+} sensing protein called CAMKII (Wang et al., 2012). One study showed

that the glucagon activates the release of Ca^{2+} from the ER and it then activates the CAMKII (Ozcan et al., 2013). There was a noticeable increase in the cytoplasmic Ca^{2+} levels observed in HI treated HepG2 cells by Fura-2AM staining and this result was further confirmed with the increased expression of p-CAMKII levels in the HI treated cells. VA and metformin treatments lowered the intracellular Ca^{2+} by the decreased expression of p-CAMKII levels and the reduced fluorescence of Fura-2AM. However, during obesity the cytoplasmic Ca^{2+} levels become increased and it activates the JNK. Activation of JNK resulted in the excess glucose production and initiation of inflammatory cascade in the liver (Ozcan et al., 2013). JNK is a key inflammatory/stress kinase, and an inhibitor of IP3R (Hirosumi et al., 2002; Manning and Davis, 2003; Vallerie and Hotamisligil, 2010). In the current study also there is an increased level of JNK observed in HI. Furthermore, ER is the organelle that has an important role in maintaining the Ca^{2+} homeostasis. The entry of Ca^{2+} into the ER and its regulation across ER membrane is controlled by the presence of three types of proteins such as SERCA, IP3Rs and ryanodine receptors (RyRs). Among these, SERCA is the Ca^{2+} pump while IP3R and RyRs are the Ca^{2+} channels (Clapham, 2007; Mekahli et al., 2011; Prins and Michalak, 2011). SERCA controls the Ca^{2+} uptake from the cytoplasm to ER (Toyoshima and Inesi, 2004) while the release of Ca^{2+} from ER to cytoplasm is done by IP3R and RyR channels. In the present study the expression of both IP3R and GRP78 were found to be increased and the SERCA levels were found to be lowered during HI. Furthermore, the expression of IP3R and GRP78 were decreased while the SERCA expression was increased in the HepG2 cells treated with VA and metformin.

ER is a multifunctional organelle as well as a dominant Ca^{2+} storing area of the cell (Mekahli et al., 2011; Prins and Michalak, 2011). ER Ca^{2+} is essential for the protein folding, synthesis and its post translational modifications. The Ca^{2+} is also necessary for the synthesis of many of the ER proteins like calsequestrin and calreticulin and chaperones like GRP78 (BiP

immunoglobulin binding protein). They regulate the folding of both the membrane and the secretory proteins like insulin receptors. In addition to this ER Ca^{2+} is necessary for many of the Ca^{2+} regulated proteins such as PDI, oxidoreductase, ERp57, ERO1L etc. (Gorlach et al., 2006). The depletion of ER Ca^{2+} resulted in the reduced activity of these proteins and finally leads to the overload of misfolded proteins and initiates ER stress. UPR is an adaptive response in which the reduced protein translation, increased the chaperone levels and also increased the protein degradation. If the UPR persists it results in the unresolved ER stress and finally leads to cell death. ER dysfunction is one of the major factors for the development of almost all metabolic diseases. The molecular mechanism underlying the initiation of ER stress and ER dysfunction in the liver is the development of obesity induced abnormal ER- Ca^{2+} transport (Fu et al., 2011). Excessive energy intake and the OS created during both HI and obesity result in the peroxidation of most of the membrane lipids of ER. Most frequently it affects the phosphatidyl choline and ethanolamine which result in the loss of membrane fluidity of the ER. As well as the increased ROS will also affect the SERCA protein in the ER. In addition to this, obesity will increase the levels of saturated fatty acids and the incorporation of saturated fatty acids to the ER membrane result in the disturbances in ER membrane fluidity (Rong et al., 2013). The end result of all these consequences is the development of ER stress during HI (Fu et al., 2011). The decreased expression of SERCA reduces the ER storage of Ca^{2+} as a result the protein folding and the synthesis machinery becomes completely disturbed. It further promotes the ER stress (Egnatchik et al., 2014; Zhang et al., 2014). During the initiation of ER stress the hepatocytes activate UPR and increase the expression of chaperones like GRP78 (Kammoun et al., 2009). In our study also there is an increased GRP78 observed in the HI treated cells. The activated UPR can cause insulin resistance in the liver. The major proteins involved in the ER stress are the p-IRE1 α , p-PERK, ATF6, p-eIF2 α , XBP1 and CHOP. The increased CAMKII activates the PERK in the ER which showed the importance of increased

cytoplasmic Ca^{2+} on ER stress. As a result the activated PERK activates the p-eIF2 α which inhibits the insulin mediated AKT phosphorylation. The activated eIF2 α decreases newly synthesized protein and reduces the ER load (Malhi and Kaufman, 2011). Inhibition of CAMKII in hepatocytes results in the reduced UPR activation and a marked improvement in the blood glucose (Ozcan et al., 2013). While activation of IRE1 α activates the XBP1 by its splicing mechanism. XBP1 is the major protein that controls the expression of genes like GRP78 and facilitates protein folding and degradation (Hotamisligil, 2010). In this study it is observed that HI increased the expression of p-IRE1 α , p-PERK, p-eIF2 α and XBP1 which indicates the initiation of ER stress. But VA has the potential to reduce the expression of all these proteins and protect the HepG2 cells from ER stress. The deletion of PERK leads to the increased protein load inside the ER through the inactivation of eIF2 α and it finally results in the ER stress mediated cell death (Scheuner et al., 2001). In addition to this, PERK activates the ATF4 which induces the expression of various genes involved in antioxidant system and apoptosis. C/EBP homologous protein (CHOP) is the main player of the execution of apoptosis (Malhi and Kaufman, 2011). Most of the ER stress inducers will activate the CHOP (Malhi and Kaufman, 2011). It has been reported that the mice lacking the CHOP showed the normal growth and the cells isolated from these mice showed a better resistance towards the ER stress (Malhi and Kaufman, 2011). This data revealed the importance of CHOP and ER stress in cell survival (Malhi and Kaufman, 2011). The VA increased the ATF6 levels and decreased the ER stress proteins like p-IRE1 α , XBP1, p-PERK and p-eIF2 α which were increased in the HI treated cells. One of the reports suggests that the levels of ATF6 was decreased in the livers of obese mouse, it reveals the importance of ATF6 in the prevalence of obesity and T2DM (Ozcan et al., 2004). It has been reported that the complete deletion of ATF6 resulted in the embryo lethality which indicates the essential functions of this protein in early development (Malhi and Kaufman, 2011). ATF6 decreases HGP and it also reduces obesity in the liver

(Yang et al., 2010). Although the ER and mitochondria are the two distinct cell organelles and each have independent roles in hepatocytes. But at some points these organelles are physically connected and coupled with their functions. These areas are collectively called MAM. MAM connections are tight and strong and it functions as a lipid raft (Hayashi and Su, 2003). MAM has a number of variety functions such as lipid transport, energy metabolism, Ca^{2+} signaling and cell survival (Rowland and Voeltz, 2012). Some of the proteins in the both organelles participate in the MAM formation. They are VDAC of the mitochondrial membrane and IP3R on the ER membrane. Glucose regulatory protein 75 (GRP75) is the bridging protein that helps for the interaction between VDAC and IP3R. The Ca^{2+} enters into the mitochondria from ER is through MAM (Szabadkai et al., 2006). In addition to this, MAM is also enriched with several other proteins. GRP 75 is the major protein involved in the formation of MAM and it facilitates the entry of Ca^{2+} from ER to mitochondria (Szabadkai et al., 2006). Here also in HI condition the levels of GRP75 were down-regulated this indicated the disturbances in MAM integrity and also caused the damages in the intracellular Ca^{2+} levels. VA or metformin co-treatments significantly increased the GRP75 and restored the MAM association and function. MFN2 is one the MAM proteins which participates in the Ca^{2+} transport. Accumulating data suggest that both mitochondria and ER are the major organelles involved in the hepatic energy homeostasis. So the occurrence of hepatic insulin resistance is associated with both ER and mitochondrial dysfunctions (Ozcan et al., 2004; Vial et al., 2011). One of the recent studies reported that the specific silencing of MFN2 in hepatocytes is associated with the development of insulin resistance (Sebastián et al., 2012). In our study also the levels of MFN2 are down-regulated in the HI condition while both the VA and metformin noticeably improved the MFN2 levels in HepG2 cells. Furthermore, MAMs are the important areas in which it controls the insulin action and the disruption of MAM is associated with hepatic insulin resistance (Tubbs et al., 2014). So, numerous other proteins involved in the insulin signaling pathway are also

identified in the MAM. They are mTORC and PTEN. One study revealed that, the cellular loss of mTORC resulted in the distorted ER-mitochondria interactions and also is caused to mitochondrial alterations (Betz et al., 2013). As well as the liver specific knockdown of the mTORC showed an altered hepatic glucose homeostasis (Hagiwara et al., 2012). In this study, I have analyzed the expression of several protein pairs such as VDAC, CypD, MFN2 and mTORC. The expression of all these proteins are decreased in the HI treated HepG2 cells; this indicates the distortions in the MAM during HI. However the MAM are enriched with the several ER chaperones like SigR1 and calnexin and the protein CypD is also found in the MAM, it regulates the inter organelle Ca^{2+} transport (Paillard et al., 2013; Rieusset et al., 2016). It has been identified that the silencing of the liver specific mitochondrial MFN2 and the inhibition of mitochondrial CypD resulted in the genesis of the hepatic ER stress and insulin resistance (Rieusset et al., 2016; Sebastian et al., 2012). The distortion of MAM through the inactivation of CypD develops insulin resistance in mice and also creates disrupted insulin signaling in hepatocytes (Tubbs et al., 2014). Here also I observed the noticeable decrease in the CypD expression in HI treated HepG2 cells. VA dose dependently increased the CypD levels and thereby restores the MAMs integrity. Based on these results shown in this study, the mitochondrial dysfunctions, ER stress, alterations in MAM and distorted Ca^{2+} and lipid homeostasis are the main pathophysiological effects of HI. All these consequences result in the development of insulin resistance in HepG2 cells. Some of the recent evidence suggests that MAM is the hot area of research to find out the prevalence of many diseases like T2DM, obesity, NAFLD etc. However, MAM is also a hub for the nutrient and Ca^{2+} transport across the ER and mitochondria. So the ER-mitochondria miscommunication results in the development of hepatic insulin resistance. Furthermore I discovered that VA can reduce the mitochondrial dysfunction and ER stress during the HI in HepG2 cells and it also has the potential to restore the normal Ca^{2+} homeostasis. In this study I have revealed the efficacy of

VA to reduce the disturbances in MAM created in HI conditions. These results support that ER-mitochondria interactions and Ca^{2+} fluxes may play an important role in the regulation of hepatic glucose and lipid metabolism especially in the context of metabolic diseases.

References

Amaya MJ and Nathanson MH. Calcium signaling in the liver. *Compr Physiol*. 2013; 3: 515-539.

Austin S, Klimcakova E, St-Pierre J. Impact of PGC-1 α on the topology and rate of superoxide production by the mitochondrial electron transport chain. *Free Radic Biol Med*. 2011; 51: 2243-2248.

Baines CP, Kaiser RA, Purcell NH, Blair NS, Osinska H, Hambleton MA, et al. Loss of cyclophilin D reveals a critical role for mitochondrial permeability transition in cell death. *Nature*. 2005; 434: 658-662.

Barrena HC, Schiavon FP, Cararra MA, Marques ADCR, Schamber CR, Curi R, Bazotte RB. Effect of linseed oil and macadamia oil on metabolic changes induced by a high-fat diet in mice. *Cell Biochem Funct*. 2014; 32: 333-340.

Bazotte RB, Silva LG, Schiavon FP. Insulin resistance in the liver: deficiency or excess of insulin?. *Cell Cycle*. 2014; 13: 2494-2500.

Begrache K, Igoudjil A, Pessayre D, Fromenty B. Mitochondrial dysfunction in NASH: causes, consequences and possible means to prevent it. *Mitochondrion*. 2006; 6: 1-28.

Berridge MJ, Bootman MD, Roderick HL. Calcium signalling: dynamics, homeostasis and remodelling. *Nat Rev Mol Cell Biol*. 2003; 4: 517-529.

Berridge MJ. Calcium signalling remodelling and disease. *Biochem Soc Trans*. 2012; 40: 297-309.

Betz C, Stracka D, Prescianotto-Baschong C, Frieden M, Demaurex N, Hall MN. Feature article: mTOR complex 2-Akt signaling at mitochondria-associated endoplasmic reticulum

membranes (MAM) regulates mitochondrial physiology. *Proc Natl Acad Sci. U.S.A.* 2013; 110: 12526-12534

Blais JD, Filipenko V, Bi M, Harding HP, Ron D, Koumenis C, Wouters BG, et al. Activating transcription factor 4 is translationally regulated by hypoxic stress. *Mol Cell Biol.* 2004; 24: 7469-7482.

Bollen M, Kee SM, Graves DJ, Soderling TR. Substrate specificity of phosphorylase kinase: effects of heparin and calcium. *Arch Biochem Biophys.* 1987; 254: 437-447.

Bonora M, Morganti C, Morciano G, Giorgi C, Wieckowski MR, Pinton P. Comprehensive analysis of mitochondrial permeability transition pore activity in living cells using fluorescence-imaging-based techniques. *Nature protocols.* 2016; 11: 1067-1080.

Chatterjee A, Dasgupta S, Sidransky D. Mitochondrial subversion in cancer. *Cancer Prev Res.* 2011; 4: 638-654.

Choi J, Chandrasekaran K, Inoue T, Muragundla A, Russell JW. PGC-1 α regulation of mitochondrial degeneration in experimental diabetic neuropathy. *Neurobiol Dis.* 2014; 64: 118-130.

Clapham DE. Calcium signaling. *Cell.* 2007; 131: 1047-1058

Cullinan SB, Zhang D, Hannink M, Arvisais E, Kaufman RJ, Diehl JA. Nrf2 Is a Direct PERK Substrate and Effector of PERK-Dependent Cell Survival. *Mol Cell Biol.* 2003; 23: 7198-7209.

Degli Esposti D, Hamelin J, Bosselut N, Saffroy R, Sebah M, Pommier A, et al. Mitochondrial roles and cytoprotection in chronic liver injury. *Biochem Res Int.* 2012; 2012: 1-16.

Egnatchik RA, Leamy AK, Jacobson DA, Shiota M, Young JD. ER calcium release promotes mitochondrial dysfunction and hepatic cell lipotoxicity in response to palmitate overload. *Mol Metab.* 2014; 3: 544-553.

Fabbrini E, Sullivan S, Klein S. Obesity and nonalcoholic fatty liver disease: biochemical, metabolic, and clinical implications. *Hepatology.* 2010; 51: 679-689.

Fazakerley DJ, Minard AY, Krycer JR, Thomas KC, Stöckli J, Harney DJ, et al. Mitochondrial oxidative stress causes insulin resistance without disrupting oxidative phosphorylation. *J Biol Chem.* 2018; 293: 7315-7328.

Finck BN, Kelly DP. PGC-1 coactivators: inducible regulators of energy metabolism in health and disease. *J Clin Invest.* 2006; 116: 615–622.

Fu S, Watkins SM, Hotamisligil GS. The role of endoplasmic reticulum in hepatic lipid homeostasis and stress signaling. *Cell metab.* 2012; 15: 623-34.

Fu S, Yang L, Li P, Hofmann O, Dicker L, Hide W, et al. Aberrant lipid metabolism disrupts calcium homeostasis causing liver endoplasmic reticulum stress in obesity. *Nature.* 2011; 473: 528-531.

Gao X, Guo S, Zhang S, Liu A, Shi L, Zhang Y. Matrine attenuates endoplasmic reticulum stress and mitochondrion dysfunction in nonalcoholic fatty liver disease by regulating SERCA pathway. *J Transl Med.* 2018; 16: 1-16.

Giorgi C, Ito K, Lin HK, Santangelo C, Wieckowski MR, Lebedzinska M, et al. PML regulates apoptosis at endoplasmic reticulum by modulating calcium release. *Science.* 2010; 330: 1247-1251.

Gorlach A, Klappa P, Kietzmann T. The endoplasmic reticulum: folding, calcium homeostasis, signaling, and redox control. *Antioxid Redox Signal.* 2006; 8: 1391-1418.

Green DR, Galluzzi L, Kroemer G. Mitochondria and the autophagy–inflammation–cell death axis in organismal aging. *Science*. 2011; 333: 1109-1112.

Green K, Brand MD, Murphy MP. Prevention of mitochondrial oxidative damage as a therapeutic strategy in diabetes. *Diabetes*. 2004; 53: S110-S118.

Guerrero-Hernandez A and Verkhatsky A. Calcium signalling in diabetes. *Cell Calcium*. 2014; 56: 297–301.

Hagiwara A, Cornu M, Cybulski N, Polak P, Betz C, Trapani F, et al. Hepatic mTORC2 activates glycolysis and lipogenesis through Akt, glucokinase, and SREBP1c. *Cell Metab*. 2012; 15: 725-738

Hamanaka RB and Chandel NS. Mitochondrial reactive oxygen species regulate cellular signaling and dictate biological outcomes. *Trends Biochem Sci*. 2010; 35: 505-513.

Handschin C, Lin J, Rhee J, Peyer AK, Chin S, Wu PH, et al. Nutritional regulation of hepatic heme biosynthesis and porphyria through PGC-1 α . *Cell*. 2005; 122: 505-515.

Handy DE and Loscalzo J. Redox regulation of mitochondrial function. *Antioxid Redox Signal*. 2012; 16: 1323-1367.

Harding HP, Zhang Y, Zeng H, Novoa I, Lu PD, Calton M, Sadri N, et al. An Integrated Stress Response Regulates Amino Acid Metabolism and Resistance to Oxidative Stress. *Mol Cell*. 2003; 11: 619-633.

Hartman ML, Shirihai OS, Holbrook M, Xu G, Kocherla M, Shah A, et al. Relation of mitochondrial oxygen consumption in peripheral blood mononuclear cells to vascular function in type 2 diabetes mellitus. *Vasc Med*. 2014; 19: 67-74.

Hayashi T and Su TP. Sigma-1 receptors (sigma(1) binding sites) form raft-like microdomains and target lipid droplets on the endoplasmic reticulum: roles in endoplasmic reticulum lipid compartmentalization and export. *J Pharmacol Exp Ther.* 2003; 306: 718-725.

Hetz C, Chevet E, Oakes SA. Proteostasis control by the unfolded protein response. *Nat Cell Biol.* 2015; 17: 829-838.

Hirosumi J, Tuncman G, Chang L, Go¨rgu¨n CZ, Uysal KT, Maeda K, et al. A central role for JNK in obesity and insulin resistance. *Nature.* 2002; 420: 333-336.

Hotamisligil GS. Endoplasmic reticulum stress and the inflammatory basis of metabolic disease. *Cell.* 2010; 140: 900-917

Indo HP, Davidson M, Yen HC, Suenaga S, Tomita K, Nishii T, et al. Evidence of ROS generation by mitochondria in cells with impaired electron transport chain and mitochondrial DNA damage. *Mitochondrion.* 2007; 7: 106-118.

Jeon SM. Regulation and function of AMPK in physiology and diseases. *Exp Mol Med.* 2016; 48: 1-13.

Kammoun HL, Chabanon H, Hainault I, Luquet S, Magnan C, Koike T, et al. GRP78 expression inhibits insulin and ER stress-induced SREBP1c activation and reduces hepatic steatosis in mice. *J Clin Invest.* 2009; 119: 1201–1215.

Kim JA, Wei Y, Sowers JR. Role of mitochondrial dysfunction in insulin resistance. *Circ Res.* 2008; 102: 401-414.

Korshunov SS, Skulachev VP, Starkov AA. High protonic potential actuates a mechanism of production of reactive oxygen species in mitochondria. *FEBS Letters.* 1997; 416: 15-18.

Kowaltowski AJ, de Souza-Pinto NC, Castilho RF, Vercesi AE. Mitochondria and reactive oxygen species. *Free Radic Biol Med.* 2009; 47: 333-343.

Lai S, Li Y, Kuang Y, Cui H, Yang Y, Sun W, et al. PKC δ silencing alleviates saturated fatty acid induced ER stress by enhancing SERCA activity. *Biosci Rep.* 2017; 37: 1-10.

Luo M and Anderson ME. Mechanisms of altered Ca²⁺ handling in heart failure. *Circ Res.* 2013; 113, 690-708.

Malhi H and Kaufman RJ. Endoplasmic reticulum stress in liver disease. *J Hepatol.* 2011; 54: 795-809.

Manning AM and Davis RJ. Targeting JNK for therapeutic benefit: from junk to gold? *Nat Rev Drug Discov.* 2003; 2: 554-565.

Mantena SK, King AL, Andringa KK, Eccleston HB, Bailey SM. Mitochondrial dysfunction and oxidative stress in the pathogenesis of alcohol- and obesity-induced fatty liver diseases. *Free Radic Biol Med.* 2008; 44: 1259-1272.

Mantena SK, King AL, Andringa KK, Landar A, Darley-Usmar V, Bailey SM. Novel interactions of mitochondria and reactive oxygen/nitrogen species in alcohol mediated liver disease. *World J Gastroenterol.* 2007; 13: 4967- 4973.

Mao YX, Cai WJ, Sun XY, Dai PP, Li XM, Wang Q, et al. RAGE-dependent mitochondria pathway: A novel target of silibinin against apoptosis of osteoblastic cells induced by advanced glycation end products. *Cell Death Dis.* 2018; 9: 1-14.

Marchi S, Marinello M, Bononi A, Bonora M, Giorgi C, Rimessi A, Pinton P. Selective modulation of subtype III IP₃ R by Akt regulates ER Ca²⁺ release and apoptosis. *Cell Death Dis.* 2012; 3: 1-10.

Mathur A, Hong Y, Kemp BK, Barrientos AA, Erusalimsky JD. Evaluation of fluorescent dyes for the detection of mitochondrial membrane potential changes in cultured cardiomyocytes. *Cardiovasc Res.* 2000; 46: 126-138.

Mekahli D, Bultynck G, Parys JB, De Smedt H, Missiaen L. Endoplasmic-reticulum calcium depletion and disease. *Cold Spring Harb Perspect Biol.* 2011; 3: 1-30.

Mohan S, Rani MR, Brown L, Ayyappan P. Endoplasmic reticulum stress: a master regulator of metabolic syndrome. *Eur J Pharmacol.* 2019; 860: 1-10.

Nadanaka S, Yoshida H, Kano F, Murata M, Mori K. Activation of Mammalian Unfolded Protein Response Is Compatible with the Quality Control System Operating in the Endoplasmic Reticulum. *Mol Biol Cell.* 2004; 15: 2537-2548.

Nathanson MH, Gautam A, Bruck R, Isales CM, Boyer JL. Effects of Ca²⁺ agonists on cytosolic Ca²⁺ in isolated hepatocytes and on bile secretion in the isolated perfused rat liver. *Hepatology.* 1992; 15: 107-116.

Nohl H, Gille L, Staniek K. Intracellular generation of reactive oxygen species by mitochondria. *Biochem Pharmacol.* 2005; 69: 719-723.

Ozcan L, Cristina de Souza J, Harari AA, Backs J, Olson EN, Tabas I. Activation of calcium/calmodulin-dependent protein kinase II in obesity mediates suppression of hepatic insulin signaling. *Cell Metab.* 2013; 18: 803-815.

Ozcan U, Cao Q, Yilmaz E, Lee AH, Iwakoshi NN, Ozdelen E, et al. Endoplasmic reticulum stress links obesity, insulin action, and type 2 diabetes. *Science.* 2004; 306: 457-461.

Paillard M, Tubbs E, Thiebaut PA, Gomez L, Fauconnier J, Da Silva CC, et al. Depressing mitochondria-reticulum interactions protects cardiomyocytes from lethal hypoxia-reoxygenation injury. *Circulation.* 2013; 128: 1555-1565

Peng TI and Jou MJ. Oxidative stress caused by mitochondrial calcium overload. *Ann N Y Acad Sci.* 2010; 1201: 183-188.

Prins D and Michalak M. Organellar calcium buffers. *Cold Spring Harb Perspect Biol.* 2011; 3: 1-16.

Puigserver P, Rhee J, Donovan J, Walkey CJ, Yoon JC, Oriente F, et al. Insulin-regulated hepatic gluconeogenesis through FOXO1–PGC-1 α interaction. *Nature.* 2003; 423: 550-555.

Rauscher FM, Sanders RA, Watkins III JB. Effects of coenzyme Q10 treatment on antioxidant pathways in normal and streptozotocin-induced diabetic rats. *J Biochem Mol Toxicol.* 2001; 15: 41-46.

Rieusset J, Fauconnier J, Paillard M, Belaidi E, Tubbs E, Chauvin MA, et al. Disruption of calcium transfer from ER to mitochondria links alterations of mitochondria-associated ER membrane integrity to hepatic insulin resistance. *Diabetologia.* 2016; 59: 614-623.

Rieusset J. Role of endoplasmic reticulum-mitochondria communication in type 2 diabetes. *Organelle Contact Sites.* 2017; 997: 171-186.

Rizzuto R, De Stefani D, Raffaello A, Mammucari C. Mitochondria as sensors and regulators of calcium signalling. *Nat Rev Mol Cell Biol.* 2012; 13: 566-578.

Rong X, Albert CJ, Hong C, Duerr MA, Chamberlain BT, Tarling EJ, et al. LXRs regulate ER stress and inflammation through dynamic modulation of membrane phospholipid composition. *Cell Metab.* 2013; 18: 685-697.

Rovira-Llopis S, Bañuls C, Diaz-Morales N, Hernandez-Mijares A, Rocha M, Victor VM. Mitochondrial dynamics in type 2 diabetes: Pathophysiological implications. *Redox Biol.* 2017; 11: 637-645.

Rowland AA, Voeltz GK. Endoplasmic reticulum-mitochondria contacts: function of the junction. *Nat Rev Mol Cell Biol.* 2012; 13: 607-625

Scarpulla RC. Metabolic control of mitochondrial biogenesis through the PGC-1 family regulatory network. *Biochim Biophys Acta Mol Cell Res.* 2011; 1813: 1269-1278.

Scheuner D, Song B, McEwen E, Liu C, Laybutt R, Gillespie P, et al. Translational control is required for the unfolded protein response and in vivo glucose homeostasis. *Mol Cell.* 2001; 7: 1165-1176.

Sebastian D, Hernandez-Alvarez MI, Segales J, Sorianello E, Munoz JP, Sala D, et al. Mitofusin 2 (Mfn2) links mitochondrial and endoplasmic reticulum function with insulin signaling and is essential for normal glucose homeostasis. *Proc Natl Acad Sci. U.S.A.* 2012; 109: 5523-5528

Shen J, Chen X, Hendershot L, Prywes R. ER Stress Regulation of ATF6 Localization by Dissociation of BiP/GRP78 Binding and Unmasking of Golgi Localization Signals. *Dev Cell.* 2002; 3: 99-111.

Simmen T, Aslan JE, Blagoveshchenskaya AD, Thomas L, Wan L, Xiang Y, et al. PACS-2 controls endoplasmic reticulum-mitochondria communication and Bid-mediated apoptosis. *EMBO J.* 2005; 24: 717-729

Skulachev V P. Uncoupling: New approaches to an old problem of bioenergetics. *Biochim Biophys Acta Bioenerg.* 1998; 1363: 100-124.

Szabadkai G, Bianchi K, Várnai P, De Stefani D, Wieckowski MR, Cavagna D, et al. Chaperone-mediated coupling of endoplasmic reticulum and mitochondrial Ca²⁺ channels. *J Cell Biol.* 2006; 175: 901-911.

Tan M, Tang C, Zhang Y, Cheng Y, Cai L, Chen X, et al. SIRT1/PGC-1 α signaling protects hepatocytes against mitochondrial oxidative stress induced by bile acids. *Free Radic Res.* 2015; 49: 935-945.

Tang BL. Sirt1 and the mitochondria. *Mol Cells*. 2016; 39: 87-95.

Toyoshima C and Inesi G. Structural basis of ion pumping by Ca²⁺-ATPase of the sarcoplasmic reticulum. *Annu Rev Biochem*. 2004; 73: 269-292.

Tubbs E, Theurey P, Vial G, Bendridi N, Bravard A, Chauvin MA, et al. Mitochondria-associated endoplasmic reticulum membrane (MAM) integrity is required for insulin signaling and is implicated in hepatic insulin resistance. *Diabetes*. 2014; 63: 3279-3294.

Urrea H, Dufey E, Lisbona F, Rojas-Rivera D, Hetz C. When ER stress reaches a dead end. *Biochim Biophys Acta*. 2013; 1833: 3507-3517.

Valle I, Álvarez-Barrientos A, Arza E, Lamas S, Monsalve M. PGC-1 α regulates the mitochondrial antioxidant defense system in vascular endothelial cells. *Cardiovasc Res*. 2005; 66: 562-573.

Vallerie SN and Hotamisligil GS. The role of JNK proteins in metabolism. *Sci Transl Med*. 2010; 2: 1-7.

Van der Bliek AM, Shen Q, Kawajiri S. Mechanisms of mitochondrial fission and fusion. *Cold Spring Harb Perspect Biol*. 2013; 5: 1-16.

Vial G, Dubouchaud H, Couturier K, Cottet-Rousselle C, Taleux N, Athias A, et al. Effects of a high-fat diet on energy metabolism and ROS production in rat liver. *J Hepatol*. 2011; 54: 348-356.

Walter P and Ron D. The Unfolded Protein Response: From Stress Pathway to Homeostatic Regulation. *Science*. 2011; 334: 1081-1086.

Wang M and Kaufman RJ. Protein misfolding in the endoplasmic reticulum as a conduit to human disease. *Nature*. 2016; 529: 326-335.

Wang Y, Li G, Goode J, Paz JC, Ouyang K, Sreaton R, et al. Inositol-1,4,5-trisphosphate receptor regulates hepatic gluconeogenesis in fasting and diabetes. *Nature*. 2012; 485: 128-132

Yang L, Li P, Fu S, Calay ES, Hotamisligil GS. Defective hepatic autophagy in obesity promotes ER stress and causes insulin resistance. *Cell Metab*. 2010; 11: 467-478.

Yoshida H, Matsui T, Yamamoto A, Okada T, Mori K. XBP1 mRNA Is Induced by ATF6 and Spliced by IRE1 in Response to ER Stress to Produce a Highly Active Transcription Factor. *Cell*. 2001; 107: 881-891.

Youle RJ and Narendra DP. Mechanisms of mitophagy. *Nat Rev Mol Cell Biol*. 2011; 12: 9-14.

Zhang J, Li Y, Jiang S, Yu H, An W. Enhanced endoplasmic reticulum SERCA activity by overexpression of hepatic stimulator substance gene prevents hepatic cells from ER stress-induced apoptosis. *Am J Physiol Cell Physiol*. 2014; 306: C279-C290.

Zhao M, Yuan Y, Bai M, Ding G, Jia Z, Huang S, Zhang A. PGC-1 α overexpression protects against aldosterone-induced podocyte depletion: Role of mitochondria. *Oncotarget*. 2016; 7: 12150-12162.

Zhu HR, Wang ZY, Zhu XL, Wu XX, Li EG, Xu Y. Icariin protects against brain injury by enhancing SIRT1-dependent PGC-1 α expression in experimental stroke. *Neuropharmacology*. 2010; 59: 70-76.

Zorov DB, Juhaszova M, Sollott SJ. Mitochondrial reactive oxygen species (ROS) and ROS-induced ROS release. *Physiol Rev*. 2014; 94: 909-950.

Chapter 6

Summary and Conclusion

The HI created insulin resistance has been developed in the HepG2 cells by incubating with 1 μ M human insulin for 24 hrs. This led to the down-regulation of both IRS2 and the GLUT2 and resulted in the reduced glucose uptake. These confirmed the development of HI created insulin resistance in HepG2 cells.

One of the major pathophysiology of HI which affects our body is the abnormal formation of ROS in the liver. Here also I found the increased levels of ROS in HI groups and it also altered the redox status of the cell. I have found that the levels of GSH, GPx and G6PDH were down-regulated in the HI group where the SOD activity was increased. The increased levels of SOD during the increased production of ROS is an adaptive response seen in the liver. During the initial stages of oxidative stress (increased ROS production), the SOD levels were found to increase because SOD is the first line of defence in the hepatocytes. The expression studies of both cytoplasmic and mitochondrial SOD levels confirmed the development of adaptive response in the liver during OS. However the decreased levels of G6PDH represents the delay of the regeneration of reduced GSH.

During OS the glutathione undergoes oxidation to form the reduced glutathione so for the capturing of the next ROS it needs to be regenerated into reduced glutathione. G6PDH is the major enzyme which provides the reducing equivalents for the formation of reduced glutathione, but the decreased level of G6PDH in HI condition leads to the shortage of the reducing equivalents like NADPH. In addition to this the progression of polyol pathway during HI condition is another way to utilise the NADPH levels. Both the increased levels of ROS as

well as the increased polyol pathway results in the decreased NADPH levels. Furthermore, the increased ROS will affect the cellular proteins and membrane lipids and form both protein carbonyls and lipid peroxides. The increased levels of both protein carbonyls and lipid peroxides were observed in my study also.

Both HI and insulin resistance are intertwined with each other. So a decreased glucose uptake was observed in the HI and it is via the inhibition of insulin signaling pathway in the HepG2 cells. The major proteins in the insulin signaling pathway such as AKT, PI3K, and GLUT2 were down-regulated in HI. Inhibition of insulin signaling is the indication of development of insulin resistance. Besides this, a decreased IDE expression was observed in HI and it is one of the reasons for the progression of HI. The decreased expression of GLUT2 revealed the reduced glucose uptake in hepatocytes.

The master regulator of hepatic glucose metabolism is the GK in the liver. It is the rate limiting enzyme of hepatic glycolysis and it maintains the hepatic glucose homeostasis. The decreased expression of GLUT2 during HI also reduced the activity of the GK. The decreased glycolysis was observed in the HI via the reduced GK activity and the increased GKR levels. Mitochondria is linked to hepatic glucose metabolism through BAD, a mitochondrial protein. Mitochondria are the powerhouse of the cell and glucose is the prime energy source for almost all cells in our body. The expression analysis of both p-BAD and GK proved the importance of mitochondria on glucose metabolism. During HI the p-BAD levels were down-regulated; it decreased the glycolysis through reduced expression of GK.

Furthermore, in hyperinsulinemic HepG2 cells, the decreased expression of IRS2 and unaltered expression of IRS1 were observed which indicates the development of selective insulin resistance in the liver. The increased gluconeogenesis and the decreased glycogenesis during HI confirmed the development of selective insulin resistance. In addition to this, the

decreased insulin signaling in the liver leads to the increased glucose levels in the hepatocytes. The result of glucose uptake assay proved this. The increased glucose in the HepG2 cells results in the genesis of many complications like increased production of ROS, increased the production of AGEs and increased the activation of polyol pathway. Sorbitol, the first product of the polyol pathway, was found to be increased in the HI treated cells. The increased polyol pathway leads to the increased production of AGEs. In our study also the increased production of AGEs were observed in the HI treated cells. Increased AGEs were observed with the up-regulated levels of RAGE and reduced expression of DDOST in HI cells. The selective insulin resistance created by HI in hepatocytes is the crucial factor for the development of T2DM and NAFLD.

Another consequence of selective insulin resistance is the excessive DNL. The increased levels of DNL were found in HI. This leads to the increased lipid storage in the liver. The data of lipid droplet assay and the increased TG content confirmed the lipid accumulation in the HepG2 cells. Also the levels of major enzymes involved in both DNL and the fatty acid uptake were increased in HI. The levels of DGAT, the major enzyme in the TG synthesis, was also increased in HI treated cells. All these results confirmed the development of selective insulin resistance during HI. It is the major factor for the initiation of impairments in lipid metabolism in HepG2 cells. Besides this, the excess lipid accumulation in the liver is the major cause for the development of NAFLD. In my study also the lipid accumulation was increased in HI conditions.

The increased lipid levels in the liver results in the initiation of inflammation and it releases the various proinflammatory cytokines like NF- κ B, IL6 and TNF- α . These results further confirmed the prevalence of NAFLD. The adverse effects of HI such as increased levels of ROS, the development of selective insulin resistance and its associated disturbances in both glucose and lipid metabolism, and the excess production of AGEs in the liver finally leads to

the mitochondrial dysfunction. Here I have seen that the initiation of mitochondrial alterations via the increased production of mitochondrial ROS. Here I also observed a decrease of aconitase activity and the reduced mitochondrial content. During the disease condition the level of mitochondrial super oxides were increased. In my study also the increased mitochondrial super oxides was observed in the HI group. Simultaneously the increased mitochondria ROS affects the distortion in the $\Delta\psi_m$ which results in the opening of the mPTP. Continued opening of the mPTP leads to the mitochondrial Ca^{2+} dysregulation. $\Delta\psi_m$ is an indicator of mitochondrial membrane integrity. The loss of $\Delta\psi_m$, defect in Ca^{2+} homeostasis and the mitochondrial dynamics have been observed. These create the disturbances in mitochondrial bioenergetics.

In addition to this the ATP production and the oxygen consumption rate were found to be decreased in hyperinsulinemic HepG2 cells. All these consequences resulted in the reduced mitochondrial biogenesis. The proteins involved in mitochondrial biogenesis like p-AMPK, PGC-1 α and SIRT1 were found to be down regulated in HI.

Meanwhile in our study, an increased cytoplasmic Ca^{2+} level in the HI group resulted in the alterations in the Ca^{2+} homeostasis. The alterations in the mitochondrial Ca^{2+} will result in the increased cytoplasmic Ca^{2+} and it also reduced the ER Ca^{2+} storage. The decrease in ER Ca^{2+} levels and the increased production of ROS resulted in the initiation of ER stress. During the ER stress, the three UPR pathways like IRE-1 α , PERK and ATF6 are activated. Various ER stress proteins like p-IRE1 α , XBP1, p-PERK, p-eIF2 α and CHOP while the proteins involved in Ca^{2+} homeostasis such as IP3R, JNK, GRP78, p-CAMKII were increased in response to ER stress in HI. Also the levels of SERCA were found to be decreased in HI. The decreased expression is carried out mainly through the attack of ROS on the ER membrane proteins like SERCA. This indicates the reduced storage of ER Ca^{2+} . Furthermore the decreased levels of ER Ca^{2+} also affect the Ca^{2+} dependent ER proteins and chaperons. These findings

revealed the importance of Ca^{2+} in the progression of ER stress. From these results I found that the major contributor for the alterations in Ca^{2+} homeostasis is the mitochondrial alterations.

Both the mitochondrial alterations, ER stress and the Ca^{2+} dysregulation finally leads to the disturbances in the MAM. The major proteins of the MAM like VDAC, CypD, IP3R, mTORC, MFN2 and GRP75 were found to be decreased in HI treated cells which indicates the initiation of alteration in MAM also. Another major protein found in the MAM surface is the PTEN and it was observed that during HI the expression of PTEN was also increased. The up-regulated level of PTEN in HI indicated the alterations in the glucose metabolism and it further confirmed that the mitochondrial alterations also affect the hepatic glucose metabolism.

From these overall results I conclude that the increased ROS during the HI is the main causative agent for the development of almost all the adverse effects of HI. The increased ROS also attacks the membrane lipids of both ER and mitochondria which results in the mitochondrial dysfunction and ER stress. The formation of lipid peroxides during HI will affect the $\Delta\psi_m$. Here also I have observed the loss of $\Delta\psi_m$ in HI treated cells. The distorted $\Delta\psi_m$ results in the continuous opening of the mPTP which was seen in the HI group. The opening of the mPTP caused the disturbances in the mitochondrial Ca^{2+} . The decreased level of VDAC and increased expression of p-CAMKII during HI confirmed the mitochondrial Ca^{2+} distortion and the increased cytoplasmic Ca^{2+} levels. Increased cytoplasmic Ca^{2+} leads to the decreased ER Ca^{2+} storage.

The major ER proteins involved in this process are SERCA and IP3R. In this study I have observed that during HI the SERCA expression decreases while the IP3R expression increases which indicates the decreased pumping of Ca^{2+} from cytoplasm to ER. As a result the ER Ca^{2+} storage has decreased. When the ER Ca^{2+} is reduced it causes the decreased synthesis of Ca^{2+} dependent proteins which are essential for protein folding. The end result of this is the

increased accumulation of misfolded proteins inside the ER which resulted in the ER stress. Here also the increased ER stress was observed in HI.

In continuation with this, during HI due to enormous production of ROS both the lipid peroxidation and protein carbonyls levels were increased and it created the disturbances in the ER membrane lipids and proteins. This also results in the ER stress. Another factor which contributes to ER stress is the increased accumulation of lipids during HI which also creates the alterations in the lipid compositions in ER membrane and results in the ER stress. The other markers of ER stress like JNK and GRP78 were up-regulated in the HI condition which confirmed the genesis of ER stress in HI. Also the increased JNK leads to the initiation of inflammation cascade in the hepatocytes by increased production of proinflammatory cytokines like NF- κ B, IL6 and TNF- α .

The HI causes OS, altered hepatic glucose metabolism, impaired lipid metabolism, initiation of inflammation and Ca²⁺ dysregulation in the HepG2 cells. All these consequences result in the development of mitochondrial alterations, ER stress and the disturbances in MAM. So in the present study, I have found that the mitochondrial alterations and the ER stress are the main players in the progression of HI creating complications in the liver. HI is the major symptom of insulin resistance and it causes many of the diseases including metabolic syndrome.

The natural compound 'VA' and positive control metformin were also evaluated against the pathophysiology created by HI. VA is a well-known food additive and it has so many beneficial properties like hepatoprotective, anti-inflammatory, antioxidant, antihypertensive etc. According to this study also VA is a hepatoprotective and a good antioxidant during the HI condition. VA can restore the antioxidant enzyme status of the cell by increasing the activity of GPx and glutathione. Simultaneously VA treatment can reduce the levels of other products

of OS like protein carbonyls and lipid peroxides levels. In addition to this VA is effective in restoring the mitochondrial function by decreasing the mitochondrial superoxide production, increasing the mitochondrial content, increasing the mitochondrial biogenesis and increasing the aconitase activity. ATP synthesis and oxygen consumption rates were also increased by the VA treatment. VA treatment also increased the mitochondrial fusion and restored the $\Delta\psi_m$ thereby reducing the mPTP opening. So VA is also effective in maintaining the mitochondrial Ca^{2+} levels. Furthermore, VA is effective against the insulin resistance created by HI by activating the insulin signaling pathway and improving the glucose uptake. Simultaneously VA treatment increased the insulin degradation process and decreased the HI and insulin resistance in HepG2 cells.

VA treatment also increased the hepatic glycolysis and glycogenesis simultaneously it reduced the gluconeogenesis in the HI group. According to my docking experiments data VA has a potential to activate the GK so it can be considered as a new GK activator. VA also decreased the levels of sorbitol and reduced the occurrence of polyol pathways. Meanwhile it decreased the formation of the AGEs by the down-regulation of RAGE. Here VA proved its potential as an antiglycation agent. Same time VA treatment reduced the lipid accumulation in hepatocytes and thereby reduced the prevalence of NAFLD. VA treatment reduced both the DNL and the hepatic fatty acid uptake while it also reduced the cholesterol synthesis by down-regulating the expression of HMG CoA reductase. VA treatment also up-regulates the levels of FGF-21 and thereby interconnects and regulates both carbohydrates and lipid metabolism which maintains a normal hepatic homeostasis. VA also exhibits the anti-inflammatory effects in HI treated groups.

Furthermore, VA treatment is also effective against the ER stress and the disturbances in MAM during HI. It prevented the ER stress by down-regulating the levels of UPR stress proteins and also restored the MAM integrity by up-regulating the expression of MAM proteins

like VDAC, CypD, GRP75, IP3R, MFN2 and mTORC. Finally VA also shows the DPP4 inhibition property. The overall data show the pathological effects created by HI and the beneficial effect of VA against the same. Based on these I am in the opinion that HI is a very critical risk factor for liver dysfunction through multiple pathways.

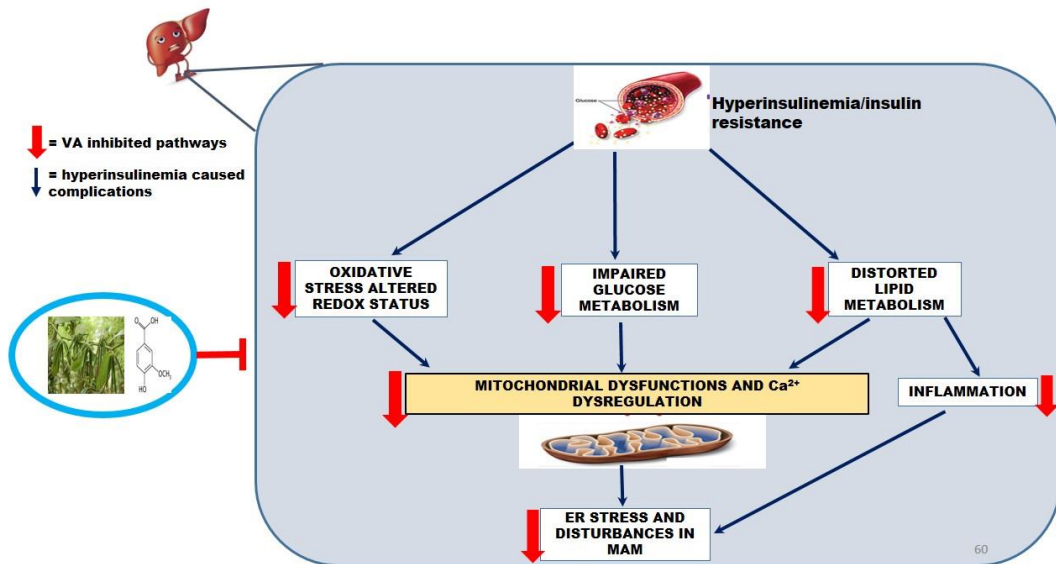


Figure. 6.1: Schematic representation of adverse biochemical alterations in HepG2 cells during hyperinsulinemia and proposed mechanism of action of VA

ABSTRACT

Name of the Student : Sreelekshmi Mohan	Registration No : 10BB16A39017
Faculty of Study : Biological Sciences	Year of Submission : November 2021
AcSIR academic centre/CSIR Lab : NIIST	Name of the Supervisor : Dr. K.G. Raghu

Title of the thesis : Investigation on adverse biochemical alterations in HepG2 cells during hyperinsulinemia and possible reversal with vanillic acid

Hyperinsulinemia (HI) and insulin resistance are the two conditions, but they are intertwined and co-exist. So in this investigation I elucidated in detail the various pathological effects of HI in the HepG2 cells and its association with insulin resistance and NAFLD via *in vitro* mechanistic study. Here I tried to study the adverse biochemical effects created by HI such as distortions in the redox status, alterations in the both hepatic glucose and lipid metabolism, mitochondrial alterations, Ca²⁺ dysregulation, ER stress and disturbances in MAM. For this investigation, an *in vitro* model of HI created insulin resistance was developed by incubating HepG2 cells with 1 μM human insulin for 24 hrs. Here I have observed that HI can cause insulin resistance and which in turn significantly affects the redox status of the cell by the increased production of reactive oxygen species (ROS). This resulted in the depletion of glutathione peroxidase levels, glucose-6-phosphate dehydrogenase levels, glutathione levels and also as an adaptive response it increased the superoxide dismutase levels in the HepG2 cells. I also observed that HI altered both the insulin signaling pathway and the glucose uptake. The decreased glucose uptake resulted in the hyperglycemia and it amplified both glycation and polyol pathway in the HepG2 cells by increased production of advanced glycation end products and sorbitol. During HI the development of insulin resistance were observed which revealed impairments in the both hepatic glucose and lipid metabolism. Based on this I studied the alterations in both hepatic glucose and lipid metabolism and from these I have noticed the association between the glucokinase (GK) and p-BAD in inducing the alterations in hepatic glucose metabolism. Also, I have found a decreased glycogenesis and reduced glycolysis through the inhibition of the GK in HepG2 cells. Simultaneously I have observed the increased gluconeogenesis and the up-regulated *de novo* lipogenesis as a result of selective insulin resistance. Both the up-regulated *de novo* lipogenesis and increased fatty acid uptake resulted in the development of lipid accumulation as well as the initiation of inflammation inside the cell, a hallmark of the initiation of NAFLD. Besides this, I have found that the increased ROS via alteration in redox status affect the mitochondrial metabolism also. Mitochondria is related to hepatic glucose metabolism via BAD protein. In addition, the decreased glucose uptake during HI created the mitochondrial dysfunction by decreased ATP synthesis. Furthermore, the increased lipid levels during selective insulin resistance and the increased production of lipid peroxides during oxidative stress caused both the ER and mitochondrial disturbances. The ER stress during the HI also created a decreased expression of SERCA. The decreased SERCA expression and the increased cytoplasmic Ca²⁺ leads to the altered Ca²⁺ homeostasis. All these consequences caused the disturbances in MAM. All these results implicated the importance of MAM, ER and mitochondria on the prevalence of HI and HI associated complications. Meanwhile VA and metformin were effective against these complications created by HI. VA could act as an antioxidant, antiglycation agent, a good glucokinase activator and a novel DPP4 inhibitor. In addition to this, VA has a potential to increase the expression of insulin degrading enzymes in the HepG2 cells and thereby reduce the occurrence of HI. Thus VA could act as a good and an attractive phytochemical against the HI and its associated complications.

Publications

From thesis

1. Sreelekshmi Mohan, Raghu KG. Vanillic acid mitigates the impairments in glucose metabolism in HepG2 cells through BAD–GK interaction during hyperinsulinemia. *J Biochem Mol Toxicol.* 2021; 35 :1-8.
2. Sreelekshmi Mohan, George George, Raghu KG. Vanillic acid retains redox status in HepG2 cells during hyperinsulinemic shock using the mitochondrial pathway. *Food Biosci.* 2021; 41: 101016.
3. Sreelekshmi Mohan, Preetha Rani MR, Lindsay Brown L, Prathapan Ayyappan, Raghu KG. Endoplasmic reticulum stress: a master regulator of metabolic syndrome. *Eur J Pharmacol.* 2019; 860:172553.

Other than thesis

1. Preetha Rani MR, Anupama Nair, Sreelekshmi, Mohan, Raghu, K.G. Chlorogenic acid attenuates glucotoxicity in H9c2 cells via inhibition of glycation and PKC α upregulation and safeguarding innate antioxidant status. *Biomed Pharmacother.* 2018; 100: 467-477

Scientific Conferences

Oral presentations

1. Vanillic acid mitigates the impairments in glucose metabolism in HepG2 cells through BAD-GK interaction during hyperinsulinemia. In National Virtual Conference on recent breakthroughs in Biotechnology (NCRBB-2021) and Annual Meet of the Society for Biotechnologists (India) held at Bharathiar University, Coimbatore, 22-23 January 2021.
2. Vanillic Acid Protects HepG2 cells From Hyperinsulinemia Induced Complications. In 8th IABS conference on Deliberation on Translation of Basic Scientific Insights into Affordable Healthcare Products held at CSIR-NIIST, Thiruvananthapuram, 25-27 February 2019.

Poster presentations

1. Hyperinsulinemia induced alterations in redox status, bioenergetics and glucose metabolism in HepG2 cells and amelioration with vanillic acid. In International Congress on Obesity and Metabolic Syndromes (ICOMES & AOCO 2019) held at Conrad Hotel, Seoul, South Korea, 29-31 August 2019 (**Received travel grant award**).
2. *Parmotrema tinctorum* (Lichen): a potent nutraceutical against oxidative stress and hyperglycemia induced complications evident from *in vitro* study in HepG2 cells. In International Seminar on Phytochemistry (ISP) held at Jawaharlal Nehru Tropical Botanical Garden and Research Institute, Palode, Trivandrum, 26-27 March 2018.
3. Licarin B, a novel insulin sensitizer from *Myristica fragrans* acts via PPAR γ and GLUT4 in the IRS-1/PI3K/AKT pathway in 3T3-L1 adipocytes. In International symposium on Current Trends in Pharmaceutical Sciences: Advances in New Drug

discovery and Development held at Gujarat University Convention and Exhibition Centre, Ahmedabad, 2-4 February 2017.

4. *Parmotrema tinctorum* (Lichen): a potent nutraceutical against oxidative stress and hyperglycemia induced complications evident from *in vitro* study in HepG2 cells. In National Conference on Recent Trends in Biotechnology and Annual Meet of the Society for Biotechnologists (India) held at National Institute of Ocean Technology, Chennai, 19-21 October 2016.

RESEARCH ARTICLE

Vanillic acid mitigates the impairments in glucose metabolism in HepG2 cells through BAD–GK interaction during hyperinsulinemia

 Mohan Sreelekshmi^{1,2} | Kozhiparambil Gopalan Raghu^{1,2} 

¹Biochemistry and Molecular Mechanism Laboratory, Agro-processing and Technology Division, CSIR-National Institute for Interdisciplinary Science and Technology, Thiruvananthapuram, Kerala, India

²Academy of Scientific and Innovative Research (AcSIR), Ghaziabad, India

Correspondence

K. G. Raghu, Biochemistry and Molecular Mechanism Laboratory, Agro-processing and Technology Division, CSIR-National Institute for Interdisciplinary Science and Technology, Thiruvananthapuram-695019, Kerala, India.
 Email: raghukgopal@niist.res.in

Funding information

University Grant Commission (UGC, New Delhi, India), Grant/Award Number: Ref. No: 21/06/2015(i)EU-V

Abstract

Glucokinase (GK), a key regulator of hepatic glucose metabolism in the liver and glucose sensor and mediator in the secretion of insulin in the pancreas, is not studied in detail for its therapeutic application in diabetes. Herein, we study the alteration in GK activity during hyperinsulinemia-induced insulin resistance in HepG2 cells. We also investigated the link between GK and Bcl-2-associated death receptor (BAD) during hyperinsulinemia. There are emerging demands for GK activators from natural resources, and we selected vanillic acid (VA) to evaluate its potential as GK activators during hyperinsulinemia in HepG2 cells. VA is a phenolic compound and a commonly used food additive in many food industries. We found that VA safeguarded GK inhibition during hyperinsulinemia significantly in HepG2 cells. VA also prevented the depletion of glycogen synthesis during hyperinsulinemia, which is evident from protein expression studies of phosphoenolpyruvate carboxykinase, glucose-6-phosphatase, glycogen synthase, and glycogen synthase kinase-3 β . This was associated with activation of BAD activity, which was also confirmed by Western blotting. Molecular docking revealed strong binding between GK active site and VA, supporting their strong interaction. These are the first in vitro data to indicate the beneficial properties of VA with respect to insulin resistance induced by hyperinsulinemia by GK activation. Since it is activated via BAD, the hypoglycemia associated with general GK activation is not expected here and therefore has significant implications for future therapies against diabetes.

KEYWORDS

BAD, glucokinase, gluconeogenesis, HepG2 cells, hyperinsulinemia

Abbreviations: BAD, Bcl-2-associated death receptor; BSA, bovine serum albumin; DMEM, Dulbecco's modified Eagle's medium; DMSO, dimethyl sulfoxide; FBS, fetal bovine serum; G-6-P, glucose-6-phosphatase; GK, glucokinase; GKR, glucokinase regulatory protein; GS, glycogen synthase; GSK-3 β , glycogen synthase kinase-3 β ; HepG2, human hepatic carcinoma; HGP, hepatic glucose production; HRP, horseradish peroxidase; IR, insulin resistance; MODY2, maturity-onset diabetes of the young type 2; PBST, phosphate-buffered saline-Tween 20; PEPC, phosphoenolpyruvate carboxykinase; SDS-PAGE, sodium dodecyl sulfate-polyacrylamide gel electrophoresis; TBST, trisbuffered saline-Tween 20; T2DM, type 2 diabetes mellitus; VA, vanillic acid.

1 | INTRODUCTION

The glucose metabolism in the human is controlled by a master regulator called glucokinase (GK),^[1] predominantly seen in both the pancreas and liver. GK controls the flux of glucose through several metabolic pathways like glycolysis, glycogenesis, glycogenolysis, and gluconeogenesis.^[2] It phosphorylates the glucose to glucose-6-phosphate (G6P) and traps glucose inside the hepatocyte, ensuring that an adequate amount of glucose enters the cell to be metabolized.^[3] To synthesize glycogen, glucose is phosphorylated upon its entrance into the hepatocytes, and it is carried out by GK. So the GK reaction is a limiting factor for glycogen synthesis from glucose in the liver.^[4] Through this mechanism, it enhances insulin secretion in pancreatic β -cells and improves hepatic glucose homeostasis.^[1] A defective glycogen synthesis after meals was observed in type 2 diabetes mellitus (T2DM) patients, which leads to postprandial hyperglycemia.

In the liver, GK regulates substrate utilization by promoting glycolysis and glycogenesis while inhibiting hepatic glucose production (HGP).^[2] HGP is central to metabolic adaptation during fasting, and its abnormal elevation is a chief determinant of fasting hyperglycemia in T2DM.^[2,5] HGP is derived from glycogen breakdown and *de novo* genesis of glucose (gluconeogenesis).^[2] In the liver, the GK activity is profoundly regulated by its binding to a glucokinase regulatory protein (GKRP).^[6] Accordingly, GKRP is a GK anchoring protein and a chaperone that mediates the GK import and export.^[7,8] This regulation of GK with its GKRP is needed for postprandial glycolysis without generating hypoglycemia. In the liver, when the glucose concentration is high, GK is released from the GKRP and enters into the cytoplasm, where it catalyzes the formation of glucose 6 phosphate from glucose.^[8,9] Recent studies postulate that when GK enters the cytoplasm, it associates with a mitochondrial complex comprising Bcl-2-associated death receptor (BAD).^[10,11] BAD-deficient hepatocytes possess diminished mitochondria-based GK activity. BAD's metabolic effect depends on its ability to activate GK and modulate glucose oxidation.^[12] Several diseases like permanent neonatal diabetes mellitus and maturity-onset diabetes of the young type 2 (MODY2) result from heterozygous inactivation of GK genes.^[13] The contribution of BAD in altered hepatic glucose metabolism during T2DM has not been examined. Also, the actual mechanism of cytoplasmic GK in regulating glucose metabolism is not fully understood, and the role of associate proteins involved in the process has not been elucidated completely. Here, we try to reveal the role of BAD in association with GK, improving its glucose uptake in the HepG2 cells. We have also selected vanillic acid (VA) to screen its potential to enhance the activity of BAD-linked GK activity in HepG2 cells. VA is a biologically safe, natural plant component, an intermediate molecule formed during the ferulic acid metabolism, and commonly used flavoring agent. It has been reported for multiple beneficial effects such as hepatoprotective,^[14] chemopreventive, cardioprotective, antihypertensive, and antioxidant.^[15]

2 | MATERIALS AND METHODS

Dulbecco's modified eagle's medium (DMEM) (Cat no. 11965118), fetal bovine serum (FBS) (Cat no. 16000044), 0.5% trypsin-ethylene diamine tetra acetic acid (trypsin-EDTA) (Cat no. R001100) and penicillin-streptomycin antibiotics (Cat no. 15070063) were purchased from Gibco-BRL Life Technologies. Dimethyl sulfoxide (DMSO) (Cat no. D8418), radioimmuno precipitation assay-radioimmuno precipitation assay (RIPA) buffer (Cat no. R0278), VA (Cat no. W398802), and metformin (Cat no. 317240) were purchased from Sigma Aldrich. GK (Cat no. sc-17819), GKRP (Cat no. sc-166841), and Bcl-2-associated death receptor (BAD) (Cat no. sc-271963) antibodies were obtained from Santa Cruz Biotechnology. Glycogen synthase (GS) (Cat no. 3893s), glycogen synthase kinase-3 β (GSK3 β) (Cat no. 12456), β -actin (Cat no. 4970), and all other secondary antibodies were purchased from Cell Signaling Technology. Phosphoenolpyruvate carboxykinase (PEPCK) (Cat no. ab-54481) and glucose-6-phosphatase (G-6-P) (Cat no. ab-93857) were from Abcam. Recombinant human insulin was from Merck (Cat no. 407709). The remaining chemicals used were of analytical grade.

2.1 | Cell culture

Human hepatic carcinoma (HepG2) cells were obtained from the National Centre for Cell Science (NCCS), Pune. The cells were cultured in DMEM containing 10% FBS, 100 U/ml penicillin, and 100 μ g/ml streptomycin at 5% CO₂ and 37°C in an incubator. A model of high insulin-induced insulin-resistant HepG2 cells was developed according to the method of Jung et al.,^[16] with slight modifications. Briefly, HepG2 cells were seeded in 96-well plates. After reaching 80% confluence, the cells were treated with 1 μ M human insulin for 24 h to induce insulin resistance; simultaneously, the cells were subjected to corresponding treatments with 1% serum-containing media. After treatment, the cells were harvested for further analysis.

2.1.1 | Experimental groups

C group: HepG2 cells without any treatment (control).

Insulin-resistant group (IR): Cells incubated with 1 μ M human insulin for 24 h.

VA1 group: IR group cotreated with 5 μ M of VA.

VA2 group: IR group cotreated with 10 μ M of VA.

M group: IR group cotreated with 1 mM of metformin.

2.2 | GK activity and regulation of GK

The activity of GK was detected and quantified calorimetrically (ELISA; My Biosource) (Cat no. MBS729636). A microtiter plate precoated with an antibody specific to GK provided in the kit was used. To perform this assay, the cells after respective treatments

were harvested. Then both standard and 100 μ l of the sample were added into the respective wells of a microtiter plate. After 2 h of incubation at 37°C, the wells were washed. Then, 100 μ l of avidin-conjugated horseradish peroxidase (HRP) was added to all the wells and incubated for 1 h at 37°C. Then the wells were washed and added 90 μ l of TMB substrate solution to the wells. Then incubated for 25 min at 37°C. Then 50 μ l of stop solution was added to terminate the reaction, and immediately the color change was read at 450 nm.

The amount of GKRP protein was quantified calorimetrically according to the ELISA method. In this assay, a 96-well plate was coated with nuclear protein samples of 50 μ l and incubated at 4°C overnight. After this, the plate was washed five times with phosphate-buffered saline-Tween 20 (PBST). Then, 100 μ l of GKRP antibody (1:1000) was added and incubated for 1 h followed by five times wash with PBST. Then, the antirabbit secondary antibody (1:2000), which is HRP-conjugated, was added and incubated for 1 h. Then, the cells were washed with PBST followed by the addition of 50 μ l of substrate solution and incubated for 20 min. After that, 50 μ l of stop solution was added to terminate the reaction, and immediately the color change was read at 450 nm.

2.3 | Glycogen assay

The glycogen level was assayed using a kit from Abcam (Cat no. ab169558). For this assay, the cells were seeded in a 24-well plate. After respective treatments, the cells were homogenized for 10 min on ice, followed by boiling of homogenates for 10 min to inactivate the enzymes. After centrifugation, the supernatant was collected. Fifty microliters of supernatants (samples) and standards were added to the 96-well plate. Then 2 μ l of hydrolysis buffer (provided by the kit) to all the wells was added and incubated for 30 min. After that, 48 μ l of reaction mix was added. Then, it was incubated for 30 min at room temperature, and the OD was measured at 450 nm. The expression levels of proteins, GS and GSK-3 β , involved in glycogen metabolism were analyzed by Western blotting (for details, refer Section 2.8).

2.4 | Gluconeogenesis

The expression levels of major proteins in hepatic gluconeogenesis like PEPCK and G-6-P were evaluated at protein levels by Western blot analysis (for details, refer Section 2.8).

2.5 | GK and BAD expression

The expression level of GK and BAD proteins during insulin resistance conditions were analyzed by Western blot analysis (for details, refer Section 2.8).

2.6 | Molecular docking

Autodock v4.2 and autodock tools were used to analyze the interaction between the GK ligand-binding domain and VA. They were used to find the most populated cluster with the lowest binding energy, which was deemed as the most stable conformation. The three-dimensional model of GK was taken from Brookhaven protein data bank, and the structure of VA was downloaded from Chemspider and converted to PDB format using Chem-3D Pro 10. The docking fitness of the VA to GK and the amino acids of GK involved in the interaction was predicted by using iGEMDOCK. The binding energy of VA-GK was analyzed using the software Autodock v4.2.

2.7 | Western blot analysis

Immunoblotting was used to analyze the expression of GK, PEPCK, G-6-P, GS, GSK-3 β , BAD, and β -actin proteins. Cells were seeded in T-25 flasks containing 5 ml DMEM medium and subjected to respective treatments. After the treatment, the cells were harvested and lysed in an ice-cold RIPA buffer containing a protease inhibitor cocktail (Sigma Aldrich). Each homogenized sample was centrifuged at 10,000g for 20 min at 4°C, and the supernatant was collected. Protein concentration in the supernatant was quantified using a bicinchoninic acid protein assay kit (Pierce). After equalization of proteins, 20 μ l of protein was mixed in 5 \times sample buffer and was boiled for 5 min and resolved in 10% sodium dodecyl sulfate-polyacrylamide gel electrophoresis at 55 V. Twenty-five microliters of each sample was loaded into each well. After separation using Mini-Trans-Blot (BioRad), the proteins were transferred to the PVDF membrane (Millipore, Merck). The membrane was blocked in bovine serum albumin (BSA) in tris-buffered saline-Tween 20 (TBST) for 1 h at room temperature. After washing with TBST, membranes were incubated with specific primary antibodies (1:1000) and β -actin in TBST overnight with gentle agitation at 37°C. After washing with TBST, membranes were incubated for 1 h at 37°C with horseradish peroxidase-conjugated secondary antibodies (1:2000) by shaking. After three washes with TBST, the membranes were developed with the enhanced chemiluminescence (Abcam) kit. After that, the membrane was visualized by ChemiDoc XRS (Bio-Rad). Proteins levels were quantified by densitometry using ImageJ software.

2.8 | Statistical analysis

All analyses were carried out in triplicates ($n = 3$) and data are presented as mean \pm standard error of the mean (SEM). The normality for the variables were analyzed using Kolmogorov-Smirnov Z test, and the variables were normally distributed. Hence, the data were subjected to a one-way analysis of variance (ANOVA), and further significantly different pairs were identified using post hoc Duncan's multiple comparison test. Values were statistically significant at

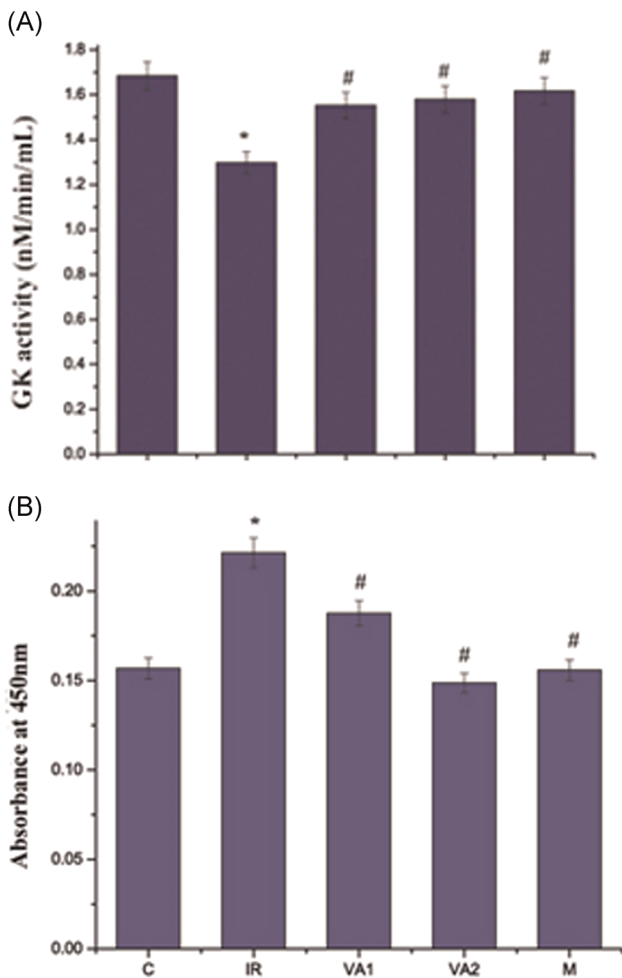


FIGURE 1 VA enhances GK activity by downregulating GKR. (A) GK activity is analyzed by GK activity assay. (B) GKR activity is analyzed by indirect ELISA. C, control cells; IR, high insulin-treated insulin-resistant cells; VA1, IR + 5 μ M vanillic acid; VA2, IR + 10 μ M vanillic acid; M, IR + metformin (1 mM). Data are presented as mean \pm SEM, where $n = 6$. *mean value was significantly different from control cells ($p \leq 0.05$). # mean value was significantly different from IR cells ($p \leq 0.05$). ELISA, enzyme-linked immunosorbent assay; GK, glucokinase; GKR, glucokinase receptor protein; VA, vanillic acid

$p \leq 0.05$. All calculations were done by using SPSS for Windows standard version 20 (SPSS Inc.).

3 | RESULTS

3.1 | GK level is declined in insulin-resistant HepG2 cells via the overexpression of GKR

Analysis of GK activity showed a significant decrease (20%) in IR cells compared with control cells (Figure 1A). While with VA cotreatment, the level of GK was increased significantly by 15% and 16.7% for 5 and 10 μ M concentrations compared with IR cells.

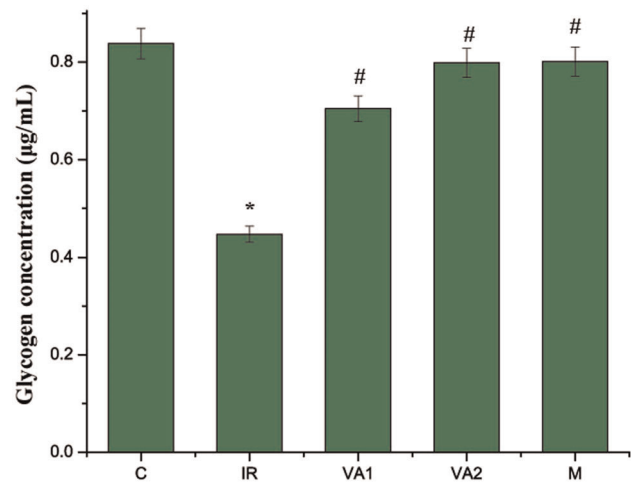


FIGURE 2 Glycogen synthesis. After VA cotreatment, the glycogen content is determined by glycogen assay. C, control cells; IR, high insulin-treated insulin-resistant cells; VA1, IR + 5 μ M vanillic acid; VA2, IR + 10 μ M vanillic acid; M, IR + metformin (1 mM). Data are presented as mean \pm SEM, where $n = 6$. * mean value was significantly different from control cells ($p \leq 0.05$). # mean value was significantly different from IR cells ($p \leq 0.05$)

Metformin caused a significant increase of the GK levels by 20% (Figure 1A).

To determine how the GK is downregulated in IR cells, the levels of GKR were analyzed. Here, we found that in IR cells, the levels of GKR were increased (41.1%) significantly compared with control cells. VA of both concentrations (5 and 10 μ M) significantly reduced the activity of GKR by 21.6% and 46.4%, respectively. Metformin also reduced the activity of GKR by 41.8% as compared with IR. Here compared with metformin, VA of 10 μ M concentration showed a better result (Figure 1B).

3.2 | Hepatic GK activation enhances the glycogenesis in the liver

During IR condition, the glycogen level was decreased drastically (46.6%) as compared with control cells (Figure 2). While with VA, the level of glycogen was increased significantly by 30.7% and 41.9% ($p \leq 0.05$) for 5 and 10 μ M concentrations, respectively, compared with IR cells (Figure 2). Metformin also significantly enhanced the glycogen content of IR cells by 42.2% as compared with IR cells.

This was also confirmed by Western blot data. Here, we checked the expression of both GS and GSK-3 β (Figure 3A). The result showed that there was a significant reduction in the GS enzyme by 38.7% ($p \leq 0.05$) and upregulation of GSK-3 β by 123.5% ($p \leq 0.05$; Figure 3B) in IR cells. The cotreatment of VA (5 and 10 μ M) caused 29.7% and 84.1% increase in GS activity and 85.7% and 94.7% decrease in GSK-3 β compared with IR cells, respectively. Metformin cotreatment also significantly increased the GS enzyme by 85.2%

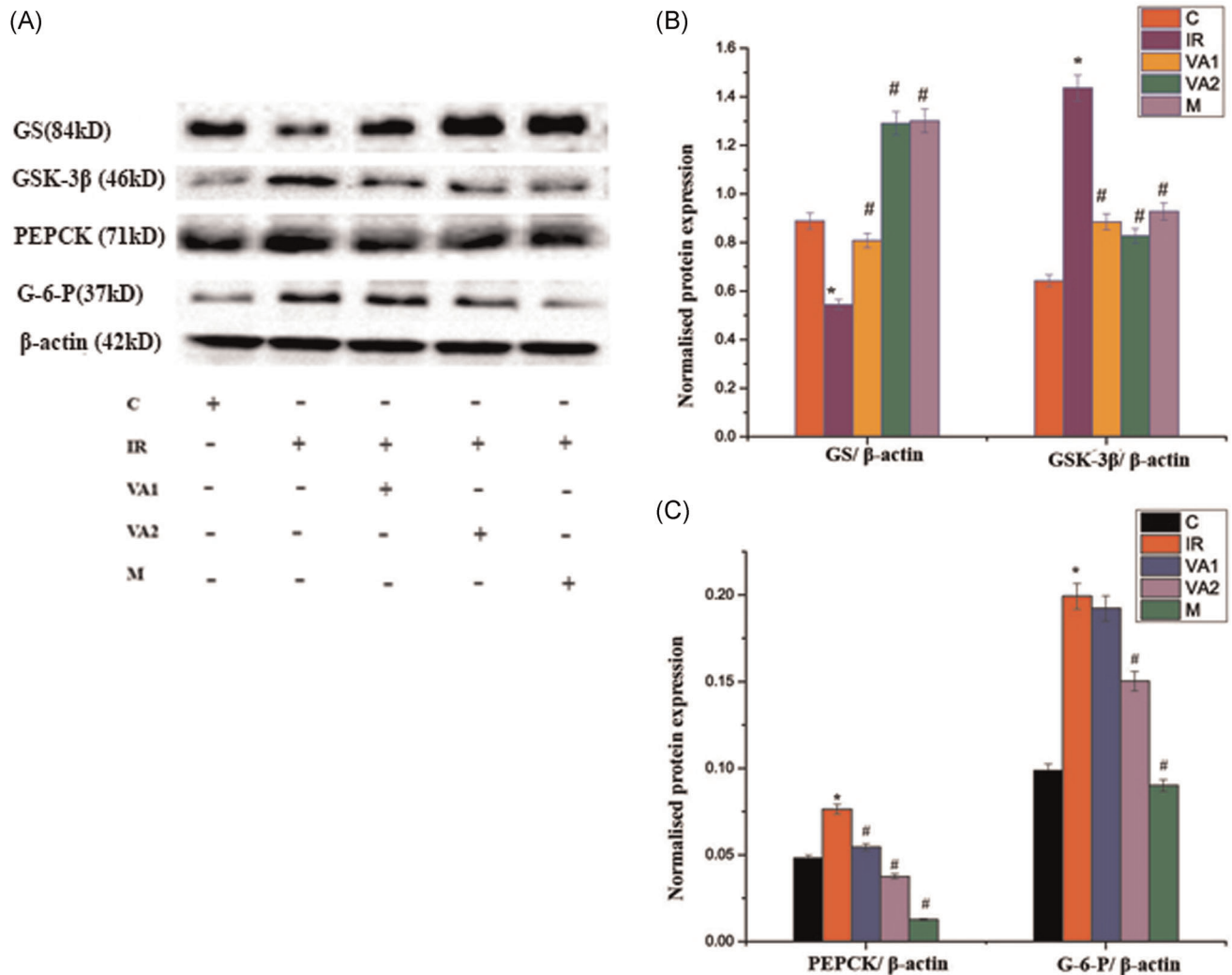


FIGURE 3 Effect of VA on glycogenesis and gluconeogenesis. (A) After VA cotreatment, the cells were lysed and GS, GSK-3 β , PEPCK, G-6-P, and β -actin expression were analyzed by Western blot analysis. (B) Densitometric quantification of GS and GSK-3 β were normalized to β -actin. (C) Densitometric quantification of PEPCK and G-6-P were normalized to β -actin. C, control cells; IR, high insulin-treated insulin-resistant cells; VA1, IR + 5 μ M vanillic acid; VA2, IR + 10 μ M vanillic acid; M, IR + metformin (1 mM). Each value represents the mean \pm SEM, where $n = 6$. *mean value was significantly different from control cells ($p \leq 0.05$). #mean value was significantly different from IR cells ($p \leq 0.05$). GS, glucokinase; GSK-3 β , glycogen synthase kinase-3 β ; G-6-P, glucose 6 phosphate; PEPCK, phosphoenolpyruvate carboxykinase

and decreased the GSK-3 β by 79.1% compared with the IR cells (Figure 3B).

3.3 | GK expression is negatively correlated with hepatic gluconeogenesis

Here, we found that during IR, the expression of PEPCK and G-6-P was significantly increased, 58.7% and 101.7%, respectively, as compared with control. VA cotreatment downregulated the expression of PEPCK by 45.4% at 5 μ M and by 80.5% at 10 μ M ($p \leq 0.05$) compared with IR (Figure 3A,C). Also, VA dose-dependently decreased G-6-P expression by 9% at 5 μ M and by 49% at 10 μ M concentrations as compared with IR cells (Figure 3A,C). Metformin significantly reduced the expression of

both PEPCK and G-6-P by 132.2% and 110.5%, respectively, when compared with IR.

3.4 | GK activation is linked with the hepatic BAD expression

Western blot analysis was performed for GK and BAD protein expression analysis (Figure 4A). IR caused a significant reduction in the expression of GK (69.7%) compared with control cells. VA cotreatment significantly upregulated the GK expression (62.7% and 108.7% for 5 and 10 μ M, respectively; $p \leq 0.05$) compared with IR cells. Metformin group noticeably enhanced (101.2%) the GK levels compared with IR. During IR condition, there was a significant downregulation in the expression of mitochondrial protein BAD by 58.6%

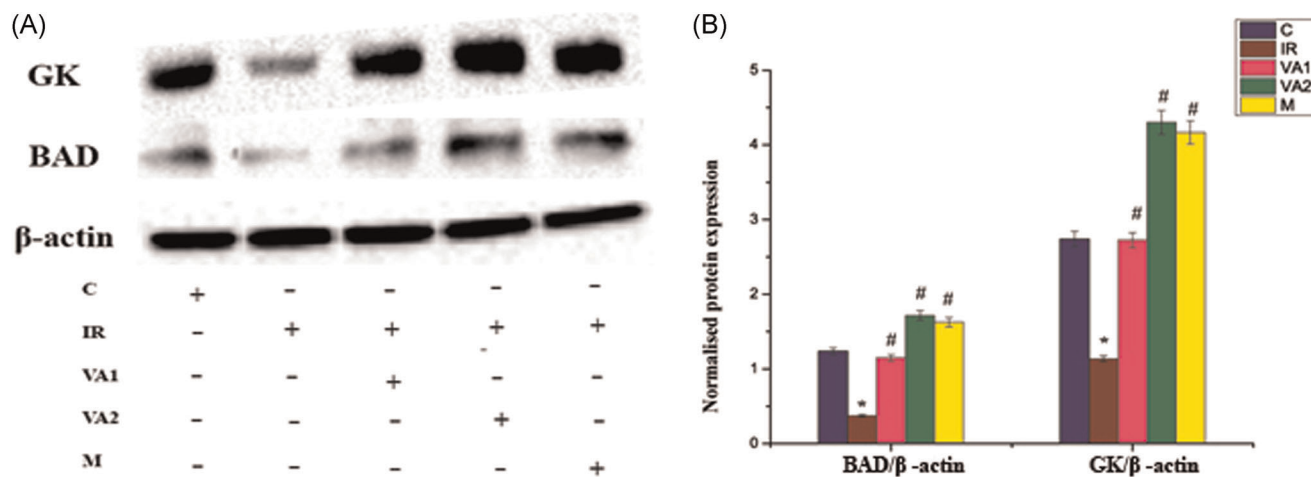


FIGURE 4 Effect of VA on GK and BAD. (A) After treatment with VA, the cells were lysed, and GK, BAD, and β -actin expression were analyzed by Western blotting. (B) Densitometric quantification of GK and BAD were normalized to β -actin. C, control cells; IR, high insulin-treated insulin-resistant cells; VA1, IR + 5 μ M vanillic acid; VA2, IR + 10 μ M vanillic acid; M, IR + metformin (1 mM). The protein contents were normalized by β -actin. Each value represents the mean \pm SEM, where $n = 6$. * indicates that the mean value was significantly different from control cells ($p \leq 0.05$). # indicates that the mean value was significantly different from IR cells ($p \leq 0.05$). BAD, Bcl-2-associated death receptor; GS, glucokinase; GK, glucokinase; VA, vanillic acid

($p \leq 0.05$) as compared with control. VA cotreatment at 5 and 10 μ M significantly ($p \leq 0.05$) upregulated the expression of BAD by 58% and 115.5%, respectively, compared with IR cells. Also, metformin treatment significantly ($p \leq 0.05$) increased the BAD protein by 110.6% compared with IR cells (Figure 4B).

3.5 | Docking of VA to GK

To determine the putative binding mode and potential ligand-target interactions of VA, it was docked to human GK using Autodock v4.2.

The VA was bound to GK with a binding energy of -4.94 kcal/mol, showing a stable binding affinity into the active site of GK (Figure 5A). The amino acid residues of GK interacting with VA was given in Figure 5B. The result of Autodock v4.2 showed that the amino acid residues in the close proximity of affinity pocket leveraged binding of VA to GK through hydrophobic as well as electrostatic interactions (Figure 5B). The amino acid residues of GK involved in the interactions with VA were Glu17, Leu20, Phe23, Gln24, Leu25, Gln26, Arg369, Glu372, Ser373, Val374, Thr376, Arg377, and His380 (Figure 5B). VA was found to form a hydrogen bond with residue Arg369 in the binding pocket of GK.

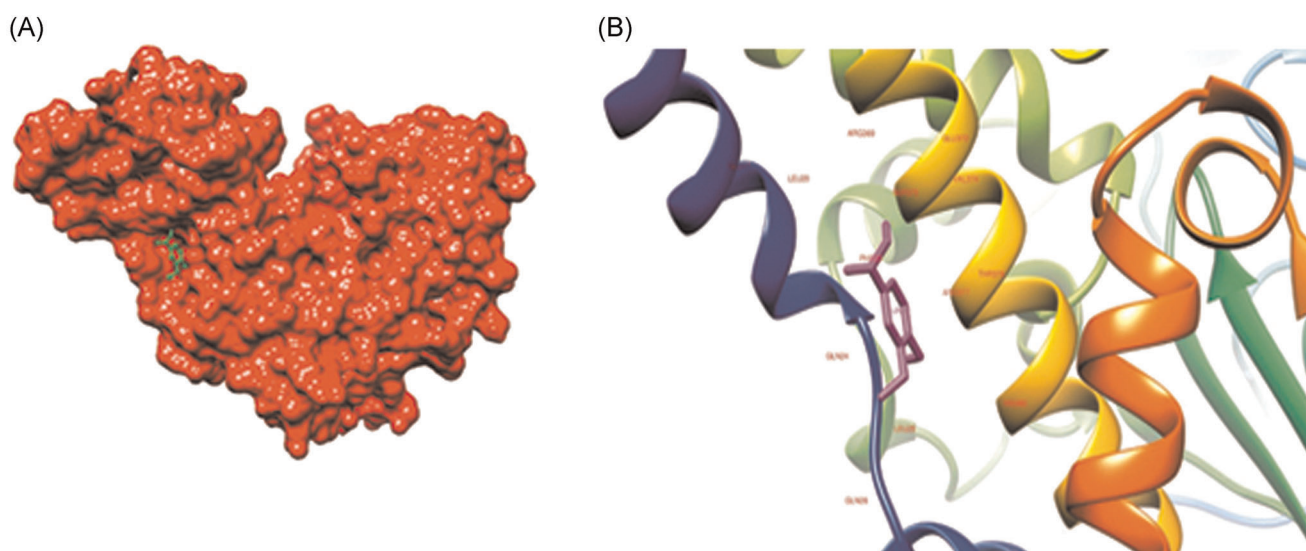


FIGURE 5 Docking model predicted interaction details between VA and GK. (A) Hydrophobicity surface representation of human glucokinase-vanillic acid complex (green stick: vanillic acid). (B) Interacting amino acid residues of glucokinase with vanillic acid. GK, glucokinase; VA, vanillic acid

4 | DISCUSSION

This study deals with alterations in GK activity during hyperinsulinemia in HepG2 cells and amelioration with VA. We also discuss the alteration in glucose metabolism and the role of BAD during this IR condition. GK is the predominant hexokinase expressed in the liver and has a major role in hepatic glucose disposal and glucose output.^[17] There are reports to argue that GK therapy is a more effective preventive measure in T2DM because it is especially important for glucose homeostasis.^[17] Hepatic GK is regulated by an inhibitory protein called GKR that traps GK at basal glucose level.^[17] During the hyperglycemic condition, GK in the liver is activated and activated GK suddenly triggers the disposal of postprandial blood glucose.^[17] In fact, decreased GK enzymatic activity has been reported in patients with T2DM.^[18]

In the human liver, the major quantitative pathway for glucose utilization is glycogen synthesis.^[3] Glucose 6 phosphate is the precursor for glycogen synthesis and is supplied by GK. Animal studies showed that even a small mutation in GK protein level has a noticeable effect on blood glucose homeostasis.^[18] There are reports in diabetic patients; the liver GK activity has been reduced when compared with normal subjects, which suggests that hepatic GK may have a role in T2DM.^[19] During IR condition, the amount of glycogen becomes downregulated by the inhibition of GS enzyme.^[20] We also reported the same result that during IR condition in HepG2 cells, the glycogen level was decreased. The increase in GK was associated with an increase in intracellular levels of glucose 6 phosphate and glycogen.^[21] Increased glucose 6 phosphate allosterically activates GS protein.^[22] Impairment of GK during T2DM decreases glucose 6 phosphate level and subsequently reduces glycogenesis.^[18] Activation of GK would repair glycogen storage in T2DM patients.^[7] Another enzyme that takes part in the glycogen synthesis is GSK-3 β , which inactivates GS and the decreased glycogen stores in the liver.^[23] It is a negative regulator of glycogenesis. Activation of GSK-3 β inhibits the GS enzyme, promotes glycogenolysis, and increases hepatic glucose output. During a diabetic condition, the GSK-3 β level increases.^[21] From our data, it is evident that during an IR condition, the level of GSK-3 β is high, which decreases GS enzyme.

In addition to glucose utilization, the human liver releases glucose to the bloodstream either through glycogenolysis or from gluconeogenesis.^[24,25] The unique ability of this organ to control glucose production and storage is important for maintaining normal blood glucose during fasting or starvation.^[19] These findings underscore the importance of maintaining normal gluconeogenic rates to avoid disease pathophysiology. In patients with T2DM, gluconeogenesis has been identified as the primary source of glucose production, while glycogenolysis was found not to contribute to glucose production.^[26] So next, we investigated the contributors of the HGP during IR in HepG2 cells. Gluconeogenesis is the de novo synthesis of glucose, initiated in the mitochondria from pyruvate, and finally, glucose is generated in the cytosol.^[27] Increased HGP is mainly due to the overexpression of PEPCK and G-6-P.^[28] They are the key players behind gluconeogenesis during T2DM.^[5] PEPCK is the rate

regulator of gluconeogenesis,^[27] it decarboxylates and phosphorylates the oxaloacetate to form phosphoenolpyruvate.^[27,29] After several reverse steps of glycolysis, G-6-P is involved in the final step of glucose generation in the liver. Here, it catalyzes the dephosphorylation of G6P and generates free glucose. Proteins involved in gluconeogenesis and GK action act in the opposite direction, so a coordinated regulation is essential to control the hepatic glucose input and output. We found that IR increased gluconeogenesis through the increased expression of G-6-P and PEPCK levels.

GK is situated in the mitochondria and forms a hetero pentameric complex on the mitochondrial membrane. Among these members, BAD is the critical component of the complex, and it integrates glycolysis and apoptosis via interaction with GK.^[2] The hepatic loss of BAD is linked to reduced glycolysis and enhanced gluconeogenesis. This shows that BAD deficiency is associated with impaired HGP.^[30] When the phosphorylated BAD level increases, it activates GK and promotes glycolysis, and when the BAD level is diminished, it will downregulate glycolysis and enhance gluconeogenesis.^[2] These observations point out that BAD may help the mitochondria to distinguish glycolysis versus gluconeogenesis.^[2] This confirms that GK is an important mechanistic component of BAD modulation in hepatic metabolism. Moreover, BAD's ability to coordinately regulate hepatic energy metabolism and gluconeogenesis is abolished in the absence of GK. This provides evidence of an epistatic relationship between these partner proteins, and GK is a downstream mediator of BAD's metabolic effects.^[2] BAD activates GK and enhances glucose metabolism in the liver and pancreas.^[12] So, we checked the expression level of BAD in IR cells and the effect of VA on it. In IR cells, the BAD level was decreased significantly as compared with control cells. The gluconeogenesis was also significantly higher in IR cells, which facilitates the HGP. This reveals the decreased activity of GS enzyme and reduced glycogenesis. From these findings, we suggest that GK is a downstream mediator of BAD in HepG2 cell's energy metabolism. The link between mitochondria and GK in connection with ATP utilization has already been established.^[1] We have already reported the depletion of ATP and oxygen consumption in our early study (data not shown here). Based on this observation, we postulate that alteration of GK and BAD activity during IR influence general bioenergetics of hepatocytes, such as ATP production and oxygen consumption.

There are reports that hepatic GK activation using phytopharmacologic tools or other agents, such as small allosteric GK activators, can lead to increased glucose utilization, decreased glucose production, and amelioration of the hyperglycemia.^[1,2] But it is also important to exclude the potential risk of hypoglycemia and hyperlipidemia associated with GK activation.^[2] Most of the GK activators are allosteric activators, and they may increase the risk of hypoglycemia and hypertriglyceridemia.^[31,32] Within this context, it is important to note that the mechanism by which the BAD activates GK is distinct from allosteric GK activators,^[33] and BAD mimetic compounds may exclude the side effects and highlight the potential therapeutic utility of these strategies in diabetes and metabolic syndrome. From our data, it is evident that VA is an activator of GK via BAD. Through this mechanism, VA could enhance glycogenesis by

inhibiting gluconeogenesis in IR cells. This was confirmed with our docking data too. According to our docking results, the binding of VA to GK is through hydrophobic and electrostatic interactions. In addition to this, the binding energy for this interaction is -4.94 kcal/mol. This means VA was stably placed in the active site of GK and promotes glucose consumption in hepatocytes. Meanwhile, docking results also revealed that VA formed a hydrogen bond with Arg369 residue in the binding pocket of GK. From these results, it is clear that VA promotes the activation of GK level in IR cells. In addition to this, VA behaves as a potential stimulator of GK through BAD activation. With this unique mode of action, we could say that VA has the potential to act as a new class of GK activators and it may be an interesting phyto molecule for further research for use in T2DM.

5 | CONCLUSION

Overall, this study revealed the potential of VA in the activation of GK level through BAD. Since the mode of action is via BAD-associated nonallosteric interaction, the fear of hypoglycemia associated with GK activation is not here. Thus, we could say that VA may be an ideal molecule to explore for its beneficial properties against diabetic complications.


ACKNOWLEDGMENT

Sreelekshmi Mohan thank the University Grants Commission (UGC, New Delhi, India) for financial assistance to conduct the research. We thank the Director, CSIR-NIIST for providing necessary facilities.

DATA AVAILABILITY STATEMENT

The data that support the findings of this study are available from the corresponding author upon reasonable request.

ORCID

Kozhiparambil Gopalan Raghu  <https://orcid.org/0000-0002-1341-5470>

REFERENCES

- [1] S. M. Sternisha, B. G. Miller, *Arch. Biochem. Biophys.* **2019**, *663*, 199.
- [2] A. Giménez-Cassina, L. Garcia-Haro, C. S. Choi, M. A. Osundiji, E. A. Lane, H. Huang, M. A. Yildirim, B. Szlyk, J. K. Fisher, K. Polak, E. Patton, J. Wiwczar, M. Godes, D. H. Lee, K. Robertson, S. Kim, A. Kulkarni, A. Distefano, V. Samuel, G. Cline, Y. B. Kim, G. I. Shulman, N. N. Danial, *Cell Metab.* **2014**, *19*, 272.
- [3] M. M. Adeva-Andany, N. Pérez-Felpete, C. Fernández-Fernández, C. Donapetry-García, C. Pazos-García, *Biosci. Rep.* **2016**, *36*, 1.
- [4] M. Bollen, S. Keppens, W. Stalmans, *Biochem. J.* **1998**, *336*, 19.
- [5] R. A. Haeusler, S. Camastra, B. Astiarraga, M. Nannipieri, M. Anselmino, E. Ferrannini, *Mol. Metab.* **2015**, *4*, 222.
- [6] E. D. Slosberg, U. J. Desai, B. Fanelli, I. S. Denny, S. Connelly, M. Kaleko, B. R. Boettcher, S. L. Caplan, *Diabetes* **2001**, *50*, 1813.
- [7] J. M. Choi, M. H. Seo, H. H. Kyeong, E. Kim, H. S. Kim, *Proc. Natl. Acad. Sci. U. S. A.* **2013**, *110*, 10171.
- [8] M. Mukhtar, M. Stubbs, L. Agius, *FEBS Lett.* **1999**, *462*, 453.
- [9] C. Shiota, J. Coffey, J. Grimsby, J. F. Grippo, M. A. Magnuson, *J. Biol. Chem.* **1999**, *274*, 37125.
- [10] N. N. Danial, C. F. Gramm, L. Scorrano, C. Y. Zhang, S. Krauss, A. M. Ranger, S. R. Datta, M. E. Greenberg, L. J. Licklider, B. B. Lowell, S. P. Gygi, S. J. Korsmeyer, *Nature* **2003**, *424*, 952.
- [11] R. S. Westphal, S. H. Soderling, N. M. Alto, L. K. Langeberg, J. D. Scott, *EMBO J.* **2000**, *19*, 4589.
- [12] N. N. Danial, L. D. Walensky, C. Y. Zhang, C. S. Choi, J. K. Fisher, A. J. A. Molina, S. R. Datta, K. L. Pitter, G. H. Bird, J. D. Wikstrom, J. T. Deeney, K. Robertson, J. Morash, A. Kulkarni, S. Neschen, S. Kim, M. E. Greenberg, B. E. Corkey, O. S. Shirihai, G. I. Shulman, B. B. Lowell, S. J. Korsmeyer, *Nat. Med.* **2008**, *14*, 144.
- [13] S. H. Kim, *Diabetes Metab.* **2015**, *39*, 468.
- [14] A. Itoh, K. Isoda, M. Kondoh, M. Kawase, A. Watari, M. Kobayashi, M. Tamesada, K. Yagi, *Biol. Pharm. Bull.* **2010**, *33*, 983.
- [15] B. N. Shyamala, M. M. Naidu, G. Sulochanamma, P. Srinivas, *J. Agric. Food Chem.* **2007**, *55*, 7738.
- [16] H. A. Jung, M. Y. Ali, H. K. Bhakta, B. S. Min, J. S. Choi, *Arch. Pharm. Res.* **2017**, *40*, 37.
- [17] L. Agius, *Diabetes* **2009**, *58*, 18.
- [18] P. J. Roach, *Curr. Mol. Med.* **2002**, *2*, 101.
- [19] N. Hariharan, D. Farrelly, D. Hagan, D. Hillyer, C. Arbeeney, T. Sabrah, A. Treloar, K. Brown, S. Kalinowski, K. Mookhtiar, *Diabetes* **1997**, *46*, 11.
- [20] J. M. Irimia, C. M. Meyer, D. M. Segvich, S. Surendran, A. A. DePaoli-Roach, N. Morral, P. J. Roach, *J. Biol. Chem.* **2017**, *292*, 10455.
- [21] H. S. Han, G. Kang, J. S. Kim, B. H. Choi, S. H. Koo, *Exp. Mol. Med.* **2016**, *48*, e218.
- [22] R. M. McDevitt, S. J. Bott, M. Harding, W. A. Coward, L. J. Bluck, A. M. Prentice, *Am. J. Clin. Nutr.* **2001**, *74*, 737.
- [23] N. Mitro, P. A. Mak, L. Vargas, C. Godio, E. Hampton, V. Molteni, A. Kreusch, E. Saez, *Nature* **2007**, *445*, 219.
- [24] A. Adkins, R. Basu, M. Persson, B. Dicke, P. Shah, A. Vella, W. F. Schwenk, R. Rizza, *Diabetes* **2003**, *52*, 2213.
- [25] A. Adina-Zada, T. N. Zeczycki, P. V. Attwood, *Arch. Biochem. Biophys.* **2012**, *519*, 118.
- [26] M. C. Petersen, D. F. Vatner, G. I. Shulman, *Nat. Rev. Endocrinol.* **2017**, *13*, 572.
- [27] R. A. Rizza, *Diabetes* **2010**, *59*, 2697.
- [28] L. Rui, *Compr. Physiol.* **2011**, *4*, 177.
- [29] M. C. Moore, K. C. Coate, J. J. Winnick, Z. An, A. D. Cherrington, *Adv. Nutr.* **2012**, *3*, 286.
- [30] C. B. Newgard, *Cell Metab.* **2012**, *15*, 606.
- [31] G. E. Meininger, R. Scott, M. Alba, Y. Shentu, E. Luo, H. Amin, M. J. Davies, K. D. Kaufman, B. J. Goldstein, *Diabetes Care* **2011**, *34*, 2560.
- [32] T. P. Torres, R. L. Catlin, R. Chan, Y. Fujimoto, N. Sasaki, R. L. Printz, C. B. Newgard, M. Shiota, *Diabetes* **2009**, *58*, 78.
- [33] B. Szlyk, C. R. Braun, S. Ljubcic, E. Patton, G. H. Bird, M. A. Osundiji, F. M. Matschinsky, L. D. Walensky, N. N. Danial, *Nat. Struct. Mol. Biol.* **2014**, *21*, 36.

How to cite this article: Sreelekshmi M., Raghu K.G., *J. Biochem. Mol. Toxicol.* **2021**, e22750.



Vanillic acid retains redox status in HepG2 cells during hyperinsulinemic shock using the mitochondrial pathway

Sreelekshmi Mohan^{a,b}, Genu George^a, K.G. Raghu^{a,b,*}

^a Biochemistry and Molecular Mechanism Laboratory, Agro-Processing and Technology Division, CSIR-National Institute for Interdisciplinary Science and Technology, Thiruvananthapuram, Kerala, 695019, India

^b Academy of Scientific and Innovative Research (AcSIR), Ghaziabad, 201002, India

ARTICLE INFO

Keywords:

Hyperinsulinemia
Reactive oxygen species
Glycation
Mitochondria
HepG2 cells
Angelica sinensis

ABSTRACT

Vanillic acid (VA) is a flavoring and nutritional agent found in many fruits and vegetables. It is an antioxidant but its nutraceutical potential has not been studied in detail. In this study, the potential of VA against hyperinsulinemia mediated changes on redox status and mitochondria in HepG2 cells were investigated. Incubation of cells with 1 μ M insulin for 24 h was found to induce insulin resistance using the inhibition of Glut2 and glucose uptake (51.9%). Hyperinsulinemia caused depletion of superoxide dismutase, glutathione, glutathione peroxidase and generation of reactive oxygen species (68%). It also caused overexpression of the receptor for advanced glycation end products (120%) and a decreases of dolichyl-diphospho-oligosaccharide-protein glycosyltransferase non-catalytic subunit (34%). Mitochondria were affected with alterations in mitochondrial transmembrane potential, aconitase activity, mitochondrial fission and fusion, biogenesis (AMPK, Sirt1 and PGC-1 α) and bioenergetics (ATP and oxygen consumption). Co-treatment with VA decreased oxidative stress by reducing reactive oxygen species and lipid peroxidation during hyperinsulinemia. Similarly, VA protected the mitochondria during insulin shock. VA also prevented glycation through the decrease of the receptor for advanced glycation end products expression. VA was found to act through the AMPK/Sirt1/PGC-1 α pathway to obtain its beneficial activity. From the overall results it was concluded that VA is expected to be a potential nutraceutical which could be explored for the development of affordable nutraceuticals after detailed *in vivo* study.

1. Introduction

Alternative approaches are needed to prevent and treat metabolic diseases such as type 2 diabetes mellitus (T2DM) and associated health issues. Non-pharmacological management with the utilization of herbal dietary products has been an option and further work is needed in the search for culinary plants for prophylactic and therapeutic use. These edible biomaterials have been shown to alleviate complex disorders using nutritional intervention (Choudhury et al., 2018). Functional foods are being developed to manage chronic diseases, such as T2DM and cardiovascular diseases. Some have enhanced antioxidant, anti-inflammatory and insulin sensitivity functions.

Hyperinsulinemia is associated with health complications of diabetes. Insulin resistance (IR) is a major issue with hyperinsulinemia (Marin-Juez et al., 2014). This has been established in animal and human studies (Shanik et al., 2008). Insulin is one of the main hormones

for regulating glucose metabolism (Wilcox, 2005). Circulating levels are controlled by the nutrients involved in glucose uptake, glycolysis and glycogen storage, lipogenesis, and protein synthesis (Czech et al., 2013; Fu et al., 2013). Insulin may also have some autocrine functions like the promotion of β -cell growth and influence its own production and release (Wang et al., 2013). Hyperinsulinemia could enhance the desensitization of the insulin receptor which results in IR (Templeman et al., 2017). Corkey (2012) showed that hyperinsulinemia is the root cause of IR and diabetes. Inhibition of hyperinsulinemia results in the reduction of IR without affecting glucose tolerance including in human studies (Reed et al., 2011). Thus, early recognition of hyperinsulinemia may be helpful to guide earlier intervention strategies to prevent or delay diabetes onset and related chronic diseases. Hyperinsulinemia could alter redox status (Kim et al., 2008) and induce surplus generation of superoxide anions, hydrogen peroxide and hydroxyl radicals (Ge et al., 2008; Li et al., 2015). These effects were reversed using antioxidants such as N-acetyl-cysteine, superoxide dismutase or catalase. Therefore, oxidative

* Corresponding author. Biochemistry and Molecular Mechanism Laboratory, Agro-Processing and Technology Division, CSIR-National Institute for Interdisciplinary Science and Technology, Thiruvananthapuram, 695019, Kerala, India.

E-mail address: raghugopal@niist.res.in (K.G. Raghu).

<https://doi.org/10.1016/j.fbio.2021.101016>

Received 15 December 2019; Received in revised form 17 March 2021; Accepted 18 March 2021

Available online 24 March 2021

2212-4292/© 2021 Elsevier Ltd. All rights reserved.

Abbreviations	
$\Delta\psi_m$	mitochondrial membrane potential
2-DG	2-deoxy-D-glucose
AGE	advanced glycation end products
ALE	advanced lipoxidation end products
AMPK	adenosine monophosphate activated kinase
ANOVA	one-way analysis of variance
ATP	adenosine triphosphate
BSA	bovine serum albumin
DCFH-DA	2,7-dichlorodihydrofluorescein diacetate
DDOST	dolichyl-diphospho-oligosaccharide-protein glycosyltransferase non-catalytic subunit
DMEM	Dulbecco's modified eagle's medium
DMSO	dimethyl sulfoxide
DTNB	5,5'-dithio-bis (2-nitrobenzoic acid)
DTT	dithiothreitol
ECL	enhanced chemiluminescence
EDTA	ethylenediaminetetraacetic acid
EGTA	ethylene glycol tetraacetic acid
FBS	fetal bovine serum
FIS1	fission 1 protein
GLUT2	glucose transporter 2
GPx	glutathione peroxidase
GSH	glutathione
HBSS	Hanks balanced saline solution
HEPES	4-(2-hydroxyethyl)-1-piperazineethanesulfonic acid
HepG2	human hepatocellular carcinoma cells
HI	high insulin
HRP	horseradish peroxidase
IR	insulin resistance
IRS2	insulin receptor substrate 2
JC-1	5,5',6,6'-tetrachloro-1,1',3,3'-tetraethyl-benzimidazol carbocyanine iodide
MDA	malondialdehyde
MES	2-(N-morpholino)ethanesulfonic acid
MTT	3-(4,5-dimethylthiazol-2-yl)-2,5-diphenyltetrazolium bromide
NAC	N-acetyl-cysteine
NADP	nicotinamide adenine dinucleotide phosphate
NCCS	National Centre for Cell Science
OPA1	optic atrophy 1
OS	oxidative stress
p-AMPK	phospho-AMP activated kinase
PBS	phosphate-buffered saline
PGC-1 α	peroxisome proliferator activated receptor γ coactivator-1 α
PVDF	polyvinylidene difluoride
RAGE	receptor for advanced glycation end products
RIPA	radioimmuno precipitation assay
ROS	reactive oxygen species
RT	room temperature
SEM	standard error of the mean
Sirt1	sirtuin 1
SOD	superoxide dismutase
SPSS	Statistical Package for the Social Sciences
T2DM	type 2 diabetes mellitus
TBST	tris buffered saline-Tween 20
VA	vanillic acid

stress (OS) could be a potential interventional target for hyperinsulinemia induced IR and related diseases. Mitochondria are the powerhouse of the cell and involved in important functions of the cell such as regulation of ATP production, redox status and apoptosis. Mitochondrial dysfunction and associated OS are often involved at the start in the genesis of metabolic syndromes. Hyperinsulinemia associated pathologies have been associated with OS and mitochondrial dysfunction but the detailed information needed to design therapeutic strategies based on molecular mechanisms might be beneficial (Gonzalez-Franquesa & Patti, 2017).

Based on the importance of antioxidants in protecting the mitochondria from OS during hyperinsulinemia, vanillic acid (VA) was selected for this study. It is a flavoring agent mainly found in the root of the Chinese medicinal plant *Angelica sinensis*. It is also found in many alcoholic beverages, cereals, dried fruits, nuts and herbs. It is a strong antioxidant (Tai et al., 2012) and anti-lipid-peroxidative agent (Vinoth & Kowsalya, 2018). It is the oxidized form of vanillin and has antibacterial, antimicrobial, and chemopreventive activities (Itoh et al., 2010). Only one report showed that VA protects against hyperinsulinemia and hyperlipidemia by decreasing the serum glucose, triglycerides, and free fatty acids (Chang et al., 2015). Similarly, not much research has been done with hyperinsulinemia induced alterations in redox status associated with mitochondrial dysfunction and glycation in human hepatocellular carcinoma (HepG2) cells. In this study the effects of VA on hyperinsulinemia in HepG2 cells, an *in vitro* model of the hyperinsulinemic insulin resistant liver, was studied.

2. Materials and methods

Dulbecco's modified eagle's medium (DMEM), fetal bovine serum (FBS), penicillin-streptomycin antibiotics (10,000 IU/mL of each) and 0.5% trypsin (porcine pancreas)- ethylenediaminetetraacetic acid

(trypsin-EDTA) were from Gibco-BRL Life Technologies (Waltham, MA, USA). 3-(4,5-Dimethylthiazol-2-yl)-2,5-diphenyltetrazolium bromide (MTT), dimethylsulfoxide (DMSO), radioimmunoprecipitation assay buffer (RIPA buffer), 2,7-dichlorodihydrofluorescein diacetate (DCFH-DA), and VA were from Sigma Aldrich Chemical Co. (St. Louis, MO, USA). Adenosine monophosphate activated kinase (AMPK), phospho-AMPK (p-AMPK), peroxisome proliferator activated receptor γ coactivator-1 α (PGC-1 α), sirtuin 1 (Sirt 1), fission 1 protein (FIS 1), optic atrophy 1 (OPA 1), β -actin and all other secondary antibodies were from Santa Cruz Biotechnology (Dallas, TX, USA). RAGE and DDOST were from Abcam (Cambridge, MA, USA). Metformin, N-acetyl-cysteine (NAC) and amino guanidine were from SRL (Mumbai, India). Recombinant human insulin, MitoSoxTM dye and JC-1 dye were from Merck (Kenilworth, NJ, USA). The remaining chemicals used were of analytical grade from SRL.

2.1. Cell culture

HepG2 cell lines which were purchased from the National Centre for Cell Science (NCCS, Maharashtra, India) were maintained in DMEM supplemented with 10% FBS and antibiotics (100 IU/mL of each penicillin and streptomycin) in a humidified atmosphere with 5% CO₂ at 37 °C.

2.2. Establishment of IR through hyperinsulinemic shock of HepG2 cells

HepG2 cells were seeded in 96-well plates at a density of 2×10^4 cells/well counted using a haemocytometer (Merck) and grown for 24 h to reach 80% confluence. Then the cells were cultured in the presence or absence of different concentrations (50 or 100 nM or 1 μ M) of insulin and parameters relevant to IR (glucose uptake, insulin receptor substrate (IRS) 2, glucose transporter 2 (Glut2)) were studied to confirm the

development of hyperinsulinemia mediated IR in HepG2 cells.

2.2.1. Glucose uptake

Briefly, the cells were incubated with various concentrations of insulin for 24 h. Then glucose uptake was assessed using a glucose uptake colorimetric assay kit (Abcam). The control and hyperinsulinemic group were incubated in 4-(2-hydroxyethyl)-1-piperazineethanesulfonic acid (HEPES) buffered saline (20 mM) containing 10 μ M 2-deoxy-D-glucose (2-DG) at room temperature (RT, 22–28 °C) for 5 min. After two washes the cells were trypsinized by adding 100 μ L of 10 \times trypsin-EDTA and centrifuged at 20,000 \times g (AG-716 rotor, model 7780 high speed refrigerated centrifuge, Kubota Laboratory Centrifuges Co., Tokyo, Japan) for 15 min at 4 °C. The pellets were dissolved in neutralizing buffer (10 μ L), centrifuged at 20,000 \times g for 15 min at 4 °C. The supernatant was collected. Reaction mix A (10 μ L) was mixed with 50 μ L supernatant and incubated for 1 h at RT. Extraction buffer (90 μ L) was added and heated to 90 °C for 40 min. Finally, 12 μ L of neutralizing buffer and 38 μ L of reaction mix B were added. Then the absorbance was measured every 2–3 min at 412 nm (BioTek Synergy 4, BioTek Instruments Corp., Winooski, VT, USA).

2.2.2. Alterations of insulin signaling pathway

The expression of IRS 2 and Glut 2 were visualized using western blotting (for details please see section 2.19).

2.3. Experimental groups to check potential of VA against hyperinsulinemic shock

The experimental groups consisted of control (C), insulin resistant (IR; 1 μ M insulin) cells (IR), IR + 5 μ M VA (VA1), IR +10 μ M VA (VA2), IR+1 mM metformin (M).

2.4. Cell viability with VA

Cell viability was measured using the MTT assay. After 80% confluency they were treated with VA. After 24 h, the medium was replaced with 100 μ L of MTT (0.05 mg/mL) solution and incubated for 3–4 h at 37 °C. The formazan crystals were dissolved in 100 μ L of DMSO and the purple color was measured after 20 min at 570 nm using a microplate reader (BioTek Synergy 4).

2.5. Intracellular ROS

Intracellular ROS levels were measured using DCFH-DA as a probe. DCFH-DA is oxidized by intracellular nonspecific esterases and high level of fluorescence occurs with ROS. Briefly, the cells were incubated with the DCFH-DA (20 μ M) at 37 °C for 20 min. Then fluorescence was measured at an excitation of 488 nm and emission of 525 nm using a fluorescence microplate reader (BioTek Synergy 4). Fluorescent imaging was done using a bioimager system (BD pathway™ Bioimager, BD Biosciences, San Jose, CA, USA). For the conformation, ROS analyses were done with a flow cytometer, by quantifying the fluorescence produced by ROS. The cells after treatment were incubated with DCFH-DA at 37 °C for 20 min. Then the cells were trypsinized as previously and analysed using a flow cytometer FACS Aria™ II (BD Biosciences).

2.6. Superoxide dismutase (SOD) activity

Total SOD activity was assayed using a SOD assay kit (Cayman Chemical, Ann Arbor, MI, USA). For this the cells were homogenized with a Tissue master 125-watt laboratory homogenizer with a 5 mm probe (Omni International, PerkinElmer Co., Kennesaw GA, USA) in cold 20 mM HEPES buffer (1 mM ethylene glycol tetraacetic acid (EGTA), 210 mM mannitol, 70 mM sucrose) and centrifuged at 1500 \times g for 5 min at 4 °C. The supernatant (10 μ L) and standards (bovine erythrocyte SOD) were added to each well containing 200 μ L of diluted

radical detector. Then 20 μ L of diluted xanthine oxidase were added quickly and incubated for 30 min. The absorbance was measured at 450 nm using the microplate reader.

2.7. Activity of glutathione (GSH)

GSH was assayed according to the manufacturer's instructions (Cayman Chemical). After treatments with VA, the cell pellets were dissolved in 2 mL sample buffer. Sample and standard of 50 μ L each were added to corresponding wells. Then 150 μ L of assay cocktail were added and kept in the dark. Then absorbance was measured every 2–3 min at 407 nm for 30 min using the microplate reader.

2.8. Glutathione peroxidase (GPx) determination

This assay measured GPx activity by a coupled reaction with glutathione reductase. The cell pellet was mixed in cold buffer containing 50 mM tris HCl (pH = 5.5), 5 mM ethylenediaminetetraacetic acid (EDTA) and 1 mM dithiothreitol (DTT). Sample (20 μ L), assay buffer (100 μ L) and co-substrate mix (50 μ L) were added to respective wells. Then 20 μ L of cumene hydroperoxide was added to initiate the reaction. The absorbance was measured at 340 nm.

2.9. Antiglycation activity assay

The method of Riya et al. (2015) was used to measure bovine serum albumin (BSA) derived advanced glycation end products (AGE) with slight modifications. VA of different concentrations was added to BSA (10 mg/mL) and glucose (500 mM). Fluorescence of AGE at an excitation/emission wavelengths of 370/440 nm was obtained after 24 h and 7 days using the fluorescence microplate reader. The two results were compared and the percentage inhibition of VA against glycation was measured.

2.10. Analysis of AGE with hyperinsulinemia

The method of Rani et al. (2018) was used to analyze the AGE. Cell samples and a standard (provided with the kit) were added to the AGE conjugate coated ELISA plate provided with the kit. After 10 min incubation at RT, 50 μ L of anti-AGE polyclonal antibody was added and incubated for 1 h. The plate was washed with 250 μ L 1 \times wash buffer. Horseradish peroxidase (HRP) conjugated secondary antibody (100 μ L) was added to the wells and incubated for 1hr at RT. Substrate solution (100 μ L) was added which was followed by the addition of 100 μ L of stop solution and measured immediately at 450 nm using the microplate reader.

2.11. Estimation of malondialdehyde (MDA)

Malondialdehyde levels were measured using a lipid peroxidation assay kit (Cayman Chemical). After treatment with VA the cells were subjected to trypsinization using 1 mL of 10 \times trypsin-EDTA as previously and the cell pellets were sonicated (Elmasonic, Elmasonic S 30 (H), 37 kHz Elma Schmidbauer GmbH, Gottlieb-Daimler, D-78224 Singen, Germany) for 5 s. Sample and standard (100 μ L each) were added to 100 μ L of sodium dodecyl sulfate (SDS). After 1 h of boiling, all the tubes were kept in ice for 10 min to terminate the reaction. After 10 min it was centrifuged at 3600 \times g rpm for 10 min at 4 °C. Then 150 μ L of samples were added into a 96 well plate and then read at 530 nm.

2.12. Mitochondrial superoxide

Mitochondrial superoxide production was evaluated with a MitoSox™ (Merck) kit. The cells were treated with 5 mM mitosox and incubated for 20 min. After three washes with HBSS, the bioimages were visualized using the bioimager system at 514 and 580 nm. Fluorescence

was measured with excitation at 514 nm and emission at 580 nm using the microplate reader.

2.13. Aconitase activity

After treatments, cells were subjected to trypsinization using 1 mL of $10\times$ trypsin-EDTA as previously and centrifugated at $800\times g$ for 10 min at 4°C and the pellet was collected. The cell pellet was resuspended in 1 mL assay buffer. The cell suspension was centrifuged at $20,000\times g$ for 10 min at 4°C . Sample (cell supernatant) of 50 μL was added to the respective wells. Then aconitase nicotinamide adenine dinucleotide phosphate (aconitase NADP) (50 μL) reagent and aconitase isocitrate dehydrogenase solution (50 μL) were added along with 50 μL of substrate. The absorbance was measured at 340 nm for 30 min at 37°C . The change in absorbance/min was determined and reaction rate was calculated. The aconitase activity was calculated as nM.

2.14. Mitochondrial membrane potential ($\Delta\psi\text{m}$)

The method of Anupama et al. (2018) was used. After treatments with VA, the medium was changed and the cells were stained with JC-1 stain (Merck) for 20 min at 37°C . In normal cells, the JC-1 dye accumulates inside the mitochondria and forms JC-1 aggregates and gave a red fluorescence. Distortion of the $\Delta\psi\text{m}$ prevents the dye entry into the mitochondria, as a result JC-1 monomers were formed and produced green fluorescence. The shift of fluorescence was visualized and fluorescence intensity was measured using the fluorescence microplate reader with an excitation 490 and emission wavelength of 530 nm for JC-1 monomers, and the excitation 525 and emission wavelength 590 nm for aggregates.

2.15. Mitochondrial dynamics

The expression levels of fission and fusion proteins were analysed using western blotting (for details please see section 2.19).

2.16. ATP content

ATP levels were measured using the ATP determination assay kit. After treatment with VA the cells were homogenized as previously described with ATP assay buffer. Then 100 μL of $1\times$ somatic cell ATP releasing agent, and 50 μL of ultrapure water provided in the kit were added into 50 μL of sample. A 100 μL aliquot was transferred to the reaction vial with 100 μL of ATP assay mix and kept at RT for 3 min. The amount of light emitted at 560 nm was measured using the microplate reader.

2.17. Oxygen consumption

This oxygen consumption rate assay kit uses a phosphorescent oxygen probe to check oxygen consumption rate. Blank wells were filled with only culture medium. After treatments with VA, the spent medium was replaced with fresh medium. MitoXpress xtra solution (10 μL) was added to all the wells except the blank. Then 100 μL of HS mineral oil (provided with the kit) was added over each well. After that the fluorescence was read at 380 nm (excitation) and 650 nm (emission) kinetically for 150 min using the microplate reader.

2.18. Mitochondrial biogenesis

The expression of proteins like AMPK, p-AMPK, Sirt1 and PGC-1 α were evaluated with western blotting (for details please see section 2.19).

2.19. Western blot

Expression of various proteins of pharmacological and functional importance in glucose transport, glycation and mitochondrial function such as IRS2, GLUT2, RAGE, DDOST, AMPK, p-AMPK, PGC-1 α , Sirt 1, FIS1 and OPA1 were studied using western blotting. Cells were cultured in T-25 flask containing 5 mL DMEM medium and the respective treatments with VA were done as described above. After that the cells were harvested and lysed in lysis buffer with a protease inhibitor cocktail and Triton X 100. Then the lysate was centrifuged at $20,000\times g$ for 15 min at 4°C . The supernatant was collected and protein content was measured and normalized using a Pierce BCA protein assay kit (Thermo Fisher Scientific Co., Waltham, MA, USA) using bovine serum albumin (BSA) as a standard and expressing the results as BSA equivalents. Samples were then run on an SDS-PAGE gel (10%) (BioRad, Hercules, CA, USA), transferred at 25 V for 15 min to polyvinylidene difluoride (PVDF) membrane (a non-reactive thermoplastic fluoropolymer produced using the polymerization of vinylidene difluoride) (Merck) using a trans blot apparatus (BioRad). The samples (25 μL) were loaded into each well. After transfer, the PVDF membrane was blocked with 3% BSA in tris buffered saline-Tween 20 (TBST, pH = 8) for 1 h at RT. After washing with TBST, the membrane was probed with primary antibodies (IRS2, GLUT2, RAGE, DDOST, AMPK, p-AMPK, PGC-1 α , Sirt 1, FIS1 and OPA1, 1:1000 dilution) in TBST and incubated for 2 h at RT with moderate shaking. The membrane was washed three times with TBST for 10 min. HRP-conjugated secondary antibody (1:2000) was added and agitated for 90 min at RT. After three TBST washes, membranes were incubated with enhanced chemiluminescence substrate (ECL substrate) (BioRad) and the proportional thickness of bands measured using Image Lab software in the Chemi Doc system (ChemiDoc MP Imaging System, BioRad) assuming all bands were in the Beer-Lambert law region.

2.20. Statistical analysis

All analyses were carried out with sextuplicates and data are shown as mean \pm standard error of the mean (SEM) for control and treated cells. The normality of the variables were tested using the Kolmogorov Smirnov Z test and the variables were found to be approximately normally distributed. Hence the significance difference between the groups were tested using one-way analysis of variance (ANOVA) and further significantly different pairs ($p \leq 0.05$) were identified using Duncan's multiple comparison test. All calculations were done using the Statistical Package for the Social Sciences for Windows standard version 20 (SPSS Inc., Chicago, IL, USA).

3. Results

3.1. Induction of IR through hyperinsulinemic shock in HepG2 cells

The results of the glucose uptake with different concentrations of insulin treated HepG2 cells are shown in Fig. 1a. The cellular uptake of 2-DG with various concentrations of insulin (50, 100 nM and 1 μM) treated cells was decreased 5.5, 35.4 and 51.9%, respectively, as compared with normal cells. Among these, 100 nM and 1 μM insulin showed significant ($p \leq 0.05$) decreases in glucose uptake. The expression levels of IRS2 and Glut2 were significantly decreased with 1 μM insulin compared to normal (Fig. 1b and c) suggesting that HI (1 μM insulin) significantly affected glucose uptake, insulin sensitivity and develop IR. Insulin (1 μM) was chosen to induce hyperinsulinemic shock in subsequent experiments.

3.2. Cell viability

To select suitable concentration of VA, cell viability was evaluated with 5, 10, 20, 30, 40, 50 and 100 μM for 24 h of incubation. Based on the results 5 and 10 μM were selected for further studies (Fig. 2a).

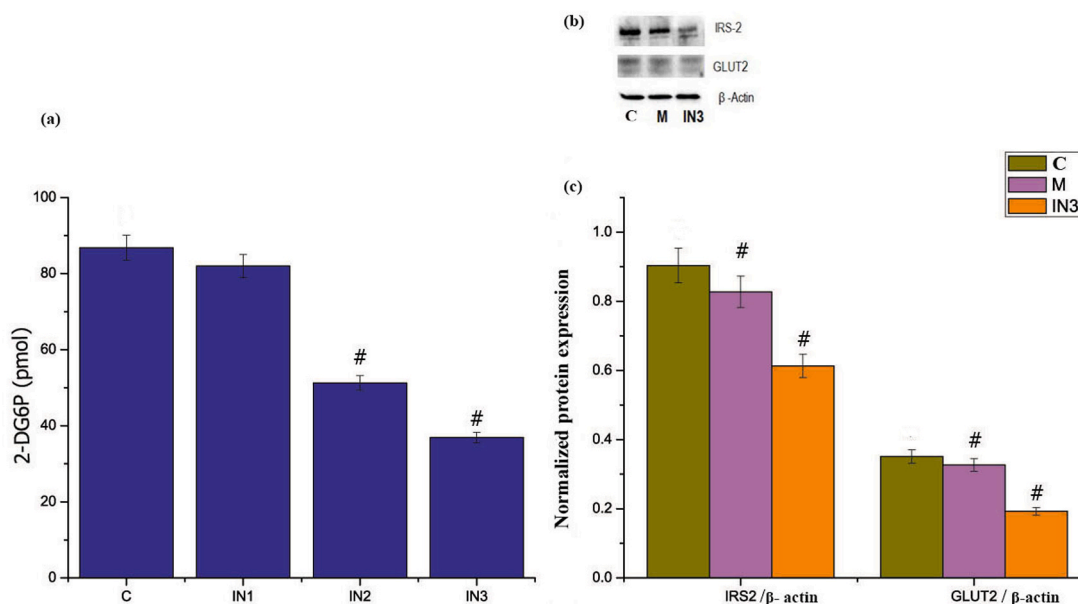


Fig. 1. Induction of IR through hyperinsulinemic shock in HepG2 cells. (a) Glucose uptake. HepG2 cells were incubated in normal medium and different concentrations of insulin for 24 h. C-control; IN1-50 nM insulin; IN2-100 nM insulin; IN3-1 μM insulin. (b) Western blot analysis of insulin receptor substrate (IRS) 2 and glucose transporter (GLUT) 2. (c) Densitometric analysis of IRS 2 and GLUT 2. C-control; M-1 mM metformin; IN3-1 μM insulin. Protein quantification was carried out using densitometric analysis, normalized using an internal control of β-actin. Values are expressed as mean ± SEM where n = 6. # indicates that the mean value was significantly different from control cells ($p \leq 0.05$).

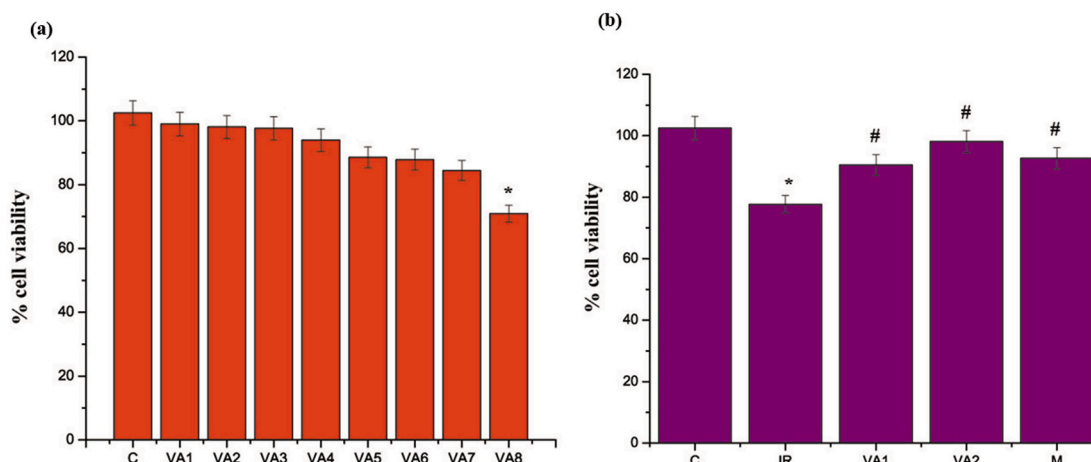


Fig. 2. Cell viability. (a) Cell viability of HepG2 cells incubated in DMEM with 1% FBS and different concentrations of vanillic acid for 24 h. C-control; VA1-5 μM; VA2-10 μM; VA3-20 μM; VA4-30 μM; VA5-40 μM; VA6-50 μM; VA7-100 μM, and VA8-500 μM. (b) Cell viability of 5 and 10 μM vanillic acid and metformin on high insulin treated insulin resistant models (IR). C-control cells; IR-high insulin treated insulin resistant cells; VA1-IR + 5 μM vanillic acid; VA2-IR + 10 μM vanillic acid; M-IR + metformin (1 mM). Values are expressed as mean ± SEM where n = 6. * indicates that the mean value was significantly different from control cells ($p \leq 0.05$). # indicates mean value was significantly different from IR cells ($p \leq 0.05$).

Effect of VA on viability of IR cells were evaluated. Incubation of HepG2 cells with HI for 24 h caused 17.2% cell death that was significant compared to control ($p \leq 0.05$). Co-treatment with 5 and 10 μM of VA and metformin (1 mM) improved (90.5, 98.1 and 92.6%, respectively) viability compared to IR (Fig. 2b).

3.3. Effect of VA on ROS generation

Determination of ROS by both spinning disk fluorescence microscopy and flow cytometry found a surplus generation of ROS in IR. IR showed a significant increase in ROS levels (68%) (Fig. 3a and b) compared to control (Fig. 3a and b). Co-treatment with VA (5 and 10 μM) was significantly ($p \leq 0.05$) effective in preventing ROS formation by 88.2 and 99.6%, respectively, compared to the IR group (Fig. 3a and b). Co-

treatment with metformin and NAC, an antioxidant significantly reduced the ROS generation by 96 and 108%, respectively (Fig. 3a and b). This was also confirmed with cytometry data (Fig. 3c and d) which determined the number of cells that could produce ROS. The IR cells showed a significantly ($p \leq 0.05$) enhanced ROS levels (40.7%) compared to control cells (Fig. 3c and d). Co-treatment with VA (5 and 10 μM concentrations) significantly ($p \leq 0.05$) decreased the ROS levels by 51.3 and 58.3%, respectively, compared with IR cells (Fig. 3c and d). Co-treatment with metformin and NAC significantly reduced the ROS levels 63.3 and 65.5%, respectively, compared to IR treated group (Fig. 3c and d).

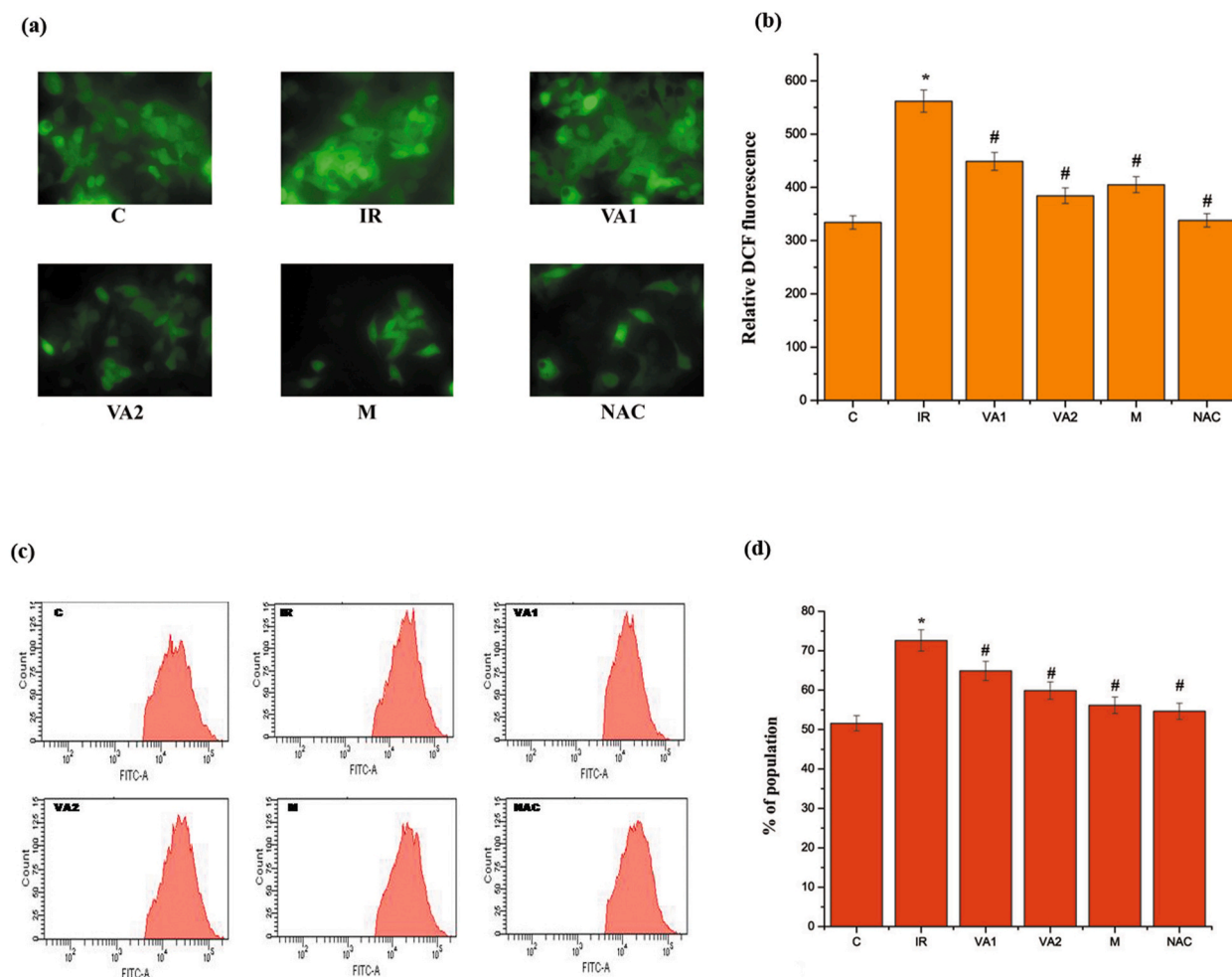


Fig. 3. Intracellular reactive oxygen species generation determined using DCFDA. (a) Fluorescent microscopic images of HepG2 cells stained with DCFDA. (b) Relative fluorescence intensity of DCFDA uptake. (c) Flow cytometric analysis of intracellular ROS generation in different groups. (d) Percentage cell population. C-control cells; IR-high insulin treated insulin resistant cells; VA1-IR + 5 μM vanillic acid; VA2-IR + 10 μM vanillic acid; M-IR + metformin (1 mM); NAC-IR + N-acetyl cysteine (1 mM). Values are expressed as mean ± SEM where n = 6. * indicates that the mean value was significantly different from control cells ($p \leq 0.05$). # indicates mean value was significantly different from IR cells ($p \leq 0.05$).

3.4. Effect of high insulin on SOD levels

Compared to control cells, the activity of SOD was significantly ($p \leq 0.05$) increased in IR treated cells (74.7%). VA co-treatment reduced the SOD activity by 92.2% at 5 μM and by 113% at 10 μM ($p \leq 0.05$) compared with IR (Fig. 4). But metformin significantly ($p \leq 0.05$) improved the SOD activity by 81.2%, respectively.

3.5. GSH levels

Compared to control IR caused a significant ($p \leq 0.05$) drop in GSH level by 31.4%. VA co-treatment at both concentrations (5 and 10 μM) caused a significant ($p \leq 0.05$) increase in GSH levels by 58 and 65.3%, respectively, compared to IR. Metformin significantly improved the GSH level by 85.3% (Fig. 5) compared to IR.

3.6. Level of GPx

GPx activity was decreased in IR by 19.9% compared to control. But VA co-treatment significantly ($p \leq 0.05$) increased the GPx activity by 29.3 (5 μM) and 35.8% (10 μM) compared to IR (Fig. 6). Metformin increased the GPx levels by 42.9%.

3.7. Antiglycation capacity of VA

VA showed a dose-response inhibition of glycation (IC_{50} ; 397 μM). The half maximal inhibitory concentration (IC_{50}) is a measure of the potency of a substance in inhibiting a specific biological or biochemical function. The effect of VA was better than that of the aminoguanidine, as the positive control (IC_{50} ; 500 μM; Fig. 7).

3.8. Production of AGE during high insulin

IR showed an increased level of AGE (221%) as compared to control. While with VA, the formation of AGE was reduced by 232 and 252% for 5 and 10 μM, respectively, with IR. Metformin significantly reduced the AGE levels by 283%. (Fig. 8a).

Western blotting was done for DDOST and RAGE proteins. IR caused a significant increase in the expression of RAGE (120%) compared to control. VA co-treatment significantly decreased the expression of RAGE (147 and 165% for 5 and 10 μM; $p \leq 0.05$) compared to the IR group (Fig. 8b and c). Metformin significantly ($p \leq 0.05$) decreased RAGE levels by 168%. Expression of DDOST was reduced by 34.5% in IR cells compared to control cells. But VA co-treatment at 5 and 10 μM concentrations significantly ($p \leq 0.05$) increased the DDOST protein levels by 56.1 and 63.3%, respectively, compared to IR. Metformin also increased the DDOST levels by 68.9% compared to IR cells (Fig. 8b and

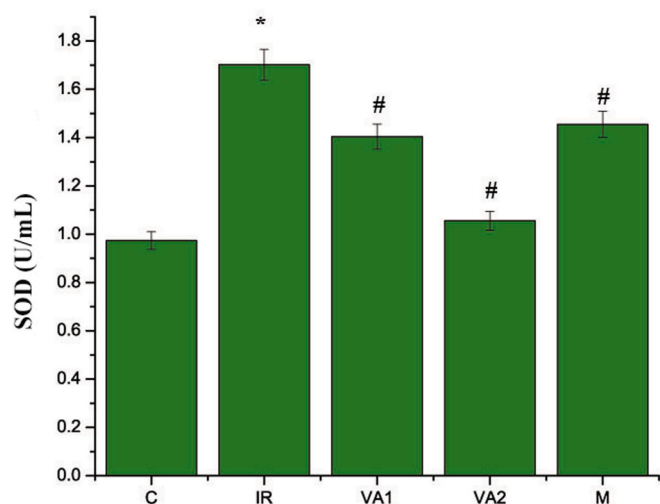


Fig. 4. Activity of SOD during IR. C-control cells; IR-high insulin treated insulin resistant cells; VA1-IR + 5 μ M vanillic acid; VA2-IR + 10 μ M vanillic acid; M-IR + metformin (1 mM). Values are expressed as mean \pm SEM where n = 6. * indicates that the mean value was significantly different from control cells ($p \leq 0.05$). # indicates mean value was significantly different from IR cells ($p \leq 0.05$).

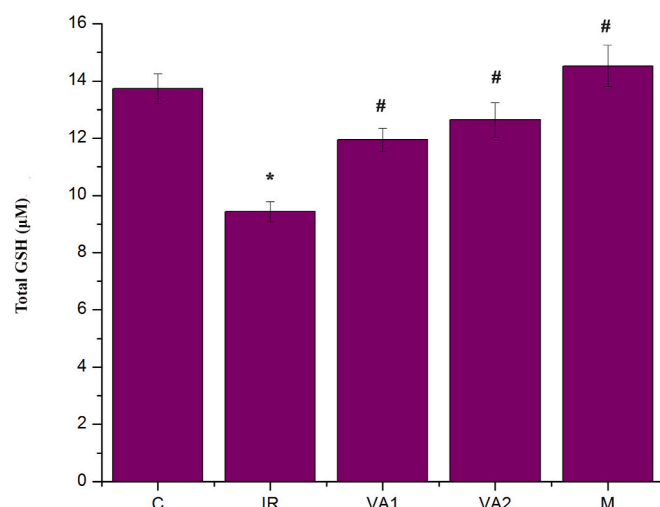


Fig. 5. Total glutathione (GSH) levels. C-control cells; IR-high insulin treated insulin resistant cells; VA1-IR + 5 μ M vanillic acid; VA2-IR + 10 μ M vanillic acid; M-IR + metformin (1 mM). Values are expressed as mean \pm SEM where n = 6. * indicates that the mean value was significantly different from control cells ($p \leq 0.05$). # indicates mean value was significantly different from IR cells ($p \leq 0.05$).

c).

3.9. Lipid peroxidation

Lipid peroxidation was also increased ($p \leq 0.05$) in IR cells by 52.8% (Fig. 9). Co-treatment with VA at 5 and 10 μ M and metformin lowered MDA by 67.6, 78.7 and 87.4%, respectively, compared to IR.

3.10. Effect of VA on mitochondrial superoxide production

Surplus generation of ROS was observed in IR groups (Fig. 10) compared to control. Fluorescence detection also showed an increment of fluorescence in IR cells (143%). VA of both concentrations (5 and 10 μ M) reduced superoxide by 161 and 193%, respectively (Fig. 10).

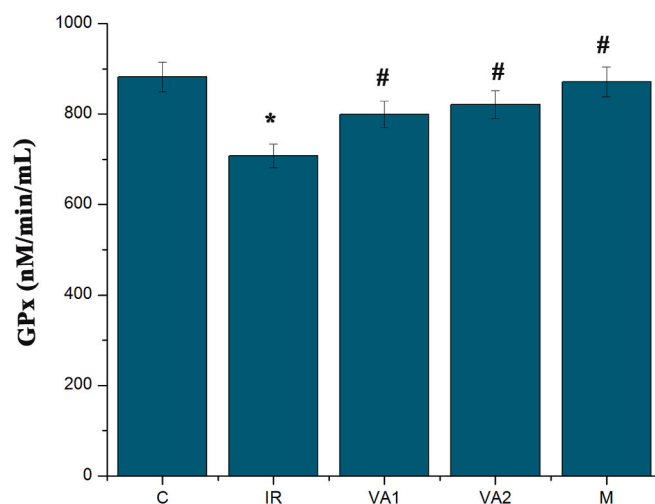


Fig. 6. Glutathione peroxidase (GPx) activity. C-control cells; IR-high insulin treated insulin resistant cells; VA1-IR + 5 μ M vanillic acid; VA2-IR + 10 μ M vanillic acid; M-IR + metformin (1 mM). Values are expressed as mean \pm SEM where n = 6. * indicates that the mean value was significantly different from control cells ($p \leq 0.05$). # indicates mean value was significantly different from IR cells ($p \leq 0.05$).

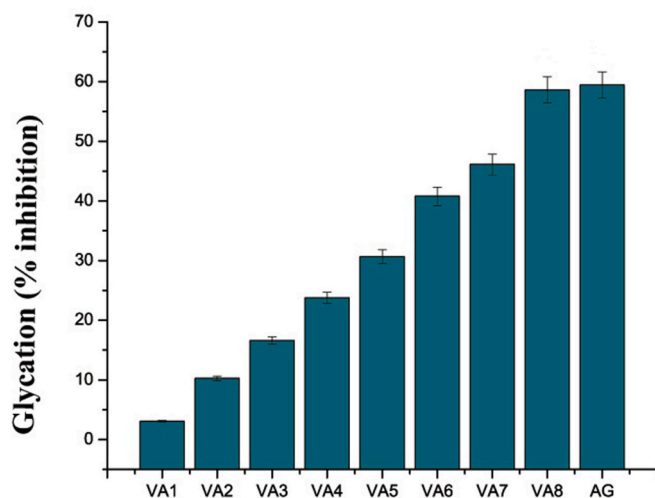


Fig. 7. Antiglycation capacity of vanillic acid. Evaluation of antiglycation effect of vanillic acid; Ex 370 nm, Em 440 nm. Different concentrations of vanillic acid (VA1-5 μ M, VA2-10 μ M, VA3-50 μ M, VA4-100 μ M, VA5-150 μ M, VA6-200 μ M, VA7-250 μ M, VA8-500 μ M) were used, IC_{50} -397 μ M/mL. Amino guanidine (AG) was used as a reference (IC_{50} - 500 μ M). Values are expressed as mean \pm SEM where n = 6.

Compared with metformin (187%) 10 μ M of VA showed better results (Fig. 10).

3.11. Aconitase activity

The aconitase activity was significantly decreased in IR (34%) groups compared to the control. VA (5 and 10 μ M) in a dose dependent manner showed a tendency to increased the enzyme level by 24.2 and 36.6% compared to IR. Co-treatment with metformin significantly increased the aconitase levels by 56.5% compared to IR (Fig. 11).

3.12. Effect of vanillic acid on $\Delta\psi_m$

Analysis of the $\Delta\psi_m$ of mitochondria during IR showed significant

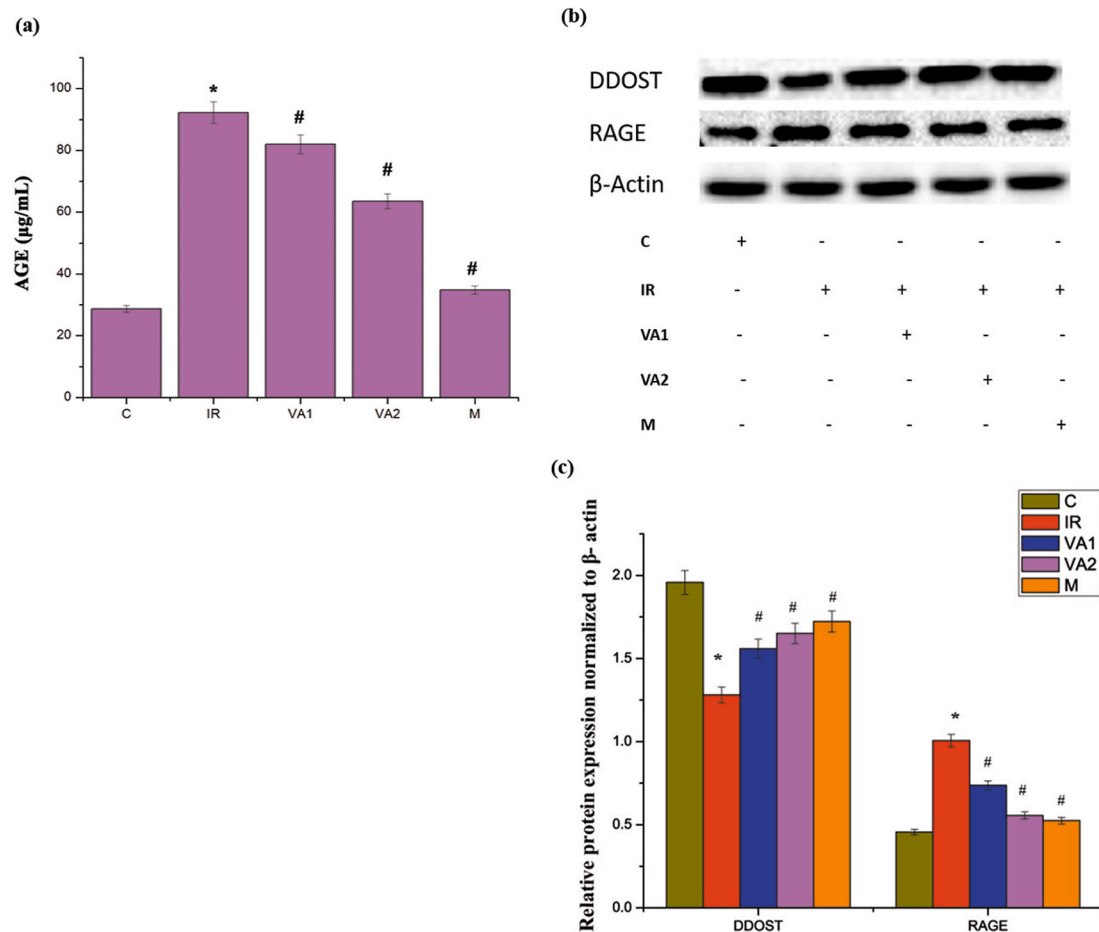


Fig. 8. Production of AGE with high insulin. (a) Quantification of advanced glycated end products (AGE) content. (b) Immunoblot analysis of RAGE and DDOST. (c) Densitometric analysis of protein expression of RAGE and DDOST, normalized to β -actin. C-control cells; IR-high insulin treated insulin resistant cells; VA1-IR + 5 μ M vanillic acid; VA2-IR + 10 μ M vanillic acid; M-IR + metformin (1 mM). Values are expressed as mean \pm SEM where $n = 6$. * indicates that the mean value was significantly different from control cells ($p \leq 0.05$). # indicates mean value was significantly different from IR cells ($p \leq 0.05$). Protein quantification was carried out by densitometric analysis, normalized using β -actin as an internal control.

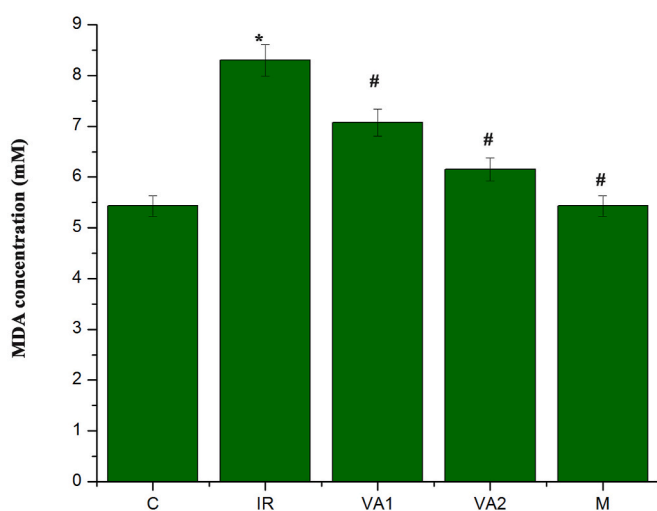


Fig. 9. Lipid peroxidation. Estimation of malondialdehyde (MDA) formation in different groups. C-control cells; IR-high insulin treated insulin resistant cells; VA1-IR + 5 μ M vanillic acid; VA2-IR + 10 μ M vanillic acid; M-IR + metformin (1 mM). Values are expressed as mean \pm SEM where $n = 6$. * indicates that the mean value was significantly different from control cells ($p \leq 0.05$). # indicates mean value was significantly different from IR cells ($p \leq 0.05$).

distortion of $\Delta\psi_m$ compared with control (Fig. 12a). In control cells, the JC-1 dye forms aggregate inside the mitochondrial matrix and emit a red fluorescence due to the potential gradient. Alteration in $\Delta\psi_m$ resulted in the prevention of entry of JC-1 in the mitochondria and resulted in green fluorescence (JC-1 monomers). IR cells showed depolarized $\Delta\psi_m$ as can be seen in Fig. 12a, which had a higher amount of green fluorescence (103%) compared to that of control. VA co-treatment with IR prevented the alteration of $\Delta\psi_m$ which was evident from the significant increase ($p \leq 0.05$) of red fluorescence by 79.9 and 93.9%, respectively, for 5 and 10 μ M of VA compared to IR (Fig. 12b). The quantity of red fluorescence (aggregates) with metformin was improved, and the green fluorescence was decreased by 116% compared to IR (Fig. 12b). Valinomycin was the negative control, and it caused a decrease of the red fluorescence by 40.4% and improved the green fluorescence by 108% compared to control.

3.13. Mitochondrial fission and fusion proteins

During IR condition there was a noticeable decrease in the levels of mitochondrial fusion protein OPA1 by 33.7% ($p \leq 0.05$; Fig. 13a and b) and an up-regulation of fission protein FIS1 by 24.2% (Fig. 13a and b). VA co-treatment at 5 and 10 μ M significantly ($p \leq 0.05$) increased the expression of OPA1 by 52.2 and 60.6%, respectively, and in a dose dependent manner decreased the FIS1 by 92.3 and 109% compared to the IR group. Metformin co-treatment also significantly ($p \leq 0.05$)

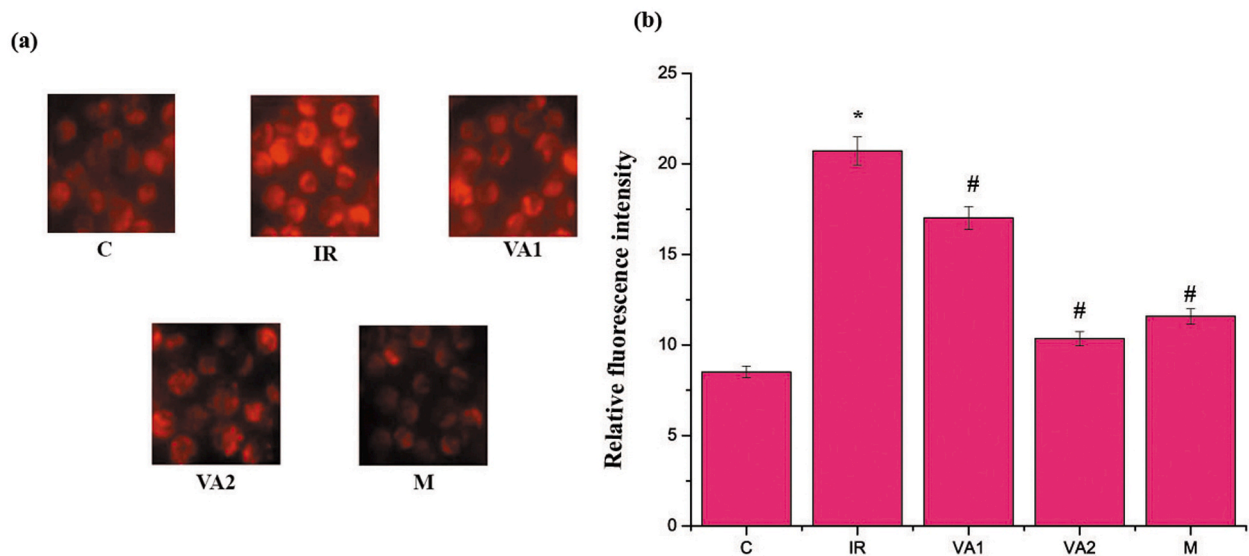


Fig. 10. Effect of vanillic acid on mitochondrial superoxide generation. (a) Mitochondrial superoxide generation determined using MitoSOXTM Red indicator (original magnification 40 \times). (b) Relative fluorescence intensity of confocal images. C-control cells; IR-high insulin treated insulin resistant cells; VA1-IR + 5 μ M vanillic acid; VA2-IR + 10 μ M vanillic acid; M-IR + metformin (1 mM). Values are expressed as mean \pm SEM where n = 6. * indicates that the mean value was significantly different from control cells ($p \leq 0.05$). # indicates mean value was significantly different from IR cells ($p \leq 0.05$).

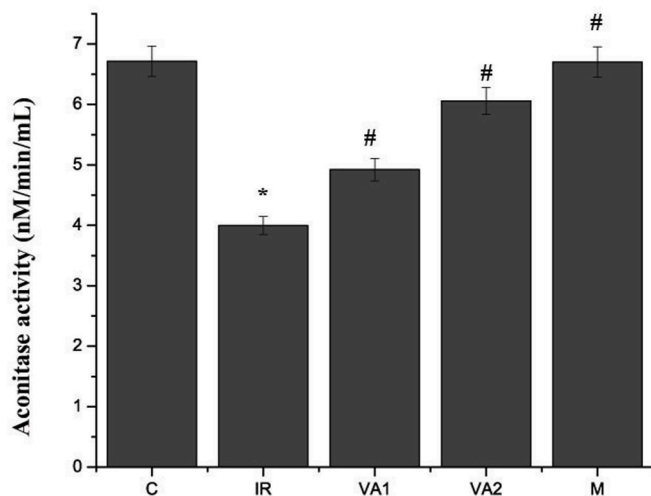


Fig. 11. Aconitase activity. Aconitase enzyme activities in different groups. C-control cells; IR-high insulin treated insulin resistant cells; VA1-IR + 5 μ M vanillic acid; VA2-IR + 10 μ M vanillic acid; M-IR + metformin (1 mM). Values are expressed as mean \pm SEM where n = 6. * indicates that the mean value was significantly different from control cells ($p \leq 0.05$). # indicates mean value was significantly different from IR cells ($p \leq 0.05$).

increased the fusion protein by 58.1% and reduced the fission protein FIS 1 by 81.6% compared to the IR group (Fig. 13a and b).

3.14. ATP levels and oxygen consumption

There was a significant decrease in ATP levels ($p \leq 0.05$, 35.6%; Fig. 14) in IR cells compared to control cells. Co-treatment with VA at both concentrations (5 and 10 μ M) significantly ($p \leq 0.05$) increased the ATP levels by 56.3 and 71.9%, respectively, compared to IR. Metformin also significantly increased the ATP levels by 133% compared with IR.

Oxygen consumption in cells was evaluated by calculating the change in fluorescence for two and a half hr. More changes in

fluorescence represent more usage of oxygen by cells. This, in turn, represented the good metabolic status of cells. With the IR group oxygen consumption rate was reduced (25%) as compared to control. Co-treatment with VA at 5 and 10 μ M significantly ($p \leq 0.05$) improved the oxygen consumption rate by 13.1 and 26.2% compared with IR group (Fig. 15). VA with better oxygen utilization seems to be effective against mitochondrial dysfunction in IR. Metformin also increased the oxygen consumption rate by 29.6% compared to IR.

3.15. Mitochondrial biogenesis regulated by VA

AMPK, PGC-1 α and Sirt1 are the major proteins responsible for mitochondrial biogenesis. The active form of AMPK was determined in various groups using the ratio of p-AMPK to total AMPK. During IR, the expression of p-AMPK/AMPK was decreased significantly by 62.3% compared to control cells whereas VA in a dose dependent manner increased the ratio significantly (193 and 185% for 5 and 10 μ M, respectively) (Fig. 16a and b). Also, VA (5 and 10 μ M) significantly ($p \leq 0.05$) increased the level of PGC-1 α by 50.4 and 71.3%, respectively, compared to the IR group (Fig. 16a and c). In IR the level of PGC-1 α was reduced to 29.5% compared to control as well as there was also a significant decrease in Sirt1 expression in IR cells (31.5%). On the other hand, VA co-treatment at 5 and 10 μ M increased the expression of Sirt1 by 115 and 119%, respectively (Fig. 16a and c). Metformin significantly ($p \leq 0.05$) increased all three proteins (p-AMPK/AMPK, PGC-1 α and Sirt1) involved in mitochondrial biogenesis by 300, 80.6 and 113%, respectively, compared to IR cells (Fig. 16a–c).

4. Discussion

During T2DM pancreatic cells are unable to compensate for the normal blood glucose level even by producing large amounts of insulin (Steneberg et al., 2015). This most often leads to the malfunction of insulin generation, which opens the pathway of hyperinsulinemia related IR (Schofield & Sutherland, 2012). Many studies have shown that hyperinsulinemia and IR are the independent risk factors for the development of T2DM (Facchini et al., 2001; Marin-Juez et al., 2014). Excessive insulin production and IR with hyperinsulinemia are due to

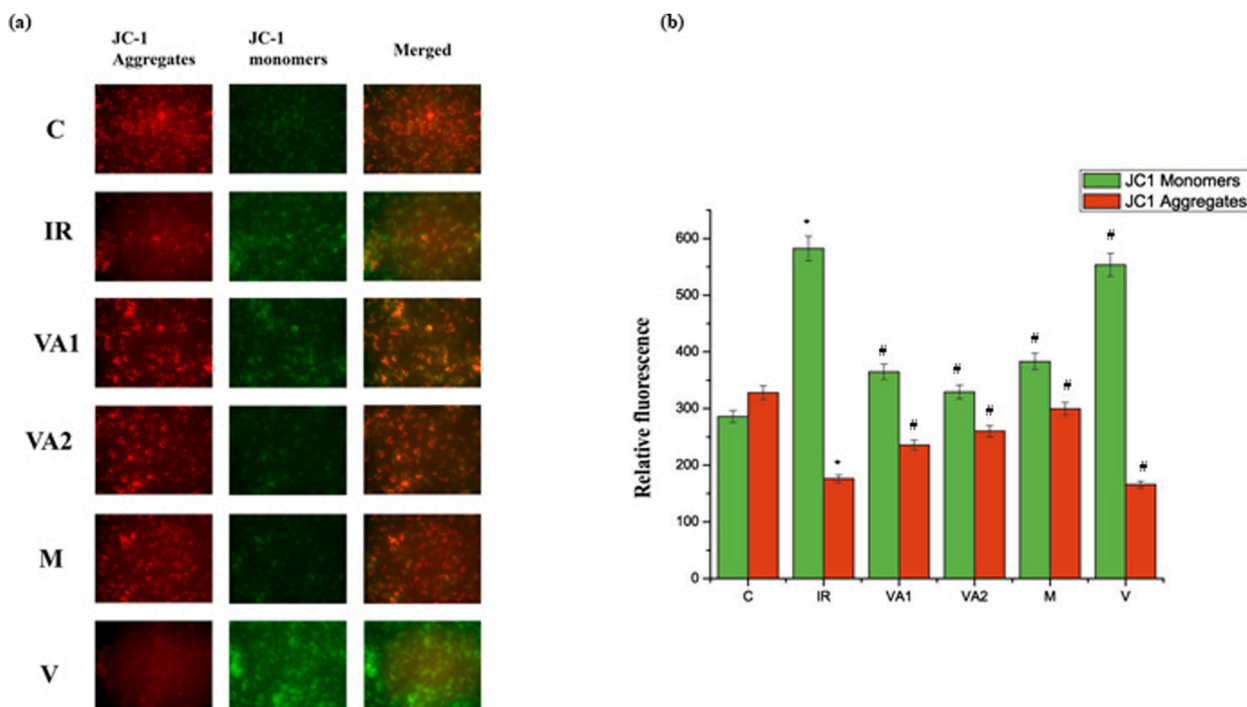


Fig. 12. Mitochondrial transmembrane potential ($\Delta\psi_m$) determined using JC-1 staining. The representative images are merged images of JC-1 aggregates and monomers. JC-1 aggregates in control cells showing intact mitochondria and JC-1 monomers in HI treated cells showing distortion of $\Delta\psi_m$. (a) Alteration in membrane potential in various groups. (b) Relative fluorescent intensity of the fluorescent images. C-control cells; IR-high insulin treated insulin resistant cells; VA1-IR + 5 μ M vanillic acid; VA2-IR + 10 μ M vanillic acid; M-IR + metformin (1 mM). Values are expressed as mean \pm SEM where n = 6. * indicates that the mean value was significantly different from control cells ($p \leq 0.05$). # indicates mean value was significantly different from IR cells ($p \leq 0.05$).

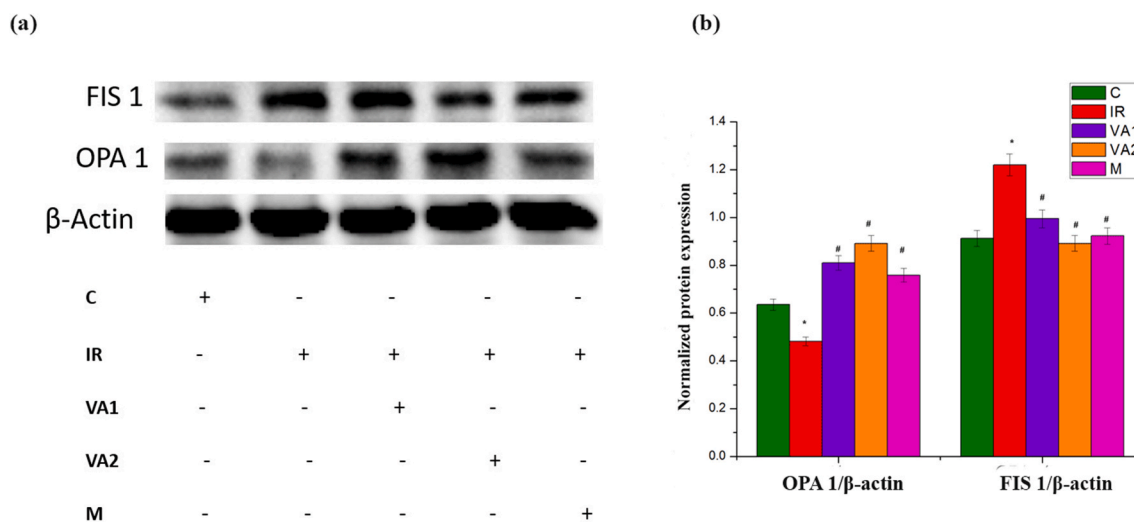


Fig. 13. Immunoblot analysis of proteins involved in mitochondrial fission and fusion (OPA 1 and FIS 1). HepG2 cells treated with high insulin (1 μ M), vanillic acid and metformin for 24 h. (a) Immunoblot of FIS 1 and OPA 1. (b) Densitometric quantification of OPA 1 and FIS 1 normalized to β -actin. C-control cells; IR-high insulin treated insulin resistant cells; VA1-IR + 5 μ M vanillic acid; VA2-IR + 10 μ M vanillic acid; M-IR + metformin (1 mM). Values are expressed as mean \pm SEM where n = 6. * indicates that the mean value was significantly different from control cells ($p \leq 0.05$). # indicates mean value was significantly different from IR cells ($p \leq 0.05$).

the impaired glucose uptake (Crofts et al., 2015). Hyperinsulinemia is not an after-effect of IR, but it is an independent driver of many metabolic consequences and IR is one of them (Shanik et al., 2008).

The liver is the depot for glucose metabolism and also the major clearance site of insulin. Insulin clearance in the liver is through a receptor-mediated mechanism (Michael et al., 2000). The main reasons for the development of hyperinsulinemia and the associated IR is the inhibition of insulin clearance and increased production of defective

insulin (Michael et al., 2000). All these consequences lead to hyperglycemia. Once these pathophysiological conditions are developed these in turn initiate IR (Bazotte et al., 2014). The after-effect in the liver is the up-regulation of hepatic glucose production, lipid accumulation and decreased glucose uptake. The end result is hyperplasia and dysfunction (Michael et al., 2000). Because of the potential role of the liver in glucose metabolism and pathogenesis of T2DM, the role of hyperinsulinemia in HepG2 with more emphasis on redox status alterations

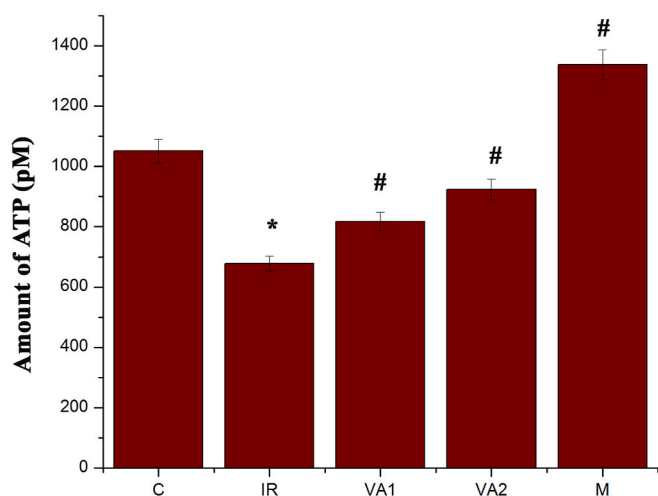


Fig. 14. Level of ATP content in different groups. C-control cells; IR-high insulin treated insulin resistant cells; VA1-IR + 5 μ M vanillic acid; VA2-IR + 10 μ M vanillic acid; M-IR + metformin (1 mM). Values are expressed as mean \pm SEM where n = 6. * indicates that the mean value was significantly different from control cells ($p \leq 0.05$). # indicates mean value was significantly different from IR cells ($p \leq 0.05$).

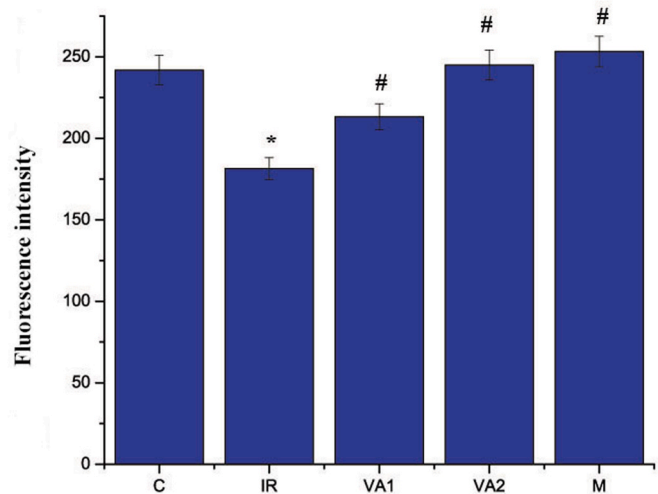


Fig. 15. Oxygen consumption rate in different groups. C-control cells; IR-high insulin treated insulin resistant cells; VA1-IR + 5 μ M vanillic acid; VA2-IR + 10 μ M vanillic acid; M-IR + metformin (1 mM). Values are expressed as mean \pm SEM where n = 6. * indicates that the mean value was significantly different from control cells ($p \leq 0.05$). # indicates mean value was significantly different from IR cells ($p \leq 0.05$).

associated mitochondrial dysfunction were studied.

Insulin (1 μ M) treatment for 24 h induced IR due to hyperinsulinemic shock in HepG2 cells consistent with previous reports (Duraisamy et al., 2003; Jung et al., 2017). This is a good model to study the toxicity of IR on the progression of T2DM and related complications (Yan et al., 2017). The efficacy of insulin-stimulated glucose uptake was also reduced with HI (Fig. 1a). Simultaneously the proteins involved in the insulin signaling pathway were also impaired. For example, HI treatment decreased the IRS 2, and GLUT2 expressions in HepG2 cells as compared to normal (Fig. 1b), suggesting the impairment of the insulin signaling pathway. Besides, with the hyperinsulinemic condition, the OS was developed by increasing the levels of ROS. Hyperinsulinemic shock could also generated IR in HepG2 cells. The effect of hyperinsulinemia on the redox status of HepG2 cells which is essential for maintaining the

normal functional status of cells was the primary focus. In addition, the potential of VA to safeguard redox status during hyperinsulinemic shock was also analysed. Alterations in the innate antioxidant system were seen with IR. Compounds involved in the innate antioxidant system such as SOD, GPx and GSH were studied. The role of hyperinsulinemia in the induction of OS in animals had been reported by Crofts et al. (2015). But no detailed studies dealing with various compounds involved in the innate antioxidant system, lipid peroxidation, mitochondrial dysfunction were found. In the present study, HI significantly increased the SOD and decreased GPx and GSH levels in HepG2 cells. They are the important enzymes for removing oxy-radicals (Ochiai et al., 2008). The increase in SOD during stress conditions might be a compensatory regulatory response in the liver (Li et al., 2015). SOD overexpression might lead to accumulation of H_2O_2 (Fukai & Ushio-Fukai, 2011). GPx is an antioxidant protein, that has an important role in the reduction of H_2O_2 (Espinosa-Diez et al., 2015). The accumulation of increased levels of peroxides inactivates the GPx and increases OS (Miyamoto et al., 2003). GSH is another antioxidant, abundantly seen in the liver and an important determinant of redox signaling (Lu, 2013). During OS, the level of GSH was reduced by decreasing the levels of H_2O_2 and lipid peroxides (Yin et al., 2017).

One of the risk factors associated with OS is glycation. Glycation is one among various pathological complications of diabetes which have a significant role in the induction of micro- and macro-vascular complications (Brownlee, 2000). Increased RAGE and decreased DOST confirmed induction of severe glycation during IR. OS with severe glycation is sufficient to affect carbohydrate, lipid and protein metabolism significantly. These results showed the consequences of HI in HepG2 cells (Hiwatashi et al., 2008). The increased RAGE-AGE axis is the main contributor of hepatic IR in diabetic patients (Yamagishi & Matsui, 2015). Glycation probably acts as an amplifier in the case of IR. In diabetes, almost all proteins undergo glycation and produce AGE (Ahmed, 2005) and insulin is the major protein subjected to glycation and impaired insulin is produced (Song & Schmidt, 2012). Surplus nonfunctional insulin induces IR and damages the pancreas affecting its insulin-producing efficiency (Cerf, 2013).

Overexpression of AGE alters innate antioxidant defence status (Nowotny et al., 2015). Therefore, the enzymes become ineffective in neutralizing the reactive radicals and accelerate the OS observed (Maritim et al., 2003). This was consistent with the current study. Binding of AGE to RAGE generated ROS, which in turn induced lipid peroxidation (Wautier et al., 2003). Lipid peroxidation resulted in the formation of reactive carbonyl intermediates capable of making conformational changes in proteins, thereby leading to advanced lipoxidation end products (ALE). The role of ALE in the pathogenesis of diabetic complications has been established (Williamson & Ido, 2012). Increased AGE can induce lipid peroxidation in diseases like Alzheimer's disease (Gasic-Milenkovic et al., 2003). MDA, a marker of lipid peroxidation with IR was also elevated. MDA is a main lipid peroxidation product and participates in the transcriptional regulation of innate antioxidant enzymes and decreases their production (Kuehne et al., 2015). These results showed that IR induced alterations in redox status of the cell is through the cross-talk between OS, lipid peroxidation and glycation.

Mitochondria are expected to be a prominent component of maintaining the redox status of cells and the epicentre of ROS production. Therefore, the next focus was on mitochondrial function during IR to determine its link with HI induced OS and glycation. The integrity, dynamics and biogenesis, which are the critical functional indicators of mitochondria were studied. Up-regulation of RAGE expression directly induces ROS formation, which alters mitochondrial homeostasis (McKillop et al., 2002). When the intracellular ROS increases, it will upregulate the mitochondrial ROS generation. Therefore, mitochondrial superoxide generation and aconitase enzyme levels were analysed. Compared to normal cells, IR HepG2 cells had increased superoxide generation (Fig. 10) and decreased aconitase level (Fig. 11). Aconitase is

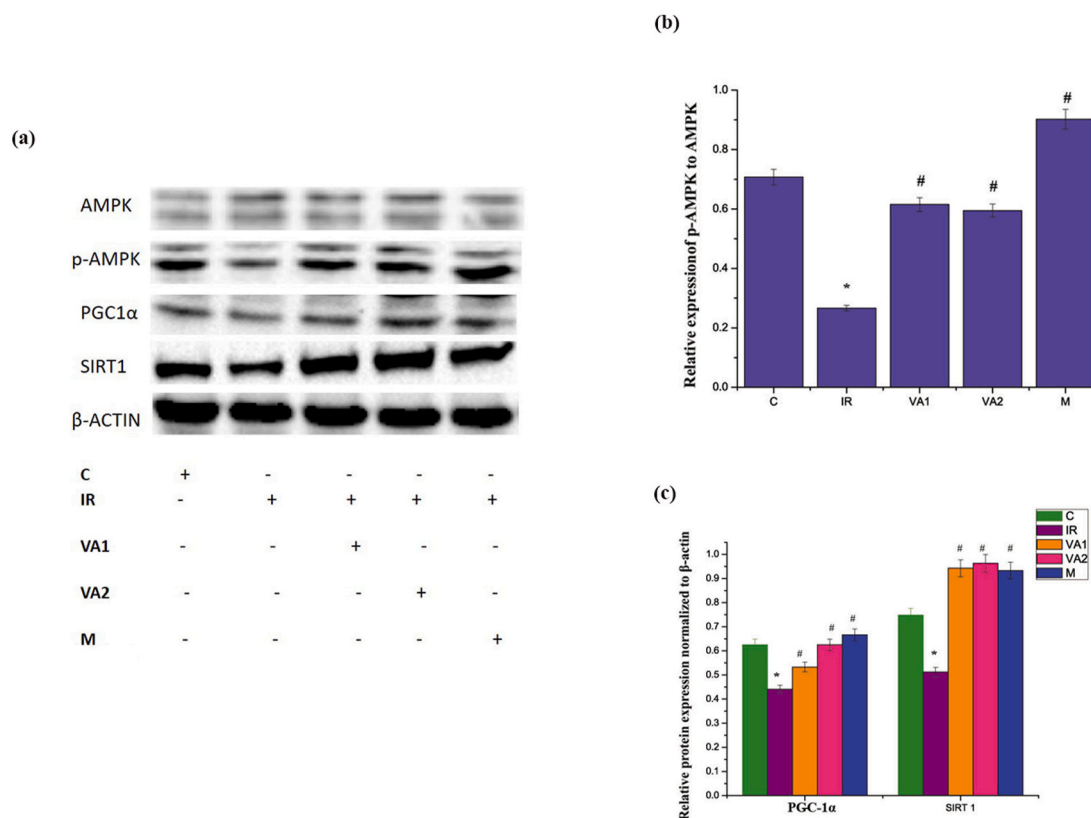


Fig. 16. Immunoblot analysis of proteins involved in mitochondrial biogenesis. (a) AMPK, p-AMPK, PGC-1 α , SIRT1 were analysed using western blotting. (b) Densitometric determination of relative expression of p-AMPK:AMPK. (c) Densitometric analysis PGC-1 α and SIRT1 normalized to β -actin. C-control cells; IR-high insulin treated insulin resistant cells; VA1-IR + 5 μ M vanillic acid; VA2-IR + 10 μ M vanillic acid; M-IR + metformin (1 mM). Values are expressed as mean \pm SEM where n = 6. * indicates that the mean value was significantly different from control cells ($p \leq 0.05$). # indicates mean value was significantly different from IR cells ($p \leq 0.05$). Protein quantification was carried out by densitometric analysis, normalized using an internal control of β -actin.

a mitochondrial protein sensitive to OS (Indo et al., 2007; Tan et al., 2015) and it detoxifies the superoxides through a suicidal inhibition (Green et al., 2004). The significant reduction of aconitase with IR was expected to cause alteration in the redox status in the cells. This results in alterations of the $\Delta\psi_m$ (Skulachev, 1998). $\Delta\psi_m$ is the major participant involved in the regulation of ROS production (Rauscher et al., 2001) and an important marker of mitochondrial integrity (Mathur et al., 2000). When the electrochemical potential difference generated by the proton gradient across the inner mitochondrial membrane is high, the lifetime of superoxide generating intermediates is increased (Korshunov et al., 1997; Zorov et al., 2014). In the present study compared to normal cells, the hyperinsulinemic model had an altered $\Delta\psi_m$. Distortion of mitochondrial dynamics towards fission along with an increase in fission proteins and dissipation of $\Delta\psi_m$ indicated poor mitochondrial health (Dorn, 2015). The loss of $\Delta\psi_m$ leads to proteolysis and degradation of mitochondrial fusion proteins (Youle & Narendra, 2011) and also increased the fission rates (Van der Bliek et al., 2013). Hyperinsulinemia results in an overexpression of fission proteins such as FIS1 and down-regulation of fusion protein such as OPA1 leading to enhanced mitochondrial fission. Reduced expression of OPA1 was linked to the distortion of mitochondrial function (Tang, 2016) and up-regulation of FIS1 resulted in mitochondrial fragmentation (Mao et al., 2018). This results in nonfunctional fragmented mitochondria in the cytoplasm. Balanced mitochondrial dynamics is important for the normal functioning of mitochondria and energy generation (Mao et al., 2018), and it is controlled by the fission and fusion balance (Rovira-Llopis et al., 2017).

The increase of mitochondrial oxidants could lead to severe IR developing in most of the tissues (Fazakerley et al., 2018). AGE initiated numerous deleterious effects on mitochondrial respiration and energy

homeostasis (Neviere et al., 2016). In addition, $\Delta\psi_m$ provides the driving force for ATP synthesis in mitochondria. When the mitochondria lose their $\Delta\psi_m$, the ATP production decreased simultaneously (Van der Bliek et al., 2013). The current study showed a significant decrease in ATP generation in hyperinsulinemic HepG2 cells. Several studies showed that accumulation of glycated mitochondrial proteins significantly influences the mitochondrial function by decreasing the oxygen consumption (Ghosh et al., 2011). To check respiration in mitochondria, basal oxygen consumption rates have been measured (Hartman et al., 2014). Ailing cells with mitochondrial dysfunction showed a decreased rate of oxygen utilization. A reduced oxygen consumption rate was observed in IR HepG2 cells.

Defective mitochondrial dynamics and imbalanced redox status affected mitochondrial biogenesis (Handy & Loscalzo, 2012). Therefore, the alterations of the important proteins in mitochondrial biogenesis were measured. The genes responsible for the regulation of mitochondrial biogenesis are AMPK, Sirt1 and PGC-1 α . AMPK is a protein kinase and it has an important role in the improvement of insulin sensitivity in insulin-resistant individuals (Jeon, 2016; Zhao et al., 2016) by stimulation of downstream genes like sirt1 and PGC-1 α (Austin et al., 2011). Sirt1 is a member of the family of sirtuins and an upstream activator of PGC-1 α through AMPK activation (Austin et al., 2011; Zhu et al., 2010). PGC-1 α is considered as the master controller of mitochondrial biogenesis and the antioxidant defence system (Valle et al., 2005). IR cells had a decreased ratio of phosphorylated to total AMPK, decreased PGC-1 α , and sirt1. These showed imbalances in mitochondrial biogenesis in the HI treated cells and that begins the process of IR development. IR decreased the sirt1, AMPK and PGC-1 α expression and altered the mitochondrial homeostasis and enhanced OS (Choi et al., 2014).

Like metformin VA co-treatment during hyperinsulinemia was

effective in maintaining the redox status of HepG2 cells to a certain extent. Most of the physiologically and pharmacologically relevant parameters altered by HI were restored with VA. These results confirmed the nutraceutical potential of VA for a broad range of pathologies, including hyperinsulinemia associated complications. These beneficial effects of VA were mainly due to its antioxidant activity. VA protects mice from OS induced complications (Amin et al., 2017), restores the antioxidant enzymes in tissues of diabetic hypertensive rats (Vinothiya & Ashokkumar, 2017), inhibits the OS by increasing antioxidant enzymes and decreases mitochondrial damage in human umbilical vein endothelial cells (Ma et al., 2019). In addition, it has cardioprotective effects in myocardial infarcted rats (Prince et al., 2015) and reduces lipid peroxidation (Chou et al., 2010). In addition to its antioxidant and associated effects, it is also beneficial in safeguarding mitochondria with various pathological states. VA protects mitochondrial dynamics and biogenesis, mitochondrial bioenergetics and mitochondrial integrity during hyperinsulinemic shock. The antiglycation property of VA, will have a significant role in the development of VA-based nutraceuticals. All these beneficial properties of VA could be utilized for the development of functional foods/nutraceuticals for the control and management of IR mediated complications mainly in T2DM after detailed *in vivo* study.

5. Conclusions

Hyperinsulinemia altered the redox status of HepG2 cells by glycation, mitochondrial dysfunction, depletion of innate antioxidant status and lipid peroxidation. VA reduced adverse biochemical effects induced by hyperinsulinemia in HepG2 cells by the AMPK and PGC-1 α signaling pathways. Its potential antioxidant and antiglycation property also contributed to its beneficial activities. Detailed *in vivo* and preclinical studies are needed before recommending applications for hyperinsulinemia in humans.

Author statement

Sreelekshmi Mohan conducted the experiments, collected, analyzed and interpreted the data and she wrote the first draft of the manuscript. Dr. Genu George edited the manuscript. Dr. K.G. Raghu designed work plan, concept, interpreted the data, contributed intellectual content.

Declaration of competing interest

The authors declare that they have no known competing interests or personal relationships that could have appeared to influence the work reported in this paper.

Acknowledgements

Sreelekshmi Mohan thanks the University Grants Commission (UGC, New Delhi, India) for financial assistance to conduct the research. Genu George thanks the Science and Engineering Research Board (SERB, New Delhi, India) for her financial assistance.

References

- Ahmed, N. (2005). Advanced glycation endproduct-Role in pathology of diabetic complications. *Diabetes Research and Clinical Practice*, *67*, 3–21.
- Amin, F. U., Shah, S. A., & Kim, M. O. (2017). Vanillic acid attenuates β 1-42-induced oxidative stress and cognitive impairment in mice. *Scientific Reports*, *7*, 1–15.
- Anupama, N., Rani, M. P., Shyni, G. L., & Raghu, K. G. (2018). Glucotoxicity results in apoptosis in H9c2 cells via alteration in redox homeostasis linked mitochondrial dynamics and polyol pathway and possible reversal with cinnamic acid. *Toxicology in Vitro*, *53*, 178–192.
- Austin, S., Klimcakova, E., & St-Pierre, J. (2011). Impact of PGC-1 α on the topology and rate of superoxide production by the mitochondrial electron transport chain. *Free Radical Biology and Medicine*, *51*, 2243–2248.
- Bazotte, R. B., Silva, L. G., & Schiavon, F. P. (2014). Insulin resistance in the liver: Deficiency or excess of insulin? *Cell Cycle*, *13*, 2494–2500.
- Brownlee, M. (2000). Negative consequences of glycation. *Metabolism*, *49*, 9–13.
- Cerf, M. E. (2013). Beta cell dysfunction and insulin resistance. *Frontiers in Endocrinology*, *4*, 1–12.
- Chang, W. C., Wu, J. S., Chen, C. W., Kuo, P. L., Chien, H. M., Wang, Y. T., et al. (2015). Protective effect of vanillic acid against hyperinsulinemia, hyperglycemia and hyperlipidemia via alleviating hepatic insulin resistance and inflammation in high-fat diet (HFD)-fed rats. *Nutrients*, *7*, 9946–9959.
- Choi, J., Chandrasekaran, K., Inoue, T., Muragundla, A., & Russell, J. W. (2014). PGC-1 α regulation of mitochondrial degeneration in experimental diabetic neuropathy. *Neurobiology of Disease*, *64*, 118–130.
- Choudhury, H., Pandey, M., Hua, C. K., Mun, C. S., Jing, J. K., Kong, L., et al. (2018). An update on natural compounds in the remedy of diabetes mellitus: A systematic review. *Journal of Traditional and Complementary Medicine*, *8*, 361–376.
- Chou, T. H., Ding, H. Y., Hung, W. J., & Liang, C. H. (2010). Antioxidative characteristics and inhibition of α -melanocyte-stimulating hormone-stimulated melanogenesis of vanillin and vanillic acid from *Origanum vulgare*. *Experimental Dermatology*, *19*, 742–750.
- Corkey, B. E. (2012). Banting lecture 2011: Hyperinsulinemia: Cause or consequence? *Diabetes*, *61*, 4–13.
- Crofts, C. A. P., Zinn, C., Wheldon, M., & Schofield, G. (2015). Hyperinsulinemia: A unifying theory of chronic disease. *Diabetes*, *1*, 34–43.
- Czech, M. P., Tencerova, M., Pedersen, D. J., & Aouadi, M. (2013). Insulin signalling mechanisms for triacylglycerol storage. *Diabetologia*, *56*, 949–964.
- Duraisamy, Y., Gaffney, J., Slevin, M., Smith, C. A., Williamson, K., & Ahmed, N. (2003). Aminosalicic acid reduces the antiproliferative effect of hyperglycaemia, advanced glycation end products and glycated basic fibroblast growth factor in cultured bovine aortic endothelial cells: Comparison with aminoguanidine. *Vascular Biochemistry*, *246*, 143–153.
- Espinosa-Diez, C., Miguel, V., Mennerich, D., Kietzmann, T., Sánchez-Pérez, P., Cadenas, S., et al. (2015). Antioxidant responses and cellular adjustments to oxidative stress. *Redox Biology*, *6*, 183–197.
- Facchini, F. S., Hua, N., Abbasi, F., & Reaven, G. M. (2001). Insulin resistance as a predictor of age-related diseases. *Journal of Clinical Endocrinology & Metabolism*, *86*, 3574–3578.
- Fazakerley, D. J., Minard, A. Y., Krycer, J. R., Thomas, K. C., Stöckli, J., Harney, D. J., et al. (2018). Mitochondrial oxidative stress causes insulin resistance without disrupting oxidative phosphorylation. *Journal of Biological Chemistry*, *293*, 7315–7328.
- Fu, Z., Gilbert, R. E., & Liu, D. (2013). Regulation of insulin synthesis and secretion and pancreatic beta-cell dysfunction in diabetes. *Current Diabetes Reviews*, *9*, 25–53.
- Fukai, T., & Ushio-Fukai, M. (2011). Superoxide dismutases: Role in redox signaling, vascular function, and diseases. *Antioxidants and Redox Signaling*, *15*, 1583–1606.
- Gasic-Milenkovic, J., Dukic-Stefanovic, S., Deuther-Conrad, W., Gärtner, U., & Münch, G. (2003). β -Amyloid peptide potentiates inflammatory responses induced by lipopolysaccharide, interferon- γ and 'advanced glycation end products' in a murine microglia cell line. *European Journal of Neuroscience*, *17*, 813–821.
- Ge, X., Yu, Q., Qi, W., Shi, X., & Zhai, Q. (2008). Chronic insulin treatment causes insulin resistance in 3T3-L1 adipocytes through oxidative stress. *Free Radical Research*, *42*, 582–591.
- Ghosh, A., Bera, S., Ray, S., Banerjee, T., & Ray, M. (2011). Methylglyoxal induces mitochondria-dependent apoptosis in sarcoma. *Biochemistry (Moscow)*, *76*, 1164–1171.
- Gonzalez-Franquesa, A., & Patti, M. E. (2017). Insulin resistance and mitochondrial dysfunction. *Mitochondrial Dynamics in Cardiovascular Medicine*, *982*, 465–520.
- Green, K., Brand, M. D., & Murphy, M. P. (2004). Prevention of mitochondrial oxidative damage as a therapeutic strategy in diabetes. *Diabetes*, *53*, S110–S118.
- Handy, D. E., & Loscalzo, J. (2012). Redox regulation of mitochondrial function. *Antioxidants and Redox Signaling*, *16*, 1323–1367.
- Hartman, M. L., Shirihai, O. S., Hollbrook, M., Xu, G., Kocherla, M., Shah, A., et al. (2014). Relation of mitochondrial oxygen consumption in peripheral blood mononuclear cells to vascular function in type 2 diabetes mellitus. *Vascular Medicine*, *19*, 67–74.
- Hiwatashi, K., Ueno, S., Abeyama, K., Kubo, F., Sakoda, M., Maruyama, I., et al. (2008). A novel function of the receptor for advanced glycation end-products (RAGE) in association with tumorigenesis and tumor differentiation of HCC. *Annals of Surgical Oncology*, *15*, 923–933.
- Indo, H. P., Davidson, M., Yen, H. C., Suenaga, S., Tomita, K., Nishii, T., et al. (2007). Evidence of ROS generation by mitochondria in cells with impaired electron transport chain and mitochondrial DNA damage. *Mitochondrion*, *7*, 106–118.
- Itoh, A., Isoda, K., Kondoh, M., Kawase, M., Watari, A., Kobayashi, M., et al. (2010). Hepatoprotective effect of syringic acid and vanillic acid on CCl4-induced liver injury. *Biological and Pharmaceutical Bulletin*, *33*, 983–987.
- Jeon, S. M. (2016). Regulation and function of AMPK in physiology and diseases. *Experimental & Molecular Medicine*, *48*(e245), 1–13.
- Jung, H. A., Ali, M. Y., Bhakta, H. K., Min, B. S., & Choi, J. S. (2017). Prunin is a highly potent flavonoid from *Prunus davidiana* stems that inhibits protein tyrosine phosphatase 1B and stimulates glucose uptake in insulin-resistant HepG2 cells. *Archives of Pharmacological Research*, *40*, 37–48.
- Kim, J. A., Wei, Y., & Sowers, J. R. (2008). Role of mitochondrial dysfunction in insulin resistance. *Circulation Research*, *102*, 401–414.
- Korshunov, S. S., Skulachev, V. P., & Starkov, A. A. (1997). High protonic potential actuates a mechanism of production of reactive oxygen species in mitochondria. *FEBS Letters*, *416*, 15–18.
- Kuehne, A., Emmert, H., Soehle, J., Winnefeld, M., Fischer, F., Wenck, H., et al. (2015). Acute activation of oxidative pentose phosphate pathway as first-line response to oxidative stress in human skin cells. *Molecular Cell*, *59*, 359–371.

- Li, W., Cao, L., Han, L., Xu, Q., & Ma, Q. (2015). Superoxide dismutase promotes the epithelial-mesenchymal transition of pancreatic cancer cells via activation of the H2O2/ERK/NF- κ B axis. *International Journal of Oncology*, *46*, 2613–2620.
- Lu, S. C. (2013). Glutathione synthesis. *Biochimica et Biophysica Acta (BBA) - General Subjects*, *1830*, 3143–3153.
- Ma, W. F., Duan, X. C., Han, L., Zhang, L. L., Meng, X. M., Li, Y. L., et al. (2019). Vanillic acid alleviates palmitic acid-induced oxidative stress in human umbilical vein endothelial cells via adenosine monophosphate-activated protein kinase signaling pathway. *Journal of Food Biochemistry*, *e12893*, 1–10.
- Mao, Y. X., Cai, W. J., Sun, X. Y., Dai, P. P., Li, X. M., Wang, Q., et al. (2018). RAGE-dependent mitochondria pathway: A novel target of silibinin against apoptosis of osteoblastic cells induced by advanced glycation end products. *Cell Death & Disease*, *9*, 1–14.
- Marin-Juez, R., Jong-Raadsen, S., Yang, S., & Spink, H. P. (2014). Hyperinsulinemia induces insulin resistance and immune suppression via Ptpn6/Shp1 in zebrafish. *Journal of Endocrinology*, *222*, 229–241.
- Maritim, A. C., Sanders, A., & Watkins, J. B., III (2003). Diabetes, oxidative stress, and antioxidants: A review. *Journal of Biochemical and Molecular Toxicology*, *17*, 24–38.
- Mathur, A., Hong, Y., Kemp, B. K., Barrientos, A. A., & Erusalimsky, J. D. (2000). Evaluation of fluorescent dyes for the detection of mitochondrial membrane potential changes in cultured cardiomyocytes. *Cardiovascular Research*, *46*, 126–138.
- McKillop, A. M., Abdel-Wahab, Y. H., Mooney, M. H., O'Harte, F. P., & Flatt, P. R. (2002). Secretion of glycated insulin from pancreatic beta-cells in diabetes represents a novel aspect of beta-cell dysfunction and glucose toxicity. *Diabetes & Metabolism*, *28*, 3861–3869.
- Michael, M. D., Kulkarni, R. N., Postic, C., Previs, S. F., Shulman, G. I., Magnuson, M. A., et al. (2000). Loss of insulin signaling in hepatocytes leads to severe insulin resistance and progressive hepatic dysfunction. *Molecular Cell*, *6*, 87–97.
- Miyamoto, Y., Koh, Y. H., Park, Y. S., Fujiwara, N., Sakiyama, H., Misonou, Y., et al. (2003). Oxidative stress caused by inactivation of glutathione peroxidase and adaptive responses. *Biological Chemistry*, *384*, 567–574.
- Neviere, R., Yu, Y., Wang, L., Tessier, F., & Boulanger, E. (2016). Implication of advanced glycation end products (AGE) and their receptor (RAGE) on myocardial contractile and mitochondrial functions. *Glycoconjugate Journal*, *33*, 607–617.
- Nowotny, K., Jung, T., Höhn, A., Weber, D., & Grune, T. (2015). Advanced glycation end products and oxidative stress in type 2 diabetes mellitus. *Biomolecules*, *5*, 194–222.
- Ochiai, Y., Kaburagi, S., Okano, Y., Masaki, H., Ichihashi, M., Funasaka, Y., et al. (2008). A Zn (II)-glycine complex suppresses UVB-induced melanin production by stimulating metallothionein expression. *International Journal of Cosmetic Science*, *30*, 105–112.
- Prince, P. S. M., Dhanasekar, K., & Rajakumar, S. (2015). Vanillic acid prevents altered ion pumps, ions, inhibits Fas-receptor and caspase mediated apoptosis-signaling pathway and cardiomyocyte death in myocardial infarcted rats. *Chemico-Biological Interactions*, *232*, 68–76.
- Rani, M. P., Anupama, N., Sreelekshmi, M., & Raghu, K. G. (2018). Chlorogenic acid attenuates glucotoxicity in H9c2 cells via inhibition of glycation and PKC α up-regulation and safeguarding innate antioxidant status. *Biomedicine & Pharmacotherapy*, *100*, 467–477.
- Rauscher, F. M., Sanders, R. A., & Watkins, J. B., III (2001). Effects of coenzyme Q10 treatment on antioxidant pathways in normal and streptozotocin-induced diabetic rats. *Journal of Biochemical and Molecular Toxicology*, *15*, 41–46.
- Reed, M. A., Pories, W. J., Chapman, W., Pender, J., Bowden, R., Barakat, H., et al. (2011). Roux-en-Y gastric bypass corrects hyperinsulinemia implications for the remission of type 2 diabetes. *Journal of Clinical Endocrinology & Metabolism*, *96*, 2525–2531.
- Riya, M. P., Antu, K. A., Pal, S., Chandrakanth, K. C., Anilkumar, K. S., Tamrakar, A. K., et al. (2015). Antidiabetic property of *Aerva lanata* (L.) Juss. ex Schult. is mediated by inhibition of alpha glucosidase, protein glycation and stimulation of adipogenesis. *Journal of Diabetes*, *7*, 548–561.
- Rovira-Llopis, S., Bañuls, C., Diaz-Morales, N., Hernandez-Mijares, A., Rocha, M., & Victor, V. M. (2017). Mitochondrial dynamics in type 2 diabetes: Pathophysiological implications. *Redox Biology*, *11*, 637–645.
- Schofield, C. J., & Sutherland, C. (2012). Disordered insulin secretion in the development of insulin resistance and type 2 diabetes. *Diabetic Medicine*, *29*, 972–979.
- Shanik, M. H., Xu, Y., Škrha, J., Dankner, R., Zick, Y., & Roth, J. (2008). Insulin resistance and hyperinsulinemia: Is hyperinsulinemia the cart or the horse? *Diabetes Care*, *31*, S262–S268.
- Skulachev, V. P. (1998). Uncoupling: New approaches to an old problem of bioenergetics. *Biochimica et Biophysica Acta (BBA) - Bioenergetics*, *1363*, 100–124.
- Song, F., & Schmidt, A. M. (2012). Glycation and insulin resistance: Novel mechanisms and unique targets? *Arteriosclerosis, Thrombosis, and Vascular Biology*, *32*, 1760–1765.
- Steneberg, P., Sykaras, A. G., Backlund, F., Straseviciene, J., Söderström, I., & Edlund, H. (2015). Hyperinsulinemia enhances hepatic expression of the fatty acid transporter Cd36 and provokes hepatosteatosis and hepatic insulin resistance. *Journal of Biological Chemistry*, *290*, 19034–19043.
- Tai, A., Sawano, T., & Ito, H. (2012). Antioxidative properties of vanillic acid esters in multiple antioxidant assays. *Bioscience Biotechnology and Biochemistry*, *76*, 314–318.
- Tang, B. L. (2016). Sirt1 and the mitochondria. *Molecules and Cells*, *39*, 87–95.
- Tan, M., Tang, C., Zhang, Y., Cheng, Y., Cai, L., Chen, X., et al. (2015). SIRT1/PGC-1 α signaling protects hepatocytes against mitochondrial oxidative stress induced by bile acids. *Free Radical Research*, *49*, 935–945.
- Templeman, N. M., Skovso, S., Page, M. M., Lim, G. E., & Johnson, J. D. (2017). A causal role for hyperinsulinemia in obesity. *Journal of Endocrinology*, *232*, R173–R183.
- Valle, I., Álvarez-Barrientos, A., Arza, E., Lamas, S., & Monsalve, M. (2005). PGC-1 α regulates the mitochondrial antioxidant defense system in vascular endothelial cells. *Cardiovascular Research*, *66*, 562–573.
- Van der Blik, A. M., Shen, Q., & Kawajiri, S. (2013). Mechanisms of mitochondrial fission and fusion. *Cold Spring Harbor Perspectives in Biology*, *5*, 1–16.
- Vinothiya, K., & Ashokkumar, N. (2017). Modulatory effect of vanillic acid on antioxidant status in high fat diet-induced changes in diabetic hypertensive rats. *Biomedicine & Pharmacotherapy*, *87*, 640–652.
- Vinoth, A., & Kowsalya, R. (2018). Chemopreventive potential of vanillic acid against 7, 12-dimethylbenz (a) anthracene-induced hamster buccal pouch carcinogenesis. *Journal of Cancer Research and Therapeutics*, *14*, 1285–1290.
- Wang, M., Li, J., Lim, G. E., & Johnson, J. D. (2013). Is dynamic autocrine insulin signaling possible? A mathematical model predicts picomolar concentrations of extracellular monomeric insulin within human pancreatic islets. *PLoS One*, *8*, 1–10.
- Wautier, M. P., Massin, P., Guillausseau, P. J., Huijberts, M., Levy, B., Boulanger, E., et al. (2003). N-(carboxy methyl) lysine as a biomarker for microvascular complications in type 2 diabetic patients. *Diabetes & Metabolism*, *29*, 44–52.
- Wilcox, G. (2005). Insulin and insulin resistance. *Clinical Biochemist Reviews*, *26*, 19–39.
- Williamson, J. R., & Ido, Y. (2012). Linking diabetic complications to sorbitol oxidation, oxidative stress and metabolic suppression. *Journal of Diabetes & Metabolism*, *3*, 2–15.
- Yamagishi, S. I., & Matsui, T. (2015). Role of receptor for advanced glycation end products (RAGE) in liver disease. *European Journal of Medical Research*, *20*, 1–7.
- Yan, F., Chen, Y., Azat, R., & Zheng, X. (2017). Mulberry anthocyanin extract ameliorates oxidative damage in HepG2 cells and prolongs the lifespan of *Caenorhabditis elegans* through MAPK and Nrf2 pathways. *Oxidative Medicine and Cellular Longevity*, *2017*, 1–12.
- Yin, L., Mano, J. I., Tanaka, K., Wang, S., Zhang, M., Deng, X., et al. (2017). High level of reduced glutathione contributes to detoxification of lipid peroxide-derived reactive carbonyl species in transgenic Arabidopsis overexpressing glutathione reductase under aluminum stress. *Physiologia Plantarum*, *161*, 211–223.
- Youle, R. J., & Narendra, D. P. (2011). Mechanisms of mitophagy. *Nature Reviews Molecular Cell Biology*, *12*, 9–14.
- Zhao, M., Yuan, Y., Bai, M., Ding, G., Jia, Z., Huang, S., et al. (2016). PGC-1 α overexpression protects against aldosterone-induced podocyte depletion: Role of mitochondria. *Oncotarget*, *7*, 12150–12162.
- Zhu, H. R., Wang, Z. Y., Zhu, X. L., Wu, X. X., Li, E. G., & Xu, Y. (2010). Icaritin protects against brain injury by enhancing SIRT1-dependent PGC-1 α expression in experimental stroke. *Neuropharmacology*, *59*, 70–76.
- Zorov, D. B., Juhaszova, M., & Sollott, S. J. (2014). Mitochondrial reactive oxygen species (ROS) and ROS-induced ROS release. *Physiological Reviews*, *94*, 909–950.



Endoplasmic reticulum stress: A master regulator of metabolic syndrome

Sreelekshmi Mohan^{a,b}, Preetha Rani M. R^{a,b}, Lindsay Brown^c, Prathapan Ayyappan^d,
Raghu K. G^{a,b,*}

^a Biochemistry and Molecular Mechanism Laboratory, Agroprocessing and Technology Division, CSIR-National Institute for Interdisciplinary Science and Technology, Industrial Estate, Thiruvananthapuram, 695019, Kerala, India

^b Academy of Scientific & Innovative Research (AcSIR), New Delhi, India

^c School of Health and Wellbeing/Functional Foods Research Group, University of Southern Queensland, Toowoomba, QLD, 4350, Australia

^d Department of Surgery-Transplant, University of Nebraska Medical Center, Omaha, NE, USA

ARTICLE INFO

Keywords:

ER stress
Unfolded protein response
Diabetes
Obesity
Cardiovascular diseases
Liver

ABSTRACT

Endoplasmic reticulum (ER) stress, a change in the ER homeostasis, leads to initiation of the unfolded protein response (UPR). The primary functions of the UPR are to restore the ER's physiological activity and coordinate the apoptotic and adaptive responses. Pathophysiological conditions that augment ER stress include hypoxia, misfolded and/or mutated protein accumulation, and high glucose. Prolonged ER stress is a critical factor in the pathogenesis of metabolic syndrome including type 2 diabetes mellitus, cardiovascular diseases, atherosclerosis, obesity, and fatty liver disease. UPR is a complex homeostatic pathway between newly synthesized proteins and their maturation, although the regulatory mechanisms contributing to the UPR and the possible therapeutic strategies are yet to be clarified. Therefore, a comprehensive understanding of the underlying molecular mechanisms is necessary to develop therapeutic interventions targeting ER stress response. In this review, we discuss the role of ER stress and UPR signaling in the pathogenesis of metabolic syndrome, highlighting the main functions of UPR components. We have emphasized the use of novel small molecular chemical chaperones, considered as modulators of ER stress. The initial studies with these chemical chaperones are promising, but detailed studies are required to define their efficacy and adverse effects during therapeutic use in humans.

1. Introduction

Endoplasmic reticulum (ER) is a well-developed membrane network as the largest organelle in the cell, which is present throughout the cytoplasm, more specifically in the endoplasm (Schwarz and Blower, 2016). It is an extra-nuclear space and provides temporary shelter for unmodified polypeptides. Nascent proteins that require maturation process enter into this specialized organelle. It is of two types, nuclear and peripheral ER. Nuclear ER consists of two sheets of a membrane, an outer and inner layer with a lumen between them. These two membranes are joined only at the nuclear pores (Voeltz et al., 2002). The leading role of nuclear ER is the synthesis of proteins and their translocation into nuclear space (Anderson and Hetzer, 2008). Peripheral ER is composed of tubules and rough sheets. Depending upon the diverse functions, the ratios of tubules and sheets change from cell to cell. Protein folding is the primary function of the ER, implemented with chaperones and folding proteins. Sometimes in the ER lumen, the nascent polypeptides are matured by disulfide bonds and undergo N-

glycosylation (Schroder and Kaufman, 2005). After maturation, the proteins are exported to Golgi, and the unfolded proteins are directed to ER-associated degradation (ERAD) followed by proteasomal attack (Boden, 2009). ERAD machinery consists of a molecular trimmer called ER mannosidase I and an ER degradation enhancing α -mannosidase-like protein (EDEEM) (Marciniak and Ron, 2006). Another important function of the ER is the storage of calcium (Ca^{2+}) and its signaling. The Ca^{2+} concentrations in the ER are very high and regulated by the sarco/endoplasmic reticulum calcium ATPase (SERCA) pump. Other main functions of ER include biosynthesis of lipids, cholesterol, phospholipids, and ceramides (Ron and Walter, 2007). Two major enzymes, HMG CoA reductase and serine palmitoyltransferase, are located on the ER membrane (Li et al., 2004). HMG CoA reductase is one of the major proteins participating in cholesterol synthesis and serine palmitoyltransferase is involved in *de novo* ceramide synthesis. The low cholesterol to phospholipid ratio and low free fatty acid (FFA) content make the ER membranes one of the most viscous layers in the cell (Cnop et al., 2012). During the depletion of cholesterol in the body, the ER-

* Corresponding author. Biochemistry and Molecular Mechanism Laboratory, Agroprocessing and Technology Division, CSIR-National Institute for Interdisciplinary Science and Technology, Industrial Estate, Thiruvananthapuram, 695019, Kerala, India.

E-mail address: raghugopal@niist.res.in (R.K. G).

<https://doi.org/10.1016/j.ejphar.2019.172553>

Received 8 April 2019; Received in revised form 4 July 2019; Accepted 16 July 2019

Available online 17 July 2019

0014-2999/ © 2019 Elsevier B.V. All rights reserved.

resident sterol regulatory element-binding proteins (SREBPs) stimulate and increase the production of the cholesterol. The newly synthesized cholesterol is then exported to other organelles for membrane synthesis. Under stress conditions, the high cholesterol and fatty acids containing phospholipids inhibit SERCA activity, which results in Ca^{2+} depletion and protein misfolding (Van Meer et al., 2008). There are a large number of regulatory proteins due to the diverse functions of the ER (Ron and Walter, 2007).

2. ER stress

ER stress can be defined as the condition where unwanted proteins accumulate in the lumen, and, as the degradation machinery does not work properly, ER stress is created inside the membranous network (Marciniak and Ron, 2006). During this condition, ER homeostasis will collapse, and an unfolded protein response (UPR) will be initiated. UPR is a homeostatic mechanism to achieve a balance between newly synthesized proteins and the capacity of ER to fold them correctly. Chronic conditions such as scarcity of ER chaperones, protein overload, imbalance of Ca^{2+} content, and cholesterol accumulation are the main factors for the development of ER stress (Cnop et al., 2012). In adipose tissue, ER stress is initiated by nutrient overload along with high demand for protein translation, which is crucial for its metabolism. Decreased vascularization and local glucose deprivation due to insulin resistance (IR) are the other factors. The high-fat diet also plays a major role in inducing ER stress (Hager et al., 2012). The role of severe ER stress in metabolic syndrome outcomes such as diabetes mellitus, obesity, fatty liver diseases, cardiovascular diseases, neuronal diseases, and some cancers has already been established (Piperi et al., 2012).

Three primary ER stress transducers (Fig. 1) regulate the stress in

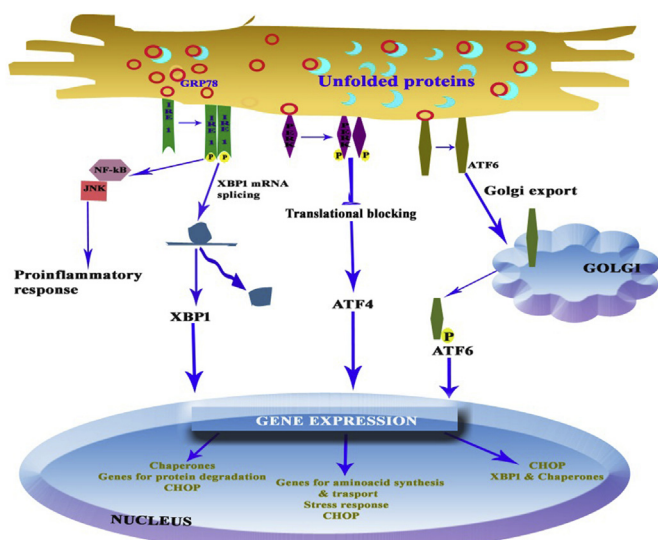


Fig. 1. UPR signaling pathways and their functions. Three ER stress sensors, ATF6, IRE1, and PERK receive the ER changes during UPR initiation. When unwanted protein levels increase, GRP-78 detaches from ER transducers, and this will result in the activation of PERK, IRE1, and ATF6. IRE1 undergoes autophosphorylation and helps the splicing of XBP1 mRNA. ATF6 activation is through Golgi by proteolysis reaction. Cleaved ATF6 along with sXBP1 induce several ER chaperones and ERAD proteins. Dimerization and transautophosphorylation of PERK lead to global translation attenuation via eIF2 α . Phosphorylated eIF2 α facilitates the translation of ATF4 and initiates the expression of many chaperones, transporters, and many genes for apoptosis. Note: ER, endoplasmic reticulum; ATF6, activating transcription factor 6; IRE1, inositol requiring 1; PERK, PKR-like ER localized kinase; UPR, unfolded protein response; XBP1, X box binding protein 1; sXBP1, spliced XBP1; ERAD, ER-associated degradation; eIF2 α , eukaryotic initiation factor 2; ATF4, activating transcription factor 4; CHOP, CCAAT-enhancer-binding protein homologous protein.

the ER network in the cytoplasm and/or nucleus: inositol-requiring enzyme 1 (IRE1); protein kinase R-like ER kinase (PERK) and activating transcription factor 6 (ATF6). Usually, they bind to glucose-regulated protein 78 (GRP-78) (also known as binding immunoglobulin protein (BiP), or heat shock 70 kDa protein 5) on the ER membrane. GRP-78 uses adenosine triphosphate (ATP) as an energy source to promote protein folding and prevent protein aggregation. Among the ER-resident chaperones, GRP-78 is the master initiator of UPR signaling. At the time of ER stress, GRP-78 binds to luminal-unfolded proteins and triggers the activation of UPR (Cnop et al., 2012). Among these transducers, the IRE1 signaling pathway is the most conserved one. This transmembrane protein is expressed on the ER membrane and acts as a bifunctional enzyme. During ER stress, the activated IRE1 promotes the splicing and expression of X-box binding protein 1 (XBP1) mRNA. As a result, the levels of components of ERAD, ER heat shock proteins, and phospholipid synthesis increase. These lead to ER membrane expansion, a structural marker of the UPR. Meanwhile, due to the RNase activity of IRE1, the protein entry into the ER lumen is reduced. In the liver, both XBP1 and IRE1 are involved in triglyceride synthesis and lipid metabolism (Wang et al., 2012).

PERK is a ubiquitous type I ER transmembrane protein kinase, structurally similar to IRE1 (Hager et al., 2012), and highly expressed in secretory cells (Marciniak and Ron, 2006). During the activation of UPR, PERK inactivates the eukaryotic initiation factor 2 alpha (eIF2 α) through serine residue phosphorylation (Cnop et al., 2012). eIF2 α is a critical factor for protein synthesis in eukaryotes. It facilitates the entry of initiator tRNA to ribosomes and starts peptide synthesis. When eIF2 α becomes inactivated, global protein synthesis will be down-regulated by decreasing the usage of AUG codon. At the time of ER stress, PERK response only depends upon the changes in chaperone level, more specifically, the GRP-78 level. Frequently, PERK is associated with GRP-78 in its monomeric form. In stress condition, GRP-78 has a high affinity towards misfolded proteins leading to detachment of PERK-GRP-78 complex. This will lead to PERK autophosphorylation and upregulation of its affinity to eIF2 α (Cao and Kaufman, 2013). Translational regulation of proteins is very important in ER stress. During stress conditions, PERK and eIF2 α are phosphorylated at a single serine residue on their substrate. However, when a mutation occurs to this substrate, the serine is changed to alanine, which prevents its phosphorylation. This results in the destruction of β -cells in mice and also the symptoms of metabolic syndrome such as hyperleptinemia, hyperinsulinemia and raised blood glucose levels (Biaison-Lauber et al., 2002). Meanwhile, the mRNA expression of activating transcription factor 4 (ATF4) is up-regulated. The activated ATF4 then stimulates the genes involved in the amino acid import and glutathione biosynthesis. Through this way, it reduces the accumulated misfolded proteins. One of the prime ATF4 regulated genes is CCAAT-enhancer-binding protein homologous protein (CHOP), a transcriptional activator of an apoptotic program (Kim et al., 2015).

Compared to IRE1 and PERK, ATF6 is a type II transmembrane protein. There are two types, ATF6 α and ATF6 β (Yoshida et al., 2000; Yoshida et al., 2001a, 2001b). When ER stress is initiated, the Golgi localization signal of ATF6 is exposed and translocated into the Golgi, where it undergoes protease digestion (Bommiasamy et al., 2009). The cleaved fragment acts as an activator of several genes involved in lipid synthesis and ERAD machinery. In addition to this, it also activates genes to produce GRP-78, glucose-regulated protein 94 (GRP-94), protein disulfide isomerase (PDI), XBP1, and CHOP (Piperi et al., 2012). ATF6 indirectly controls autophagy and apoptosis and the Wolfram syndrome 1 protein controls its activity. The function of this protein is to direct ATF6 to ubiquitination followed by proteasomal degradation (Kaneko et al., 2017). Some other ER-resident transcription factors, which mimic ATF6, include Luman/cAMP-responsive element-binding protein 3 (CREB3), CREB3L1/OASIS, and CREB3L2/BBF2H2. The differences between these factors and ATF6, and requirements need for these molecules in the ER, are unknown (Fonseca et al., 2010).

3. ER stress and metabolic syndrome

Pre-clinical and clinical studies have shown that ER stress has a major impact on metabolic syndromes including obesity, atherosclerosis, diabetes, myocardial dysfunction, and non-alcoholic fatty liver disease (NAFLD) (Ghemrawi et al., 2018).

3.1. ER stress and diabetes

The pancreatic β -cell is the primary source of insulin (Cao and Kaufman, 2013). Insulin is a hormone, initially formed as a single pro-insulin molecule. Then, within the ER, it undergoes maturation processes to form the three intramolecular disulfide bonds in insulin (Marciniak and Ron, 2006). Diabetes is a metabolic disease characterized by complex physiological changes, including inadequate insulin secretion, peripheral IR, and dysregulated hepatic glucose production. The combined results obtained from *in vitro*, *in vivo*, and human studies have confirmed that ER stress-induced pancreatic β -cell destruction is the major etiology for both type 1 and type 2 diabetes (Cnop et al., 2017). Pathological, environmental, and genetic factors that initiate ER disturbances in pancreatic β -cells include glucolipotoxicity, inflammatory responses, amyloid accumulation, and expression of mutant proinsulin (Fonseca et al., 2010; Wang and Kaufman, 2012). Congenital diabetes is a type of neonatal diabetes, which is characterized by the changes in one of the two alleles of the insulin gene. In this condition, the complete folding of the proinsulin does not take place, and this leads to prolonged ER stress and β -cell dysfunction. This mutation is induced in Akita diabetic mice that also show β -cell disruption and diabetes (Danilova and Lindahl, 2018). The development of type 2 diabetes mellitus increases the demand for pancreatic β -cells to increase insulin production, which eventually leads to ER disturbances. IR is one of the major consequences of type 2 diabetes mellitus and obesity. Recent studies reveal that ER stress might be an important contributing factor to IR (Kaneko et al., 2017). In the liver, IR leads to increased hepatic gluconeogenesis and lipogenesis, which will cause hyperglycemia-associated hyperlipidemia (Wang and Kaufman, 2012). IR initially mediates hyperglycemia during type 2 diabetes mellitus, but later insulin deficiency contributes to the development of the disease. In the liver, ER stress is initiated through IRE1-mediated activation of c-Jun N-terminal kinase (JNK) and inhibitor kappa B (I κ B) (Bhuvaneswari et al., 2014). The activated JNK impairs insulin action by phosphorylating serine residues of insulin receptor substrate (IRS) 1 and 2 (Fonseca et al., 2011).

During ER stress, the activation of the IRE1 branch is necessary for the synthesis and maturation of nascent insulin (Lee et al., 2011). Here IRE1 directly activates the complete expression of insulin mRNA, and it is necessary for optimal β -cell function. Meanwhile, hyperactivated IRE1 could result in β -cell loss via the initiation of JNK and caspases (Hetz, 2012). The PERK-eIF2 α -CHOP pathway acts as a switch between the normal functioning of the β -cell and its survival ability. Wolcott Rallison syndrome is a rare autosomal juvenile form of diabetes, which affects bone, liver, kidney, and neurons (Cnop et al., 2017). It is characterized by the inactivation of both alleles of the PERK gene and shows a loss of insulin-secreting β -cells followed by destruction of α -cells. Both of these effects result in failure of the pancreas (Danilova and Lindahl, 2018). These findings demonstrate the importance of PERK in pancreas for maintaining glucose metabolism. FFAs such as palmitate activate all three branches of the UPR, which results in the apoptosis of β -cells (Bommiasamy et al., 2009). Both *in vitro* and animal studies show that increased blood levels of glucose and saturated FFAs are the prime factors to induce proapoptotic UPR. CHOP shows its total proapoptotic effect only when there is an imbalance between ER stress and the amounts of unwanted and/or misfolded proteins. At this time, CHOP up-regulates the expression of Bcl-2-like protein 11 (BIM) and down-regulates the antiapoptotic, B-cell lymphoma 2 (Bcl-2) (Papa, 2012). Apoptosis is a planned cell death, which is carried out either

through death receptor or is mitochondria-endoplasmic mediated (Delepine et al., 2000). In contrast, deletion of CHOP will protect the β -cells in genetic and diet-induced diabetes models in mice (Zhang et al., 2006).

In contrast, ATF6 α suppresses glucose formation through CREB-regulated transcription coactivator 2 (CRT2) (Wang et al., 2009). The p85 regulatory subunits of phosphoinositide 3-kinase (PI3K) and p38 mitogen-activated protein kinases (MAPK) increase insulin activity by activating the translocation of XBP1 to the nucleus (Piperi et al., 2012). XBP1 promotes the proteasomal degradation of fork head box protein O1 (FOXO1) and thereby down-regulates several gluconeogenic enzymes including phosphoenolpyruvate carboxykinase (PEPCK) and glucose 6-phosphatase (G6Pase) (Zhou et al., 2011).

Advanced glycation end products (AGEs) directly or indirectly induce an ER stress response. Glycation is a reaction between reducing carbohydrates and proteins, initiating many post-translational changes in proteins, nucleic acids (DNA and RNA), and fats. AGEs levels become increased during cellular stress, high blood glucose levels, and oxygen depletion conditions. Moreover, AGEs have a vital role in the progression of metabolic syndrome. Therefore, inhibitors of AGEs are important to restore ER homeostasis and AGEs can be an attractive target to treat metabolic syndrome (Piperi et al., 2012).

3.2. ER stress in obesity and lipid metabolism

Inside the cell, ER is just like a kitchen where phospholipids and sterols are synthesized. They constitute the lipid components of all cellular membranes. During obesity, excess energy is stored as triglycerides inside the lipid droplets in adipocytes (Surmi and Hasty, 2008) and other tissues such as liver, pancreas, heart, and muscle (Tripathi and Pandey, 2012). Adipocytes are cells meant for storing energy but also act as a central endocrine organ (Bays et al., 2008). They are involved both in inflammation and energy metabolism, which are the critical factors of metabolic syndrome (Kabir et al., 2005). Lipotoxicity is one of the leading causes of cellular damage in pathophysiological conditions (Nicklas and O'Neil, 2014). During lipotoxicity, cells undergo severe stress to amalgamate more proteins for lipid droplet generation as well as to meet the energy expenditure for metabolism and maintain glucose deprivation. Many hormones and adipokines such as insulin, visfatin, leptin and omentin work together for the utilization and storage of this excess energy (Rosen and Spiegelman, 2006). This reveals the role of ER in lipid droplet formation and thereby to sustain lipid metabolism. Excessive protein formation and their transportation within the ER initiate the UPR signaling and IR with a low grade of inflammation (Verdile et al., 2015). Numerous reports suggest that UPR plays an important role in metabolic and lipid homeostasis (Achar and Laybutt, 2012). Over-expression of XBP1, a major protein involved in ER biogenesis and expansion, in pre-adipocytes up-regulates the enzyme choline phosphate cytidyltransferase (CCT) which participates in the formation of phosphatidylcholine (Sriburi et al., 2004), the major membrane lipid found in the ER (Zha and Zhou, 2012). The loss of CCT affects the fusion of lipid droplets (Lewy et al., 2017). In some studies, in *Drosophila* by knockout, up-regulation of one of the CCT genes produces increased triacylglycerols (Lewy et al., 2017). Thus, XBP1 is the major protein involved in lipid metabolism. Over-expression of GRP-78 in liver regulates glucose homeostasis and decreases hepatic steatosis by reducing the SREBP-1c activity, which proved the importance of ER in liver lipid metabolism (Lewy et al., 2017). SREBPs are proteins that have a specific site for deoxyribonucleic acid (DNA) binding and thereby regulate the expression of genes responsible for sterol/lipid biosynthesis (Shimano, 2001). They are mainly situated on the ER surface and bind to SREBP-cleavage-activating-protein (SCAP) through the insulin-induced gene (Insig) (Gianfrancesco et al., 2018). Three isoforms of SREBPs are SREBP-1a, -1c, and -2. SREBP-1c and 2 are involved in lipogenesis and cholesterol synthesis (Zha and Zhou, 2012). During low cholesterol levels, SREBP-Insig complex is

dissociated and targeted to Golgi. Inside the Golgi, the complexes are attacked by proteases and release mature SREBP. Then the mature SREBP relocates to the nucleus and activates the genes responsible for cholesterol and lipid metabolism. This involves the disruption of ER homeostasis and alters cholesterol and fat synthesis (Shao and Espenshade, 2014). IRE1, PERK and ATF6 are ER stress-responsive proteins and they have independent roles in lipid metabolism. The major regulator of hepatic lipid metabolism is IRE1-XBP1 pathway. Specific IRE1 deletion in liver cells results in the upregulation of hepatic lipid levels by increased expression of genes such as CCAAT/enhancer binding protein and genes responsible for triglycerides synthesis (Qiu et al., 2013). At the same time the silencing of XBP1 leads to down-regulation of FFAs and cholesterol by decreased lipogenic genes such as SCD and ACC (So et al., 2012). The ATF6 pathway also has a prominent role in lipid metabolism. It controls lipid metabolism through a negative interaction with SREBPs and down-regulates the lipid accumulation in both liver and kidney (Yamamoto et al., 2010). In kidney, the prime factor for the renal lipid accumulation and ER stress is SREBP-2 (DeZwaan-McCabe et al., 2017). ER stress in hepatocytes activates SREBP-1c through proteolytic cleavage of the insig protein and activates lipogenesis (Baiceanu et al., 2016). The role of PERK in hepatocytes is not fully understood but one study reported that antipsychotic drugs activate SREBP-1 and 2 through this pathway (Han and Kaufman, 2016). PERK pathway is also critical for adipocyte differentiation through the activation of SREBP-1. The effect of PERK on adipogenesis is due to the activation of eIF2 α and results in inhibition of general translation (Damiano et al., 2010). Meanwhile, PERK up-regulates the translation of mRNAs of GRP-78, SREBP-1, and ATF4 (Lewy et al., 2017). Furthermore, SREBP-1 is a critical activating factor of adipogenesis, so it has an additional name as adipocyte determination and differentiation 1 (ADD1) (Fig. 2: Zha and Zhou, 2012).

3.3. ER stress and inflammation

The mechanism underlying obesity-related IR and diabetes is the development of chronic low-grade inflammation. During ER stress, the IRE1-XBP branch activates tumor necrosis factor alpha (TNF α) expression. At the same time, the PERK arm of ER stress initiates cellular inflammatory cascade through activation of the JNK pathway

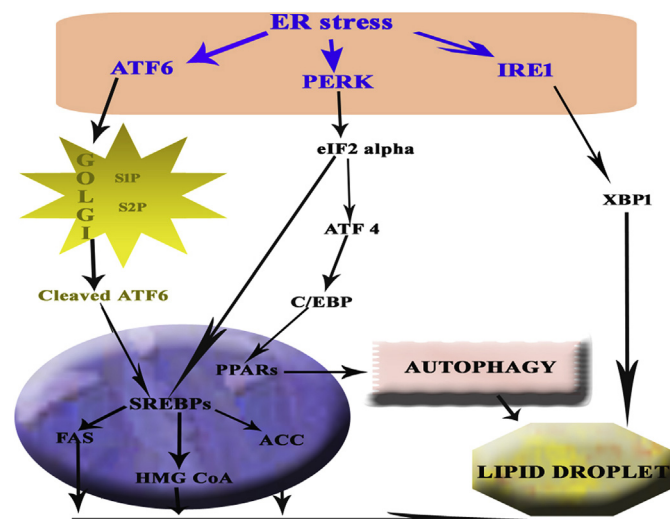


Fig. 2. Involvement of ER stress in adipogenesis. Role of UPR in the formation of lipid globules in adipose tissues during ER stress; the activated SREBPs upregulates the levels of enzymes participating in lipid metabolism. As a result, the lipid droplets are generated in the tissues which are responsible for fatty acid metabolism. ER stress also activates XBP1, which encourages the formation of triglyceride and finally leads to adipogenesis. Note: SREBPs, sterol regulatory element-binding proteins.

(O'Rourke, 2009). Lastly, the activated ATF6 upregulates interleukin 6 (IL6) and TNF α expression and also the nuclear factor kappa-light-chain-enhancer of activated B cells (NF- κ B) signaling. It finally inhibits the anti-inflammatory protein kinase B (PKB) pathway (Thoudam et al., 2016). Meanwhile, the increased JNK activates pro-inflammatory cytokines (IL6) and several chemokines. They are the main activators of macrophages in the vicinity of inflammation as well as in the circulation (Hirosumi et al., 2002). Then these macrophages engulf the adipocytes and create crown-like structures, which is the hallmark of obesity. Meanwhile, these structures activate lipolysis in adipocytes. As a result, FFA levels are increased, and FFAs deposited in the liver as well as in muscles induce cellular dysfunction (Zha and Zhou, 2012). This is one of the primary causes of fatty liver and cardiovascular disease. In diabetes, high diacylglycerols activate protein kinase C (PKC), which inhibits the insulin signaling through serine/threonine kinases and finally leads to IR. During ER stress, PERK induces I κ B kinase β (IKK β) activation and subsequently decreases the production of adiponectin. Adiponectin is one of the major anti-inflammatory cytokines produced by adipocytes that negatively regulates cardiovascular disease and fatty liver disease (Boden and Merali, 2011).

3.4. ER stress and fatty liver disease

ER stress has a prominent role in the pathogenesis of fatty liver diseases. UPR pathway is a critical factor for the initiation of hepatocyte death and a potential promoter of inflammation. Hepatocytes perform many metabolic functions such as the metabolism of xenobiotics, synthesis of proteins such as plasma proteins, lipoproteins, and very low-density lipoproteins, and the formation of cholesterol (Rutkowski, 2019). These are the major functions of ER, so hepatocytes are enriched with both rough and smooth ER (Malhi and Kaufman, 2011). Smooth ER lacks ribosomes and they are the prime site for lipid synthesis. Smooth ER has a connection with cytoskeleton so through this way ER moves the lipids as well as Ca²⁺ to adjacent membranes and organelles (Baiceanu et al., 2016).

As the name suggests, fatty liver is the condition when the liver is loaded with fats, mainly the triglycerides, described as either alcoholic fatty liver diseases (AFLD) or NAFLD (Dara et al., 2011). NAFLD is defined as an aggregation of lipids inside the liver in the absence of alcohol consumption or other liver diseases (Pagliassotti, 2012). The primary entry of these lipids is either from the diet, from *de novo* lipogenesis or through release from adipose tissue. Compared to unsaturated fatty acids, saturated fatty acids cause severe ER stress and finally result in liver damage, because saturated fatty acids do not degrade into triglycerides. They can freely move to the ER and destroy ER compatibility (Dara et al., 2011).

The three UPR pathways behave differentially in ER stress (Malhi and Kaufman, 2011). Both IRE1 and PERK are activated through autophosphorylation, and ATF6 activation is via its Golgi localization. Activated IRE1 increases the levels of chaperones, growth arrest and DNA damage (GADD) and ERAD genes in the nucleus through the activation of XBP1 mRNA. The activated GADD then sensitizes the liver cells to apoptosis. In stressed cells, the IRE1 initiates the inflammation and IR through the activation of JNK. The activated JNK inhibits IRS1 and finally results in hyperinsulinemia and increased lipogenesis (Sarvani et al., 2017). At the same time in hepatocytes, nucleotide-binding oligomerization domain, leucine-rich repeat and pyrin domain containing 3 (NLRP3) inflammasome is activated. It is a multi-protein complex coming under the family of nucleotide-binding oligomerization domain (NOD)-like receptors (Olivares and Henkel, 2015). NLRP3 initiates IR and promotes inflammation in liver cells (Lebeaupin et al., 2016). Formation of this complex activates caspase 1 and 11 and many other proinflammatory cytokines including IL6 and interleukin 8 (IL8). The combined action of caspases and cytokines finally results in programmed cell death. IRE1 also has a prominent role in liver steatosis through XBP1. XBP1 independently controls the genes responsible for

fatty acid synthesis such as acetyl CoA carboxylase (ACC), and stearoyl CoA desaturase (SCD). In addition, XBP1 protein has a role in adipocyte differentiation. Selective silencing of XBP1 in the liver leads to decreased plasma triglyceride and cholesterol in mice and reduces adipogenesis in XBP1-deficient preadipocytes (Wu et al., 2016). XBP1 also protects the cells from oxidative damage, and it can increase the level of antioxidant enzymes in the liver (Gentile et al., 2011).

Activated PERK inhibits the protein synthesis and decreases the Insig1 protein, a negative regulator of lipogenesis. Hence, inhibition of this protein will increase the level of SREBP. Raised SREBP alters the biosynthesis of lipids that increase the formation of cholesterol and triglycerides, one of the hallmarks of the fatty liver disease. When mice lack the SREBP gene, they are protected from both AFLD and NAFLD (Dara et al., 2011). *De novo* fatty acid synthesis is one of the crucial factors for the pathogenesis of fatty liver disease. Over-expression of the chaperone GRP-78 reduces the level of SREBP in liver cells, improves insulin sensitivity and reduces steatosis (Dara et al., 2011).

To maintain the UPR-generated reactive oxygen species, the phosphorylated-PERK (p-PERK) initiates the transcription of nuclear erythroid-related factor 2 (Nrf2), which maintains the redox status. PERK pathway also reduces reactive oxygen species via the activation of Nrf2 (Zhang et al., 2019). In the fatty liver, the reactive oxygen species generation is mainly done by the protein CHOP (GADD153). The expression of CHOP is down-regulated by PERK and ATF6 (Lebeauupin et al., 2016). Similar results occur when the animals are exposed to ethanol. In AFLD models, increased gene expression of GRP-78, SREBP, Ca²⁺, CHOP, calnexin, ER oxidoreductin 1 (ERO1), Bcl-2 associated X protein (BAX), and caspase 12 is detected in the ER (Wu et al., 2016). Alcohol has a predominant role in the generation of ER stress. Thus, all three UPR sensors IRE1, PERK, and ATF6 regulate lipid stores in the liver.

3.5. ER stress and cardiovascular diseases

Endothelial dysfunction is one of the initial responses in many cardiovascular complications (Di Francescomarino et al., 2009). The heart is very sensitive to ER stress as the endothelium is the critical site to maintain vascular homeostasis (Hong et al., 2017). Temperature, oxygen and nutrient depletion, infection, hyperglycemia, oxidative stress, and altered lipid metabolism are the main inducers of the ER stress pathway. Among these, deficiency of oxygen is one of the critical stresses of the myocardium (Shohet and Garcia, 2007). UPR has an important function in the pathophysiology of many cardiovascular diseases including myocardial hypertrophy, ischemic stroke, and congestive heart failure (Maamoun et al., 2019). During ER stress, all the three arms of UPR, PERK, ATF6, and IRE1, are activated. The activity of PDI is reduced, so the disulfide bonds are not formed correctly, and the level of unwanted proteins will increase ensuring increasing severity of ER stress (Szegezdi et al., 2006). The IRE1-XBP1 pathway plays a protective role against hypoxic effect in the heart. During hypoxia, the XBP1 mRNA splicing and GRP-78 levels are increased, indicating the initiation of UPR. Moreover, the upregulation of GRP-78 is controlled by XBP1; at the time of UPR, the activated ATF6 reduces cell death due to high Ca²⁺ levels in H9c2 cardiomyocytes (Vitadello et al., 2003). The sudden decrease of protein translation is regulated by PERK that inhibits the nascent protein transport into the ER lumen and upregulates CHOP, the most widely investigated biomarker involved in ER stress-associated apoptotic signaling in cardiovascular disease (Minamino and Kitakaze, 2010). CHOP, in turn, activates ERO1 expression, which is the protein necessary for the optimal activity of the enzymes such as PDI and prolyl hydroxylase (Marciniak et al., 2004).

Nrf2 is a well-known promoter of the antioxidant defense system in cardiomyocytes (da Costa et al., 2019; Tu et al., 2019). It protects against oxidative stress during ischemia-reperfusion injury and aging. The upregulation of Nrf2 is another function of p-PERK. Through this mechanism, PERK upregulates the antioxidant proteins and detoxifying

enzymes (Ooi et al., 2018). Nrf2-deficient cells show increased cell death when exposed to ER stress. From these data, it is clear that phosphorylated Nrf2 is essential for the survival of cardiac myocytes against ER stress (Howden, 2013).

The other two ER stress sensors, IRE1 and ATF6, are involved in upregulation of the genes encoding the proteins that participate in nascent protein maturation, transport, and ubiquitination (Groenendyk et al., 2010). The activation of ATF6 during ischemia and its inactivation during reperfusion showed its participation in the production of ER stress. In this event, the blood flow becomes reduced, which limits the cell exposure to an energy source by activation of ATF4 and 6. Then they initiate the genes involved in glycogenolysis and inactivate cholesterol synthesis to conserve carbon units. In addition, reperfusion after ischemia generates oxidative stress through the surplus amount of reactive oxygen species (Avery et al., 2010). This condition results in the disruption of ER oxidative state and Ca²⁺ homeostasis. The development of cardiac hypertrophy is mainly due to Ca²⁺ dysregulation and abnormal protein synthesis. In cardiomyocytes, the sarcoplasmic reticulum (SR) is recognized as the regulator of Ca²⁺ levels and controls the excitation-contraction coupling in the heart. Strict regulation of ER luminal Ca²⁺ concentration is vital for maintaining cellular integrity. Disruption of homeostasis will impair all ER functions leading to ER stress. Decreased ER Ca²⁺ levels increase the chaperones and proteins (CHOP, eIF2 α , p-PERK, calnexin, caspase 12 and JNK) and initiate cell death in H9c2 cardiomyocytes (Brostrom and Brostrom, 2003; Thuerlauf et al., 2006). In this condition, the cytosolic Ca²⁺ is increased which increases the level of Ca²⁺-mobilizing agents. Ca²⁺-mobilizing agents are Ca²⁺ ionophores that are responsible for the regulation of Ca²⁺ levels in cytoplasm and extracellular space. These effects were modulated by calcineurin, a phosphatase that activates the nuclear factor of activated T cells (Fig. 3; Liu et al., 2016).

Atherosclerosis is one of the common and important cardiovascular diseases. ER stress has a prominent role in the pathogenesis of this disease by affecting lipid metabolism inside the ER (Zhang et al.,

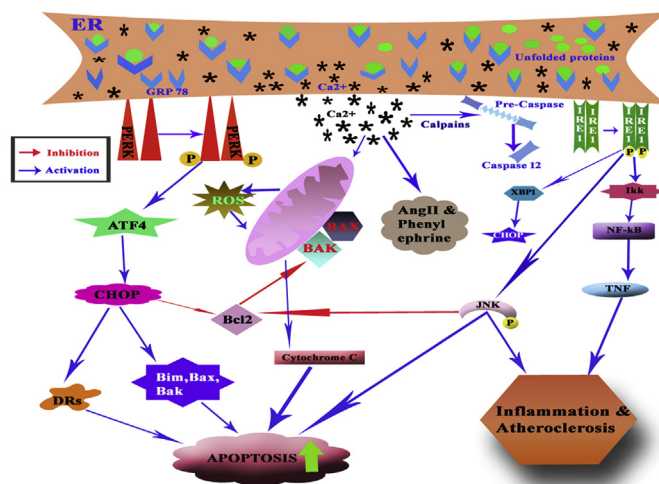


Fig. 3. ER stress-induced inflammation in cardiovascular diseases & atherosclerosis. During chronic ER stress, both CHOP & jun N-terminal kinase (JNK) are activated and induce apoptosis in cardiomyocytes. The IRE1-TRAF activates the XBP1, JNK & Ikk leading to apoptosis and inflammation. Inflammation is the major contributing factor to the development of cardiovascular diseases and atherosclerosis. Inflammation creates a fatal amount of reactive oxygen species and this initiates mitochondrial dysfunction and apoptosis. In cardiomyocytes, strict regulation of ER Ca²⁺ concentration is necessary for the maintenance of cellular integrity. Decreased level of calcium increase GRP-78 expression, the same time as it initiates the calcium mobilizing agents in the cytoplasm. Note: CHOP, CCAAT-enhancer-binding protein homologous protein; JNK, Jun N-terminal kinase; Ikk, IKB kinase β ; GRP-78, Glucose-regulated protein 78.

2017a). During UPR activation, lipid formation and hepatic lipid reserves are decreased, triggering the entry of inflammatory cells into the damaged site and initiation of an inflammatory response. These inflammatory cells produce cytokines and reactive oxygen species (Gotoh et al., 2011). When these reactive oxygen species are produced, PERK and IRE1/TNF- α -receptor-associated factor 2 (TRAF2) complex becomes activated. The activated TRAF2 then initiates the activation of I κ B kinase and JNK (Villalobos-Labra et al., 2018). It results in the translocation of NF- κ B, activates several downstream inflammatory signals, and thereby induces atherosclerosis (Hu et al., 2006). Inflammation is an immunological response where ER stress and inflammation pathways connect through various mechanisms that can produce cardiovascular diseases. Moreover, one of the central contributors of cardiovascular disease is chronic ER stress (Hong et al., 2017). How ER stress modulates endothelium-dependent vascular function and nitric oxide (NO) signaling pathway is not precisely understood (Maamoun et al., 2019).

4. Targets for the management of ER stress

The UPRs were uncovered 20 years ago. Recently, it has been found that activated UPR is involved in the pathogenesis of metabolic syndrome (Lee and Ozcan, 2014). Therefore, ER could act as an important target for the amelioration of different signs of metabolic syndrome (Eizirik et al., 2007). A common factor for the pathogenesis of many of these disorders is the appearance of unwanted proteins. It reveals the relationship between ER stress and metabolic syndrome, so targeting UPR is an important area for the alleviation of many of these metabolic changes. There are several approaches to target the UPR. Agents that can reduce the factors of the pro-apoptotic pathway or activate the adaptive UPR components could be used as a possible approach for managing the disease. Small molecular agents that promote ER protein folding capacity and protein stability are first among them (Fig. 4). They are heat shock proteins (chaperones) having a low molecular weight and ER stress inhibitors (Welch and Brown, 1996). Tauroursodeoxycholate (TUDCA) and 4-phenyl butyrate (PBA) are two chaperones already accepted by Food and Drug Administration (FDA) (Bouchecareilh et al., 2011). They have been studied for their potential

to diminish UPR-induced dysfunction in several cell lines including adipocytes, hepatocytes, and β -cells (Zha and Zhou, 2012). TUDCA is a bile acid derivative, used as a hepatoprotective agent in humans with fatty liver disease (Kaplan and Gershwin, 2005). It markedly reduces aortic clot development and ER stress in cardiovascular disease patients. PBA is approved for many urea cycle disorders as an ammonia-scavenging molecule and also used for other diseases linked with unfolded proteins such as cystic fibrosis and thalassemia (Kim et al., 2009). In neurodegenerative diseases, PBA will stimulate amyloid- β precursor protein (APP) proteolysis and apoptosis (Wiley et al., 2010). It can also be used for cardiovascular diseases (Erbay et al., 2009). One of the major limitations of this chaperone treatment is the requirement of a high dose for a satisfactory response. Another problem is that the molecular mechanism for the reduction of the protein misfolding is not known.

PBA and TUDCA reduce UPR activation in obese mice (Bouchecareilh et al., 2011). They can nonselectively reduce the UPR by acting as leptin-sensitizing agents. Leptin is an adipokine from adipose tissue that is increased when fat is increased (Minamino et al., 2010). It binds to the hypothalamus and reduces food intake. Importantly, leptin resistance is documented in many obese people and some reports link leptin resistance to ER stress (Sarvani et al., 2017). Other studies showed both compounds improve insulin sensitivity in obese individuals. TUDCA improved the insulin sensitivity in liver and muscle, and PBA reduced IR and β -cell dysfunction (Kars et al., 2010; Xiao et al., 2011).

Moreover, TUDCA and PBA are capable of reducing hyperglycemia in diabetic patients and restoring β -cell function in humans (Sarvani et al., 2017). In addition, treatment of ApoE $^{-/-}$ mice with PBA reduced ER stress and apoptosis of macrophages (Sarvani et al., 2017). TUDCA has anti-aggregation activity so that it can be used for the amelioration of atherosclerotic lesions (Erbay et al., 2009). In hepatocytes and adipocytes, both TUDCA and PBA decrease ER stress by reducing inflammation and weight gain (Bouchecareilh et al., 2011; Kim et al., 2009), so these compounds might be considered as relevant interventions against metabolic syndrome.

Next type includes ER stress sensors and transcription factors. They are collectively called GRP-78 activators. Elevated levels of BiP/GRP-78 prevent UPR-induced cell death (Morris et al., 1997). Several small molecules, BiP inducer X (BIX) and valproate, induce GRP-78 in animal models. Valproate is a compound used in neurodegenerative diseases but it also protects β -cells from palmitate-induced injury (Zhang et al., 2011). BIX is also used against neurological diseases and in animal models to prevent ER stress and cell death (Inokuchi et al., 2009; Kudo et al., 2008; Oida et al., 2010), but the exact mechanism by which BIX activates GRP-78 expression is not known. Therefore, GRP-78 activators including valproate and BIX in metabolic syndrome need further investigation of their efficacy and safety through preclinical and clinical studies. Regulators of the PERK-eIF2 α -CHOP pathway are included in the third category. There are many inhibitors that reduce phosphorylation and dephosphorylation. An optimal level of eIF2 α phosphorylation is protective in several metabolic pathologies, including β -cell failure. Among the inhibitors, the major one is guanabenz, an FDA-authorized drug used for hypertension. Guanabenz is a small molecule, which binds to GADD and activates eIF2 α phosphorylation to reduce protein translation and decrease UPR stress. Therefore, it represents a hopeful candidate for the treatment of metabolic syndrome (Tsaytler et al., 2011). Another small molecule, salubrinal, protects cells from UPR-induced death by reducing the dephosphorylation of eIF2 α (Boyce et al., 2005). However, its efficacy and safety under *in vivo* conditions have not been demonstrated. Further, a normal level of eIF2 α phosphorylation is required for the proper functioning of β -cells, and an increased level could result in pancreatic cell death, atherosclerosis or hepatosteatosis (Boyce et al., 2005). Tight regulation of ER stress is necessary, and it may provide therapeutic advantages to some signs of metabolic syndrome. One example is the rational design of PERK

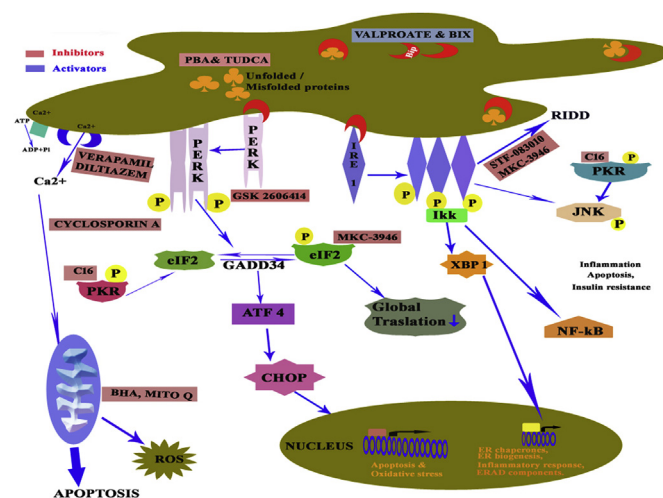


Fig. 4. ER stress and their targeted therapies. Many compounds have now been identified to target ER stress (Green box-activators, Red box-inhibitors). The two chemical chaperones approved by FDA (PBA and TUDCA) can reduce protein misfolding in a nonspecific manner. MKC3946 is a chemical inhibitor that targets specific UPR components, at the same time cyclosporin A and MitoQ suppress the mitochondrial oxidative stress. Mitochondrial stress has an intimate relationship with ER stress and its protein homeostasis. Note: ER, endoplasmic reticulum; PBA, 4-phenyl butyrate; TUDCA, tauroursodeoxycholate; MitoQ, mitoquinone.

inhibitors such as GSK2606414 which is an attractive tool for targeting UPR (Axten et al., 2012; Wang et al., 2010). PERK is a major antiviral component of the interferon response and is activated by a variety of cellular stresses. Cl6A is a small molecular inhibitor of PERK, which can prevent ER stress-induced cell death and alleviate neurological disorders. However, this molecule warrants further preclinical investigation for the management of many diseases including diabetes, cardiovascular disease, obesity and fatty liver disease (Harding et al., 2012; Jammi et al., 2003; Shimazawa and Hara, 2006). One of the exciting UPR targets for metabolic disorders is CHOP. It is a major proapoptotic component induced by ER stress. Unfortunately, the lack of selective inhibitors of CHOP has delayed the current efforts in this field. Modulators of IRE1, a highly conserved UPR transducer, are the next promising target for ameliorating ER stress and thereby metabolic syndrome. Hyperactivation of IRE1 causes multiple pathologies, including IR, inflammation, and apoptosis (Han et al., 2009; Zhu et al., 2011). A group of small molecules including STF-083010, 4μ8C, and MKC-3946 selectively inhibit the RNase activity of IRE1 (So et al., 2012; Volkmann et al., 2011). These inhibitors are based on a similar structure and have a similar mechanism of action. A synthetic peptide promoted IRE1 oligomerization and XBP1 splicing thereby improving cell survival upon ER stress challenge (Cross et al., 2012; Mimura et al., 2012; Papandreou et al., 2011). From these data, we suggest that it is worthwhile to give more effort to demonstrate the safety and efficacy of these compounds in pre-clinical studies. Another important target is the regulation of ER Ca^{2+} homeostasis. Ca^{2+} is a second messenger which can regulate many signaling pathways. The ER lumen has high levels of Ca^{2+} , which is essential for nascent protein modification and trafficking. The disturbances of Ca^{2+} levels initiate ER stress mainly in insulin-secreting β -cells. Therefore, regulators of ER Ca^{2+} homeostasis may demonstrate beneficial effects in metabolic syndrome. Two therapeutic approaches have been used to decrease the Ca^{2+} -efflux from the ER lumen and improve Ca^{2+} -influx into the ER. First one is to reduce the Ca^{2+} -leakage from the ER. In some studies, antihypertensive drugs such as verapamil were used to block the Ca^{2+} channel; verapamil protects the β -cells in diabetic patients through the inhibition of proapoptotic genes (Xu et al., 2012). Next one is the upregulation of Ca^{2+} -influx through increased SERCA expression (Ghemrawi et al., 2018). Forced activation of SERCA reduced UPR and improved glucose homeostasis in obese mice *in vivo* (Bouchecareilh et al., 2011). In obese mice, altered hepatic lipid composition inhibits the Ca^{2+} -ATPase pump and limits the glucose metabolism in the liver (Fu et al., 2011). Increased Ca^{2+} -leakage from the ER could also lead to Ca^{2+} -overload in the mitochondria, causing mitochondrial oxidative stress and apoptosis. Cyclophilin D, a component on the mitochondrial inner membrane, is required for an influx of cytosolic Ca^{2+} into the mitochondrial matrix. Cyclosporine A is a cyclophilin D inhibitor which protects cells from ER stress by preventing Ca^{2+} -influx into the mitochondria (Baines et al., 2005; Park et al., 2010). Another drug approved by the FDA for hypertension is diltiazem. It functions as Ca^{2+} channel blocker to inhibit ER Ca^{2+} -efflux and enhances ER protein folding capacity (Zamorano et al., 2012; Zhang and Armstrong, 2007).

4.1. Targeting ER stress by natural products

Targeting ER stress associated complications by natural products opens an exciting therapeutic window for alleviating many signs of metabolic syndrome. Many phytochemicals showed the potential to reduce and/or normalize the ER stress with their antioxidant properties (Tripathi and Pandey, 2012). Two major cellular causes for the development of metabolic syndrome are reactive oxygen species-generated and ER-related stress. Therefore, antioxidant therapy might have a crucial role in reducing these types of stress. Butylated hydroxyanisole (BHA) is a widely used antioxidant and food additive, which reduces UPR stress, and reactive oxygen species-mediated damage of membrane proteins and programmed cell death (Han et al., 2013). It protects

genetically engineered β -cells from damage caused by UPR and oxidative insult during proinsulin synthesis (Ong and Kelly, 2011). Quercetin is a well-known antioxidant and abundantly present natural compound. It restored the ER homeostasis through the normalization of antioxidant enzymes (Suganya et al., 2014). Another possibility is elatolide, a terpenoid derived from *Aralia elata*, which inhibited ER stress by reducing the levels of GRP-78, CHOP, and JNK in cardiomyocytes (Wang et al., 2014). Sulforaphane from cruciferous vegetables inhibits ER stress through activation of Sirt1 (Danilov et al., 2009). Sirt1 inhibits ER stress by reducing PERK-eIF2 α activation (Prola et al., 2017). Phytochemicals that modulate ER stress include baicalin and resveratrol (Lin et al., 2016; Shen et al., 2014). Next one is an alkaloid, berberine, for its potential to suppress ER stress by downregulating the PERK-eIF2 α generation and the expression of ATF4 and CHOP in heart tissues (Zhao et al., 2016). Hydroxycitric acid, mostly found in *Garcinia* species, acts as a promising ER stress modulator (Nisha et al., 2014). Kaempferol, a ubiquitous flavonoid, inhibits ER stress mediated cell death in neuroblastoma cells using *in vitro* models (Abdullah and Ravanan, 2018). Nobiletin, another flavonoid mostly found in citrus plants, mitigates ER stress and thereby offers protection against cardiac hypertrophy (Zhang et al., 2017b). In addition, mitochondrial oxidative stress also disrupts ER protein folding homeostasis and causes a variety of human diseases. Mitoquinone (MitoQ) is a mitochondria-targeted antioxidant that protects against cardiac ischemic injury and Parkinson's disease (Fernández-Moriano et al., 2015). In clinical trials, it had an excellent safety profile (Ong et al., 2010). A combination of MitoQ with another mitochondrion-targeted antioxidant, MitoTempol, reduce mitochondrial oxidative damage, ER stress, and apoptosis in β -cell models of glucotoxicity and glucolipotoxicity (Back et al., 2009).

In addition to these compounds, there are many plant-derived compounds with the potential to maintain ER homeostasis (Choy et al., 2018). Preclinical and clinical studies demonstrate that a wide range of small molecular modulators and regulators of UPR-related stress have great therapeutic potential against signs of metabolic syndrome (Smith and Murphy, 2010). Some of the compounds such as chemical chaperones have shown efficacy in animal and clinical studies, while other molecules including the regulators of IRE1 and GRP-78 still need extensive preclinical investigation (Lim et al., 2011). However, one of the major problems that we need to consider is the multifunctional nature of UPR signaling in different cell types. Hence, the dosing of drugs will be critical for success in clinical settings. However, more mechanistic and physiological studies are still needed to elucidate the efficiency and safety of these interventions to target ER stress.

5. Conclusion

The ER is a large membranous network that participates in lipid and protein metabolism. High nutritional and protein load initiates ER stress. UPR regulate protein modification, secretion, and alter the receptor protein expression. Chronic ER stress results in cellular apoptosis. Many studies have been conducted to exploit protein-folding signaling as a target for therapy. Therefore, a variety of strategies and dozens of compounds have been tested in *in vitro*, *in vivo* and some are under clinical study. Some of these compounds alleviate ER stress by promoting protein folding and preventing aggregation in the cell. Increased understanding of ER stress in metabolic syndrome will allow the rational design of small molecules for more selective pharmacological interventions. The ideal examples are TUDCA and PBA. They are synthetic pharmacological agents tested in clinical studies. UPR pathways have a different role in many tissues/organs. Optimization of dose and treatment duration is necessary to avoid adverse effects. Organ-specific drug delivery might be a good solution to increase the safety profile of therapeutic agents. Some of the conditions such as NAFLD and type 2 diabetes mellitus may require long-term dosing of therapeutic agents. In such situations, long-term clinical trials are necessary to reveal potential side effects. Apart from this, many gaps have to be filled,

which require the complete understanding of ER stress response pathway in different aspects of metabolic syndrome.

Conflict of interest

The authors declare no conflict of interest.

Acknowledgements:

Sreelekshmi Mohan thanks University Grants Commission (UGC, New Delhi, India) for providing fellowship to conduct research, on the role of ER stress and metabolic syndrome. Preetha Rani M R thanks Council of Scientific and Industrial Research (CSIR), Government of India, for providing fellowship.

References

- Abdullah, A., Ravanan, P., 2018. Kaempferol mitigates endoplasmic reticulum stress induced cell death by targeting caspase 3/7. *Sci. Rep.* 8, 1–15.
- Achard, C.S., Laybutt, D.R., 2012. Lipid-induced endoplasmic reticulum stress in liver cells results in two distinct outcomes: adaptation with enhanced insulin signaling or insulin resistance. *Endocrinology* 153, 2164–2177.
- Anderson, D.J., Hetzer, M.W., 2008. Shaping the endoplasmic reticulum into the nuclear envelope. *J. Cell Sci.* 121, 137–142.
- Avery, J., Etzion, S., DeBosch, B.J., Jin, X., Lupu, T.S., Beitinjaneh, B., Muslin, A.J., 2010. TRB3 function in cardiac endoplasmic reticulum stress. *Circ. Res.* 106, 1516–1523.
- Axten, J.M., Medina, J.R., Feng, Y., Shu, A., Romeril, S.P., Grant, S.W., Atkins, C., 2012. Discovery of 7-methyl-5-(1-([3-(trifluoromethyl) phenyl] acetyl)-2, 3-dihydro-1 H-indol-5-yl)-7 H-pyrrolo [2, 3-d] pyrimidin-4-amine (GSK2606414), a potent and selective first-in-class inhibitor of protein kinase R (PKR)-like endoplasmic reticulum kinase (PERK). *J. Med. Chem.* 55, 7193–7207.
- Back, S.H., Scheuner, D., Han, J., Song, B., Ribick, M., Wang, J., Kaufman, R.J., 2009. Translation attenuation through eIF2 α phosphorylation prevents oxidative stress and maintains the differentiated state in β cells. *Cell Metabol.* 10, 13–26.
- Baiceanu, A., Mesdom, P., Lagouge, M., Foufelle, F., 2016. Endoplasmic reticulum proteostasis in hepatic steatosis. *Nat. Rev. Endocrinol.* 12, 710–722.
- Baines, C.P., Kaiser, R.A., Purcell, N.H., Blair, N.S., Osinska, H., Hambleton, M.A., Robbins, J., 2005. Loss of cyclophilin D reveals a critical role for mitochondrial permeability transition in cell death. *Nature* 434, 658–662.
- Bays, H.E., Gonzalez-Campoy, J.M., Henry, R.R., Bergman, D.A., Kitabchi, A.E., Schorr, A.B., 2008. Adiposopathy Working Group. Is adiposopathy (sick fat) an endocrine disease? *Int. J. Clin. Pract.* 62, 1474–1483.
- Bhuvanawari, S., Yagalakshmi, B., Sreeja, S., Anuradha, C.V., 2014. Astaxanthin reduces hepatic endoplasmic reticulum stress and nuclear factor- κ B-mediated inflammation in high fructose and high fat diet-fed mice. *Cell Stress Chaperones* 19, 183–191.
- Biason-Laubert, A., Lang-Muritano, M., Vaccaro, T., Schoenle, E.J., 2002. Loss of kinase activity in a patient with Wolcott-Rallison syndrome caused by a novel mutation in the EIF2AK3 gene. *Diabetes* 51, 2301–2305.
- Boden, G., 2009. Endoplasmic reticulum stress: another link between obesity and insulin resistance/inflammation? *Diabetes* 58, 518–519.
- Boden, G., Merali, S., 2011. Measurement of the increase in endoplasmic reticulum stress-related proteins and genes in adipose tissue of obese, insulin-resistant individuals. *Methods Enzymol.* 489, 67–82.
- Bommiasamy, H., Back, S.H., Fagone, P., Lee, K., Meshinchi, S., Vink, E., Brewer, J.W., 2009. ATF6 α induces XBP1-independent expansion of the endoplasmic reticulum. *J. Cell Sci.* 122, 1626–1636.
- Bouchecareilh, M., Higa, A., Fribourg, S., Moenner, M., Chevet, E., 2011. Peptides derived from the bifunctional kinase/RNase enzyme IRE1 α modulate IRE1 α activity and protect cells from endoplasmic reticulum stress. *FASEB J.* 25, 3115–3129.
- Boyce, M., Bryant, K.F., Jousse, C., Long, K., Harding, H.P., Scheuner, D., Yuan, J., 2005. A selective inhibitor of eIF2 α dephosphorylation protects cells from ER stress. *Science* 307, 935–939.
- Brostrom, M.A., Brostrom, C.O., 2003. Calcium dynamics and endoplasmic reticulum function in the regulation of protein synthesis: implications for cell growth and adaptability. *Cell Calcium* 34, 345–363.
- Cao, S.S., Kaufman, R.J., 2013. Targeting endoplasmic reticulum stress in metabolic disease. *Expert Opin. Ther. Targets* 17, 437–448.
- Choy, K.W., Murugan, D., Mustafa, M.R., 2018. Natural products targeting ER stress pathway for the treatment of cardiovascular diseases. *Pharmacol. Res.* 132, 119–129.
- Cnop, M., Foufelle, F., Velloso, L.A., 2012. Endoplasmic reticulum stress, obesity and diabetes. *Trends Mol. Med.* 18, 59–68.
- Cnop, M., Toivonen, S., Igoillo-Esteve, M., Salpea, P., 2017. Endoplasmic reticulum stress and eIF2 α phosphorylation: the Achilles heel of pancreatic β cells. *Mol. Metab.* 6, 1024–1039.
- Cross, B.C., Bond, P.J., Sadowski, P.G., Jha, B.K., Zak, J., Goodman, J.M., Harding, H.P., 2012. The molecular basis for selective inhibition of unconventional mRNA splicing by an IRE1-binding small molecule. *Proc. Natl. Acad. Sci. U.S.A.* 109, E869–E878.
- da Costa, R.M., Rodrigues, D., Pereira, C.A., Silva, J.F., Alves, J.V., Lobato, N.S., Tostes, R.C., 2019. Nrf2 as a potential mediator of cardiovascular risk in metabolic diseases. *Front. Pharmacol.* 10, 1–12.
- Damiano, F., Alemanno, S., Gnoni, G.V., Siculella, L., 2010. Translational control of the sterol-regulatory transcription factor SREBP-1 mRNA in response to serum starvation or ER stress is mediated by an internal ribosome entry site. *Biochem. J.* 429, 603–612.
- Danilov, C.A., Chandrasekaran, K., Raczy, J., Soane, L., Zielke, C., Fiskum, G., 2009. Sulforaphane protects astrocytes against oxidative stress and delayed death caused by oxygen and glucose deprivation. *Glia* 57, 645–656.
- Danilova, T., Lindahl, M., 2018. Emerging roles for mesencephalic astrocyte-derived neurotrophic factor (MANF) in pancreatic beta cells and diabetes. *Front. Physiol.* 9, 1–21.
- Dara, L., Ji, C., Kaplowitz, N., 2011. The contribution of endoplasmic reticulum stress to liver diseases. *Hepatology* 53, 1752–1763.
- Delepine, M., Nicolino, M., Barrett, T., Golamaully, M., Lathrop, G.M., Julier, C., 2000. EIF2AK3, encoding translation initiation factor 2- α kinase 3, is mutated in patients with Wolcott-Rallison syndrome. *Nat. Genet.* 25, 406–409.
- DeZwaan-McCabe, D., Sheldon, R.D., Gorecki, M.C., Guo, D.F., Gansemer, E.R., Kaufman, R.J., Rahmouni, K., Gillum, M.P., Taylor, E.B., Teesch, L.M., Rutkowski, D.T., 2017. ER stress inhibits liver fatty acid oxidation while unmitigated stress leads to anorexia-induced lipolysis and both liver and kidney steatosis. *Cell Rep.* 19, 1794–1806.
- Di Francescomarino, S., Sciartilli, A., Di Valerio, V., Di Baldassarre, A., Gallina, S., 2009. The effect of physical exercise on endothelial function. *Sport. Med.* 39, 797–812.
- Eizirik, D.L., Cardozo, A.K., Cnop, M., 2007. The role for endoplasmic reticulum stress in diabetes mellitus. *Endocr. Rev.* 29, 42–61.
- Erbay, E., Babaev, V.R., Mayers, J.R., Makowski, L., Charles, K.N., Snitow, M.E., Hotamisligil, G.S., 2009. Reducing endoplasmic reticulum stress through a macrophage lipid chaperone alleviates atherosclerosis. *Nat. Med.* 15, 1383–1391.
- Fernández-Moriano, C., González-Burgos, E., Gómez-Serranillos, M.P., 2015. Mitochondria-targeted protective compounds in Parkinson's and Alzheimer's diseases. *Oxid. Med. Cell Longev.* 1–30 2015.
- Fonseca, S.G., Gromada, J., Urano, F., 2011. Endoplasmic reticulum stress and pancreatic β -cell death. *Trends Endocrinol. Metab.* 22, 266–274.
- Fonseca, S.G., Ishigaki, S., Osowski, C.M., Lu, S., Lipson, K.L., Ghosh, R., Urano, F., 2010. Wolfram syndrome 1 gene negatively regulates ER stress signaling in rodent and human cells. *J. Clin. Investig.* 120, 744–755.
- Fu, S., Yang, L., Li, P., Hofmann, O., Dicker, L., Hide, W., Hotamisligil, G.S., 2011. Aberrant lipid metabolism disrupts calcium homeostasis causing liver endoplasmic reticulum stress in obesity. *Nature* 473, 528–531.
- Gentile, C.L., Frye, M.A., Pagliassotti, M.J., 2011. Fatty acids and the endoplasmic reticulum in nonalcoholic fatty liver disease. *Biofactors* 37, 8–16.
- Ghemrawi, R., Battaglia-Hsu, S.F., Arnold, C., 2018. Endoplasmic reticulum stress in metabolic disorders. *Cells* 7, 1–35.
- Gianfrancesco, M.A., Paquot, N., Piette, J., Legrand-Poels, S., 2018. Lipid bilayer stress in obesity-linked inflammatory and metabolic disorders. *Biochem. Pharmacol.* 153, 168–183.
- Gotoh, T., Endo, M., Oike, Y., 2011. Endoplasmic reticulum stress-related inflammation and cardiovascular diseases. *Int. J. Inflamm.* 1–8 2011.
- Groenendyk, J., Sreenivasiah, P.K., Kim, D.H., Agellon, L.B., Michalak, M., 2010. Biology of endoplasmic reticulum stress in the heart. *Circ. Res.* 107, 1185–1197.
- Hager, L., Li, L., Pun, H., Liu, L., Hossain, M.A., Maguire, G.F., Adeli, K., 2012. Lecithin: cholesterol acyltransferase deficiency protects against cholesterol-induced hepatic endoplasmic reticulum stress in mice. *J. Biol. Chem.* 287, 20755–20768.
- Han, D., Lerner, A.G., Walle, L.V., Upton, J.P., Xu, W., Hagen, A., Papa, F.R., 2009. IRE1 α kinase activation modes control alternate endoribonuclease outputs to determine divergent cell fates. *Cell* 138, 562–575.
- Han, J., Kaufman, R.J., 2016. The role of ER stress in lipid metabolism and lipotoxicity. *J. Lipid Res.* 57, 1329–1338.
- Han, J., Back, S.H., Hur, J., Lin, Y.H., Gildersleeve, R., Shan, J., Yuan, C.L., Krokowski, D., Wang, S., Hatzoglou, M., Kilberg, M.S., 2013. ER-stress-induced transcriptional regulation increases protein synthesis leading to cell death. *Nat. Cell Biol.* 15, 481–490.
- Harding, H.P., Zryanova, A.F., Ron, D., 2012. Uncoupling proteostasis and development in vitro with a small molecule inhibitor of the pancreatic endoplasmic reticulum kinase, PERK. *J. Biol. Chem.* 287, 44338–44344.
- Hetz, C., 2012. The unfolded protein response: controlling cell fate decisions under ER stress and beyond. *Nat. Rev. Mol. Cell Biol.* 13, 89–102.
- Hirosumi, J., Tuncman, G., Chang, L., Görgün, C.Z., Uysal, K.T., Maeda, K., Hotamisligil, G.S., 2002. A central role for JNK in obesity and insulin resistance. *Nature* 420, 333–336.
- Hong, J., Kim, K., Kim, J.H., Park, Y., 2017. The role of endoplasmic reticulum stress in cardiovascular disease and exercise. *Int. J. Vasc. Med.* 1–9 2017.
- Howden, R., 2013. Nrf2 and cardiovascular defense. *Oxid. Med. Cell Longev.* 1–10 2013.
- Hu, P., Han, Z., Couvillon, A.D., Kaufman, R.J., Exton, J.H., 2006. Autocrine tumor necrosis factor alpha links endoplasmic reticulum stress to the membrane death receptor pathway through IRE1 α -mediated NF- κ B activation and down-regulation of TRAF2 expression. *Mol. Cell Biol.* 26, 3071–3084.
- Inokuchi, Y., Nakajima, Y., Shimazawa, M., Kurita, T., Kubo, M., Saito, A., Araie, M., 2009. Effect of an inducer of BiP, a molecular chaperone, on endoplasmic reticulum (ER) stress-induced retinal cell death. *Investig. Ophthalmol. Vis. Sci.* 50, 334–344.
- Jammi, N.V., Whitby, L.R., Beal, P.A., 2003. Small molecule inhibitors of the RNA-dependent protein kinase. *Biochem. Biophys. Res. Commun.* 308, 50–57.
- Kabir, M., Catalano, K.J., Ananthnarayan, S., Kim, S.P., Van Citters, G.W., Dea, M.K., Bergman, R.N., 2005. Molecular evidence supporting the portal theory: a causative link between visceral adiposity and hepatic insulin resistance. *Am. J. Physiol. Endocrinol. Metab.* 288, E454–E461.
- Kaneko, M., Imaizumi, K., Saito, A., Kanemoto, S., Asada, R., Matsuhisa, K., Ohtake, Y., 2017. ER stress and disease: toward prevention and treatment. *Biol. Pharm. Bull.* 40, 1337–1343.
- Kaplan, M.M., Gershwin, M.E., 2005. Primary biliary cirrhosis. *N. Engl. J. Med.* 353,

- 1261–1273.
- Kars, M., Yang, L., Gregor, M.F., Mohammed, B.S., Pietka, T.A., Finck, B.N., Klein, S., 2010. Tauroursodeoxycholic acid may improve liver and muscle but not adipose tissue insulin sensitivity in obese men and women. *Diabetes* 59, 1899–1905.
- Kim, I., Shu, C.W., Xu, W., Shiau, C.W., Grant, D., Vasile, S., Reed, J.C., 2009. Chemical biology investigation of cell death pathways activated by endoplasmic reticulum stress reveals cytoprotective modulators of ASK1. *J. Biol. Chem.* 284, 1593–1603.
- Kim, O.K., Jun, W., Lee, J., 2015. Mechanism of ER stress and inflammation for hepatic insulin resistance in obesity. *Ann. Nutr. Metab.* 67, 218–227.
- Kudo, T., Kanemoto, S., Hara, H., Morimoto, N., Morihara, T., Kimura, R., Takeda, M., 2008. A molecular chaperone inducer protects neurons from ER stress. *Cell Death Differ.* 15, 364–375.
- Lebeauapin, C., Vallee, D., Gual, P., Bailly-Maitre, B., 2016. Role of ER stress in inflammation activation and non-alcoholic fatty liver disease progression. *Single Cell Biol.* 5, 1–3.
- Lee, A.H., Heidtman, K., Hotamisligil, G.S., Glimcher, L.H., 2011. Dual and opposing roles of the unfolded protein response regulated by IRE1 α and XBP1 in proinsulin processing and insulin secretion. *Proc. Natl. Acad. Sci. U.S.A.* 108, 8885–8890.
- Lee, J., Ozcan, U., 2014. Unfolded protein response signaling and metabolic diseases. *J. Biol. Chem.* 289, 1203–1211.
- Lewy, T.G., Grabowski, J.M., Bloom, M.E., 2017. Focus: infectious diseases: BiP: master regulator of the unfolded protein response and crucial factor in flavivirus biology. *Yale J. Biol. Med.* 90, 291–300.
- Li, Y., Ge, M., Ciani, L., Kuriakose, G., Westover, E.J., Dura, M., Tabas, I., 2004. Enrichment of endoplasmic reticulum with cholesterol inhibits sarcoplasmic-endoplasmic reticulum calcium ATPase-2b activity in parallel with increased order of membrane lipids implications for depletion of endoplasmic reticulum calcium stores and apoptosis in cholesterol-loaded macrophages. *J. Biol. Chem.* 279, 37030–37039.
- Lim, S., Rashid, M.A., Jang, M., Kim, Y., Won, H., Lee, J., Ha, J., 2011. Mitochondria-targeted antioxidants protect pancreatic β -cells against oxidative stress and improve insulin secretion in glucotoxicity and glucolipotoxicity. *Cell. Physiol. Biochem.* 28, 873–886.
- Lin, Y., Zhu, J., Zhang, X., Wang, J., Xiao, W., Li, B., Jin, L., Lian, J., Zhou, L., Liu, J., 2016. Inhibition of cardiomyocytes hypertrophy by resveratrol is associated with amelioration of endoplasmic reticulum stress. *Cell. Physiol. Biochem.* 39, 780–789.
- Liu, M.Q., Chen, Z., Chen, L.X., 2016. Endoplasmic reticulum stress: a novel mechanism and therapeutic target for cardiovascular diseases. *Acta Pharmacol. Sin.* 37, 425–443.
- Maamoun, H., Abdelsalam, S.S., Zeidan, A., Korashy, H.M., Agouni, A., 2019. Endoplasmic Reticulum Stress: a critical molecular driver of endothelial dysfunction and cardiovascular disturbances associated with diabetes. *Int. J. Mol. Sci.* 20, 1–21.
- Malhi, H., Kaufman, R.J., 2011. Endoplasmic reticulum stress in liver disease. *J. Hepatol.* 54, 795–809.
- Marciniak, S.J., Yun, C.Y., Oyadomari, S., Novoa, I., Zhang, Y., Jungreis, R., Ron, D., 2004. CHOP induces death by promoting protein synthesis and oxidation in the stressed endoplasmic reticulum. *Genes Dev.* 18, 3066–3077.
- Marciniak, S.J., Ron, D., 2006. Endoplasmic reticulum stress signaling in disease. *Physiol. Rev.* 86, 1133–1149.
- Mimura, N., Fulciniti, M., Gorgun, G., Tai, Y.T., Cirstea, D., Santo, L., Kiziltepe, T., 2012. Blockade of XBP1 splicing by inhibition of IRE1 α is a promising therapeutic option in multiple myeloma. *Blood* 119, 5772–5781.
- Minamino, T., Kitakaze, M., 2010. ER stress in cardiovascular disease. *J. Mol. Cell. Cardiol.* 48, 1105–1110.
- Minamino, T., Komuro, I., Kitakaze, M., 2010. Endoplasmic reticulum stress as a therapeutic target in cardiovascular disease. *Circ. Res.* 107, 1071–1082.
- Morris, J.A., Dorner, A.J., Edwards, C.A., Hendershot, L.M., Kaufman, R.J., 1997. Immunoglobulin binding protein (BiP) function is required to protect cells from endoplasmic reticulum stress but is not required for the secretion of selective proteins. *J. Biol. Chem.* 272, 4327–4334.
- Nicklas, T.A., O'Neil, C.E., 2014. Prevalence of obesity: a public health problem poorly understood. *AIMS Public Health* 1, 109–122.
- Nisha, V.M., Priyanka, A., Anusree, S.S., Raghunath, K.G., 2014. (-)-Hydroxycitric acid attenuates endoplasmic reticulum stress-mediated alterations in 3T3-L1 adipocytes by protecting mitochondria and downregulating inflammatory markers. *Free Radic. Res.* 48, 1386–1396.
- O'Rourke, R.W., 2009. Inflammation in obesity-related diseases. *Surgery* 145, 255–259.
- Oida, Y., Hamanaka, J., Hyakkoku, K., Shimazawa, M., Kudo, T., Imaizumi, K., Hara, H., 2010. Post-treatment of a BiP inducer prevents cell death after middle cerebral artery occlusion in mice. *Neurosci. Lett.* 484, 43–46.
- Olivares, S., Henkel, A.S., 2015. Hepatic Xbp1 gene deletion promotes endoplasmic reticulum stress-induced liver injury and apoptosis. *J. Biol. Chem.* 290, 30142–30151.
- Ong, D.S.T., Kelly, J.W., 2011. Chemical and/or biological therapeutic strategies to ameliorate protein misfolding diseases. *Curr. Opin. Cell Biol.* 23, 231–238.
- Ong, D.S.T., Mu, T.W., Palmer, A.E., Kelly, J.W., 2010. Endoplasmic reticulum Ca²⁺ increases enhance mutant glucocerebrosidase proteostasis. *Nat. Chem. Biol.* 6, 424–432.
- Ooi, B.K., Chan, K.G., Goh, B.H., Yap, W.H., 2018. The role of natural products in targeting cardiovascular diseases via Nrf2 Pathway: novel molecular mechanisms and therapeutic approaches. *Front. Pharmacol.* 9, 1–18.
- Pagliassotti, M.J., 2012. Endoplasmic reticulum stress in nonalcoholic fatty liver disease. *Annu. Rev. Nutr.* 32, 17–33.
- Papa, F.R., 2012. Endoplasmic reticulum stress, pancreatic β -cell degeneration, and diabetes. *Cold Spring Harb. Perspect. Med.* 2, 1–17.
- Papandreou, I., Denko, N.C., Olson, M., Van Melckebeke, H., Lust, S., Tam, A., Koong, A.C., 2011. Identification of an IRE1 α endonuclease specific inhibitor with cytotoxic activity against human multiple myeloma. *Blood* 117, 1311–1314.
- Park, S.W., Zhou, Y., Lee, J., Lee, J., Ozcan, U., 2010. Sarco (endo) plasmic reticulum Ca²⁺ ATPase 2b is a major regulator of endoplasmic reticulum stress and glucose homeostasis in obesity. *Proc. Natl. Acad. Sci. U.S.A.* 107, 19320–19325.
- Piperi, C., Adamopoulos, C., Dalagiorgou, G., Diamanti-Kandaraki, E., Papavassiliou, A.G., 2012. Crosstalk between advanced glycation and endoplasmic reticulum stress: emerging therapeutic targeting for metabolic diseases. *J. Clin. Endocrinol. Metab.* 97, 2231–2242.
- Prola, A., Pires Da Silva, J., Guilbert, A., Lecru, L., Piquereau, J., Ribeiro, M., Mateo, P., Gressette, M., Fortin, D., Boursier, C., Gallerne, C., Caillard, A., Samuel, J.L., François, H., Sinclair, D.A., Eid, P., Ventura-Clapier, R., Garnier, A., Lemaire, C., 2017. SIRT1 protects the heart from ER stress-induced cell death through eIF2 α deacetylation. *Cell Death Differ.* 24, 343–356.
- Qiu, Q., Zheng, Z., Chang, L., Zhao, Y.S., Tan, C., Dandekar, A., Zhang, Z., Lin, Z., Gui, M., Li, X., Zhang, T., 2013. Toll-like receptor-mediated IRE1 α activation as a therapeutic target for inflammatory arthritis. *EMBO J.* 32, 2477–2490.
- Ron, D., Walter, P., 2007. Signal integration in the endoplasmic reticulum unfolded protein response. *Nat. Rev. Mol. Cell Biol.* 8, 519–529.
- Rosen, E.D., Spiegelman, B.M., 2006. Adipocytes as regulators of energy balance and glucose homeostasis. *Nature* 444, 847–853.
- Rutkowski, D.T., 2019. Liver function and dysfunction—a unique window into the physiological reach of ER stress and the unfolded protein response. *FEBS J.* 286, 356–378.
- Sarvani, C., Sireesh, D., Ramkumar, K.M., 2017. Unraveling the role of ER stress inhibitors in the context of metabolic diseases. *Pharmacol. Res.* 119, 412–421.
- Schroder, M., Kaufman, R.J., 2005. The mammalian unfolded protein response. *Annu. Rev. Biochem.* 74, 739–789.
- Schwarz, D.S., Blower, M.D., 2016. The endoplasmic reticulum: structure, function and response to cellular signaling. *Cell. Mol. Life Sci.* 73, 79–94.
- Shao, W., Espenshade, P.J., 2014. Sterol regulatory element-binding protein (SREBP) cleavage regulates Golgi-to-endoplasmic reticulum recycling of SREBP cleavage-activating protein (SCAP). *J. Biol. Chem.* 289, 7547–7557.
- Shen, M., Wang, L., Yang, G., Gao, L., Wang, B., Guo, X., Zeng, C., Xu, Y., Shen, L., Cheng, K., Xia, Y., 2014. Baicalin protects the cardiomyocytes from ER stress-induced apoptosis: inhibition of CHOP through induction of endothelial nitric oxide synthase. *PLoS One* 9, e88389.
- Shimano, H., 2001. Sterol regulatory element-binding proteins (SREBPs): transcriptional regulators of lipid synthetic genes. *Prog. Lipid Res.* 40, 439–452.
- Shimazawa, M., Hara, H., 2006. Inhibitor of double stranded RNA-dependent protein kinase protects against cell damage induced by ER stress. *Neurosci. Lett.* 409, 192–195.
- Shohet, R.V., Garcia, J.A., 2007. Keeping the engine primed: HIF factors as key regulators of cardiac metabolism and angiogenesis during ischemia. *J. Mol. Med. (Berl.)* 85, 1309–1315.
- Smith, R.A., Murphy, M.P., 2010. Animal and human studies with the mitochondria-targeted antioxidant MitoQ. *Ann. N. Y. Acad. Sci.* 1201, 96–103.
- So, J.S., Hur, K.Y., Tarrío, M., Ruda, V., Frank-Kamenetsky, M., Fitzgerald, K., Lee, A.H., 2012. Silencing of lipid metabolism genes through IRE1 α -mediated mRNA decay lowers plasma lipids in mice. *Cell Metabol.* 16, 487–499.
- Sriburi, R., Jackowski, S., Mori, K., Brewer, J.W., 2004. XBP1: a link between the unfolded protein response, lipid biosynthesis, and biogenesis of the endoplasmic reticulum. *J. Cell Biol.* 167, 35–41.
- Suganya, N., Bhakkiyalakshmi, E., Suriyanarayanan, S., Paulmurugan, R., Ramkumar, K.M., 2014. Quercetin ameliorates tunicamycin-induced endoplasmic reticulum stress in endothelial cells. *Cell Prolif* 47, 231–240.
- Surmi, B., Hastay, A., 2008. Macrophage infiltration into adipose tissue: initiation, propagation and remodeling. *Future Lipidol.* 3, 545–556.
- Szegezdi, E., Duffy, A., O'Mahoney, M.E., Logue, S.E., Mylotte, L.A., O'Brien, T., Samali, A., 2006. ER stress contributes to ischemia-induced cardiomyocyte apoptosis. *Biochem. Biophys. Res. Commun.* 349, 1406–1411.
- Thoudam, T., Jeon, J.H., Ha, C.M., Lee, I.K., 2016. Role of mitochondria-associated endoplasmic reticulum membrane in inflammation-mediated metabolic diseases. *Mediat. Inflamm.* 1–18 2016.
- Thurauf, D.J., Marcinko, M., Gude, N., Rubio, M., Sussman, M.A., Glembofski, C.C., 2006. Activation of the unfolded protein response in infarcted mouse heart and hypoxic cultured cardiac myocytes. *Circ. Res.* 99, 275–282.
- Tripathi, Y.B.T., Pandey, V.P., 2012. Obesity and endoplasmic reticulum (ER) stresses. *Front. Immunol.* 3, 1–9.
- Tsaytler, P., Harding, H.P., Ron, D., Bertolotti, A., 2011. Selective inhibition of a regulatory subunit of protein phosphatase 1 restores proteostasis. *Science* 332, 91–94.
- Tu, W., Wang, H., Li, S., Liu, Q., Sha, H., 2019. The anti-inflammatory and anti-oxidant mechanisms of the Keap1/Nrf2/ARE signaling pathway in chronic diseases. *Aging Dis.* 10, 637–651.
- Van Meer, G., Voelker, D.R., Feigenson, G.W., 2008. Membrane lipids: where they are and how they behave. *Nat. Rev. Mol. Cell Biol.* 9, 112–124.
- Verdile, G., Keane, K.N., Cruzat, V.F., Medice, S., Sabale, M., Rowles, J., Newsholme, P., 2015. Inflammation and oxidative stress: the molecular connectivity between insulin resistance, obesity, and Alzheimer's disease. *Mediat. Inflamm.* 1–17 2015.
- Villalobos-Labra, R., Subiabre, M., Toledo, F., Pardo, F., Sobrevia, L., 2018. Endoplasmic reticulum stress and development of insulin resistance in adipose, skeletal, liver, and foetoplacental tissue in diabetes. *Mol. Asp. Med.* 66, 49–61.
- Vitadello, M., Penzo, D., Petronilli, V., Michieli, G., Gomirato, S., Menabo, R., Di Liza, F., Gorza, L., 2003. Overexpression of the stress protein Grp94 reduces cardiomyocyte necrosis due to calcium overload and simulated ischemia. *FASEB J.* 17, 923–925.
- Voeltz, G.K., Rolls, M.M., Rapoport, T.A., 2002. Structural organization of the endoplasmic reticulum. *EMBO Rep.* 3, 944–950.
- Volkmann, K., Lucas, J.L., Vuga, D., Wang, X., Brumm, D., Stiles, C., Liu, Z., 2011. Potent and selective inhibitors of the inositol-requiring enzyme 1 endoribonuclease. *J. Biol.*

- Chem. 286, 12743–12755.
- Wang, H., Blais, J., Ron, D., Cardozo, T., 2010. Structural determinants of PERK inhibitor potency and selectivity. *Chem. Biol. Drug Des.* 76, 480–495.
- Wang, M., Meng, X.B., Yu, Y.L., Sun, G.B., Xu, X.D., Zhang, X.P., Dong, X., Ye, J.X., Xu, H.B., Sun, Y.F., Sun, X.B., 2014. Elatoside C protects against hypoxia/reoxygenation-induced apoptosis in H9c2 cardiomyocytes through the reduction of endoplasmic reticulum stress partially depending on STAT3 activation. *Apoptosis* 19, 1727–1735.
- Wang, S., Kaufman, R.J., 2012. The impact of the unfolded protein response on human disease. *J. Cell Biol.* 197, 857–867.
- Wang, S., Chen, Z., Lam, V., Han, J., Hassler, J., Finck, B.N., Davidson, N.O., Kaufman, R.J., 2012. IRE1 α -XBP1s induces PDI expression to increase MTP activity for hepatic VLDL assembly and lipid homeostasis. *Cell Metabol.* 6, 473–486.
- Wang, Y., Vera, L., Fischer, W.H., Montminy, M., 2009. The CREB coactivator CRTC2 links hepatic ER stress and fasting gluconeogenesis. *Nature* 460, 534–537.
- Welch, W.J., Brown, C.R., 1996. Influence of molecular and chemical chaperones on protein folding. *Cell Stress Chaperones* 1, 109–115.
- Wiley, J.C., Meabon, J.S., Frankowski, H., Smith, E.A., Schecterson, L.C., Bothwell, M., Ladiges, W.C., 2010. Phenylbutyric acid rescues endoplasmic reticulum stress-induced suppression of APP proteolysis and prevents apoptosis in neuronal cells. *PLoS One* 5, e9135.
- Wu, F.L., Liu, W.Y., Van Poucke, S., Braddock, M., Jin, W.M., Xiao, J., Zheng, M.H., 2016. Targeting endoplasmic reticulum stress in liver disease. *Expert Rev. Gastroenterol. Hepatol.* 10, 1041–1052.
- Xiao, C., Giacca, A., Lewis, G.F., 2011. Sodium phenylbutyrate, a drug with known capacity to reduce endoplasmic reticulum stress, partially alleviates lipid-induced insulin resistance and β -cell dysfunction in humans. *Diabetes* 60, 918–924.
- Xu, G., Chen, J., Jing, G., Shalev, A., 2012. Preventing β -cell loss and diabetes with calcium channel blockers. *Diabetes* 61, 848–856.
- Yamamoto, K., Takahara, K., Oyadomari, S., Okada, T., Sato, T., Harada, A., Mori, K., 2010. Induction of liver steatosis and lipid droplet formation in ATF6 α -knockout mice burdened with pharmacological endoplasmic reticulum stress. *Mol. Biol. Cell* 21, 2975–2986.
- Yoshida, H., Matsui, T., Yamamoto, A., Okada, T., Mori, K., 2001a. XBP1 mRNA is induced by ATF6 and spliced by IRE1 in response to ER stress to produce a highly active transcription factor. *Cell* 107, 881–891.
- Yoshida, H., Okada, T., Haze, K., Yanagi, H., Yura, T., Negishi, M., Mori, K., 2000. ATF6 activated by proteolysis binds in the presence of NF-Y (CBF) directly to the cis-acting element responsible for the mammalian unfolded protein response. *Mol. Cell Biol.* 20, 6755–6767.
- Yoshida, H., Okada, T., Haze, K., Yanagi, H., Yura, T., Negishi, M., Mori, K., 2001b. Endoplasmic reticulum stress-induced formation of transcription factor complex ERSF including NF-Y (CBF) and activating transcription factors 6 α and 6 β that activates the mammalian unfolded protein response. *Mol. Cell Biol.* 21, 1239–1248.
- Zamorano, S., Rojas-Rivera, D., Lisbona, F., Parra, V., Villegas, R., Cheng, E.H., Hetz, C., 2012. A BAX/BAK and cyclophilin D-independent intrinsic apoptosis pathway. *PLoS One* 7, e37782.
- Zha, B.S., Zhou, H., 2012. ER stress and lipid metabolism in adipocytes. *Biochem. Res. Int.* 1–9 2012.
- Zhang, C., Syed, T.W., Liu, R., Yu, J., 2017a. Role of endoplasmic reticulum stress, autophagy, and inflammation in cardiovascular disease. *Front. Cardiovasc. Med.* 4, 1–8.
- Zhang, D., Armstrong, J.S., 2007. Bax and the mitochondrial permeability transition cooperate in the release of cytochrome c during endoplasmic reticulum-stress-induced apoptosis. *Cell Death Differ.* 14, 703–715.
- Zhang, G., Yang, W., Jiang, F., Zou, P., Zeng, Y., Ling, X., Zhou, Z., Cao, J., Ao, L., 2019. PERK regulates Nrf2/ARE antioxidant pathway against dibutyl phthalate-induced mitochondrial damage and apoptosis dependent of reactive oxygen species in mouse spermatocyte-derived cells. *Toxicol. Lett.* 308, 24–33.
- Zhang, N., Wei, W.Y., Yang, Z., Che, Y., Jin, Y.G., Liao, H.H., Wang, S.S., Deng, W., Tang, Q.Z., 2017b. Nobiletin, a polymethoxy flavonoid, protects against cardiac hypertrophy induced by pressure-overload via inhibition of NADPH oxidases and endoplasmic reticulum stress. *Cell. Physiol. Biochem.* 42, 1313–1325.
- Zhang, W., Feng, D., Li, Y., Iida, K., McGrath, B., Cavener, D.R., 2006. PERK EIF2AK3 control of pancreatic β cell differentiation and proliferation is required for postnatal glucose homeostasis. *Cell Metabol.* 4, 491–497.
- Zhang, Z., Tong, N., Gong, Y., Qiu, Q., Yin, L., Lv, X., Wu, X., 2011. Valproate protects the retina from endoplasmic reticulum stress-induced apoptosis after ischemia–reperfusion injury. *Neurosci. Lett.* 504, 88–92.
- Zhao, G.L., Yu, L.M., Gao, W.L., Duan, W.X., Jiang, B., Liu, X.D., Zhang, B., Liu, Z.H., Zhai, M.E., Jin, Z.X., Yu, S.Q., 2016. Berberine protects rat heart from ischemia/reperfusion injury via activating JAK2/STAT3 signaling and attenuating endoplasmic reticulum stress. *Acta Pharmacol. Sin.* 37, 354–367.
- Zhou, Y., Lee, J., Reno, C.M., Sun, C., Park, S.W., Chung, J., Ozcan, U., 2011. Regulation of glucose homeostasis through a XBP1–FoxO1 interaction. *Nat. Med.* 17, 356–365.
- Zhu, P.J., Huang, W., Kalikulov, D., Yoo, J.W., Placzek, A.N., Stoica, L., Noebels, J.L., 2011. Suppression of PKR promotes network excitability and enhanced cognition by interferon- γ -mediated disinhibition. *Cell* 147, 1384–1396.